Die approbierte Originalversion dieser Dissertation ist an der Hauptbibliothek der Technischen Universität Wien aufgestellt (http://www.ub.tuwien.ac.at).

The approved original version of this thesis is available at the main library of the Vienna University of Technology (http://www.ub.tuwien.ac.at/englweb/).

DISSERTATION

CGE-on-the-chip, planar SDS-PAGE and MALDI-TOF-MS investigations of proteins and dendrimers with molecular weights beyond 200 kDa

ausgeführt zum Zwecke der Erlangung des akademischen Grades eines Doktors der technischen Wissenschaften unter der Leitung von

Prof. Dr. Günter Allmaier
E164
Institut für chemische Technologien und Analytik

eingereicht an der Technischen Universität Wien
Fakultät für technische Chemie

von

Mag. Roland Müller
e9700409
Gartengasse 18/1/3
2500 Baden

Wien, am 23.10.2006

Name des Kandidaten: Mag. Roland Müller

Name des Prüfers: Prof. Dr. Günter Allmaier

Titel der Dissertation: CGE-on-the-chip, planar SDS-PAGE and MALDI-TOF-MS investigations of proteins and dendrimers with molecular weights beyond 200 kDa

Kurzfassung der Dissertation (deutsch):

Der Schwerpunkt dieser Dissertation liegt bei der Molekulargewichtsbestimmung und systematischen Charakterisierung von Proteinen und Poly(amido amine) (PAMAM) Dendrimeren mit Molekulargewichten jenseits von 200 kDa mittels zweier auf dem Prinzip der Gelelektrophorese basierenden Methoden (planare SDS-PAGE und CGE-on-the-chip) sowie einer massenspektrometrischen Technik (MALDI-TOF-MS). Zu diesem Zweck wurde ein neuer Protein Kit für Hochmolekulargewichtsproteine entwickelt. CGE-on-the-chip ist die jüngste aller drei angewandten Techniken und war bisher auf die Analyse von Proteinen mit einem Molekulargewicht kleiner als 250 kDa beschränkt. Die Analyse von Hochmolekulargewichtsproteinen mittels MALDI-TOF-MS war bis jetzt nur spärlich in der Literatur beschrieben. In der vorliegenden Arbeit wurde gezeigt, daß alle drei beschriebenen Analysentechniken in der Lage waren Hochmolekulargewichtsproteine erfolgreich zu untersuchen. Die Ergebnisse der CGE-on-the-chip Messungen waren in guter Übereinstimmung mit den Ergebnissen die mittels planarer SDS-PAGE bestimmt wurden. Mittels MALDI-TOF-MS und unter Verwendung eines einfachen und kommerziell erhältlichen Geräts konnte für alle untersuchten Hochmolekulargewichtsproteine ein exaktes Molekulargewicht bestimmt werden. Ein weiterer Schwerpunkt war die exakte Molekulargewichtsbestimmung von PAMAM Dendrimeren mittels MALDI-TOF-MS. Bisher wurden nur PAMAM Dendrimere mit niedrigem Molekulargewicht mittels MALDI-TOF-MS untersucht. Es konnte gezeigt werden, daß für sämtliche untersuchte PAMAM Dendrimere bis zur 10. Generation MALDI-TOF-MS Untersuchungen möglich waren. Weiters hat sich gezeigt, daß die Polydispersität der untersuchten Dendrimerproben wesentlich höher war als jene von Proteinen mit einer vergleichbaren Größe. Aufgrund einer unvollständigen Synthese der PAMAM Dendrimere waren die mittels MALDI-TOF-MS ermittelten Molekulargewichts deutlich kleiner als erwartet.

Summary of the PhD thesis (englisch):

This PhD thesis is focused on the molecular weight determination and systematic characterization of proteins and poly(amido amine) (PAMAM) dendrimers with molecular weights higher than 200 kDa using two gel electrophoretical (planar SDS-PAGE and CGE-on-the-chip) and one mass spectrometric technique (MALDI-TOF-MS). For this purpose a novel high molecular weight protein assay for CGE-on-the-chip was developed. CGE-on-the-chip is the most recent of all three applied analytical techniques and was so far only applied for the analysis of proteins with molecular weights lower than 250 kDa. Analysis of high molecular weight proteins with MALDI-TOF-MS was only sparely described in literature. In this work it was demonstrated that all three described analytical techniques were capable of analyzing high molecular weight protein samples. The results obtained with CGE-on-the-chip were in very good agreement with the protein bands found with traditional planar SDS-PAGE. For all high molecular weight proteins exact molecular weights could be determined with MALDI-TOF-MS using a commercial standard instrument. Another issue was the exact molecular weight determination of PAMAM dendrimers using MALDI-TOF-MS. So far only the molecular weight of smaller dendrimers was determined with MALDI-TOF-MS. It was shown that exact molecular mass determination of PAMAM dendrimers up to generation 10 was generally possible using MALDI-TOF-MS. Moreover it was found out that the polydispersity of the analysed dendrimer samples was significantly higher than the polydispersity of proteins in the same mass and size range. Due to imperfect dendrimer growth/synthesis the molecular weights determined with MALDI-TOF-MS for PAMAM dendrimers were significantly lower than the expected molecular weights.

Danksagung

Folgenden Personen möchte ich an dieser Stelle herzlich danken:

Univ.-Prof. Dr. Günter Allmaier für die Betreuung der Dissertation sowie für das in die Wege leiten einer Firmenkooperation mit Agilent Technologies

Dr. Helmuth Elgass und Dr. Martin Kratzmeier von Agilent Technologies, die diese Kooperation finanziell und thematisch ermöglichten und auch trotz der geographischen Distanz die Arbeiten mitbetreut haben

Meinen Arbeitsgruppenkollegen Mag. Roswitha Braunrath, Mag. Tom Grunert, Mag. Jasmin Hirschmann, DI Christian Laschober, Dr. Martina Marchetti, Mag. Corina Mayrhofer, Dr. Ernst Pittenauer, Reingard Schandl, Dr. Gerald Stübiger, Mag. Wolfgang Winkler und Dr. Martin Zehl für das gute Arbeitsklima und die produktive Zusammenarbeit

Meinen Eltern Ilse und Harald Müller für ihre Unterstützung während der Dissertation

Meiner Gattin Sabine Müller für ihren Rückhalt

Table of Contents

I. Introduction 1

I.1. General considerations of intact protein characterization 1

I.2. Electrophoresis 3

I.2.1. Principles of gel electrophoresis 3

I.2.2. History of gel electrophoresis 4

I.2.3. Planar gel electrophoresis 5

I.2.3.1. Introduction to planar SDS-PAGE 5

I.2.3.2. Sample preparation for SDS-PAGE 6

I.2.3.3. Cross-linked polyacrylamide gel matrices 6

I.2.3.4. Gel electrophoretical separation 8

I.2.3.5. Protein visualization 9

I.2.4. CGE-on-the-chip and the Lab-on-the-chip Bioanalyzer 11

I.2.4.1. Introduction to CGE 11

I.2.4.2. Lab-on-the-chip technology 13

I.2.4.3. Instrumentation for CGE-on-the-chip 13

I.2.4.4. Sample preparation for CGE-on-the-chip 14

I.2.4.5. Linear gel matrices based on polyacrylamide 15

I.2.4.6. Sample injection and separation 17

I.2.4.7. Laser induced fluorescence detection 19

I.2.5. Differences between planar gel electrophoresis and CGE-on-the-chip 21

I.3. MALDI-TOF mass spectrometry 22

I.3.1. Development and concept of MALDI mass spectrometry of biopolymers 22

I.3.2. MALDI sample preparation 23

I.3.3. The MALDI process 27

I.3.4. TOF analyzer and detector 28

I.4. High molecular weight proteins and glycoproteins 32
I.4.1. Classification of high molecular weight proteins 32
I.4.2. High molecular weight proteins consisting of only one single polypeptide backbone with a molecular weight higher than 200 kDa 33
I.4.2.1. Apolipoprotein B-100 33
I.4.2.2. Hemocyanin 34
I.4.3. High molecular weight proteins consisting of covalently linked subunits with molecular weights higher than 200 kDa 35
I.4.3.1. Thyroglobulin 35
I.4.3.2. Fibronectin 36
I.4.4. High molecular weight proteins consisting of covalently linked subunits with molecular weights lower than 200 kDa 37
I.4.4.1. α2-Macroglobulin 37
I.4.4.2. Fibrinogen 39
I.4.4.3. Immunoglobulin M 40

I.5. Complex Glycoproteins 42
I.5.1. Importance of post-translational protein modifications 42
I.5.2. Structures and sequons of protein glycosylations 43
I.5.3. Analysis of N-glycan residues 45

I.6. High molecular weight PAMAM dendrimers 48
I.6.1. Dendrimers – overview and applications 48
I.6.2. Structure, synthesis and characterization of PAMAM dendrimers 49

I.7. Aims of the thesis 53

I.8. References 54

II. Publications **72**

Molecular weight determination of several high molecular weight proteins using CGE-on-the-chip, planar SDS-PAGE and MALDI-TOF-MS 74

Comparison of planar SDS-PAGE, CGE-on-the-chip and MALDI-TOF mass spectrometry for the analysis of the enzymatic de-N-glycosylation of Antithrombin III and Coagulation Factor IX with PNGase F 137

Determination of molecular weight, particle size and density of high number generation PAMAM dendrimers using MALDI-TOF-MS and nES-GEMMA 173

Molecular weight determination of ultra-high mass compounds on a standard MALDI TOF mass spectrometer: PAMAM dendrimer G10 and Ig M 205

III. Conclusion **219**

Abbreviations

CE – capillary electrophoresis

CGE – capillary gel electrophoresis

CMC – critical micelle concentration

Da – Dalton

DNA – dexoxyribonucleic acid

EOF – electroosmotic flow

ESI – electrospray ionization

Fig – figure

HPLC – high performance liquid chromatography

HMW – high molecular weight

IgG – immunoglobulin G

IgM – immunoglobulin M

IR – infrared

KLH – keyhole limpet hemocyanin

LDS – lithium dodecyl sulfate

LIF – laser induced fluorescence

MALDI – matrix assisted laser desorption ionization

MS – mass spectrometry

PAGE – polyacrylamid gel electrophoresis

PAMAM – poly(amido amine)

PTM – posttranslational modification

RNA – ribonucleic acid

SDS – sodium dodecyl sulfate

TOF – time-of-flight

UV - ultraviolet

w/v – weight per volume

I.1. General considerations of intact protein characterization

The existence and macroscopic properties of proteins are known for more than 200 years. Nevertheless, the term protein was first introduced in 1838 by the Swedish chemist Berzelius who was at this point not aware of the exact composition and physiological importance of proteins. In the middle of the last century both, structure and composition of proteins was discovered by various chemists who found out that proteins are linear biopolymers consisting of several different types of amino acids. Today, the characterization of proteins is a major bioanalytical issue. Proteins are not only the by far most abundant organic molecules found in living cells, but are also responsible for a large variety of biological functions like catalysis, immunology, the maintenance of cell shape, cell-cell recognizition, signalling and intra- as well as extracellular molecular transport [1,2]. Hence, proteins are essentially for maintaining the cycle of life in all organisms. Basically the sequence of polypeptide backbones is encoded by DNA and RNA molecules. Nevertheless the exact composition and quantity of proteins cannot be sufficiently predicted by the analysis of DNA or RNA, so the analysis of intact proteins is an important issue [3]. Alternative splicing and post-translational modifications are known to lead to differences between the calculated and actual molecular weight of proteins. Important parameters of proteins are the amino acid composition and sequence of the polypeptide backbone, molecular weight, three-dimensional structure, post-translational modifications and the quantity of protein found in a particular protein sample. For many applications the enzymatic activity of protein samples is an important parameter too. The amino acid composition is usually analyzed by quantitative hydrolysis of all peptide bonds followed by chromatographic separation and quantitation. This technique also allows the determination of the total protein concentration in a sample. For experimentally determining the amino acid sequence of a polypeptide backbone several N- and C-terminal sequencing techniques are available. The most common N-terminal sequencing technique is Edman degradation. De-novo sequencing of proteins or peptides with the aid of mass spectrometry is another, less automated technique which is an alternative to chemical or enzymatical sequencing techniques. Molecular weight determination of intact proteins is commonly performed using mass spectrometry [4-7], denaturing gel electrophoresis [8-9] or gel filtration [10-12]. Another less commonly applied technique is based on measuring the intensity of Rayleigh light scattering of protein samples [13-14]. Proteins may consist of more than one

polypeptide backbone. In such a case the polypeptide subunits can be linked either covalently through disulfide bridges or non-covalently through hydrogen interactions and charge interactions. Interactions of protein subunits are often crucial for the formation of functional protein aggregates. For studying protein aggregates subunits can be covalently cross-linked using cross-linking reagents and further analyzed using mass spectrometry [15-18]. Determination of 3-dimensional structures of proteins is mainly based on nuclear magnetic resonance (NMR) spectroscopy, electron microscopy, atomic force microscopy (AFM), circular dichroism (CD) and x-ray crystallography. Analysis of post-translational modifications is not as straight forward as the analysis of other protein features and gravely depends on the individual type of modification [19-20]. Quantitative analysis of proteins is usually performed with gravimetric, colorimetric, spectroscopic or radioactive techniques [21].

I.2. Electrophoresis

I.2.1. Principles of gel electrophoresis

Electrophoresis is based on the migration of charged particles in an electric field in the liquid phase. Differences in the charge state and size of particles lead to differences in the electrophoretic mobility, so separations within an electric field are feasible. Since various particles have different electrophoretic mobilities, separations can be achieved. Today, electrophoresis is a commonly applied analytical and preparative separation technique with plenty of various applications in the fields of molecular biology, medicine and chemistry. Electrophoretic separations can be performed either in aqueous or organic media or with the aid of gels as stabilizing matrix. In aqueous or organic liquid media electrophoretic separation is mainly based on charge differences, whereas in the case of electrophoretic separations with gel matrices particles are separated according to their size and charge state. Systematically electrophoresis can be divided into the three sub-classes zone electrophoresis, isotachophoresis (ITP) and isoelectric focusing (IEF). While isotachophoresis uses a discontinous buffer system and is used mainly for concentrating particles between two buffer zones of different electrophoretic mobilities, isoelectric focusing uses a pH gradient for separating particles according to their pI value. Unlike the other two electrophoretic techniques zone electrophoresis uses a homogenous buffer system and a constant pH value. All three sub-classes of electrophoresis can also be realized in capillaries too. The migration velocity v of a particle in an electric field is directly proportional with the electric field strength E (equ. 1). The proportional factor between the two parameters v and E is called electrophoretic mobility u. As shown in equation II-1 higher electrophoretic mobilities are correlated with higher migration velocities. For small spherical particles the Stokes law can be applied for the calculation of the electrophoretial mobility u, which depends on the charge valence z, the Stokes radius r and the viscosity of the solution η (equ. 2). The value e stands for the elementary charge. For non-spherical particles like proteins or peptides the electrophoretic mobility u can be described with equation 3. Hence, given constant electric field strength the electrophoretic mobility u of non-spherical particles is determined by their molecular weight and their charge valence z. While a higher charge valence leads to a higher mobility and thus a fast migration velocity, higher molecular weights are correlated with a lower mobility.

$$v = u * E \qquad \text{(equation 1)}$$

$$u = \frac{z * e}{6\pi * \eta * r} \qquad \text{(equation 2)}$$

$$u \propto \frac{z * e}{(MW)^{2/3}} \qquad \text{(equation 3)}$$

The importance of high electric field strengths can be described by equations 4 and 5. The value *N* stands for the theoretical number of plates, *D* for the diffusion coefficient, *U* for the applied voltage and *L* for the separation distance. Since the achieved separation efficiency increases with the theoretical number of plates *N*, high *N* values are desired. As shown in equation 4 the theoretical number of plates *N* is directly proportional to the applied voltage *U*, so the most obvious way to increase separation efficiency is to increase the applied voltage. This approach, however, is limited by the generation of Joule heat due to high voltages. Equation 6 describes the generation of Joule heat. The value *W* stands for the generated Joule heat per volume, *c* for the concentration of the electrolyte in solution and *F* for the Faraday constant. Because the generated Joule heat is correlated with the square of the applied electric field strength a 10-fold increase of the voltage leads to a 100-fold increase of the generated Joule heat. A significant heat increase during electrophoresis results in a poorer separation efficiency due to convective mixing caused by an increased diffusion coefficient. Therefore efficient cooling systems are required when high electrical field strengths are applied.

$$N = \frac{u}{2 * D} * U \approx 20 * z \ * U \qquad \text{(equation 4)}$$

$$E = \frac{U}{L} \qquad \text{(equation 5)}$$

$$W = E^2 * u * z * F * c \qquad \text{(equation 6)}$$

I.2.2. History of gel electrophoresis

The first electrophoretic system was introduced by the Swedish scientist Tiselius in the 1930s [8]. In his work Tiselius focused on the electrophoretic separation of serum proteins. For his experiments Tiselius was awarded with the Nobel Prize in 1948. The first application of polyacrylamide gels for the gel electrophoretic separation of biopolymers was introduced in 1959 by Raymond and Weintraub. Two years later the application of agarose gels for separating large biopolymers like DNA fragments was described by Hjerten. In 1966 the

invention of carrier ampholytes capable of forming stable pH gradients was a major break-through for the isoelectric focusing technique [22]. O'Farrell and Klose introduced the technique of two-dimensional gel electrophoresis in 1975 and hence established a valuable tool for future proteomic applications [23]. In 1988 two-dimensional gel electrophoresis and isoelectric focusing was further improved by the invention of immobilized pH gradients which offered higher loading capacities, resolution and reproducibility [24]. Capillary zone electrophoresis was first introduced by Jorgenson in 1981 [25,26]. In his experiment Jorgenson separated derivatised amino acids and peptides with the aid of an open fused silica capillary with an inner diameter of 75 μm and a voltage of 30 kV. The applied detection technique was based on fluorescence. Capillary gel electrophoresis was first described in the 1980s [27].

I.2.3. Planar gel electrophoresis

I.2.3.1. Introduction to planar SDS-PAGE

Today, planar SDS-PAGE is the most common method for separating proteins electrophoretically. The popularity of this technique comes from its simplicity, efficiency, reproducibility and sensitivity. In 1969 the reliability of molecular weight determination of several proteins in the molecular weight range between 12 and 200 kDa was demonstrated by Weber and Osborn [28]. In 1970 Laemmli introduced a sample preparation procedure for planar SDS-PAGE which still commonly applied today [29]. Consequently, planar SDS-PAGE became a generally accepted technique for determining the molecular weights of proteins. For the analysis of proteins with SDS-PAGE the analytes are denatured with the aid of heat and sodium dodecyl sulphate (SDS), an ionic detergent. In turn SDS/protein complexes are formed which consist of a rather constant weight ratio of 1,4 g SDS to 1 g protein. Due to the high molar ratio of SDS the intrinsic charge of the protein becomes insignificant. Afterwards the SDS/protein complexes are separated electrophoretically with the aid of a sieving polymer, which is also called gel matrix. Since the SDS/protein complexes have identical charge densities and conformations migration through the gel matrix is only based on the size of the SDS/protein complexes. Molecular weight determination in SDS gel electrophoresis is performed by comparing the migration behaviour of individual SDS/protein complexes with the migration behaviour of known standards [9].

I.2.3.2. Sample preparation for SDS-PAGE

During the preparation of protein samples for planar SDS-PAGE, the samples have to be denatured. For this purpose the samples are mixed with SDS, a negatively charged detergent. The detergent not only denatures and unfolds the proteins, but also improves the solubility of the analyte molecules. In the next step the protein samples are heat denatured at temperatures between 80°C and 100°C. Since SDS is non-covalently attached to the proteins and increases their solubility, protein precipitation is hindered. Moreover, the overall negatively charged SDS/protein complexes are repelled from each other thus preventing protein aggregation. In solution the hydrodynamic shape of SDS/protein complexes is ellipsoid. For completely unfolding proteins the existing disulfide bridges have to be reduced. For this purpose a reducing agent is added to the sample solution. Common reducing agents applied for gel electrophoresis are dithiotreitol (DTT) and β-mercaptoethanol. After sample preparation the shape of the proteins is changed to rod-like particles whose migration through the gel is only a function of size and molecular weight. There are several other theories for explaining the structure of protein/SDS complexes, but the "necklace" model introduced by Shirahama in 1974 seems to be supported best by experimental data [30]. In this model SDS micelles are formed along the polypeptide backbone like pearls on a string. Therefore, the ratio of SDS to protein depends on the hydrophobic and hydrophilic regions of the polypeptide backbone as well as on the charges of the individual domains.

I.2.3.3. Cross-linked polyacrylamide gel matrices

For the analysis with planar SDS-PAGE cross-linked polyarcylamide gels are used. Polyacrylamide gels are chemically inert, stable and transparent. Cross-linked polyacrylamide gels are produced by the free radical polymerization of acrylamide monomers and a bifunctional cross-linker. Most commonly N,N'-methylenbisacrylamide (Bis) is applied as cross-linker. Other applied cross-linkers are ethylene diacrylate, N,N'-diallyltartardiamide, N,N'-(1,2-dihydroxyethlene)bisacrylamide and N,N',N''-triallyl citric triamide. Polymerization is achieved with an initiator like ammonium persulfate and a catalyst like N,N,N',N'-tetramethylenediamine (TEMED). For obtaining optimal gels acrylamide monomers with high purity are desired. Impurities like acrylic acid contents cause unwanted chain terminations during polymerization. After polymerization polyacrylamide gels consist of sieve-like structures with pores. SDS-PAGE gels can be either continous or discontinous

systems. In a continuous system the gel is made with a single buffer and a constant acrylamide concentration. In the contrary a discontinous system uses gels with two different gel layers. The top gel layer, also called stacking gel, is composed of a lower acrylamid concentration and its function is to focus and concentrate proteins before they enter the lower gel layer. After passing the stacking gel the proteins are separated in the second gel layer, also called resolving gel. Due to the focusing in the stacking gel higher resolutions can be obtained. The most important parameter which describes cross-linked polyacrylamide gels is the average pore size, which is determined by the total acrylamide concentration *T* and the amount of cross-linker *C*. Equations 6 and 7 show the formulas for the calculation of the *T* and *C* value of cross-linked polyacrylamide gels. Given a constant amount of cross-linker *C*, pore sizes decrease with an increasing total acrylamide concentration *T*. Large pore sizes are obtained with small and high amounts of cross-linker, but high amounts of cross-linker ($C > 5\%$) are rarely used because such gels are hydrophobic and rough. The smallest pore sizes can be produced with a *C* value of 5%. For protein separation typical pore sizes are between 3,5 and 5,5 nm. Generally cross-linked gels with larger pore sizes are applied for the analysis of high molecular weight analytes. Pore sizes of polyacrylamide gels can be determined experimentally with light scattering [31-34] or calculated using a three-dimensional Monte Carlo simulation [35].

$$T = \frac{Acrylamide\,[g] + Bis\,[g]}{100\,mL} * 100\ [\%] \qquad \text{(equation 7)}$$

$$C = \frac{Bis\ [g]}{Acrylamide\ [g] + Bis\ [g]} * 100\ [\%] \qquad \text{(equation 8)}$$

Next to polyacrylamide another type of gel matrix commonly applied for planar gel electrophoresis is agarose [36-37]. Typical pore sizes of agarose gels are between 150 and 500 nm and are hence much larger compared to polyacrylamide gels. Due to their large pore sizes agarose gels are mainly applied of the separation of large biopolymers like DNA or RNA fragments. Agarose is a polysaccharide isolated from red seaweed and can be dissolved in water at high temperatures. When cooling aqueous agarose solutions down to room temperature agarose gelantinises. The resulting gels are ready-to-use for gel electrophoresis. Another approach especially suitable for the analysis of large protein complexes is the use of agarose-acrylamide composite gels [38].

I.2.3.4. Gel electrophoretic separation

Molecular weight determination of proteins with denaturing gel electrophoretic methods is feasible due to the correlation of the electrophoretic mobility of the SDS/protein complex and the according molecular weight of the protein (Fig. 1) [39]. Depending on gel type, pore size and buffer system of the applied gel electrophoretic system the correlation curve has at least one linear region. For this linear region the slope of the correlation curve is lower than for the rest of the correlation curve and consequently the best separation efficiency can be obtained in this molecular weight and electrophoretic mobility range.

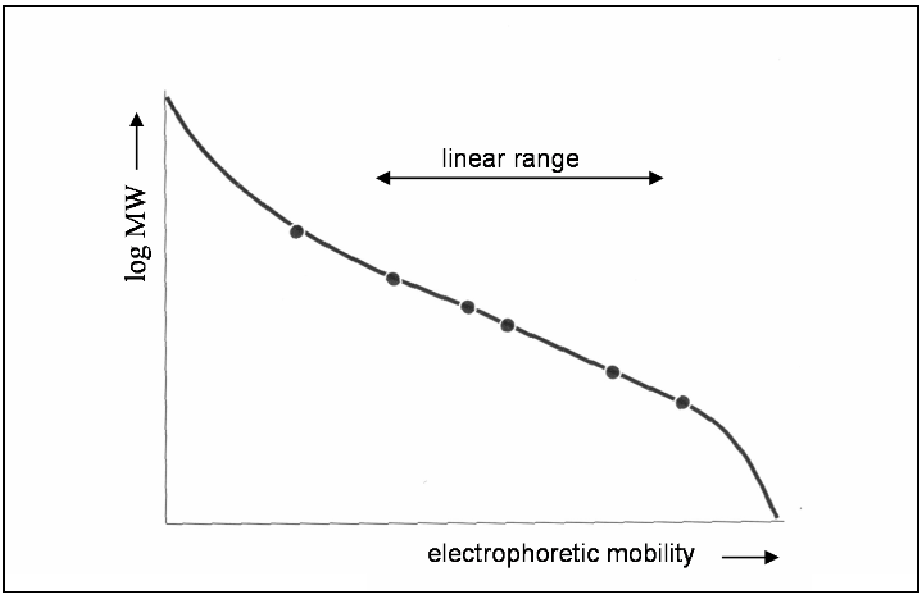

Fig. 1: Molecular weight determination of proteins with SDS gel electrophoresis. The logarithm of the molecular weight is plotted against the electrophoretic mobility.

Since the electrophoretic mobility of SDS/protein micelles also depends upon temperature, constant temperature conditions are required in order to generate reproducible results. Moreover, proteins with unusual amino acid compositions or certain post-translational modifications can show anomalously migration behaviours [40]. One of the most obvious post-translational modifications which affect the migration behaviour of proteins are disulfide bridges. With intact (non-reduced) disulfide bridges only incomplete denaturation and unfolding is achieved, so the original shape of the protein is partly maintained. Because the analyte shape plays an important role in gel electrophoretic separations, proteins which are analyzed under completely reducing conditions and can hence be completely unfolded usually show distinct migration behaviours. Further, proteins are reported to bind lower amounts of

SDS under non-reducing conditions due to the more compact protein structure under non-reducing conditions [41]. Extensively glycosylated proteins behave anomalously in SDS-PAGE as well. Since SDS only binds to the polypeptide backbone and not to glycan residues the mobility of glycoproteins is lower than expected, which results in a too high molecular weight estimated with gel electrophoresis. Furthermore, large carbohydrate structures interfere with the "necklace structure" of the SDS/protein complex and hence the glycoprotein is sterically larger than comparable non-glycosylated proteins resulting in a lower electrophoretic mobility [42]. Phosphorylations and covalently attached lipid residues are examples for other types of post-translational modifications which affect the migration behaviour of proteins in SDS-PAGE. Finally basic proteins with a high positive net charge like histones typically migrate slower than ordinary standard proteins. Hence, the molecular weight estimated with gel electrophoresis is higher than the actual molecular weight. Due to the large number of positive charges, the overall charge of the protein/SDS micelle is still affected by the intrinsic charge of the polypeptide backbone, even in the presence of large amounts of SDS. Generally for smaller proteins or peptides intrinsic charge and conformation have relatively more influence on the electrophoretic migration behaviour compared with larger proteins [43].

I.2.3.5. Protein visualization

In gel electrophoresis the most commonly used way of visualizing proteins is based on staining procedures which are performed after the electrophoretic separation is finished. For this purpose staining with Coomassie Brilliant Blue R or G-250 is a fast and simple method (Fig. 2). Both Coomassie dyes are triphenylmethane dyes with high extinction coefficients and high protein affinities [44]. Because Coomassie binds to the hydrophobic parts of amino acid residues the achieved staining efficiency depends on the number of hydrophobic amino acids present in the protein. For staining gels with Coomassie, SDS-PAGE gels are placed into a Coomassie solution first and into a destaining solution afterwards which removes excess Coomassie from the polyacrylamide gel background. Depending on the type of protein typical limits of detection observed with Coomassie staining are about 30 ng protein per band or spot. Next to Coomassie staining another widespread staining technique for gel electrophoresis is silver staining which is a method based on the high affinity of silver ions to proteins. [45]. Silver ions bind to the proteins and are form silver seed crystals in the presence of peptide bonds. Afterwards a reducing agent is added and all silver ions are slowly reduced

to elemental silver. Due to the presence of silver seed crystals the silver ions are reduced more rapidly and thus the protein spots are stained more intensely than the rest of the gel. Compared with Coomassie staining the silver staining procedure is more labour intensive but 10 times more sensitive [46].

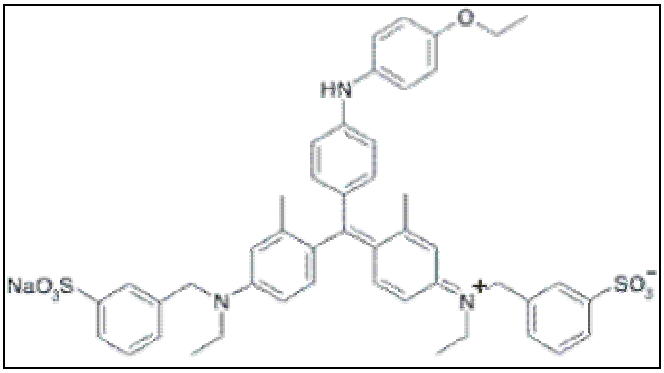

Fig. 2: Chemical structure of Coomassie Brilliant Blue G-250

Further sensitive methods, which allow the detection of proteins down to the fmol range are autoradiography (AR) and fluorography [47]. Since autoradiography makes use of radioactive isotopes this detection technique is not as widespread as staining with Coomassie or silver [48]. While fluorography is an extremely sensitive detection technique the required dyes and instrumentation is very expensive. An example for common and commercially available fluorescence dyes are SYPRO dyes [49]. Another approach of visualizing proteins is to transfer the proteins from the gel onto an inert membrane like polyvinyldifluorid (PVDF) or nitrocellulose and visualize the analytes afterwards. In such a case immunodetection based on chemilumiscence which is one of the most sensitive protein detection methods available is feasible. For immunodetection highly specific primary antibodies are applied which bind only to one particular protein. Prior to detection another less specific secondary antibody is applied which is conjugated with a functional group promoting chemiluminiscence and binds to the first antibody. After the addition of a proper substrate a light-emitting reaction used for detection takes place.

I.2.4. CGE-on-the-chip and the Lab-on-the-chip Bioanalyzer

I.2.4.1. Introduction to CGE

Capillary gel electrophoresis (CGE) is a subset of capillary zone electrophoresis. Basically sample preparation and separation principle of SDS-CGE are identical to gel electrophoresis with planar gels. CGE is not only suited for the analysis of proteins but also for the analysis of various other biomolecules like nucleic acids and carbohydrates [50]. While the latter technique applies a planar gel for sample separation, SDS-CGE makes use of a separation in capillaries. Without the presence of an electroosmatic flow (EOF) the number of theoretical plates *N* obtainable with CGE is given in equation 1 [51] and depends on the applied electric field strength *E*, the effective length of the separation capillary *L*, temperature *T* and the charge of the analyte *Q*. The Boltzmann constant is given as k.

$$N = \frac{E * L * Q}{2 * k * T} \quad \text{(equation 9)}$$

One major difference is the applied type of gel matrix. Instead of using cross-linked polyacrylamide, linear polymers which assemble to non covalent polymer networks are mostly applied in SDS-CGE. Detection in CGE is performed “on”-capillary and differs from detection in planar gel electrophoresis. Due to the small dimensions of the capillary and the low sample amounts applied for analysis and because of the fact that Coomassie and silver staining cannot be realized in CGE, fluorescence detection is the most common approach for protein visualization. Other detectors applied for CGE are the ultraviolet (UV) detector and diode array detector (DAD). Laser induced fluorescence detection is the most sensitive detection method available for CGE and achieves limits of detection similar to MALDI-TOF mass spectrometry [52]. Unlike in the case of planar SDS-PAGE where the sample is simply applied into a gel pocket located at the top of the gel, sample injection into the separation capillary is required for analysis with SDS-CGE. Sample injection into the separation capillary can be either performed with pressure (hydrodynamic injection) or with an electrical field (electrokinetic injection). In both cases the exact volume of sample solution injected into the separation capillary is unknown, but it is possible to estimate the injected volume with the aid of the injection parameters. For the electrokinetic injection field strengths lower than the field strength applied for sample separation is used in order to inject the sample into the separation capillary. Generally, hydrodynamic injections are more reproducible than electrokinectic injection. A benefit of electrokinetic injection is that no additional

instrumentation is required. Advantages of CGE over planar gel electrophoresis are the use of 10 to 100 times higher electrical fields which enable significantly faster analysis times [53]. Capillaries inside a thermostat are not affected by the deleterious effects of Joule heating like planar gels, because Joule heat is efficiently dissipated due to the large area to volume ratio of capillaries. Consequently, higher electrical fields can be applied which improve the obtainable separation efficiency and reduce analysis time. Another benefit of SDS-CGE is that fewer working steps are required because detection is performed on-line and data evaluation is usually automatic which results in a further reduction of analysis time [54]. The main disadvantage of CGE compared with planar gel electrophoresis is that CGE can not be easily combined with other analytical techniques. However, it was shown that DNA fragments separated with CGE can be further analyzed e.g. by inductively coupled plasma mass spectrometry (ICP-MS) [55]. From a technical point of view the instrumental set up of a conventional CGE device is rather simple. All compounds required are a capillary, a thermostat system, a power supply and a detector. The material of which the capillary is manufactured has to be chemically and electrically inert, flexible, robust and inexpensive. Fused silica capillaries match most of these requirements. In order to make the fused silica capillaries more robust and easier to handle, the outer surface of the capillary is usually coated with a polyimide layer. Teflon capillaries are an alterative to fused silica capillaries, but poor heat transfer properties and inhomogenous inner surfaces limit their usefulness. Most capillaries applied for CGE have an inner diameter between 25 and 75 μm and an outer diameter of 350 to 400 μm with typical lengths of about 50 to 150 cm. For achieving a good run-to-run reproducibility regular conditioning of the capillary with buffer solutions or bases is required. Another issue which is crucial for reproducibility in CGE is temperature constancy. Either liquid or air cooling can be applied. While liquid cooling is more efficient, air cooling is the simpler technique. For CGE a more efficient cooling system is required than for planar gel electrophoresis because CGE uses higher voltages and thus generates more Joule heat. A stable power supply is also a perquisite for obtaining reproducible results with CGE. Typical voltages applied for CGE are up to 30 kV with field strengths ranging from 100 to 500 V/cm^2.

1.2.4.2. Lab-on-the-chip technology

Next to planar SDS-PAGE and CGE the invention of microfluidics offered a novel and powerful tool for the analysis of biomolecules. Generally, the term microfluidics merely refers to microstructures carrying fluids which can be applied for the analysis of proteins, DNA, RNA, drugs or entire cells [56-62]. The term Lab-on-a-chip technology is even more irritating than microfluidics. At the moment no exact scientific definition of this term can be given. However, all commercially available Lab-on-the-chip devices are based on microfluidic systems and are capable of performing multiple functions [63]. Major benefits of Lab-on-the-chip instruments over conventional analysis systems are a higher degree of automatisation and lower volumes of sample solution required for analysis. Due to lower analysis times high-throughput analysis is possible. Lab-on-the-chip technology is not limited to CGE-on-the-chip. Other analytical techniques available as Lab-on-a-chip systems are primarily based on liquid chromatography, multiplex assays and immunoassays. More recently, capillary isoelectric focusing has also been adopted to the chip format [64]. Other non commercial microfluidic systems are described in literature. Examples are microfluidic chips for the analysis of amino acids [65] and lipoprotein particles [66] as well as on-chip based immunoassays for the analysis of tetanus antibodies and toxins [67]. Moreover, CGE-on-the-chip devices which work under native conditions are described in literature [68]. Drawbacks of the Lab-on-a-chip technology are comparable high prices for consumables and chips. Because several chip systems are one-way devices capillary conditioning, which is crucial for conventional CGE systems, is not necessary. The first commercially available lab-on-a-chip system was introduced in 1999 by Agilent Technologies and is based on CGE [69]. Despite commercial CGE-on-the-chip devices are available from more than one company in the following chapter the term CGE-on-the-chip is primarily associated with the 2100 Bioanalyzer from Agilent Technologies. Other commercial CGE-on-the-chip systems (e.g. from Biorad or Caliper) are principally similar to the described instrument.

I.2.4.3. Instrumentation for CGE-on-the-chip

The 2100 Bioanalyzer is a CGE Lab-on-a-chip instrument which uses microfluidic technology and integrates and automates sample handling, separation, staining, destaining, detection and data analysis. At the moment the application range extends to the automated analysis of DNA, RNA, cells and protein samples. For these four major types of analytes ten different ready-to-

use chip kits (assays) which differ in chip design, chemicals and run conditions are currently available. Two of the ten different chip kits are dedicated to the analysis of proteins. The provided chemicals of both protein assays include sample buffer, a ladder solution for external size calibration, gel matrix and a fluorescence dye concentrate. With the Protein 80 assay proteins with molecular weights between 5 and 80 kDa can be analyzed, while the analyzable molecular weight range of the Protein 230 assay is between 14 and 230 kDa. In both cases linear polymers are used as gel matrix. Sample separation is performed using disposable chips with micro-channels. The instrument contains 16 individual programmable high-voltage electrodes which are required for sample injection and separation. The chips are made of glass with photolithographically defined wet-etched channels and have a dimension of 17,5 to 17,5 mm. The channels have a depth of 13 μm and a width of 36 μm. Up to 10 different protein samples can be analyzed serially with one single chip. Detection is based on laser induced fluorescence (LIF) and the instrument is equipped with a 10 mW semiconductor laser which emits laser light with a wavelength of 630 nm. In order to maintain a constant temperature of 30°C during sample injection and separation the instrument is equipped with a thermostat and an air based cooling system.

I.2.4.4. Sample preparation for CGE-on-the-chip

The sample preparation procedure for CGE-on-the-chip is generally similar to the procedure for planar SDS-PAGE. The first step of sample preparation includes mixing of 2 volume parts protein sample with 1 volume part sample buffer. Unlike in the case of planar SDS-PAGE the sample buffer contains lithium dodecyl sulphate (LDS) instead of SDS as negatively charged detergent. LDS has better storage properties in solution compared with SDS but otherwise has identical chemical properties in denaturing gel electrophoresis. The concentration of LDS in the sample buffer is rather high because separations of complex mixtures like cell lysates require LDS levels significantly above the critical micelle concentration (CMC) to achieve sufficiently high separation efficiencies, presumably due to the need of maintaining a complete denaturation. After further heat denaturation the protein samples are diluted 15 times with water. 4 uL protein sample with 2 uL sample buffer were mixed and finally diluted with 84 uL water to give a final volume of 90 uL. For performing an analysis under reducing conditions either dithiotreitol or β-mercaptoethanol may be added to the sample solution together with the sample buffer. As in the case of planar SDS-PAGE the proteins' shape is changed to a rod-like particle after sample preparation. Before the protein samples are applied

on the chip the micro-channel network has to be filled with gel matrix. The applied gel matrix solution filled into the microfluidic system not only contains linear polymer but also SDS and fluorescence dye and is hence called gel-dye-mix. Air pressure is used to fill all capillaries with gel-dye-mix. Finally 6 uL of the final sample solutions are pipetted into the 10 sample wells located on the protein chip. One well is reserved for external molecular weight calibration and is filled with the ladder solution containing several recombinant standard proteins.

I.2.4.5. Linear gel matrices based on polyacrylamide

The first capillary gel electrophoretic systems applied cross-linked polyacrylamide as sieving matrix (Fig. 3). Since polymerization had to be performed inside the capillary bubble formation was a common problem due to gel shrinking during polymerization. Because of bubble formation reproducible high-quality separations were problematic. To circumvent such problems linear polyacrylamide gels were introduced in 1990s as replacements for cross-linked gels. First “in-column polymerization” was performed with linear gel matrices, which improved the situation by reducing bubble formation. However, the lifetime of such columns was limited and run-to-run reproducibility was poor. The next approach was the use of replaceable sieving gel matrices, which is still the most widespread approach for capillary gel electrophoresis today [70]. Because the gel matrix is replaced after each electrophoretic separation run-to-run reproducibility is improved. Moreover, the highest resolutions of capillary gel electrophoretic separations of proteins have been achieved with linear polyacrylamide and its derivatives as sieving gel matrices. Unlike in the case of planar gel electrophoresis where pores are static and pore sizes are constant, linear gel matrices possess dynamic pores and variable pore sizes. The sieving effect in a linear polymer solution is a function of the polymer network structure which is influenced by polymer-polymer and polymer-solvent interactions as well as the polymer concentration, the presence of additives and external parameters such as temperature [71]. Typical polymer concentrations applied for CGE vary from 0,1% to 6% (w/v). Based on the temperature dependence of the separation efficiency and the viscosity of polymers the use of thermo-responsive polymer solutions with “switchable” viscosities was also described in literature [72]. Generally, linear polymers are described by the chemical composition of its monomers and the average chain lengths of the polymer. Capillary coating is not required in the case of CGE-on-the-chip because the sieving matrix reduces the electroosmotic flow (EOF) sufficiently. Without the use of a sieving gel

matrix the observed EOF mobility of the CGE-on-the-chip technique would be about 60 times higher. The reduction of the EOF can be contributed to a combination of viscosity increase at the surface interface and adsorption of the polymer to the capillary wall [73]. Consequently only the electrophoretic movement of the ions and no significant flow of solution is observed during the electrophoretic separation. Moreover, it has been shown that the electrophoretic separation of proteins in untreated fused silica capillaries has not been very successful due to the interaction of proteins with silanol groups on the inner capillary wall [74]. This problem can be further circumvented by physically coating the capillary wall with chemical compounds like polyacrylamide, polyacrylamide derivates, polyethyleneimine, cellulose-acetete or polyvinyl alcohol [75-79]. Temperature constancy is not only important because of the temperature dependence of SDS-protein micelles but also because of the temperature dependence of the viscosity of the linear gel matrix. Viscosity of the sieving gel matrix is crucial for the obtainable reproducibility and separation efficiency with CGE. Therefore the use of thermostats is absolutely necessary. Next to linear polyacrylamide and its derivatives some other linear polymers are also more or less frequently used as sieving gel matrices in CGE. Such linear polymers include poly(ethylene oxide), poly(vinyl acetate), poly(vinylpyrrolidone) and some polymers based on cellulose derivatives (Fig. 4) [80-84]. Furthermore branched polymers like dextran are applied as sieving gel matrix in CGE too.

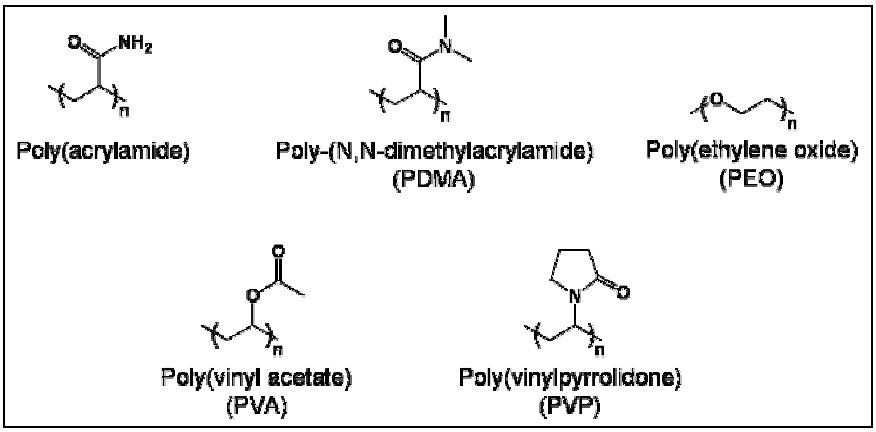

Fig. 3: Chemical structures of the monomers of various linear polymers applied as sievering gel matrices for CGE

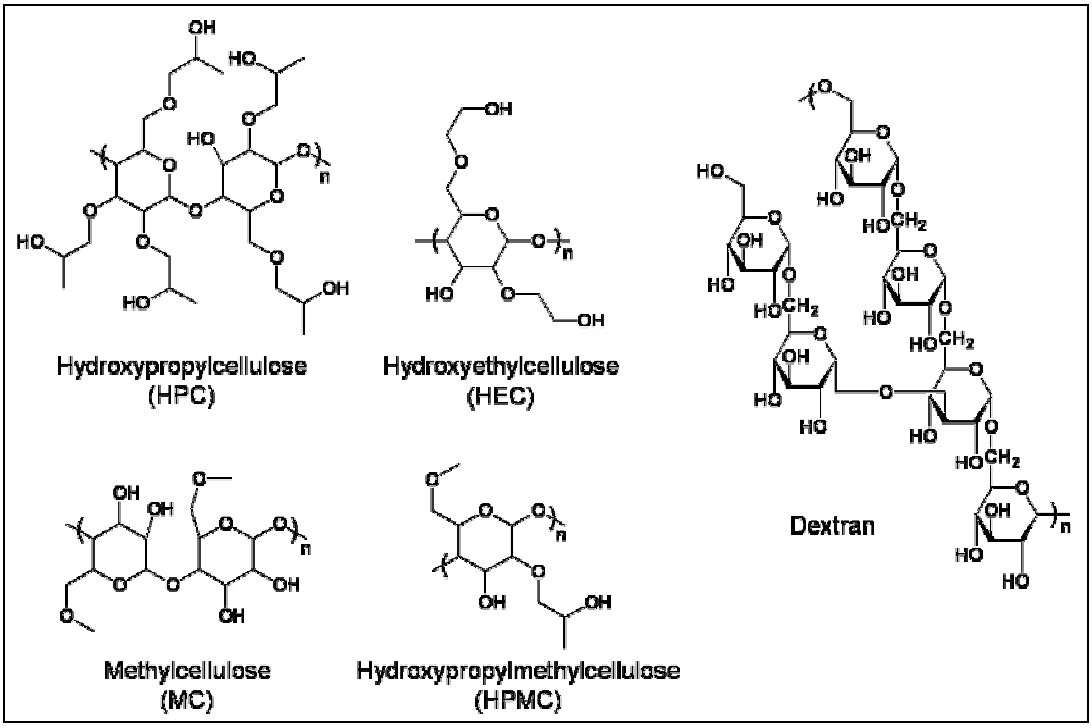

Fig. 4: Chemical structures of the monomers of various linear polymers based on carbohydrates which are applied as sieving gel matrices for CGE

I.2.4.6. Sample injection and separation

The analysis of proteins with CGE-on-the-chip is performed with the aid of microfabricated silica chips which consist of a network of connected micro-channels (Fig. 5). Each chip contains 16 wells in a 4 by 4 array. 10 wells are available for protein samples, one well is assigned for the external molecular weight calibration (sizing calibration) and the remaining five wells are needed for assay. Of these five wells one well is filled with destaining solution and the remaining four wells are filled with gel-dye-mix. As already mentioned earlier the CGE-on-the-chip device is equipped with 16 individual programmable high-voltage electrodes which are applied for the electrokinetic injection and separation of protein samples. After chip introduction the thermostat is activated and the laser is focused on a particular point of the separation capillary. Prior to the electrophoretic separation within the separation capillary located in the middle of the protein chip the samples have to be injected into the micro-channel network. The sample flow is directed orthogonal over the start of the separation capillary and a small sample plug is injected into the separation capillary by applying an electric current along the separation capillary. Based on the dimensions of the capillary the estimated volume of the sample plug which is transferred into the separation capillary is only about 25 pL. While the total length of the separation capillary is 1,7 cm, the

effective separation length is 1,25 cm. In the case of capillary electrophoresis (CE) without a gel matrix the obtainable separation efficiency under ideal conditions (no EOF, infinitely short injection plug, diffusion is the only source of analyte dispersion) is independent of the length of the separation capillary so longer capillaries provide no advantages for separations with CE (equation 4) [85]. On the other hand in CGE the number of theoretical plates depends on the length of the separation capillary. For CGE the shortest separation capillary applied for the separation of proteins reported in literature has a length of 3 mm [86]. This system allows the electrophoretic separation of one single protein sample within 8 seconds. The separation efficiency obtained with CGE-on-the-chip is 1-2 magnitudes better than in the case of SDS-CGE. Superior separation efficiencies in CGE-on-the-chip can be achieved by using a very small sample plug injected into the separation capillary in comparison to the dimension of the channel width. Moreover the use of a sufficiently high SDS concentration during the electrophoretic separation and the application of a non covalently binding fluorescence dye for detection which circumvents non quantitative covalent labelling and thus peak broading are important factors for the achieving high separation efficiencies of about 10^6 plates/m [87].

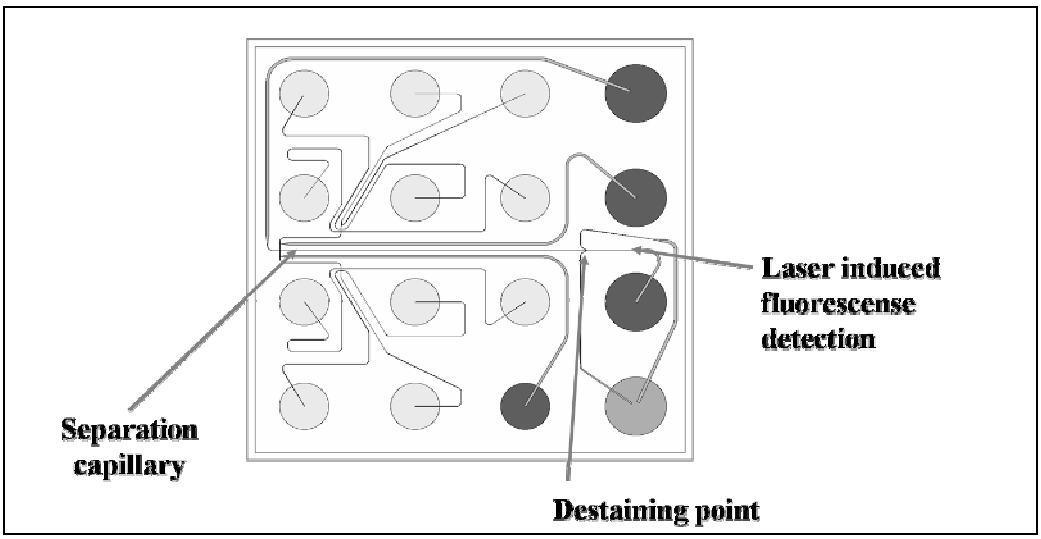

Fig. 5: Illustration of a silica chip commonly used for the analysis of proteins with CGE-on-the-chip. The chip consists of 16 wells which are all linked through micro-channels. The separation capillary is located in the middle of the chip. Five wells at the right side of the chip are filled with gel matrix (marked in dark-grey and grey) and eleven wells at the left side of the chip are filled with samples and ladder (marked in pale-grey). The picture was provided by Agilent Technologies.

Since all protein samples contain two internal standards, which are part of the sample buffer and are thus added during sample preparation, all CGE-on-the-chip protein assays make use of two internal reference peaks. These reference peaks are applied for automated sizing and normalization of peak areas. Therefore, fluctuations in the electric field can be corrected and the run-to-run reproducibility can be greatly enhanced. The molecular weight range analyzable with a particular protein assay is determined by the internal reference peaks and the external ladder applied for calibration. These internal reference peaks are referred to as lower and upper marker. Sample peaks which have a migration time higher than the upper marker and smaller than the lower marker are still detected but are not integrated.

I.2.4.7. Laser induced fluorescence detection

The detection technique applied for CGE-on-the-chip is based on laser-induced fluorescence (LIF) and uses a fluorescence dye which non covalently attaches to SDS/protein complexes. This technique is also referred to as dynamic labelling [88]. Since the sample volumes injected into the micro-channels are very small, an extremely sensitive detection technique like LIF is necessary [89]. In order to obtain a universal and quantitative labelling on-chip dye staining is applied. Because the gel matrix contains fluorescence dye molecules the SDS/protein complex is already labelled as soon as separation begins. While the exact type of applied fluorescence dye is proprietary it is known to have a molecular weight of about 500 Da and to be positively charged and hydrophobic, so the dye attaches not only to SDS-protein micelles but also to SDS micelles without protein content. The applied type of fluorescence dye has an exitation maximum at about 650 nm and an emission maximum at about 680 nm. It is reported that the fluorescence dyes binds to the SDS coating of the protein rather than to any specific amino acid residue of the protein [90]. Due to the high SDS concentration in the gel matrix most micelles present in the separation capillary are LDS/SDS micelles without protein content which would greatly increase the amount of background signals and hence reduce the obtainable signal to noise ratio. For this reason a destaining step which removes the majority of SDS micelles not containing proteins and thus significantly increases the signal to noise ratio is applied after sample separation and prior to detection (Fig. 6).

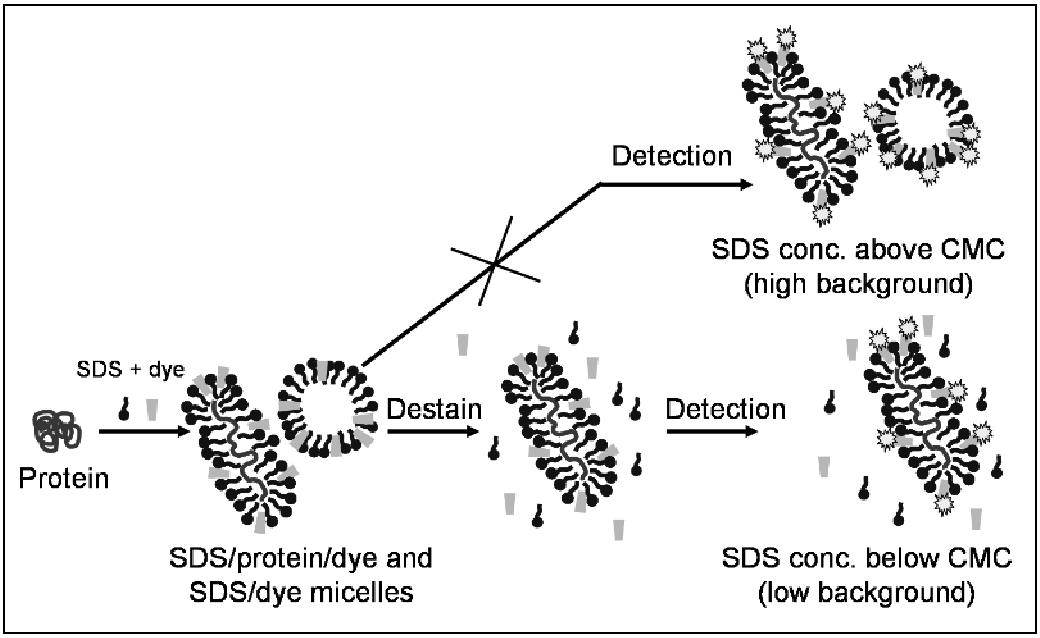

Fig. 6: Schematic illustration of the destaining and detection process used for CGE-on-the-chip. Without destaining the background noise level would be significant higher due to a large amount of SDS/dye micelles reaching the detector. After the destaining step most SDS/dye micelles not containing proteins are eliminated and the background noise level is reduced. The picture was provided by Agilent Technologies.

Technically the destaining technique is realized by an post-column channel intersection at the end of the separation channel which is not only used to dilute the SDS concentration below the critical micelle concentration (CMC) before the detection point but also to increase the signal amplitude by one order of magnitude by increasing the number of fluorescence dye molecules bound to the individual SDS/protein micelles. Two channels on each side of the separation capillary contain destaining solution which only consists of gel matrix and buffer, but neither fluorescence dye nor SDS [91]. The CMC of SDS in the presence of sieving gel matrix und the ion strength of the buffer solution was found out to be 1,7 mM [87]. After the destaining procedure SDS micelles without protein content are broken up and the SDS concentration after destaining is about 2 times below the CMC. Both on-chip staining and destaining steps occur in the time scale of some 100 ms. The destaining process, which is basically a SDS dilution step, can be compared to the destaining process applied for conventional planar SDS-PAGE gels because in both cases the background intensity is reduced. However, the major difference between both destaining techniques is that in the case of CGE-on-the-chip unbound dye molecules are not removed but SDS dilution breaks up SDS micelles and thereby the released dye molecules bind to SDS-protein micelles. In turn more released fluorescence dye molecules binding to the existing SDS-protein micelles which

results in an increase of the signal amplitude. As already mentioned earlier before, the destaining step has to be performed shortly before detection, because a SDS concentration above the CMC is required during the electrophoretic separation in order to maintain a complete denaturation of the protein sample. The sensitivity observed with CGE-on-the-chip is dependant of the ion strength of the protein sample solution. At low salt concentrations the microchip assay was about 5 times more sensitive than standard Coomassie stained SDS-PAGE gels, while at physiological salt concentrations CGE-on-the-chip is only about twice as sensitive as planar gels stained with Coomassie. Linearity of the CGE-on-the-chip protein assays is limited by an insufficient amount of fluorescence dye. Hence in the case of high protein concentrations there is not enough dye available in order to bind quantitatively to the SDS/protein micelles. Nevertheless, the linearity of CGE-on-the-chip is given in a protein concentration range between 10 and 2000 ng/uL which is similar to other protein quantification techniques like planar gel electrophoresis using Coomassie staining or Bradford quantitation assays.

I.2.5. Differences between planar gel electrophoresis and CGE-on-the-chip

As already mentioned earlier planar SDS-PAGE is still the most widespread approach for the electrophoretic separation of proteins. However, planar SDS-PAGE is time-consuming and labour-intensive. All major steps like sample loading, staining and destaining are manual steps which are difficult to automate. CGE-on-the-chip offers high analysis speed, quantitative “on-chip” detection and full automation and can therefore potentially overcome some problems of planar SDS-PAGE. Furthermore, the amount of chemicals applied for analysis is minimized supporting green chemistry. Depending on the analytical question the rather fixed instrumental settings chemistry may be disadvantageous for CGE-on-the-chip. On the other hand the establishment and validation of documented procedures is facilitated. The major drawback of CGE-on-the-chip is that the technique can not be easily combined with other analytical techniques. Therefore, CGE-on-the-chip can be considered as an analytical screening technique. An advantage of planar SDS-PAGE it that after the gel electrophoretic separation the biopolymer samples can be further analyzed by eluting proteins out of the gel. The elution can be performed either with or without the application of an electrical field [92-93].

I.3. MALDI-TOF mass spectrometry

I.3.1. Development and concept of MALDI mass spectrometry of biopolymers

Mass spectrometry is an analytical technique used for the determination of exact molecular weights of compounds as ions in a high vacuum. All mass spectrometers consist of an ion source, a mass analyzer and a detector. The ion source is required for the generation of gaseous intact analyte ions, which are then separated by the mass analyzer. Finally, the ions are detected and quantified with the aid of a detector. Plenty of different ion sources based on different principles are commercially available, but for the analysis of proteins and other biopolymers matrix assisted laser desorption/ionization (MALDI) and electrospray ionization (ESI) are most widespread [94,95]. For the analysis of intact high molecular weight proteins MALDI-MS is better suited than ESI-MS because in most cases MALDI mass spectrometers are coupled with time-of-flight mass analyzers, whereas ESI mass spectrometers are most commonly equipped with quadrupols and ion-traps as mass analyzers. Even before the introduction of the MALDI technique, lasers were used for desorbing and ionizing small organic molecules. For the laser desorpiton/ionization (LDI) technique the sample was dispersed over a metal surface and irradiated by a laser beam. Because the analyte molecules absorbed a considerable amount of the applied laser power strong fragmentations were observed and only a small amount of the analyte molecules was detected as intact molecular ions. Sensitivity was limited and accessible molecular weight was below 2 kDa. Due to these limitations LDI mass spectrometry had only minimal relevance for the analysis of biopolymers.

In 1988 MALDI mass spectrometry was invented by Hillenkamp, Karas and Tanaka. Because of the impact of MALDI mass spectrometry on the analysis of biomolecules Tanaka was rewarded for his work with the Nobel Prize in 2002 [96]. In the case of MALDI the analyte molecules were distributed in a solid or liquid matrix, which absorbed ultraviolet (UV) light generated by a laser [97,98]. Since most of the laser power was absorbed by the matrix and not by the analyte molecules direct photodissociation was circumvented and fragmentation was minimal [99]. Today MALDI-TOF-MS is a well established analytical method for the molecular weight determination of biopolymers. The linear TOF mass analyzer offers a large analyzable molecular weight range, high sensitivity and high mass accuracy, which cannot be obtained with other biochemical or electrophoretical methods. Today MALDI-TOF-MS is not

only used for the analysis of proteins and peptides [100-103], but also for the analysis of oligosaccharides [104-105], synthetic polymers [106-107] and nucleic acids.

I.3.2. MALDI sample preparation

Obviously, the most important parameter concerning sample preparation for MALDI mass spectrometry is the matrix itself. The MALDI matrix serves several purposes [108]. First, the matrix absorbs and transfers laser power to the crystal lattice supports the ionization of the analyte molecules. Typically a 10^3 to 10^4 times molar excess of matrix molecules compared to analyte molecules is applied. Second, the matrix isolates the analyte molecules and thus prevents clustering. There are some universal criteria which should be fulfilled by a MALDI matrix. High absorption at the applied laser wave length, low molecular weight, chemical inertness and miscibility with the sample solution are required characteristics for MALDI matrices. Figure 7 shows the chemical structures of some commonly applied solid matrices for UV-MALDI mass spectrometry.

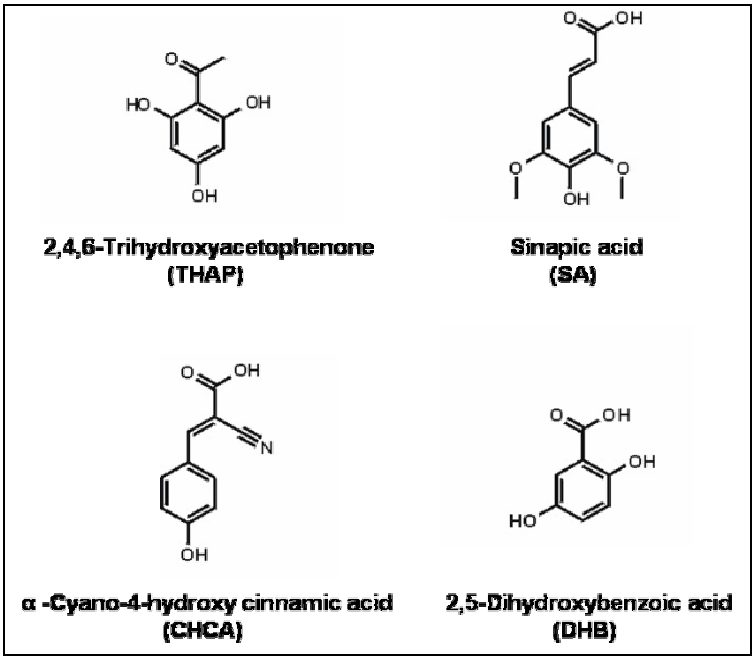

Fig. 7: Chemical structures of some MALDI matrices commonly used for the analysis of proteins and peptides

Generally, most solid MALDI matrices are cinnamic acid or benzoic acid derivatives. While 3,5-dimethoxy-4-hydroxy cinnamic acid (sinapinic acid) is mainly used for the analysis of proteins and peptides, 2,4,6-trihydroxyacetophenone is used for the analysis of glycoproteins and synthetic polymers [4]. α-Cyano-4-hydroxy cinnamic acid and 2,5-dihydroxy benzoic acid are both common matrices for the analysis of peptides [109]. Other commonly applied UV-MALDI matrices for the analysis of proteins and peptides are 3-methoxy-4-hydroxy

cinnamic acid (ferulic acid), 3,4-dihydroxy cinnamic acid (caffeic acid), 2,6-dihydroxyacetophenone and 2-(4-hydroxyphenylazo)benzoic acid [110-113]. For the analysis of synthetic polymers typical MALDI matrices are 2,5-dihydroxybenzoic acid, 2-(4-hydroxyphenylazo)benzoic acid, trans-3-indolacrylic acid and 1,8,9-anthracenetriol [114-115]. It is also reported that mixtures of different types of matrices enhance the achievable performance of MALDI-MS experiments [116].

There are several different commonly applied sample preparation techniques for MALDI mass spectrometry. In the case of all solid MALDI matrices co-crystallisation of matrix and analyte molecules has to be achieved. The simplest way of combining matrix and analyte is the direct mixing of both solutions in a tube. Afterwards a small aliquot of this mixture is pipetted on the MALDI target. This technique is called volume technique. Another sample preparation technique similar to the volume technique is the dried-droplet technique. For this technique aliquots of the matrix and analyte solutions are pipetted on the MALDI target. Both solutions are then mixed directly on the MALDI target. For both techniques the matrix can be dissolved in a variety of different solvents as long as both, matrix and sample solutions are mixable in order to obtain co-crystallization. A third sample preparation technique is called thin-layer or fast evaporation technique. First, a surface consisting of a homogenous, microcrystalline matrix layer is produced by applying a concentrated matrix solution on the MALDI target [117]. For this purpose the matrix is dissolved in a highly volatile solvent like acetone. Then the sample solution is pipetted onto the matrix layer and in turn analyte molecules are incorporated in the uppermost layer of the matrix surface. The proper sample preparation technique is crucial for a successful analysis with MALDI mass spectrometry. Despite of the availability of several good standard sample preparation techniques trial-and-error experiments are often necessary to obtain optimal analysis results. Next to the type of applied matrix substance and sample preparation technique another important factor for a successful analysis with MALDI mass spectrometry is the purity of the sample. Salts and detergents are frequently used in protein chemistry in order to stabilize protein samples. Further salts are often required as cofactors for enzymes and salts are also often applied for protein purification procedures like ion exchange chromatography. Salts and detergents disturb the crystallisation process of MALDI matrices and hamper the desorption and ionization process, which leads to a poorer MALDI mass spectrometric performance. While some non-ionic detergents like n-octyl glucoside are reported to be compatible with MALDI mass spectrometric experiments without causing severe interference, a lot of other detergents like sodium dodecylsulfate (SDS), Triton X-100 and 3-[(3-

cholamidopropyl)dimethylammonio]-1-propanesulfonate (CHAPS) are known to interfere with MALDI-MS analysis by reducing signals of analyte ions and degrading mass resolution [109,113,118,119]. However, non-ionic surfactants usually have only mild solubilizing properties. Interestingly, ammonium dodecylsulfate hampers the MALDI process less than SDS does [120]. This is explained by the fact that ammonium suppresses sodium adduct ion formation in MALDI-MS. The covalent attachment of cleavable detergents to proteins for increasing the solubility of very hydrophobic proteins is also reported in literature [121-122]. A benefit of this technique is that the detergent properties, which interfere with MALDI-MS, can be eliminated prior to analysis. In order to improve the performance of MALDI mass spectrometric experiments it is often necessary to purify protein samples by removing salts and detergents. However, sample purification is a critical issue because every purification steps is inevitably coupled with a loss of analyte [123]. Since MALDI-TOF mass spectrometry is a sensitive analytical technique and somehow tolerant against small amounts of impurities the simplest way of reducing the amount of detergents and salts in a sample is to dilute the sample solution. In some cases sample dilution is sufficient in order to obtain suitable results. The more advanced and old-fashioned way of purifying protein samples is the use of high-performance liquid chromatography (HPLC).

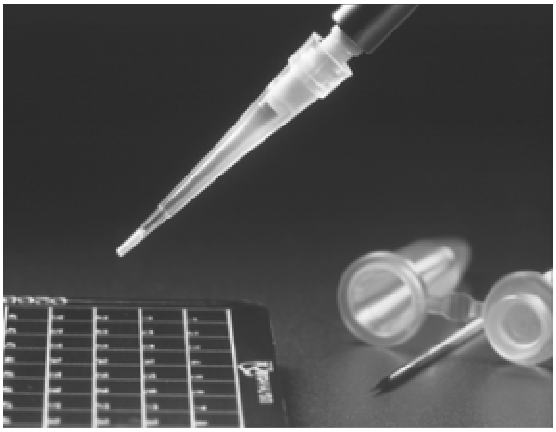

Fig. 8: Photograph of a ZipTip pipette tip from Millipore. At the end of the pipette tip the miniaturized chromatographic bed is visible. The photograph was provided by Millipore.

Today, the most convenient way of desalting a smaller number of protein samples is the use of pipette tip based chromatographic columns. Such miniaturized chromatographic columns fixed on the end of a pipette tip are available from various providers and are primary applied as tools for desalting and concentrating protein and peptide samples for the subsequent analysis with MALDI mass spectrometry. The first commercially available pipette tips with chromatographic columns were provided by Millipore and are named ZipTips (Fig. 8). ZipTips are 10 µL polypropylene pipette tips containing a bed of spherical silica particles fixed within a polymer matrix located at the end of the pipette tip. These silica particles have

typical diameters of 15 µm and are modified with various surface residues. Reversed phase (RP) residues and hydrophilic interaction residues, which are subsets of normal phase (NP) residues, are most commonly applied. RP residues are available with C-4 and C-18 alkyl surface groups. While reversed phase micro-columns are mainly used for the removal of salts, hydrophilic interaction micro-columns are used for the removal of detergents. The chromatographic bed has a bed volume of only 0,6 µL and maximum sample binding capacities of about 1 to 2 µg. Working procedures for ZipTips are fast and easy to use. First the micro-column is conditioned then the protein solution is aspired over the chromatographic bed. In turn proteins are adsorbed to the surface residues of the silica particles. Afterwards the sample is washed and finally eluted with a gradient of organic solvent. Since ZipTips are operated with a bi-directional flow automatisation is feasible. In the case of reversed phase columns proteins and peptides bind to the chromatographic material in the absence of solutions with a high percentage of organic solvent. Maximum binding to the chromatographic is obtained when an ion-pairing agent is present and when the solution has a pH value of 4 or lower. The sample is eluted with the aid of a solution containing a higher percentage of organic solvent. On the contrary proteins bind to hydrophilic interaction columns in the presence of a solution containing a high percentage of organic solvent. In this case the sample is eluted by using solutions with a lower percentage of organic solvent. Other techniques used for the desalting of protein samples are size exclusion chromatography (SEC), ultrafiltration and dialysis. Because the latter two techniques use membranes with a comparably large surface unspecific adsorption of proteins on the membrane is a common phenomenon. Size exclusion chromatography is mainly based on cross-linked dextrans or agarose as separation medium. Since size exclusion chromatography requires a minimum length of the column for the separation of large molecules, like proteins, from low molecular weight impurities a more or less significant loss of sample is observed due to unspecific adsorption. Especially for low concentrations of protein sample unspecific adsorption effects are critical. Due to the small dimensions of the chromatographic bed of pipette tip based chromatographic columns sample loss can be minimized in the case of ZipTips.

I.3.3. The MALDI process

Next to the matrix and sample preparation technique lasers are crucial for the desorption and ionization process in MALDI-MS [124]. Typical laser beams used for MALDI mass spectrometry have spot diameters of 30 to 150 μm and power intensities between 10^6 and 10^7 W/cm^2. While lower laser power intensities simply provide no analyte signals at all, higher intensities ablate a shallow surface layer from the matrix crystals which results in fragmentation of analyte molecules. Consequently there is one optimal laser power intensity for each sample which depends not only on the matrix substance and sample preparation but also on the amount and type of analyte as well as the amount and type of impurities within the sample. The duration of each laser pulse depends on the type of laser applied and can usually not be varied by the operator. There are two types of lasers available for MALDI-MS: ultraviolet (UV)-lasers and infrared (IR)-lasers. One of the most common lasers applied for MALDI mass spectrometry are nitrogen lasers with an emission wavelength of 337 nm and a pulse length of 3 to 20 ns. Another UV-laser used for MALDI-MS is the Neodym-YAG-laser with laser pulse durations of 0,5 to 20 ns and an emission wavelength of 355 nm. There are some differences in the MALDI-MS performance between UV-lasers and IR-lasers. IR-MALDI is a softer desorption and ionization technique than UV-MALDI, so labile and very large analytes provide better result with IR-MALDI-MS than with UV-MALDI-MS. Further IR-lasers have longer pulse durations (5 to 200 ns) and since IR radiation has a greater material penetration depth than UV radiation a larger desorption depth is achieved. IR-MALDI-MS is thus often used for the analysis of proteins blotted on a poly(vinyl difluorid) (PVDF) membrane after gel electrophoresis. A significant drawback of IR-lasers is their cost, which is several times higher compared to UV-lasers. After excitation of a sample spot with the laser beam matrix and analyte molecules are evaporated and matrix molecules are photoexicitated in the vapour phase through the laser beam. Finally it is assumed that a charge transfer caused by photochemical reactions occurs in the gas phase between the ionized matrix molecules and the analyte molecules (Fig. 9) [125].

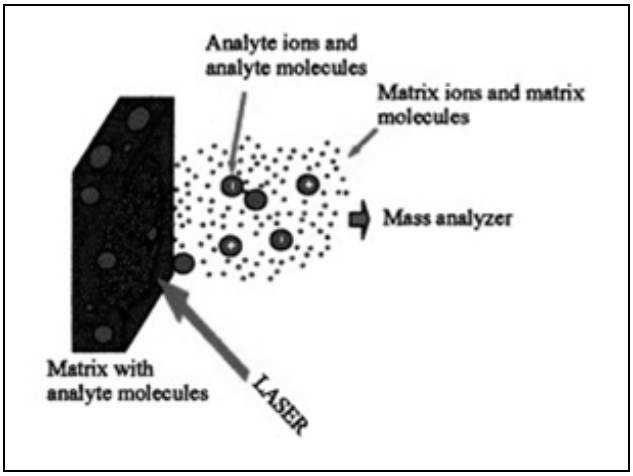

Fig. 9: Schematic illustration of the matrix assisted laser desorption and ionization process

With the aid of the photoionized and radical matrix molecules a high yield of electrically charged analyte molecules is obtained. Regardless of the type of applied laser, there are four basic types of different ionisation mechanisms in MALDI-MS [126-127]:

1. Desorption of pre-formed ions
2. Generation of radical ions by electron loss
3. Addition or removal of protons
4. Addition of cations or anions

Addition of alkali cations or protons and removal of protons are most commonly observed ionization mechanisms in MALDI mass spectrometry. Whether alkali ions or protons are added to the analyte molecule is determined by the chemical composition of the substance, the type of applied matrix and the amount of alkali and protons present in the prepared MALDI-MS target spot.

I.3.4. TOF analyzer and detector

After the analyte molecules have been desorbed and ionized, the molecular ions are accelerated and separated by a mass analyzer. While several different types of mass analyzers are applied for MALDI mass spectrometry the time-of-flight (TOF) mass analyzer is by far most widespread. Other mass analyzer which are applied for MALDI-MS experiments are Fourier transform ion cyclotron resonance (FT-ICR), quadrupol-TOF (Q-TOF) and quadrupol ion trap – TOF (QIT-TOF) mass analyzers. Basically TOF systems are rather simply consisting only of a metallic drift tube which has high voltage accelerating grids or lenses, laser and sample slide on one end and a detector on the other end. Inside the drift tube a high vacuum of 10^{-6} to 10^{-7} torr is applied. Except for the electric field between sample slide and

high voltage acceleration grids no electric fields are applied inside the drift tube, so the actual separation of the molecular ions takes place in the field free drift region. The principle of TOF mass analyzers is based on the fact that the time which particular molecular ions require for reaching the detector at the end of the TOF flight tube is directly correlated with their mass to charge (m/z) ratio (Fig. 10).

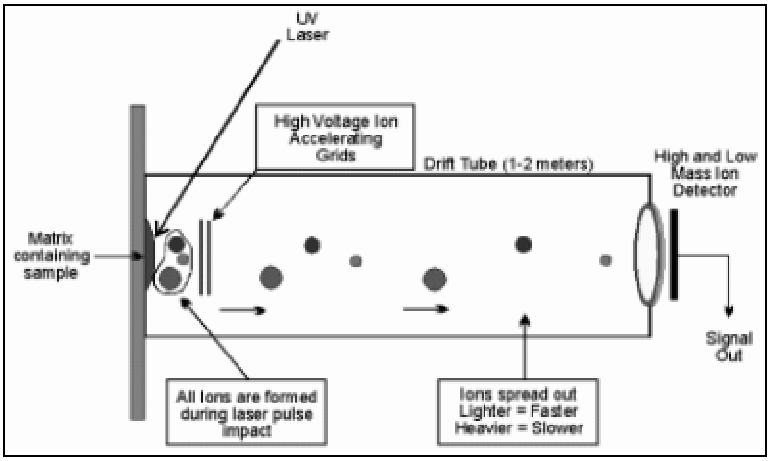

Fig. 10: Schematic illustration of a MALDI linear time-of-flight mass spectrometer. The picture was provided by mpc.

The correlation between the mass to charge ratio of a molecular ion and the time this ion requires to reach to detector at the end of the drift tube can be described mathematically through equations 7 to 8. The kinetic energy of an accelerated ion E_{kin} depends on the mass of the ion m and its velocity v. Alternatively the kinetic energy of an accelerated ion can also be described as a function of the applied potential difference U and the number of elementary charges of the ion z (equ. 7).

$$E_{kin} = U * z * e_0 = \frac{m * v^2}{2} \qquad \text{(equation 7)}$$

The elementary electric charge is termed as e_0. Further the velocity of an ion v can be calculated by dividing the length of the field free drift tube s by the time the ion requires to pass the field free drift tube and reach the detector t (equ. 8).

$$v = \frac{s}{t} \qquad \text{(equation 8)}$$

Combining equations 7 and 8 provides equation 9, which describes the obtained mass to charge ratio as a function of the applied potential difference, the time the ions require to reach the detector and the length of the field free drift tube.

$$\frac{m}{z} = \frac{2 * U * t^2}{s^2} \qquad \text{(equation 9)}$$

Because the field free drift region is determined by the instrument and the applied potential difference is kept constant, the mass to charge ratio of a particular molecular ion is only correlated with the square of its flight time. The conversion of the flight time into a usable mass to charge ratio is performed by an empirically determined calibration function. Since ion formation in MALDI occurs in the dimension of several ns after the laser was fired, the start of the TOF analysis can be timed precisely. Analysis of the desorbed and ionized molecules begins by applying an electrostatic field of several 100 to several 1000 V/mm. This process is also called ion extraction and is achieved by applying a high potential difference of 3 to 40 kV between the sample slide and a grid/lens system mounted 3 to 15 mm away from the sample slide [128]. The polarity of the electric field can be switched so either positive or negative molecular ions are analyzed. After applying the electric field the molecular ions generated through the MALDI process are instantly accelerated into the TOF mass analyzer. Initial velocities of the accelerated ions are independent of the laser wavelength and are in the dimension of 180 to 660 m/s [129]. An advantage of TOF mass analyzers is their theoretically unlimited analyzable mass to charge ratio [130]. However, there are several factors which limit the analyzable mass to charge ratio. The first limitation is the MALDI process itself. Generally desorption of larger molecules is more difficult than desorption of smaller molecules. Consequently higher laser powers must be applied which in turn facilitate the fragmentation of high molecular weight analytes. Second the molecular ions generated by the MALDI process have to be stable long enough to reach the detector. Since the time an ion needs to reach the detector increases to the second compared with the mass to charge ratio which increases only linear. It is obvious that larger molecular ions have significantly longer flight times in the drift tube and hence more time for fragmentation. The third limitation is the detector itself. Most commercial detectors used in MALDI-TOF mass spectrometers have a very poor sensitivity and poor detection efficiencies in the very high mass to charge range. All in all, the practical mass to charge range analyzable with MALDI-TOF-MS is limited with about 10^6. Another advantage of MALDI-TOF-MS is that nearly all generated ions are accelerated and reach the detector. Unlike quadrupols or ion traps which are scanning detection techniques the TOF method is an ion counting method and mass spectra acquisition is much faster compared to other mass analyzers. Because the length of most drift tubes is between 0,1 and 3 m TOF mass analyzers are rather bulky compared with other mass analyzers. What is important to remember when comparing the detection efficiency between gel electrophoresis and MALDI-TOF-MS is that the latter detection technique is based on the number of molecular ions which reach the detector, while the first detection technique is mass

sensitive. Correlation between mass and the number of molecules is given in equation 10. The molecular weight of a substance is termed *M*, its mass *m* and the corresponding number of molecules *n*.

$$n = \frac{m}{M} \qquad \text{(equation 10)}$$

The issue becomes obvious when comparing analytes with molecular weights of 10 kDa and 1000 kDa. 1 ug of the 10 kDa analyte contains 100 pmol molecules, while 1 ug of the 1000 kDa analyte contains only 1 pmol molecules. Next to the problems of MALDI-TOF-MS and high molecular weight analysis described earlier above this instance underlines the challenge of analyzing high molecular weight samples with MALDI-TOF-MS. Peak resolution in MALDI-TOF-MS is another important issue. Resolution is usually expressed in units of full width at half peak maximum (R_{FWHM}) and is calculated by dividing the average mass to charge ratio of an analyte peak by its peak width at half of its maximum height. There are mainly five factors which decrease and limit the achievable peak resolution in MALDI-TOF mass spectrometry [131]. First, the molecular ions are generated at various times due to the finite duration of the laser pulse. Second, the kinetic energy of the generated molecular ions is not uniform because the initial velocity of the generated ions with the same m/z ratio has a certain distribution. Third, the molecular ions possess a spatial distribution which influences the kinetic energy of the ions. Spatial distribution is caused by ionization at different locations within the desorption plume. Fourth, an additional kinetic energy distribution is caused by collisions between matrix and analyte molecules during the early acceleration phase. Fifth, the maximal achievable resolution of the detector is technically limited. It is possible to enhance peak resolution in MALDI-TOF mass spectrometry with the aid of a reflectron or the pulsed extraction technique. A reflectron increases resolution through mass-independent kinetic energy focusing which is achieved by correcting differences in kinetic energies of molecular ions and longer flight times [132]. Typically time-of-flight mass analyzers with reflectrons are applied only for the analysis of samples with molecular weights below 10 kDa. For analyte ions with higher molecular weights a poorer signal to noise ratio is observed due to the loss of analyte ions. Similar to a reflectron, the pulsed extraction technique, which is also called delayed extraction technique, is mainly used for enhancing the resolution of smaller molecular ions at a narrow m/z range by compensating differences in the kinetic energies of analyte ions [133]. In the pulsed extraction technique no electric field is applied when the laser is fired. Instead, the electric field is applied after an appropriate time delay after the laser was fired.

I.4. High Molecular Weight Proteins and Glycoproteins

I.4.1. Classification of high molecular weight proteins

In this chapter the term high molecular weight (HMW) protein is referred to proteins which have molecular weights higher than 200 kDa. Such HMW proteins can be systematically divided into four classes depending on their structural composition. The first type consists of HMW proteins which contain only of one single polypeptide backbone with a molecular weight higher than 200 kDa. Such proteins might form non covalent aggregates but under denaturing conditions only high molecular weight polypeptide backbones are observed. Reducing agents have no significant influence on this type of protein. The second type comprises HMW proteins which consist of polypeptide chains with molecular weights higher than 200 kDa linked together through disulfide bridges. Unlike the first type described above these HMW proteins are significantly affected by reducing agents. Analysis with SDS-PAGE of this type of protein provides different results whether reducing agents are added to the sample solutions or not. The third type of HMW proteins contains of proteins which consist of polypeptide chains smaller than 200 kDa which are linked together through disulfide bridges. With SDS-PAGE under reducing conditions protein subunits with molecular weights below 200 kDa are detected. However, under denaturing conditions without reducing agent HMW proteins are observed. The fourth and last type of HMW proteins consists of protein subunits which form non covalent aggregates under native conditions. While such proteins are often referred to as high molecular weight proteins in literature this terminology is questionable. The term high molecular weight protein aggregate would be more suitable, because under denaturing analysis conditions no high molecular weight analytes are found. Proteins like urease, ferritin and catalase belong to this group of HMW proteins [134]. Generally most high molecular weight proteins are produced in higher organisms, but some exceptions are known. While the majority of mammalian proteins have molecular weights below 100 kDa the importance of HMW proteins should not be underestimated. Some of the most abundant human blood serum proteins like fibrinogen, α2-macroglobulin, immunoglobulin M and apolipoprotein B-100 belong to the class of HMW proteins [135]. In the rest of this chapter some commercially available and important high molecular weight proteins will be discussed more closely.

I.4.2. High molecular weight proteins consisting of only one single polypeptide backbone with a molecular weight higher than 200 kDa

I.4.2.1. Apolipoprotein B-100

Expasy accession number: P04114

Structure and post-translational modifications:

Apolipoprotein B-100 (Apo B-100) consists of one single polypeptide backbone which is modified with 19 N-linked glycan residues, one S-palmitoyl cysteine and 8 intra-chain disulfide bridges. Palmitoylation is required for the proper assembly of the hydrophobic core of the lipoprotein particle (Fig. 11). The Apo B-100 molecule is modelled as a belt which surrounds the low density lipoprotein (LDL) particle [136]. The calculated molecular weight of the unmodified polypeptide backbone is 512,8 kDa. According to literature Apolipoprotein B-100 has a molecular weight of about 550 kDa [137]. One of the analytical problems in characterizing Apo B-100 is that in the free form the protein is insoluble in aqueous solutions and tends to form aggregates. Further equilibrium dialysis showed that Apo B-100 binds 2,6 times its mass in SDS, which is a much higher uptake ratio than for other high molecular weight proteins [138].

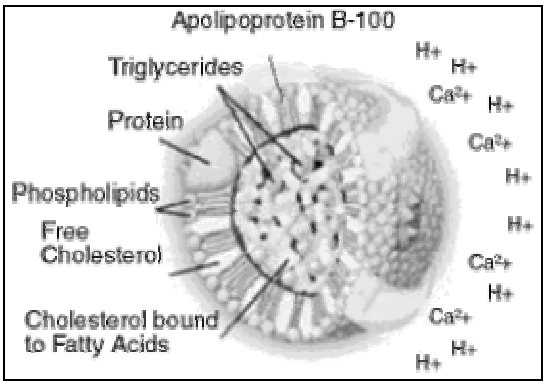

Fig. 11: Schematic image of a low density lipoprotein (LDL) particle. Apolipoprotein B-100 is the most abdundant protein found in LDL particles. The picture was provided by Souzao Enterprises.

Biological relevance:

Apolipoprotein B-100 is the dominant protein constituent of low density lipoproteins (LDL) and is also found in very low density lipoproteins (VLDL). It is a ligand for the LDL receptor and acts as a cofactor in enzymatic reactions and as a recognition signal for the cellular

binding and internalization of LDL particles. Furthermore Apo B-100 is necessary for the assembly of VLDL particles. Apolipoprotein B-100 is produced in the liver and has a mean serum concentration of about 1 mg/mL.

I.4.2.2. Hemocyanin

Expasy accession numbers: Q6KC55 and Q6KC56

Structure and post-translational modifications:

Keyhole limpet hemocyanin (KLH) consists of two structurally and physiologically distinct isoforms (KLH1 and KLH2), each being based on a subunit consisting of a single polypeptide chain with a molecular weight of approximately 400 kDa [139]. Every KLH subunit comprises 8 different globular functional units of about 50 kDa. At the level of the quaternary structure KLH1 occurs as a cylindrical didecamer, whereas KLH2 exists as a mixture of didecamers and tubular multidecamers with molecular weights of roughly 8 MDa for each didecamer. Such didecamer have diameters of about 35 nm [140]. Based on the nucleotide sequence Hemocyanin form 1 has a molecular weight of 358,9 kDa and form 2 a molecular weight of 391,5 kDa. Moreover both KLH forms have different glycosylation patterns. KLH 1 has a total carbohydrate content of 3,0%, while KLH 2 has a carbohydrate content of 3,4% [141]. KLH can exist in different aggregation states depending on pH and the concentration of divalent ions. Above pH 9,5 the protein aggregate completely dissociates into its subunits. At pH 7,4 and in the presence of divalent ions higher-order assemblies of the protein are stabilized.

Biological relevance:

KLH is found in the hemolymph of the mollusc *Megathura crenulata* and belongs to a large family of giant extracellular respiratory proteins responsible for the oxygen-transport in blood. Hemocyanins are found in many mollusc and athropod species. Each oxygen binding site of a KLH subunit contains two copper ions, resulting in the characteristic blue color of the oxygenated molecule. Due to its high molecular weight hemocyanin is widely used as a hepten carrier and immune stimulant. Since hemocyanin has many available primary amines

protein conjugation is facilitated. Haptens can be coupled to KLH using various cross-linking reagents and conjugation methods [142].

I.4.3. High molecular weight proteins consisting of covalently linked subunits with molecular weights higher than 200 kDa

I.4.3.1. Thyroglobulin

Expasy accession number: P01267

Structure and post-translational modifications:

Thyroglobulin is an extensively post-translational modified homodimeric protein which consists of two polypeptide subunits. Known post-translational modifications (PTMs) are 14 N-linked glycan residues, three thyroxine residues and one triiodothyronine per subunit. The presence of inter-chain or intra-chain disulfide bridges is not exactly described in literature. The calculated molecular weight of one polypeptide chain based on the nucleotide sequence is 301,2 kDa. According to literature intact, dimeric Thyroglobulin has a molecular weight of 660 kDa and a stokes radius of 8,6 nm [143-144]. The protein is known to be an excellent source of N-linked glycan residues of various structures [145]. The carbohydrate content of thyroglobulin comprises about 10% of the total molecular weight [146]. Despite the presence of two intact polypeptide chains in each thyroglobulin dimer smaller protein fragments ranging down to 20 kDa were observed in SDS-PAGE under reducing conditions and reported in literature [147-148]. While most proteins which contain tyrosine may be iodinated *in vitro* to form mono- and diiodotyrosine residues, no significant thyroid hormone formation occurs. Thus, thyroglobulin is the only vertebrate protein known to be iodinated in vivo under normal circumstances [149]. It is further assumed that thyroglobulin contains covalently linked phosphate residues. About half of these phosphorylations are attached to serine and tyrosine residues and the other half is attached to the carbohydrate moieties [150].

Biological relevance:

Thyroglobulin is an iodine-containing protein stored in thyroid gland. When the thyroid is stimulated by thyroid stimulating hormone (TSH) thyroglobulin is coverted into circulating

thyroxines. The protein is produced in the thyroid gland and is a precursor of the iodinated thyroid hormones thyroxine (T4) and triiodothyronine (T3). Due to its large size and absence from plasma under normal conditions thyroglobulin is very immunogenic and hence often used as carrier protein for the production of antibodies.

I.4.3.2. Fibronectin

Expasy accession number: P07589

Structure and post-translational modifications:

Fibronectin mostly forms heterodimers or multimers of alternatively spliced variants which are connected by two disulfide bridges near the carboxyl ends of the polypeptide backbones. To a lesser extend homodimers are observed as well. Fibronectin is found either as soluble plasma protein or as fibrils in the extracellular matrix. Plasma Fibrinogen has a dimeric form, whereas cellular Fibronectin is found as dimer or cross-linked multimer (Fig. 12). According to the Expasy database the N-terminus of Fibronectin subunits is modified with a pyrrolidone carboxylic acid. Other known PTMs are seven N-linked and two O-linked glycan residues and one phosphoserine. The carbohydrate content is only about 5% of the total molecular weight of the protein. Next to two inter-chain disulfide bridges which connect the individual subunits, each Fibronectin subunit has almost 30 intra-chain disulfide bridges. Two Tyrosine residues are potentially sulfonated. A molecular weight of about 220 kDa for each polypeptide chain is reported in literature [151].

Biological relevance:

Plasma Fibrinogen is secreted by hepatocytes, whereas cellular Fibronectin is produced by fibroblasts, epithelial cells or other cell types. Fibronectin has the ability to bind to collagenous and glycosaminoglycan constituents of the connective tissue, to actin, DNA, heparin, fibrinogen and some other plasma proteins as well as to various cell surfaces. Moreover, fibronectins have a variety of different functions like cell adhesion, wound healing, cell motility and maintenance of cell shape.

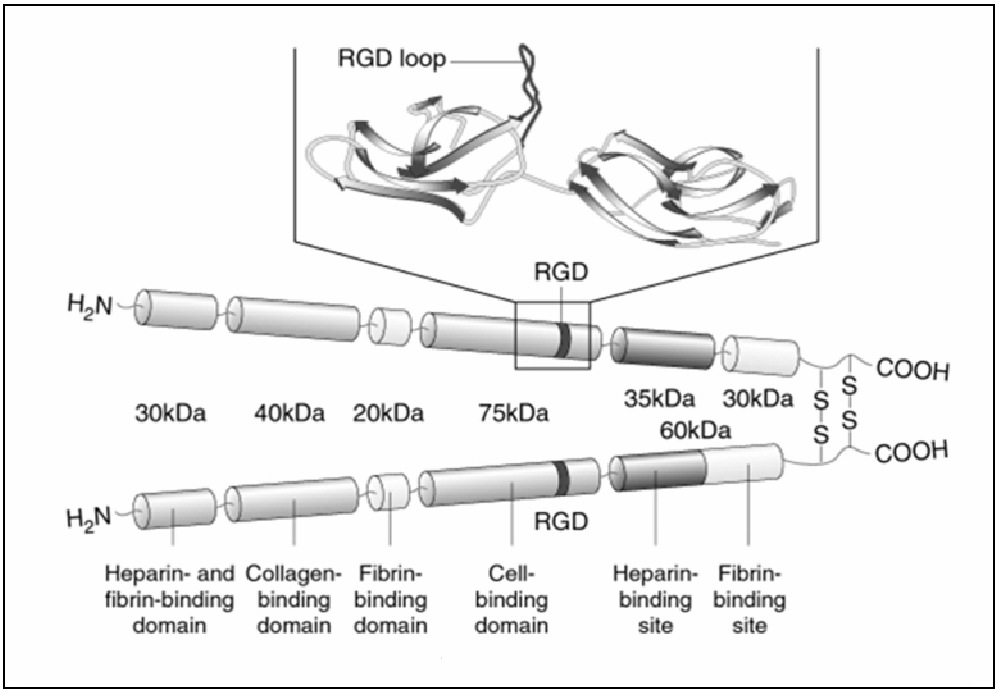

Fig. 12: Structure of plasma fibronectin. The protein is a heterodimer consisting of two similar polypeptide chains which are linked together by disulfide bridges located close to the C-termini of the polypeptide chains. The picture was provided from J. Wiley and Sohns, Inc.

I.4.4. High molecular weight proteins consisting of covalently linked subunits with molecular weights lower than 200 kDa

I.4.4.1. α2-Macroglobulin

Expasy accession number: P01023

Structure and post-translational modifications:

α2-Macroglobulin is a homotetramer and consists of two pairs of disulfide-linked polypeptide chains. While two subunits are linked covalently through two disulfide bridges, the resulting dimer forms non covalent homotetrameric protein complexes with other dimers. In literature α2-Macroglobulin is described to resemble a hollow cylinder which is comprised of two identical functional halves with three C_2 axes of symmetry and no mirror planes (Fig. 13) [152]. The calculated molecular weight of a non modified polypeptide chain based on the nucleotide sequence is 160,8 kDa. Known PTMs are 11 intra-chain disulfide bridges and 8 N-linked sugar residues. According to literature intact, tetrameric α2-Macroglobulin has a molecular weight of 725 kDa and a stokes radius of 8,8 to 9,4 nm [153-154].

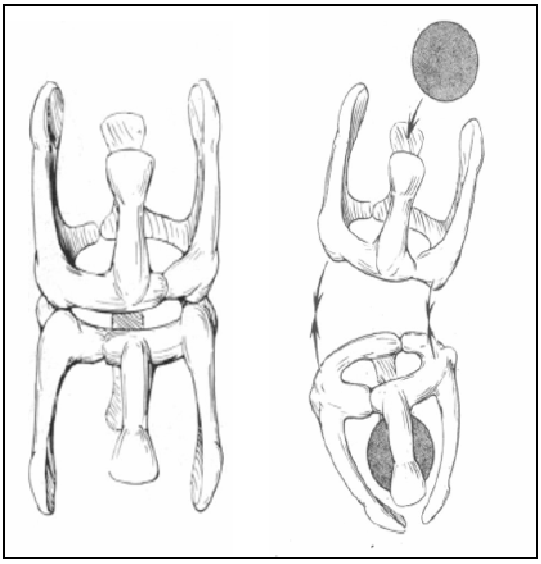

Fig. 13: Structure of homotetrameric α2-Macroglobulin. Two polypeptide chains are linked covalently through disulfide bridges. The dimers assemble without covalent bounds to tetramers. The picture was published by Feldmann et al. [152]

Biological relevance:

α2-Macroglobulin is a major serum protein which belongs to the class of protease inhibitors and is capable of irreversible inhibiting all four classes of proteases by a unique trapping mechanism which forms a molecular trap around proteases. The protein has a peptide stretch, called bait region, which contains specific cleavage sites for different proteases. A maximum of two proteases can be bound per α2-Macroglobulin tetramer and generally two subunits are cleaved per protease molecule bound [155]. When a protease cleaves the peptide stretch a conformational change is induced and in turn the protease is trapped by α2-Macroglobulin. Covalent binding of the protease to α2-Macroglobulin is not required for irreversible inhibition. Nevertheless in addition to non covalent trapping most of the bound protease is covalently bound to α2-Macroglobulin via amide bonds formed between lysyl amino groups and internal cysteine-glutamate thioesters [156]. The protein also controls the clotting and fibrinolytic system. Further α2-Macroglobulin is reported to promote the growth of mammalian cells in culture and to regulate macrophage nitric oxide synthesis.

I.4.4.2. Fibrinogen

Expasy accession numbers: P02671, P02675, P02679

Structure and post-translational modifications:

Fibrinogen is a 340 kDa glycoprotein composed of two pairs of three separate polypeptide chains (Fig. 14) [157]. The three types of subunits are called α-, β- and γ-chains. While the α-chain has no sugar residues, the β-chain has one N-linked and the γ-chain two N-linked glycan residues. In the literature a molecular weight of 66,2 kDa is stated for the α-chain, while for the β- and γ- chain a molecular weights of 54,2 and 48,4 kDa are given [158]. The α-chain contains one phosphoserine. About one-third of all α-chains are phosphorylated. While the β-chain has one N-linked glycan the γ-chain has two N-linked glycan residues. The total reported carbohydrate content of fibrinogen is only about 3% [159]. Further post-translational modifications are two sulfotyrosine residues in the case of the γ-chain and one pyrrolidone carboxylic acid located at the N-terminus of the β-chain. Next to multiple intra-chain disulfide bridges the individual fibrinogen subunits are linked together by several inter-chain disulfide bridges: α- and β-chains are linked by three disulfide bridges, while α- and γ-, β- and γ- and two γ- chains are linked with two disulfide bridges each. By electron microscopy fibrinogen appears as a trinodular structure in which the central nodule contains the amino termini of all six chains [160].

Biological relevance:

Fibrinogen, also called coagulation factor I, is a plasma glycoprotein essential for blood clotting and produced by hepatic parentchymal cells. Mean serum concentrations of human fibrinogen are about 3 mg/mL. The conversion of soluble fibrinogen monomers into insoluble fibrin monomers which is followed by polymerization and aggregation of fibrin monomers is the terminal step of the blood clotting cascade. Thrombin triggers the conversion of fibrinogen to fibrin by cleaving fibrinopeptides A and B from the N-termini of α- and β-chains and thus exposing the polymerization sites responsible for clot formation. The resulting fibrin monomers form soft clots which are then converted into hard clots by factor XIIIa which catalyzes the covalent cross-linking of glutamate and lysine amino acid residues between gamma chains and between alpha chains of different monomers. Calcium is reported

to promote the polymerization of fibrin monomers and the cross-linking of fibrin by factor XIIIa. Fibrinogen is found at elevated levels after surgical trauma and pregnancy and is decreased in cases of liver cirrhosis and serum hepatitis. Further fibrinogen acts as a cofactor in platelet aggregation.

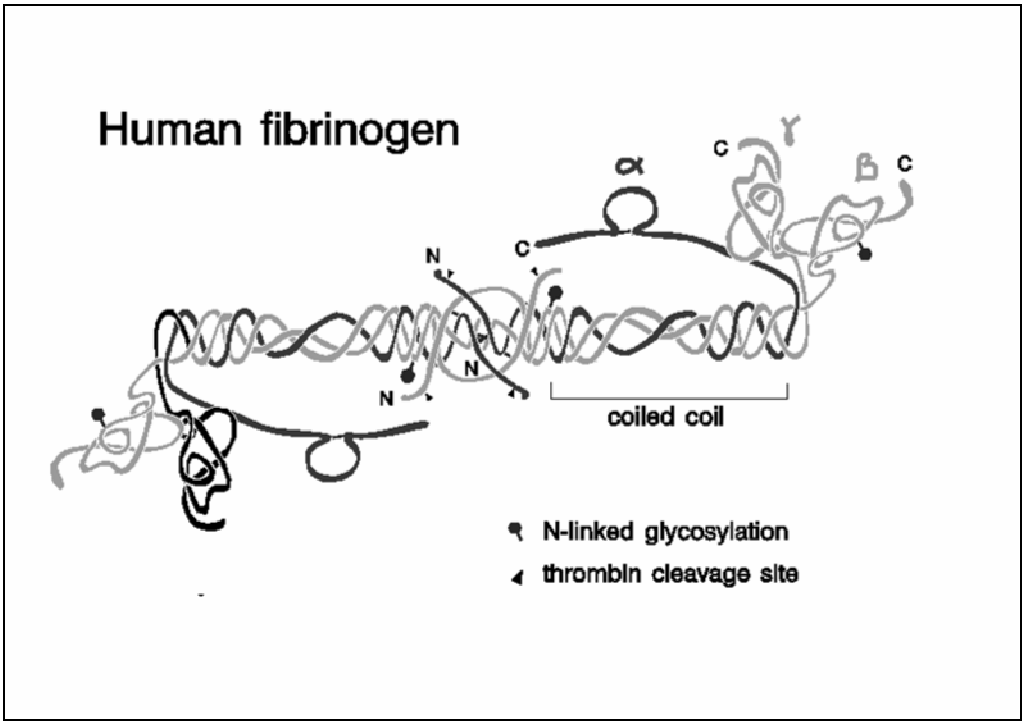

Fig. 14: Structure of fibrinogen. The protein has a hexameric structure and consists of 3 pairs of α-, β- and γ- chains. All six polypeptide chains are linked together by disulfide bridges. The picture was provided by Professor Teller from the Department of Washington (USA).

I.4.4.3. Immunoglobulin M

Expasy accession number: n/a

Structure and post-translational modifications:

Normally immunoglobulin M (IgM) is a pentameric molecule composed of five immunoglobulin subunits and a joining J-chain (Fig. 15). The various subunits are covalently linked through disulfide bridges thus forming one single molecule. The reported average molecular weight of intact IgM is between 900 and 1000 kDa [161-162]. Each immunoglobulin subunit consists of two heavy and two light chains. Only the heavy chain which has a molecular weight of about 70 to 75 kDa is glycosylated. The glycosylation of IgM is more complex than that of immunoglobin G (IgG) because the constant region of IgM

has six potential N-glycosylation sites compared with only one glycosylation site in the IgG constant region [163]. The J-chain has a molecular weight of about 15 kDa and contains one N-linked glycan residue and one pyrrolidine carboxylic acid [164]. Further the J-chain helps to bind IgM and immunoglobulin A (IgA) to secretory components. Next to IgM J-chains are also found in Immunoglobulin A. The J-chain facilitates the polymerization process of IgM subunits so pentameric IgM is preferentially synthesized [165-166].

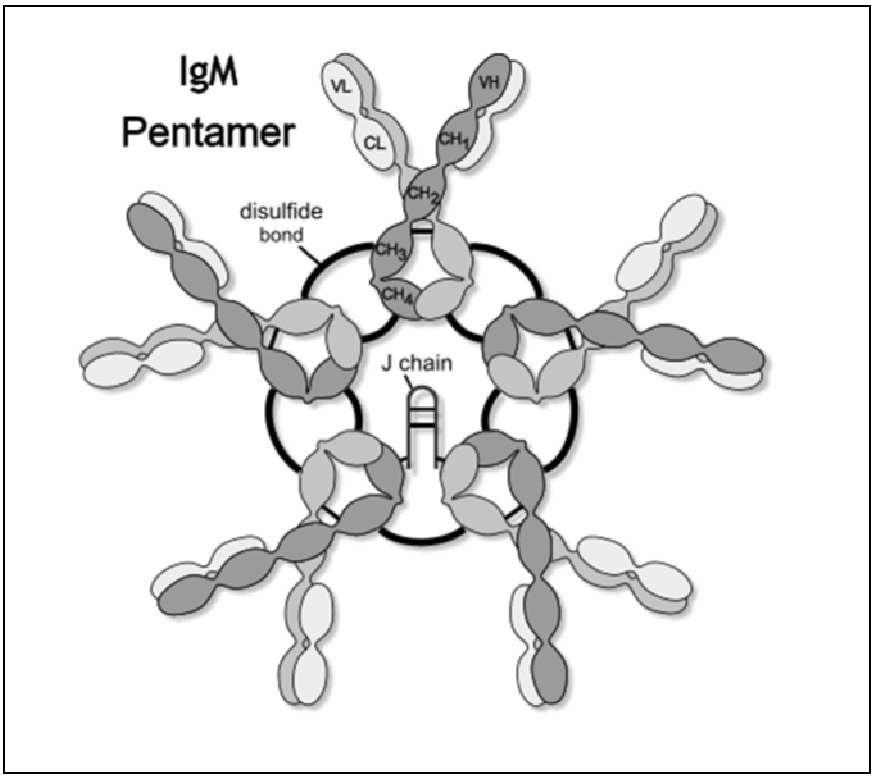

Fig. 15: Structure of immunoglobulin M. The protein consists of 5 Y-shaped subunits. Each subunit in turn consists of two light and two heavy chains. The subunits are linked together by multiple disulfide bridges and one single J-chain. The picture was provided by Alerchek, Inc.

Biological relevance:

Immunoglobulin M is an antibody and an important product of the immune system because it plays a critical role in the early protection against bacterial infections. It is the predominant antibody class made against certain antigens such as microbial polysaccharides. The mean serum concentration of human IgM is about 1,5 mg/mL.

I.5. Complex Glycoproteins

I.5.1. Importance of post-translational protein modifications

Today the analysis of entire genoms, which is also called genomics, is a well established procedure. On the other hand the analysis of complete proteoms, also called proteomics, poses several difficulties and cannot be performed in a high throughput process like genomics. One reason for this is evidence is that proteoms are actually much more complicated than genoms. While DNA is build up of only four different nucleotides, proteins consist of 20 common amino acids. A further challenge of proteomics is the presence of post-translational protein modifications (PTMs). In some cases typical amino acid sequences called sequons with the length of 3 to 10 amino acids are indications for specific post-translational modifications. Nevertheless post-translational modifications often cannot be predicted by the DNA sequence of a protein encoding gene [167]. At the moment more than 400 post-translational modifications are known. While some modifications are found only in one particular species some PTMs are rather common. Among the most common PTMs are disulfide-bridges, glycosylations, phosphorylations, sulfations, acetylations, methylations and covalent linkages with lipid residues. Generally post-translational modifications affect physiochemical parameters of proteins, like charge distribution, hydrophobicity, conformation and stability. What makes the analysis of post-translational modifications extremely challenging is the fact that not each copy of a particular protein in a given tissue must contain identical post-translational modifications. Thus a large variety of different protein forms with the same polypeptide backbone and different post-translational modifications is commonly observed in higher organisms. Proteins which contain one or more covalently attached carbohydrate chains are termed glycoproteins. Protein glycosylations have influence on physiochemical parameters of proteins like viscosity, isoelectric point, degree of hydration, solubility, thermal stability and resistance to proteolysis. For a long time the importance of protein glycosylations was underestimated, whereas today even a peculiar research field exists which is concerned with the characterization of glycan structures attached to glycoproteins. This research field is called glycomics and is considered as a sub-group of proteomics [168]. It is known that glycosylations play an important role in the fields of immunology, neurology, development biology, biological recognition, enzyme activity and pathology. Several diseases are caused by wrong or missing glycosylations [169]. Despite the importance of protein glycosylations the advances in the field of glycoproteomics are comparably low due to the

molecular complexity of oligosaccharides and the lack of appropriate analytical techniques. In contrast to linear protein and nucleic acid biopolymers the analysis of oligosaccharides involves characterization of sugar sequence, branching pattern, linkage positions, anomeric configuration and ring forms of the monosaccharide units present. Based on the genetic informations obtained from the Human Genome Project it is assumed that about 1% of all human genes encode for enzymes which are associated with protein glycosylation.

I.5.2. Structures and sequons of protein glycosylations

Oligosaccharides attached to glycoproteins of higher organisms are composed of about 10 different monosaccharide units. Commonly monosaccharide units found in the glycan residues of animal glycoproteins are glucose, galactose and mannose (all hexoses), xylose (a pentose), fucose (a desoxyhexose), N-acetylglucosamine and N-acetylgalactosamine (both N-acetylhexosamines), N-acetylneuraminic acid and N-glycolyl neuraminic acid (both sialic acids). The chemical structures of some monosaccharides are shown in Figure 16.

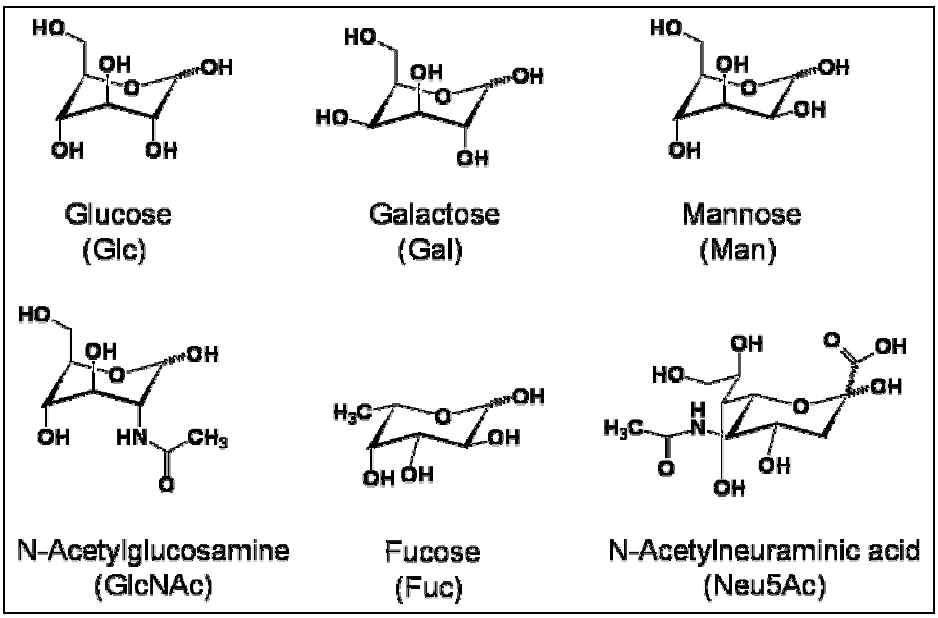

Fig. 16: Chemical structures of six monosaccharides commonly found in mammalian glycan structures

The glycan residues of glycoproteins are always covalently attached to specific amino acids and can be distinguished in N- and O-linked glycans. N-linked glycan residues are always linked via asparagine to the polypeptide backbone while O-linked glycans are always linked via serine or threonine. Moreover, N-linked oligosaccharides are always linked via N-

acetylglucoseamine to asparagines and O-linked carbohydrates are always linked via N-acetylgalactoseamine to serine or threonine residues. In mammalian glycoproteins N-linked oligosaccharides are more frequently found than O-linked sugar residues. N-glycosylations are always correlated with a specific amino acid sequence (sequone). The amino acid C-terminal adjacent to the asparagine residue with the N-linked glycan may be any amino acid except proline or aspartate and the next adjacent C-terminal amino acid has to be a serine or threonine residue. Unlike for N-glycans there is no particular sequone for O-glycans which aggravates the predictability. Glycoproteins do not possess a single, consistent structure but usually consist of several different glycoforms which differ not only in the number of attached glycans but also in the structure of the glycan itself. This phenomenon is called microheterogeneity. As already shortly mentioned earlier oligosaccharides attached to proteins are not linear, but have a tree-like structure. These antenna structures contain not only various hydroxy groups as possible linkage sites but might also contain either α- or β-glycosidic linkages. Nevertheless also some similarities exist between all N-linked mammalian glycan residues. Due to the similarity of glycosyltransferases all mammalian cells have a unique core structure found in all N-linked carbohydrates (Fig. 17). This core structure consists of two N-acetylglucoseamine and three mannose units. The two N-acetylglucosamine units attached to asparagine are called chitobiose core structure.

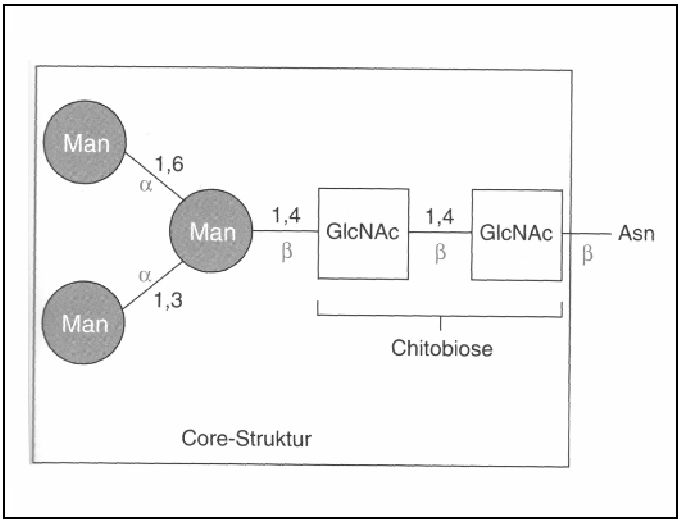

Fig. 17: Schematic illustration of the core structure of all mammalian N-linked glycan residues. The illustration was published by Lottspeich et al. [170]

N-glycans can be systematically divided into three different groups: the high mannose type, complex type and hydrid type. The first contains from 2 to 6 additional mannose residues linked to the pentasaccharide core structure (Fig. 18).

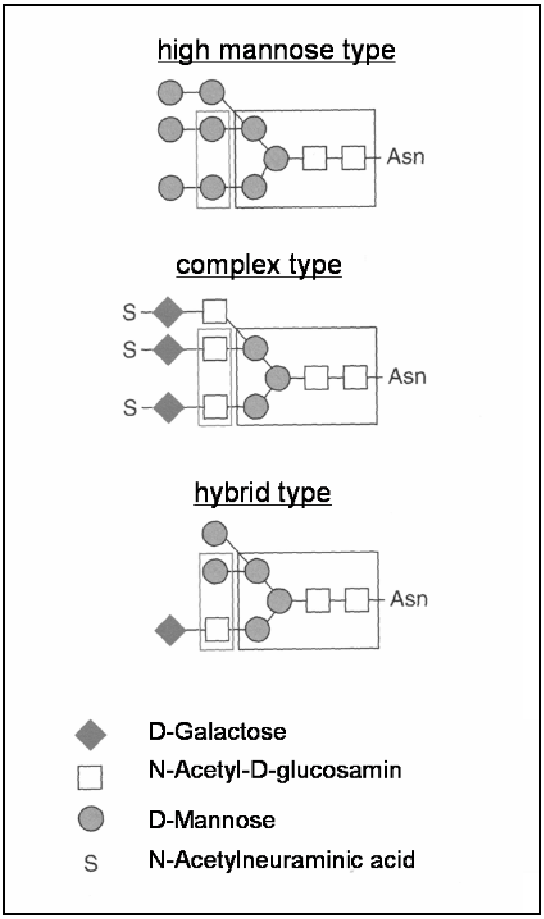

Fig. 18: Schematic illustration of the three base types of mammalian N-glycans: high mannose type, complex type and hybrid type; in all three types of N-glycans contain the same pentasaccharide core structure shown in Fig. VII-2. The illustration was published by Lottspeich et al. [170]

The complex type has 2 to 4 branches attached to the pentasaccharide core structure and consists mainly of N-acetylglucosamine, galactose and N-acetylneuraminic acid monomers. Hybrid type oligosaccharides are a mixture of high mannose and complex type. Glycans are often termed according to their number of antennas (diantennary, triantennary, etc.).

I.5.3. Analysis of N-glycan residues

For analysis of carbohydrates attached to proteins the usual procedure includes the cleavage of all oligosaccharide residues from the protein. The detachment of glycan residues can be either be performed chemically or enzymatically. Both methods have advantages and disadvantages, so it mainly depends on how much is known about the structure of the oligosaccharides and their linkage to the protein and also on the amount of glycoprotein available. Concerning the chemical cleavage of oligosaccharides from glycoproteins there are two commonly applied methods: hydrazinolysis and β-eliminiation. Both chemical methods take advantage of the high stability of glycoside bonds to alkaline conditions. However, the main focus of the chapter is the enzymatic cleavage of N-glycans from glycoproteins. There are two enzymatic approaches for the de-N-glycosylation of glycoproteins: the application of

glycopeptidases or the application of endoglycosidases. To the first type of enzyme the protein N-Glycosidase F is belonging, which is also called PNGase F, Glycoamidase F, peptide-N-glycosidase or N-glycanase [171-173]. This enzyme cleaves the linkage between the chitobiose unit and the polypeptide backbone, thus releasing the complete oligosaccharide unit (Fig. 19).

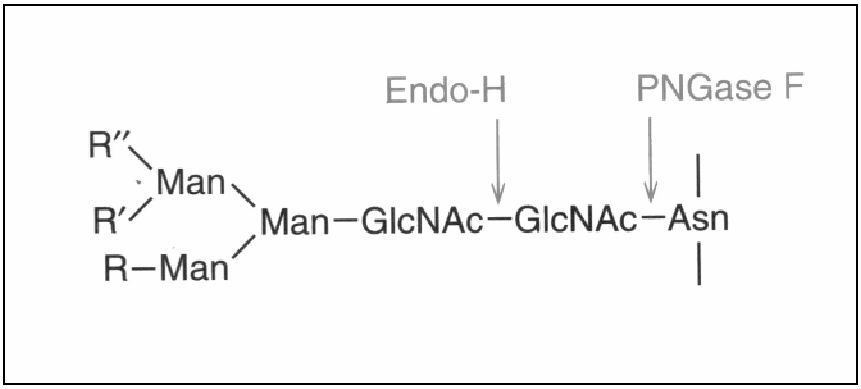

Fig. 19: Schematic illustration of the cleavage sites of endo-β-N-acetylglucosamindase (Endo-H) and peptide-N-glycosidase (PNGase F). The image was published by Lottspeich et at. [170]

PNGase F is a 35,5 kDa protein and cleaves all types of asparagine bound N-glycans provided that the amino group as well as the carboxyl group are present in a peptide linkage and that the oligosaccharide has the minimum length of the chitobiose core unit. It is known that the presence of some specific monosaccharides in the N-linked glycan residue prevents this enzymatic de-N-glycosylation. The enzyme activity of PNGase F has its pH optimum between pH 7 and 9, but the enzyme is also active at a pH of 5 to 7. De-N-glycosylation with PNGase F is a two step reaction. In the first step the amide bond which links the N-glycan is hydrolyzed. In the second step the primary amine of the recently released N-glycan residue is hydrolyzed to a hydroxy group and ammonium is released. Because of the hydrolysis of the amide bond in the first reaction step the involved asparagine residue is converted into asparatate. The second type of enzyme comprises endo-β-N-acetylglucosamidases. These enzymes cleave the linkage between the two N-acetylglucosamine residues in the chitobiose core unit. Consequently the released oligosaccharide unit contains one GlcNAc residue at the reducing end, while the other GlcNAc residue is still attached to the polypeptide backbone. Common endo-β-N-acetylglucosamidases are endo-β-N-acetylglucosamindase D (endo-D), H (endo-H) and C_{II} (endo-C_{II}). All three types of endoglycosidases release N-glycans from the high mannose and hybrid type but not from the complex type. Unlike for N-linked glycan structures there is no enzymatic method for removing all types of O-linked glycans from

glycoproteins. After releasing glycan residues from the glycoprotein, the oligosaccharides have to be isolated and further analyzed. Well established techniques for the characterization of released oligosaccharide chains are MALDI-TOF-MS and ESI-IT-MS [174-175].

I.6. High molecular weight PAMAM Dendrimers

I.6.1. Dendrimers – overview and applications

Dendrimers are synthetic polymers with multiple branched structures. In 1926 Herman Staudinger first described the principles of dendrimeric architecture [176]. The main differences between dendrimers and other polymers are the well defined structure, the defined size in the nm range and a clear distinction between core and surface. Since dendrimers are nano-particles and possess particle sizes and structures similar to common biopolymers various interesting biological applications like biocatalysis and drug delivery are described in literature (Fig. 20) [177-178]. Today dendrimers are recognized as a new type of functionalised building blocs suitable for nano-technology [179-181]. This is also due to the fact that different types of dendrimers can be self-assembled into novel macromolecular structures and that dendrimers can be coupled with various polymers in different arrangements [182-184]. Hence, macromolecules with completely new properties can be created.

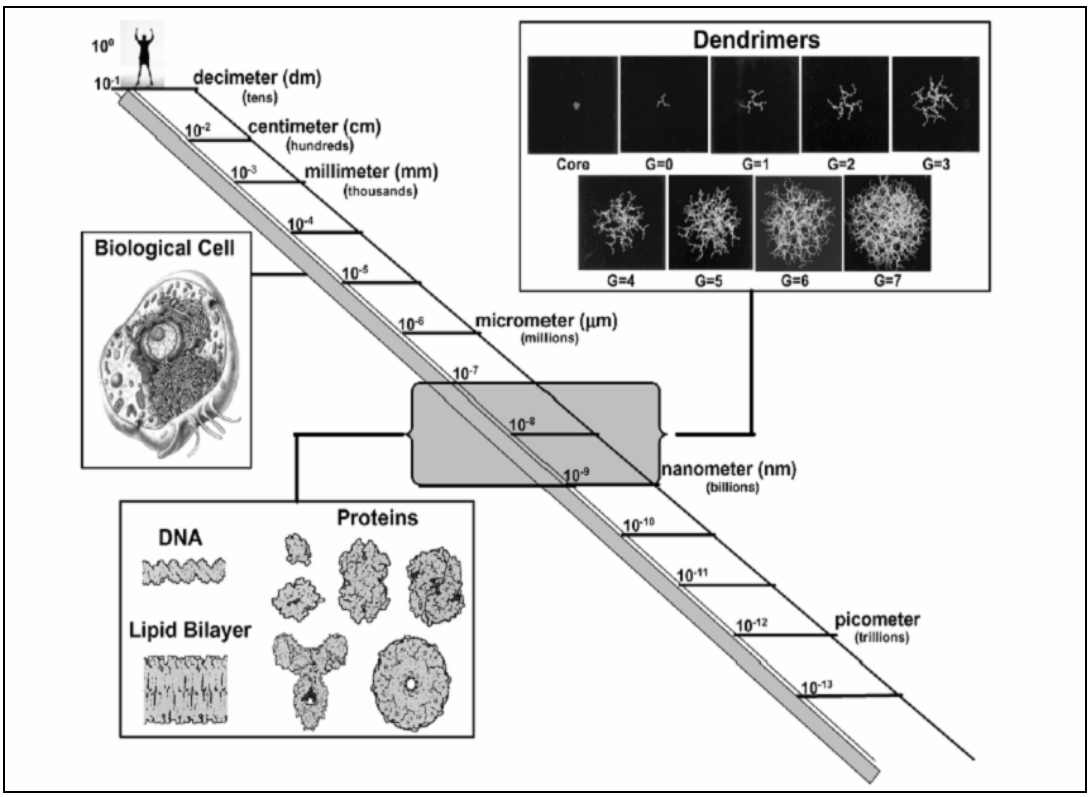

Fig. 20: Nanoscale dimensional comparison of PAMAM dendrimers with proteins, DNA, lipid bilayer and cells. The picture was published by Tomalia et al. [185]

I.6.2. Structure, synthesis and characterization of PAMAM dendrimers

While several different types of dendrimers are described in literature, this chapter focuses on poly(amido amine) (PAMAM) dendrimers which are also the best described type of dendrimers today. Moreover, PAMAM dendrimers were the first complete dendrimer family to be synthesized, characterized and commercialized [186]. Other types of dendrimers are based upon poly(propylene imine), polylysine, arborols, poly(benzyl ether) and polyphenylene [187]. At the moment more than 100 compositionally different dendrimer families have been synthesized and characterized [188]. Since 1970 two major strategies have evolved for dendrimer synthesis. The "divergent" method was the main synthesis method during the 1980s and starts with a core molecule. During this type of synthesis concentric shells are added around the core (starter) molecule and the dendrimer grows in a branch-upon-branch motif from the core to the surface. Consequently, the dendrimer grows linearly in diameter as a function of added shells and the number of surface groups is amplified exponentially (Table 1).

PAMAM Generation	calculated MW in Da	surface groups
G0	516,7	4
G1	1429,8	8
G2	3256,2	16
G3	6908,8	32
G4	14214,2	64
G5	28824,8	128
G6	58046,2	256
G7	116488,8	512
G8	233374,1	1024
G9	467144,7	2048
G10	934685,9	4096

Table 1: Table of calculated molecular weights and the number of surface groups of various PAMAM dendrimer generations

Due to the large number of terminal surface groups macromolecular properties such as size, molecular weight, topology and surface functionality can be controlled [189]. The second technique is called "covergent" synthesis and begins with starter molecules which will later become the surface of the dendrimer. Hence, synthesis route in from the surface to the focal point in the core. PAMAM dendrimers are synthesized by the "divergent" method which involves an iterative 2-step reaction sequence that produces concentric shells around a central

starter molecule (Fig. 21) [190]. The first reaction step is a Michael addition and involves the exhaustive alkylation of primary amines with methyl acrylate. In the second reaction step the amplified ester groups is amidated with a large excess of ethylene diamine. Starting with a core molecule the first reaction sequence creates a PAMAM dendrimer of generation 0. Repeating this iterative sequence produces higher generations of PAMAM dendrimers.

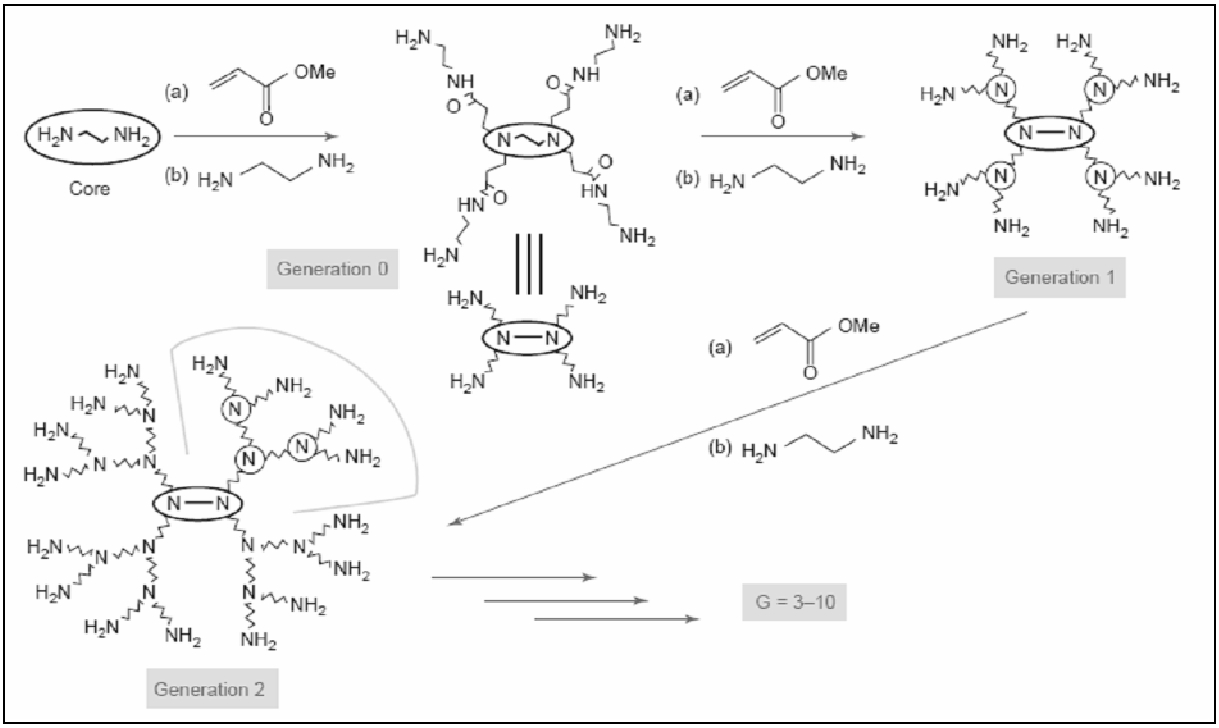

Fig. 21: Reaction scheme of the "divergent" PAMAM dendrimers synthesis. The shown PAMAM dendrimer possesses primary amines as surface groups and ethylenediamine as core. The illustration was published by Esfand et al. [188]

All PAMAM dendrimers contain multiple peptide like amide bonds but differ in three parameters: dendrimer generation, the type of core molecule and the type of terminal surface groups. PAMAM dendrimers of generation 0 to 10 are commercially available. The simplest and most common type of PAMAM dendrimer consists of ethylene diamine as core molecule and primary amines as surface groups. Further common types of PAMAM surface groups are 3-carbomethoxypyrrolidinone, amidoethanol, amidoethylethanolamine, hexylamide, trimethoxysilyl, sodium carboxylate, succinamic acid and tris(hydroxymethyl)amidomethane. Next to ethylene diamine common core molecules of PAMAM dendrimers are 1,12-diaminododecane, 1,6-diaminohexane, 1,4-diaminobutane and cystamine. Unlike several other dendrimer families PAMAM dendrimers resemble proteins not only in their size but also, due to the large number of peptide like bonds, in their particular chemical structure. The major difference between PAMAM dendrimers and proteins is that the latter consist of linear

polypeptide backbones while PAMAM dendrimers consist of a tree-like branched structure (Fig. 22).

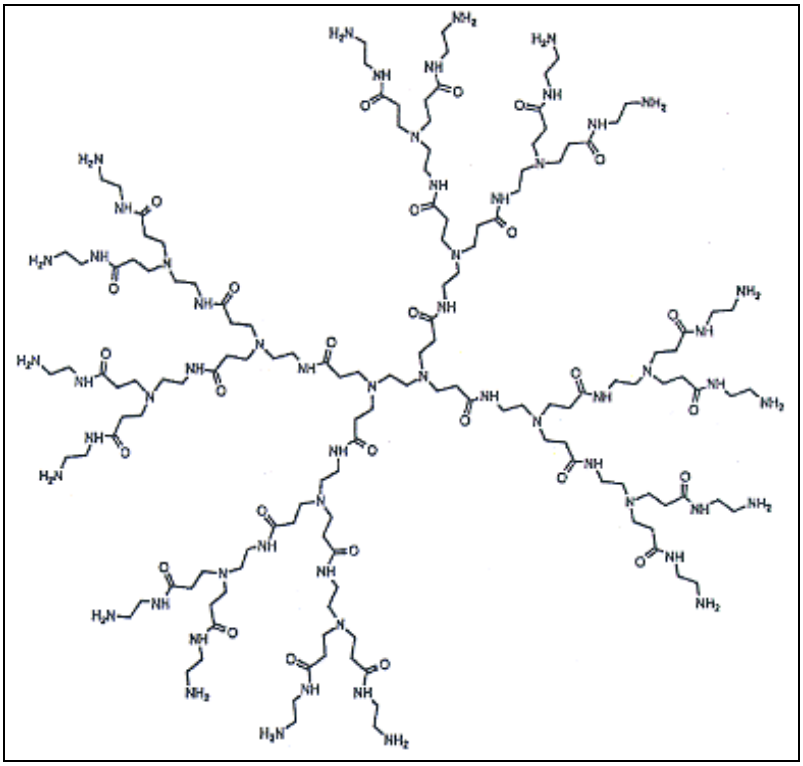

Fig. 22: Chemical structure of a generation 2 PAMAM dendrimer molecule with primary amine surface groups and an ethylene diamine core. The picture was provided by Dendritech, Inc. (USA)

While several different analytical techniques are applied for the characterization of dendrimers, analytical methods seem to be one step behind the importance of dendrimers. Due to the exponentional growth of dendrimers, molecular weight as well as the number of surface groups covers a range of about 3 magnitudes. For the analysis of molecular weight, particle diameter and shape of PAMAM dendrimers the most common analytical techniques are based on electrophoresis, chromatography, microscopy, light scattering and mass spectrometry. The electrophoretical techniques include slab gel electrophoresis [191] and capillary electrophoresis [192], while the most commonly applied chromatographic technique for the characterization of dendrimers is size exclusion chromatography (SEC) [193-197]. With the aid of size exclusion chromatography particle diameters can be measured which correlate with molecular weights of globular proteins or polystyrol polymers. Small angle x-ray scattering (SAXS) [198-199] and small angle neutron scattering (SANS) [200] are both scattering techniques which allow the determination of the gyration radius and electron density distribution of dendrimers. Atomic force microscopy (AFM) [201-204] and transmission electron microscopy (TEM) [205] are two microscopic methods which allow the visualization and diameter characterization of dendrimers particles. The most commonly applied mass

spectrometric techniques for the molecular weight determination of dendrimers are MALDI-MS [206-210] and ESI-MS [211-213]. Furthermore nuclear magnetic resonance (NMR) and other techniques are applied for the analysis of surface groups and for verifying the presence of certain structure elements [214]. Characterization of PAMAM dendrimers is not only performed experimentally but also theoretically with the aid of molecular dynamics simulation [215].

I.7. Aims of the thesis

This PhD thesis is focused on the molecular weight determination and systematic characterization of proteins and dendrimers with molecular weights higher than 200 kDa using two gel electrophoretical (planar SDS-PAGE and CGE-on-the-chip) and one mass spectrometric technique (MALDI-TOF-MS). For this purpose the first issue was the development of a novel high molecular weight protein assay for CGE-on-the-chip. CGE-on-the-chip is the most recent of all three applied analytical techniques and was so far only applied for the analysis of proteins with molecular weights lower than 250 kDa. In order to adopt an existing CGE-on-the-chip protein assay for a future high molecular weight protein assay a general feasibility study was necessary which was performed in close cooperation with Agilent Technologies in Waldbronn (Germany). During the course of this feasibility study it was necessary to modify the existing CGE-on-the-chip electrokinetic injection profiles, characterize various gel matrices in terms of separation efficiency in the high molecular weight range and develop a protein calibration in the high molecular weight range. Due to a nondisclosure agreement with Agilent Technologies details of the novel high molecular weight protein assay are not presented in this thesis. The second issue was the comparison of all three analytical techniques for the analysis of high molecular weight proteins. Planar SDS-PAGE of several high molecular weight proteins was already described in literature and today SDS-PAGE is the most straight forward commercial analytical technique for high molecular weight proteins. Analysis of high molecular weight proteins with MALDI-TOF-MS was only sparely described in literature. The main concerns for this analytical technique were the choice of an appropriate MALDI matrix as well as a suitable sample preparation technique. Moreover, high molecular weight analytes are known to have poorer desorption and ionization behaviour than analytes with lower molecular weights. Another difficulty of MALDI-TOF-MS was that most high molecular weight proteins are often heavily post-translational modified. The third issue of this PhD thesis was the molecular weight and particle size determination of high molecular weight PAMAM dendrimers using MALDI-TOF-MS and nano-electrospray gas-phase electrophoretic mobility molecular analysis (nES-GEMMA). While the analysis of PAMAM dendrimers with various analytical methods was already described in literature, analysis of PAMAM dendrimers with MALDI-TOF-MS was only performed of low molecular weight dendrimers so far. A final issue was to test the feasibility of MALDI-TOF-MS for the molecular weight determination of biopolymers with molecular weights of 1 MDa.

I.9. References

[1] Marcotte, E., Pellegrini, M., Thompson, M., Yeates, T., Eisenberg, D. (1999) A combined algorithm for genome-wide prediction of protein function. *Nature*, **402**: 83-86

[2] Sali, A., Glaeser, R., Earnest, T., Baumeister, W. (2003) From words to literature in structural proteomics. *Nature,* **422**: 216-225

[3] Peng, J., Gygi, S. (2001) Proteomics: the move to mixtures. *Journal of Mass Spectrometry,* **36**: 1083-1091

[4] Belgacem, O., Buchacher, A., Pock, K., Josic, D., Sutton, C., Rizzi, A., Allmaier, G. (2002) Molecular weight determination of plasma-derived glycoproteins by ultraviolet MALDI-TOF-MS with internal calibration. *Journal of Mass Spectrometry*, **37**: 1118-1130

[5] Luque-Garcia, J.L., Zhou, G., Sun, T., Neubert, T.A. (2006) Use of nitrocellulose membranes for protein characterization by MALDI-MS. *Analytical Chemistry*, **78**: 5102-5108

[6] Liu, Z., Schey, K.L. (2005) Optimization of a MALDI TOF-TOF mass spectrometer for intact protein analysis. *Journal of the American Society of Mass Spectrometry*, **16**: 482-490

[7] Kleinova, M., Belgacem, O., Pock, K., Rizzi, A., Buchacher, A., Allmaier, G. (2005) Characterization of cysteinylation of pharmaceutical-grade human serum albumin by ESI-MS and low-energy collision-induced dissociation tandem mass spectrometry. *Rapid Communications in Mass Spectrometry*, **19**: 2965-2973

[8] Putnam, F. (1993) Alpha-, beta-, gamma-globulin—Arne Tiselius and the advent of electrophoresis, *Perspectives in Biology and Medicine*, **36**: 323-337

[9] Shapiro, A.L., Vinuela, E., Maizel, J.V. (1967) Molecular weight estimation of polypeptide chains by electrophoresis in SDS polyacrylamide gels. *Biochemical and Biophysical Research Communications*, **28**: 815-820

[10] Whitaker, J.R. (1981) Determination of molecular weights of proteins by gel filtration on sephadex. *Analytical Chemistry*, **35**: 1950-1953

[11] Andrews, P. (1962) Estimation of molecular weights of proteins by gel filtration. *Nature*, **196**: 36-39

[12] Steere, R.L., Ackers, G.K. (1962) Restricted-diffusion chromatography through calibrated columns of granulated agar gel: a simple method for particle size determination. *Nature*, **196**: 475-476

[13] Folta-Stogniew, E., Williams, K.R. (1999) Determination of molecular masses of proteins in solution: implementation of an HPLC size exclusion chromatography and laser light scattering service in a core laboratory. *Journal of Biomolecular Techniques*, **10**: 51-63

[14] Wyatt, P.J. (1993) Light scattering and the absolute characterization of macromolecules. *Analytica Chimica Acta*, **272**: 1-40

[15] Sinz, A. (2003) Chemical cross-linking and mass spectrometry for mapping three-dimensional structures of proteins and protein complexes. *Journal of Mass Spectrometry*, **38**: 1225-1237

[16] Pearson, K.M., Pannell, L.K., Fales, H.M. (2002) Intramolecular cross-linking experiments on cytochrome c and ribonuclease A using an isotope multiplet method. *Rapid Communications in Mass Spectrometry*, **16**: 149-159

[17] Back, J.W., Hartog, A.F., Dekker, H.L., Muijsers, A.O., de oning, L.J., de Jong, L. (2001) A new crosslinker for mass spectrometric analysis of the quaternary structure of protein complexes. *Journal of the American Society of Mass Spectrometry*, **12**: 222-227

[18] Sinz, A. (2005) Chemical cross-linking and FT-ICR mass spectrometry for protein structure characterization. *Analytical and Bioanalytical Chemstry*, **381**: 44-47

[19] Baumann, M., Meri, S. (2004) Techniques for studying protein heterogeneity and post-translational modifications. *Expert Review of Proteomics*, **1**: 207-217

[20] Seo, J., Lee, K.J. (2004) Post-translational modifications and their biological functions: Proteomic analysis and systematic approaches. *Journal of Biochemistry and Molecular Biology*, **37**: 35-44

[21] Moritz, B., Meyer, H.E. (2003) Approaches for the quantification of protein concentration ratios. *Proteomics*, **3**: 2208-2220

[22] Görg, A. (1998) 2-D Electrophoresis using immobilized pH gradients – Principles and Methods (80-6429-60), Amersham Biosciences, München

[23] O'Farrell, P. (1975) High resolution two-dimensional electrophoresis of proteins. *Journal of Biological Chemistry,* **250**: 4007-4021

[24] Görg, A., Postel, W., Gunther, S. (1988) The current state of two-dimensional electrophoresis with immobilized pH gradients. *Electrophoresis,* **9**: 531-546

[25] Jorgenson, J.W., Lukacs, K.D. (1981) Zone electrophoresis in open-tubular glass capillaries. *Analytical Chemistry*, **53**: 1298-1302

[26] Jorgenson, J.W., Lukacs, K.D. (1983) Capillary Zone Electrophoresis. *Science*, **222**: 266-272

[27] Karger, B.L., Cohen, A.S., Guttmann, A. (1989) High-performance capillary electrophoresis in the biological sciences. *Journal of Chromatography – Biomedical Applications*, **492**: 585-614

[28] Weber, K., Osborn, M. (1969) The Reliability of molecular weight determinations by SDS-PAGE. *Journal of biological chemistry*, **244**: 4406-4412

[29] Laemmli, U.K. (1970) Cleavage of structural proteins during the assembly of the head of bacteriophage T4. *Nature*, **227**: 680-685

[30] Shirahama, K., Tsujii, K., Takagi, T. (1974) Free-boundary electrophoresis of SDS-protein polypeptide complexes with special reference to SDS-PAGE. *Journal of Biochemistry*, **75**: 309-319

[31] Fatin-Rouge, N., Starchev, K., Buffle, J. (2004) Size effects on diffusion processes within agarose gels. *Biophysical Journal*, **86**: 2710-2719

[32] Joosten, J.G.H., Gelade, E.T.F., Pusey, P.N. (1990) Dynamic light scattering by nonergodic media – Brownian particles trapped in polyacrylamide gels. *Physical Review A*, **42**: 2161-2175

[33] Joosten, J.G.H., McCarthy, J.L., Pusey, P.N. (1991) Dynamic and static light scattering by aqueous polyacrylamide gels. *Macromolecules*, **24**: 6690-6699

[34] Suzuki, Y., Nishio, I. (1992) Quasielastic light scattering study of the movement of particles in gels – topological structure of pores in gels. *Physical Review B*, **45**: 4614-4619

[35] Netz, P.A., Dorfmüller, T. (1995) Computer simulation studies of anomalous diffusion in gels – structural properties and probe-size dependence. *Journal of Chemical Physics*, **20**: 9074-9082

[36] Serwer, P. (1989) Sieving of double-stranded DNA during agarose gel electrophoresis. *Electrophoresis*, **10**: 327-331

[37] Serwer, P. (1990) Sieving by agarose gels and its use during pulsed-field electrophoresis. *Biotechnology and Genetic Engineering Reviews*, **8**: 319-343

[38] Suh, M., Ye, P., Datta, A.B., Zhang, M., Fu, J. (2005) An agarose-acrylamide composite native gel system suitable for separating ultra-large protein complexes. *Analytical Biochemistry*, **343**: 166-175

[39] Lambin, P. (1978) Reliability of molecular weight determination of proteins by polyacrylamide gradient gel electrophoresis in the presence of SDS. *Analytical Biochemistry*, **85**: 114-125

[40] Frank, R.N., Rodbard, D. (1975) Precision of SDS-PAGE for the molecular weight estimation of a membrane glycoprotein – studies on bovine rhodopsin. *Archives of Biochemistry and Biophysics*, **171**: 1-13

[41] Pitt-Rivers, R., Impiombato, F.S.A. (1968) The binding of SDS to various proteins. *Biochemical Journal*, **109**: 825-830

[42] Sadeghi, M., Hajivandi, M., Bogoev, R., Amshey, J. (2003) Molecular weight estimation of proteins by gel electrophoresis revisited. *Focus*, Vol. 25.3, 35-39

[43] Swank, R.T., Munkres, K.D. (1971) Molecular weight analysis of oligopeptides by electrophoresis in polyacrylamide gel with SDS. *Analytical Biochemistry*, **39**: 462-477

[44] Fazekas de St. Groth S., Webster R, Datyner A. (1963) Two new staining procedures for quantitative estimation of proteins on electrophoresis strips. *Biochimica and Biophysica Acta,* **71**: 377-391

[45] Oakley, B.R., Kirsch, D.R., Morris, N.R. (1980) A simplified ultrasensitive silver stain for detecting proteins in polyacrylamide gels. *Analytical Biochemistry*, **105**: 361-363

[46] Heukeshoven J., Dernick R. (1988) Improved silver staining procedure for fast staining in PhastSystem Development Unit. I. Staining of sodium dodecyl sulfate gels. *Electrophoresis*, **9**: 28-32

[47] Tribollet E., Dreifuss J., Charpak G., Dominik W., Zaganidis N. (1991) Location and quantitation of tritiated compounds in tissue sections with a gaseous detector of beta particles: comparison with film autoradiography. *Proceedings of the National Academy of Sciences of the United States of America*, **88**: 1466-1468

[48] Rogers, A.W. (1979) Techniques of Autoradiography, 3rd edition. Elsevier North Holland (NL)

[49] Steinberg, T.H., Jones, L.J., Haugland, R.P., Singer, V.L. (1996) SYPRO Orange and SYPRO Red protein gel stains: one-step fluorescent staining of denaturing gels for detection of nanogram levels of protein. *Analytical Biochemistry*, **239**: 223-237

[50] Hutterer, K.M., Jorgenson, J.W. (2005) Separation of hyaluronic acid by ultrahigh-voltage CGE. *Electrophoresis*, **26**: 2027-2033

[51] Guttmann, A. (1996) Effect of temperature on separation efficiency in CGE. *Trends in analytical chemistry*, **15**: 194-198

[52] Heiger, D. (2000) High performance capillary electrophoresis - an introduction, Agilent Technologies, Waldbronn

[53] Ngapo, T.M., Alexander, M. (1999) CGE versus SDS-PAGE of exudate from fresh pork. *Meat Science*, **53**: 145-148

[54] Rodriguez-Delgado, M.A., Malovana, S., Montelongo, F.J., Cifuentes, A. (2002) Fast analysis of proteins in wines by CGE. *European Food Research and Technology*, **214**: 536-540

[55] Brüchert, W., Bettmer, J. (2005) On-line coupling of gel electrophoresis and inductively coupled plasma-sector field-MS for the determination of dsDNA fragments. *Analytical Chemistry*, **77**: 5072-5075

[56] Pfohl, T., Mugele, F., Seemann, R., Herminghaus, S. (2003) Trends in Microfluidics with complex fluids. *ChemPhysChem*, **4**: 1291-1298

[57] Lion, N., Reymond, F., Girault, H.H., Rossier, J.S. (2004) Why the move to microfluidics for protein analysis?. *Current Opinion in Biotechnology*, **15**: 31-37

[58] Stone, H.A., Kim, S. (2001) Microfluidics: Basic issues, applications and challenges. *American Institute of Chemical Engineers*, **47**: 1250-1254

[59] Mueller, O., Hahnenberger, K., Dittmann, M., Yee, H., Dubrow, R., Nagle, R., Ilsley, D. (2000) A microfluidic system for high-speed reproducible DNA sizing and quantitation. *Electrophoresis*, **21**: 128-134

[60] Ogura, M., Agata, Y., Watanabe, K., McCormick, R., Hamaguchi, Y., Aso, Y., Mitsuhashi, M. (1998) RNA chip: quality assessment of RNA by microchannel linear gel electrophoresis in injection-molded plastic chips. *Clinical Chemistry*, **44**: 2249-2255

[61] Woolley, A., Mathies, R. (1995) Ultra-High-Speed DNA Sequencing Using Capillary Electrophoresis Chips. *Analytical Chemistry*, **67**: 3676-3680

[62] Woolley, A.T., Mathies, R.A. (1994) Ultra-high speed DNA fragment separations using microfabricated capillary assay electrophoresis chips. *Proceedings of the National Academy of Sciences of the United States of America*. **91**, 11348-11352

[63] Felton, M. (2003) Lab on a Chip: Poised on the brink. *Analytical Chemistry*, **75**: 505A-508A

[64] Yao, S., Anex, D.S., Caldwell, W.B., Arnold, D.W., Smith, K.B., Schultz, P.G. (1999) SDS-CGE of proteins in microfabricated channels. *Proceedings of the National Academy of Sciences of the United States of America*, **96**: 5372-5377

[65] Kato, M., Gyoten, Y., Sakai-Kato, K., Nakajima, T., Toyo'oka, T. (2005) Analysis of amino acids and proteins using a poly(methylmethacrylate) microfluidic system. *Electrophoresis*, **26**: 3682-3688

[66] Ping, G., Zhu, B., Jabasini, M., Xu, F., Oka, H., Sugihara, H., Baba, Y. (2005) Analysis of Lipoproteins by Microchip electrophoresis with high speed and high reproducibility. *Analytical Chemistry*, **77**: 7282-7287

[67] Herr, A.E., Throckmorton, D.J., Davenport, A.A., Singh, A.K. (2005) On-chip native gel electrophoresis-based immunoassays for Tetanus antibody and toxin. *Analytical Chemistry*, **77**: 585-590

[68] Tsai, S., Loughran, M., Suzuki, H., Karube, I. (2004) Native and sodium SDS-CGE of proteins on a single microchip. *Electrophoresis*, **25**: 494-501

[69] Hawtin, P., Hardern, I., Wittig, R., Mollenhauser, J., Poustka, A.M., Salowsky, R., Wulff, T., Rizzo, C., Wilson, B. (2005) Utility of lab-on-a-chip technology for high-throughput nucleic acid and protein analysis. *Elelectrophoresis*, **26**: 3674-3681

[70] Lu, J.J., Liu, S., Pu, Q. (2005) Replaceable cross-linked polyacrylamide for high performance separation of proteins. *Journal of Proteome Research*, **4**: 1012-1016

[71] Guttmann, A., Horvath, J., Cooke, N. (1993) Influence of temperature on the sieving effect of different polymer matrices in capillary SDS gel electrophoresis of proteins. *Analytical Chemistry*, **65**, 199-203

[72] Buchholz, B.A., Shi, W., Barron, A. (2002) Microchannel DNA sequencing matrices with switchable viscosities. *Electrophoresis*, **23**: 1398-1409

[73] Wu, D., Regnier, F.E. (1992) Sodium dodecyl sulfate-capillary gel electrophoresis of proteins using non-cross-linked polyacrylamide. *Journal of Chromatography A*, **608**: 349-56

[74] Issaq, H.J. (2000) A decade of CE. *Electrophoresis*, **21**: 1921-1939

[75] Verzola, B., Gelfi, C., Righetti, P.G. (2000) Quantitative studies on the adsorption of proteins to the bare silica wall in CE – effects of adsorbed, neutral polymers on quenching the interaction. *Journal of Chromatography* A, **874**: 293-303

[76] Dolnik, V. (2004) Wall coating for CE on microchips. *Electrophoresis*, **25**: 3589-3601

[77] Horvath, J., Dolnik, V. (2001) Polymer wall coatings for CE. *Electrophoresis*, **22**: 644-655

[78] Erim, F.B., Cifuentes, A., Poppe, H., Kraak, J.C. (1995) Performance of a physically absorbed high-molecular-mass polyethyleneimine layer as coating for the separation of basic proteins and peptides by CE. *Journal of Chromatography A*, **708**: 356-361

[79] Busch, M.H.A., Kraak, J.C., Poppe, H. (1995) Cellulose acetate-coated fused-silica capillaries for the separation of proteins by CZE. *Journal of Chromatography A*, **695**: 287-296

[80] Chiari, M., Melis, A. (1998) Low viscosity DNA sieving matrices for CE. *Trends in analytical chemistry*, **17**: 623-632

[81] Brahmasandra, S.N., Ugaz, V.M., Burke, D.T., Mastrangelo, C.H., Burns, M.A. (2001) Electrophoresis in microfabricated devices using photopolymerized polyacrylamid gels and electrode-defined sample injection. *Electrophoresis*, **22**: 300-311

[82] Ganzler, K., Greve, K.S., Cohen, A.S., Karger, B.K., Guttmann, A., Cooke, N.C. (1992) High performance CE of SDS-protein complexes using UV-transparent polymer networks. *Analytical Chemistry*, **64**: 2665-2671

[83] Xu, F., Baba, Y. (2004) Polymer solutions and entropic-based systems for double-stranded DNA CE and microchip electrophoresis. *Electrophoresis*, **25**: 2332-2345

[84] Bergman, M., Claessens, H., Cramers, C. (1998) Properties of entangled polymer solutions in high-performance CE. *Journal of microcolumn separations*, **10**: 19-26

[85] Gas, B., Kenndler, E. (2002) Peak broadening in microchip electrophoresis: a discussion of the theoretical background. *Electrophoresis*, **23**: 3817-3826

[86] Nagata, H., Tabuchi, M., Hirano, K., Baba, Y. (2005) High-speed separation of proteins by microchip electrophoresis using a polyethylen glicol-coated plastic chip with a SDS linear polyacrylamide solution. *Electrophoresis*, **26**: 2687-2691

[87] Bousse L. (2001) Protein sizing on a microchip. *Analytical Chemistry*, **76**: 1207-1212

[88] Jin, L.J., Giordano, B.C., Landers, J.P. (2001) Dynamic Labeling during capillary or microchip electrophoresis for LIF detection of protein-SDS complexes without pre- or postcolumn labeling. *Analytical Chemistry*, **73**: 4994-4999

[89] Sano, M., Nishino, I., Ueno, K., Kamimori, H. (2004) Assay of collagenase activity for native triple-helical collagen using CGE with laser-induced fluorescence detection. *Journal of Chromatography B*, **809**: 251-256

[90] Steinberg, T.H., Haugland, R.P., Singer, V.L. (1996) Applications of SYPRO Orange and SYPRO Red protein gel stains. *Analytical Biochemistry*, **239**: 238-245

[91] Jacobson, S.C., Ramsey, J.M. (1997) Electrokinetic focusing in microfabricated channel structures. *Analytical Chemistry*, **69**, 3212-3217

[92] Scheer, J.M., Ryan, C.A. (2001) A method for the quantitative recovery of proteins from polyacrylamide gels. *Analytical Biochemistry*, **298**: 130-132

[93] Cohen, S.L., Chait, B.T. (1997) Mass spectrometry of whole proteins eluted from SDS polyacrylamide gel electrophoresis gels. *Analytical Biochemistry*, **247**: 257-267

[94] Burlingame, A.L., Boyd, R.K., Gaskell, S.J. (1996) Mass spectrometry. *Analytical Chemistry*, **68**: 599-651R

[95] Burlingame, A.L., Baillie, T.A., Russell, D.H. (1992) Mass spectrometry. *Analytical Chemistry*, **64**: 467-502R

[96] In www.nobelprize.org

[97] Karas, M., Hillenkamp, F. (1988) Laser desorption ionization of proteins with molecular masses exceeding 10.000 daltons. *Analytical Chemistry*, **60**: 2299-2301

[98] Tanaka, K., Waki, H., Ido, Y., Akita, S., Yoshida, Y., Yohida, T. (1988) Protein and polymer analyses up to m/z 100.000 by laser ionization time-of-flight mass spectrometry. *Rapid Communications in Mass Spectrometry,* **2**: 151-153

[99] Karas, M., Bachmann, D., Bahr, U., Hillenkamp, F. (1987) Matrix-assisted ultraviolet laser desorption of non-volatile compounds. *International Journal of Mass Spectrometry and Ion Processes,* **78**: 53-68

[100] Perera, I.K., Kantartzoglou, S., Dyer, P.E. (1996) Some characteristics of matrix-assisted UV laser desorption/ionization mass spectrometry analysis of large proteins. *International Journal of Mass Spectrometry and Ion Porcesses*, **156**: 151-172

[101] Hillenkamp, F., Karas, M., Beavis, R.C., Chait, B.T. (1991) MALDI mass spectrometry of biopolymers. *Analytical Chemistry*, **63**: 1193-1203

[102] Gross, J., Strupat, K. (1998) MALDI mass spectrometry applied to biological macromolcules. t*rends in analytical chemistry*, **17**: 470-484

[103] Beavis, R.C., Chait, B.T. (1990) High-accuracy molecular mass determination of proteins using MALDI mass spectrometry. *Analytical chemistry*, **62**: 1836-1840

[104] Peacock, P.M., McEwen, C.N. (2004) Mass Spectrometry of synthetic polymers. *Analytical Chemistry*, **76**: 3417-3428

[105] Nielen, M.W.F. (1999) MALDI-TOF mass spectrometry of synthetic polymers. *Mass Spectrometric Reviews*, **18**: 309-344

[106] Mechref, Y., Novotny, M.V., Krishnan, C. (2003) Structural characterization of oligosaccharides using MALDI-TOF/TOF tandem mass spectrometry. *Analytical Chemistry*, **75**: 4895-4903

[107] Cabalkova, J., Zidkova, J., Pribyla, L., Chmelik, J. (2004) Determination of carbohydrates in juices by CE, HPLC and MALDI-TOF mass spectrometry. *Electrophoresis*, **25**: 487-493

[108] Karas, M. (1990) Neue Perspektiven der Massenspektrometrie von Biomakromolekülen. *Physikalische Blätter*, **5**: 149-154

[109] Zhang, N., Li, L. (2004) Effects of common surfactants on protein digestion and MALDI-MS analysis of digested peptides using two-layer sample preparation. *Rapid Communications in Mass Spectrometry*, **18**: 889-896

[110] Stikarovska, M., Chmelik, J. (2004) Determination of neutral oligosaccharides in vegetables by MALDI-MS. *Analytica Chimica Acta*, **520**: 47-55

[111] Zehl, M., Allmaier, G. (2004) Ultraviolet MALDI-TOF-MS of intact haemoglobin complex from whole human blood. *Rapid Communications in Mass Spectrometry*, **18**: 1932-1938

[112] He, L., Wei, G., Murray, K.K. (1997) Fragmentation of vitamin B12 in aerosol MALDI. *Journal of the American Society for Mass Spectrometry*, **8**: 140-147

[113] Meetani, M.A., Voorhees, K.J. (2005) MALDI-MS analysis of high molecular weight proteins from whole bacterial cells – pre-treatment of samples with surfactants. *Journal of the American Society for Mass Spectrometry*, **16**: 1422-1426

[114] Montaudo, G., Samperi, F., Montaudo, M.S. (2006) Characterization of synthetic polymers by MALDI-MS. *Progress in Polymer Science (Oxford)*, **31**: 277-357

[115] Montaudo, G., Scamporrino, E., Vitalizi, D., Mineo, P. (1996) Novel procedure for molecular weight averages measurement of polydisperse polymers directly from MALDI-TOF mass spectra. *Rapid Communications in Mass Spectrometry*, **10**: 1551-1559

[116] Laugesen, S., Roepstroff, P. (2003) Combination of two matrices results in improved performance of MALDI-MS for peptide mass mapping and protein analysis. *Journal of the American Society for Mass Spectrometry*, **14**: 992-1002

[117] Vorm, O., Roepstroff, P., Mann, M. (1994) Improved resolution and very high sensitivity in MALDI TOF of matrix surfaces made by fast evaporation. *Analytical Chemistry*, **66**: 3281-3287

[118] Amado, F.M., Santana-Marques, M.G., Ferrer-Correia, A.J., Tomer, K.B. (1997) Analysis of peptide and protein samples containing surfactants by MALDI-MS. *Analytical Chemistry*, **69**: 1102-1106

[119] Börnsen, K.O., Gass, M.A.S., Bruin, G.J.M., Adrichem, J.H.M., Biro, M.C., Kresbach, G.M., Ehrat, M. (1997) Influence of solvents and detergents on MALDI-MS measurements of proteins and oligonucleotides. *Rapid Communications in Mass Spectrometry*, **11**: 603-609

[120] Zhang, N., Li, L. (2002) Ammonium dodecyl sulphate as an alternative to SDS for protein sample preparation with improved performance in MALDI-MS. *Analytical Chemistry*, **74**: 1729-1736

[121] Norris, J.L., Porter, N.A., Caprioli, R.M. (2003) Mass Spectrometry of intracellular and membrane proteins using cleavable detergents. *Analytical Chemistry*, **75**: 6642-6647

[122] Norris, J.L., Porter, N.A., Caprioli, R.M. (2005) Combination detergents/MALDI matrix: functional cleavable detergents for mass spectrometry. *Analytical Chemistry*, **77**: 5036-5040

[123] Linnemayr, K., Rizzi, A., Josic, D., Allmaier, G. (1998) Comparison of microscale cleaning procedures for (Glyco) proteins prior to positive ion MALDI mass spectrometry. *Analytica Chimica Acta*, **372**: 187-199

[124] Dreisewerd, K. (2003) The desorption process in MALDI. *Chemical Reviews*, **103**: 395-425

[125] Ehring, H., Karas, M., Hillenkamp, F. (1992) Role of photoionization and photochemistry in ionization processes of organic molecules and relevance for matrix-assisted laser desorption ionization mass spectrometry. *Organic Mass Spectrometry*, **27**: 472-480

[126] Zenobi, R., Knochenmuss, R. (1998) Ion Formation in MALDI mass spectrometry. *Mass Spectrometry Reviews*, **17**: 337-366

[127] Berkenkamp, S., Kirpekar, F., Hillenkamp, F. (1998) Infrared MALDI Mass Spectrometry of Large Nucleic Acids. *Science,* **281**: 260-262

[128] Spengler, B., Kaufmann, R. (1992) Gentle probe for tough molecules: matrix-assisted laser desorption mass spectrometry. *Analusis*, **20**: 91-101

[129] Glückmann, M., Karas, M. (1999) The initial ion velocity and its dependence on matrix, analyte and preparation method in ultraviolet matrix-assisted laser desorption/ionization. *Journal of Mass Spectrometry*, **34**: 467-477

[130] Mamyrin, B.A. (2001) Time-of-flight mass spectrometry (concepts, achievements and prospects). *International Journal of Mass Spectrometry*, **206**: 251-266

[131] Guilhaus, M., Mlynski, V., Selby, D. (1997) Perfect Timing: Time-of-flight mass spectrometry. *Rapid Communications in Mass Spectrometry*, **11**: 951-962

[132] Mamyrin, B., Karataev, V, Shmikk, D., Zagulin, V. (1973) Mass reflectron. New nonmagnetic time-of-flight high-resolution mass spectrometer. *Zhurnal Eksperimental'noi i Teoreticheskoi Fiziki*, **64**: 82-89

[133] Cotter, R. (1999) The new time-of-flight mass spectrometry. *Analytical Chemistry*, **71**: 445-451A

[134] Grady, J.K., Zang, J., Laue, T.M., Arosio, P., Chasteen, N.D. (2002) Characterization of the H- and L-subunit ratios of Ferritins by SDS-CGE. *Analytical Biochemistry*, **302**: 263-268

[135] Anderson, N.L., Anderson, N.G. (2002) The human plasma proteome. *Molecular and Cellular Proteomics*, **1**: 845-867

[136] Vrablik, M., Ceska, R., Horinek, A. (2001) Major Apolipoprotein B-100 mutations in lipoprotein metabolism and atherosclerosis. *Physiological Research*, **50**: 337-343

[137] Chulkova, T.M., Tertov, V.V. (1993) Degradation of human apolipoprotein B-100 by apolipoprotein(a*). Federation of European Biochemical Societies*, **336**: 327-329

[138] Cruzado, I.D., Cockrill, S.L., McNeal, C.J., Macfarlane, R.D. (1998) Characterization and quantitation of apolipoprotein B-100 by capillary electrophoresis. *Journal of Lipid Research*, **39**: 205-217

[139] Kurokawa, T., Wuhrer, M., Lochnit, G., Geyer, H., Markl, J., Geyer, R. (2002) Hemocyanin from the keyhole limpet *Megathura crenulata* carries a novel type of N-glycans with Gal(b1-6)Man-motifs. *European Journal of Biochemistry*, **269**: 5459-5473

[140] Markl, J., Lieb, B., Gebauer, W., Altenhein, B., Meissner, U., Harris, J.R. (2001) Marine tumor vaccine carriers: structure of the molluscan hemocyanins KLH and HtH. *Journal of Cancer Research and Clinical Oncology*, **127**: R3-R9

[141] Idakieva, K., Stoeva, S., Voelter, W., Gielens, C. (2004) Glycosylations of *Rapana thomasiana* hemocyanin. Comparison with other prosobranch (gastropod) hemocyanins. *Comparative Biochemistry and Physiology, Part B: Biochemistry and Molecular Biology*, **138B**: 221-228

[142] Harris, J.R., Markl, J. (1999) Keyhole limpet hemocyanin: a biomedical review. *Micron*, **30**: 597-623

[143] Vassart, G., Verstreken, L., Dinsart, C. (1977) Molecular weight determination of thyroglobulin 33 S messenger RNA as determined by polyacrylamide gel electrophoresis in the presence of formamide. *Federation of European Biochemical Societies*, **79**: 15-18

[144] Edelhoch, H. (1960) The properties of Thyroglobulin – the effects of alkali. *Journal of Biological Chemistry*, **235**: 1326-1334

[145] Spiro, M.J. (1977) Presence of glucuronic acid-containing carbohydrate unit in human thyroglobulin. *Journal of Biological Chemistry*, **252**: 5424-5430

[146] Alvino, C.G., Tassi, V., Paterson, B.M., DiLauro, R. (1982) In vitro synthesis of 300000 M_r rat thyroglobulin subunit. *Federation of European Biochemical Societies*, **137**: 307-313

[147] Chernoff, S.B., Rawitch, A.B. (1981) Thyroglobulin structure-function. Isolation and characterization of a thyroxine-containing polypeptide from bovine thyroglobulin. *Journal of Biological Chemistry*, **256**: 9425-9430

[148] Spiro, M.J. (1973) Subunit heterogeneity of thyroglobulin. *Journal of Biological Chemistry*, **248**: 4446-4460

[149] Rawitch, A.B., Chernoff, S.B., Litwer, M.R., Rouse, J.B., Hamilton, J.W. (1983) Thyroglobulin structure-function. The amino acid sequence surrounding thyroxine. *Journal of Biological Chemistry*, **258**: 2079-2082

[150] Consiglio, E., Acquaviva, A.M., Formisano, S., Ligouro, D., Gallo, A., Vittorio, T., Santisteban, P., DeLuca, M., Shifrin, S., Yeh, H.J.C., Kohn, L.D. (1987) Characterization of phosphate residues on thyroglobulin. *Journal of Biological Chemistry*, **262**: 10304-10314

[151] Ingham, K.C., Brew, S.A., Broekelmann, T.J., McDonald, J.A. (1984) Thermal stability of human plasma fibronectin and its constituent domains. *Journal of Biological Chemistry*, **259**: 11901-11907

[152] Feldman, S.R., Gonias, S.L., Pizzo, S.V. (1985) Model of α2-macroglobulin structure and function. *Proceedings of the National Academy of Sciences of the United States of America*, **82**: 5700-5704

[153] Roche, P.A., Salvesen, G.S., Pizzo, S.V. (1988) Symmetry of the inhibitory unit of human α2-Macroglobulin. *Biochemistry*, **27**: 7876-7881

[154] Dangott, L.J., Puett, D., Cunningham, L.W. (1983) Conformational changes induced in human α2-macroglobulin by protease and nucleophilic modification. *Biochemistry*, **22**: 3647-3653

[155] Chen, B.J., Wang, D., Yuan, A.I., Feinman, R.D. (1992) Structure of α2-macroglobulin-protease complexes. Methylamine competition shows that proteases bridge two disulfide-bonded half-molecules. *Biochemistry*, **31**: 8960-8966

[156] Gettins, P., Cunningham, L.W. (1986) Identification of ^1H resonances from the bait region of human α2-macroglobulin and effects of proteases and methylamine. *Biochemistry*, **25**: 5011-5017

[157] Peng, H., Sahni, A., Fay, P., Bellum, S., Prudovsky, I., Maciag, T., Francis, C.W. (2004) Identification of a binding site on human FGF-2 for fibrinogen. *Blood*, **103**: 2114-2120

[158] Vecchione, G., Casetta, B., Santacroce, R., Margaglione, M. (2001) A comprehensive on-line digestion-liquid chromatography/mass spectrometry/collision-induced-dissociation MS approach for the characterization of human Fibrinogen. *Rapid Communications in Mass Spectrometry*, **15**: 1383-1390

[159] Townsend, R.R., Hilliker, E., Li, Y.T., Laine, R.A., Bell, W.R., Lee, Y.C. (1982) Carbohydrate structure of human fibrinogen. *Journal of Biological Chemistry*, **257**: 9704-9710

[160] Cote, H.C.F., Pratt, K.P., Davie, E.W., Chung, D.W. (1997) The polymerization pocket "a" within the carboxyl-terminal region of the gamma chain of human fibrinogen is adjacent to but independent from the calcium binding site. *Journal of Biological Chemistry*, **272**: 23792-23798

[161] Yilmaz, H., Tantas, A., Ilgaz, A., Morgan, K.L. (1999) Isolation and preparation of monoclonal antibody to ovine immunoglobulin M. *Turkish Journal of Veterinary and Animal Sciences*, **23**: 135-140

[162] Plaut, A.G., Tomasi, T.B. (1970) Immunoglobulin M: Pentameric Fc_{μ} fragments released by trypsin at higher temperatures. *Proceedings of the National Academy of Sciences of the United States of America*, **65**: 318-322

[163] Wang, F., Nakouzi, A., Angeletti, R.H., Casadevall, A. (2003) Site-specific characterization of the N-linked oligosaccharides of a murine immunoglobulin M by HPLC-ESI-MS. *Analytical Biochemistry*, **314**: 266-280

[164] Symersky, J., Novak, J., McPherson, D.T., DeLucas, L., Mestecky, J. (2000) Expression of the recombinant human immunoglobulin J chain in *E. Coli*. *Molecular Immunology*, **37**: 133-140

[165] Niles, M.J., Matsuuchi, L., Koshland, M.E. (1995) Polymer IgM assembly and secretion in lymphoid and nonlymphoid cell lines: Evidence that J chain is required for pentamer IgM synthesis. *Proceedings of the National Academy of Sciences of the United States of America*, **92**: 2884-2888

[166] Fazel, S., Wiersma, E.J., Shulman, M.J. (1997) Interplay of J chain and disulfide bonding in assembly of polymeric IgM. *International Immunology*, **9**: 1149-1158

[167] Peng J., Gygi S. Proteomics: the move to mixtures. *Journal of Mass Spectrometry*. 2001; **36**: 1083-1091

[168] Schmidt, K. Sugar Rush. *New Scientist* 2002; **176**: 34-36

[169] Durand G., Seta N. (2000) Protein glycosylation and diseases: blood and urinary oligosaccharides as markers for diagnosis and therapeutic monitoring. *Clinical Chemistry,* **46**: 795-805

[170] Lottspeich, F., Zorbas H. (1998) Bioanalytik. Spektrum Verlag, Heidelberg (D)

[171] Chu, F.K. (1986) Requirements of cleavage of high mannose oligosaccharides in glycoproteins by Peptide N-Glycosidase F. *Journal of Biological Chemistry*, **261**: 172-177

[172] Lemp, D., Haselbeck, A., Klebl, F. (1990) Molecular cloning and heterologous expression of N-Glycosidase F from *Flavobacterium meningosepticum*. *Journal of Biological Chemistry*, **265**: 15606-15610

[173] Plummer, T.H., Elder, J.H., Alexander, S., Phelan, A.W., Tarentino, A.L. (1984) Demonstration of Peptide:N-Glycosidase F activity in Endo-b-N-acetylglucosaminidase F preparations. *Journal of Biological Chemistry*, **259**: 10700-10704

[174] Weiskopf, A.S., Vouros, P., Harvey, D.J. (1998) Electrospray ionization-ion trap mass spectrometry for structural analysis of complex N-linked glycoprotein oligosaccharides. *Analytical Chemistry*, **70**: 4441-4447

[175] Rahbek-Nielsen, H., Roepstorff, P., Reischl, H., Wozny, M., Koll, H., Haselbeck, A. (1997) Glycopeptide profiling of human urinary erythropoietin by MALDI-MS. *Journal of mass spectrometry*, **32**: 948-958

[176] Staudinger, H. *From organic chemistry to macromolecules*; Wiley-Interscience: New York, 1970.

[177] Hecht, S., Frechet, J.M.J. (2001) Dendritic Encapsulation of Function: Applying Nature's Site Isolation Principle from Biomimetics to Materials Science. *Angewandte Chemie Internationale Edition*, **40**: 74-91

[178] Boas, U., Heegaard, P.M.H. (2004) Dendrimers in drug research. *Chemical Society Reviews*, **33**: 43-63

[179] Tomalia, D.A., Naylor, A.M., Goddard, I. (1990) Starburst Dendrimers: Molecular-Level Control of Size, Shape, Surface Chemistry, Topology, and Flexibility from Atoms to Macroscopic Matter. *Angewandte Chemie Internationale Edition Englisch*, **29**: 138-175

[180] Voit, B I. (1995) Dendritic polymers: from aesthetic macromolecules to commercially interesting materials. *Acta Polymerica*, **46**: 87-99

[181] Fischer, M.; Vögtle, F. (1999) Dendrimers: From Design to Application - a Progress Report. *Angewandte Chemie Internationale Edition*, **38**: 884-905

[182] van Heerbeek, R.; Kamer, P.C.J.; van Leeuwin, P.W.N.M.; Reek, J.N.H. (2002) Dendrimers as Support for Recoverable Catalysts and Reagents. *Chemical Reviews*, **102**: 3717-3756

[183] Hedrick, J. L.; Magbitang, T.; Conner, E. F.; Glauser, T.; Volksen, W.; Hawker, C. J.; Lee, V. Y.; Miller, R. D. (2002) Application of Complex Macromolecular Architectures for Advanced Microelectronic Materials. *Chemistry - A European Journal*, **8**: 3308-3319.

[184] Schlüter, A. D. (1998) Dendrimers with Polymeric Core: Towards Nanocylinders. T*opics in current chemistry*, **197**: 165-191

[185] Tomalia, D.A., Huang, B., Swanson, D.R., Brothers, H.M., Klimash, J.W. (2003) Structure control within PAMAM dendrimers: size, shape and region-chemical mimicry of globular proteins. *Tetrahedron*, **59**: 3799-3813

[186] Tomalia, D.A.; Baker, H.; Dewald, J.R.; Hall, M.J.; Kallos, G.; Matrin, S. Roeck, J., Ryder, J., Smith, P. (1985) A New Class of Polymers: Starburst-Dendritic Macromolecules. *Polymer Journal (Tokyo)*, **17**: 117-132

[187] Caminade, A.M., Laurent, R., Majoral, J.P. (2005) Characterization of dendrimers. *Advanced Drug Delivery Reviews*, **57**: 2130-2146

[188] Esfand, R., Tomalia, D.A. (2001) PAMAM dendrimers: from biomimicry to drug delivery and biomedical applications. *Drug Delivery Today*, **6**: 427-436

[189] Wang, S., Gaylord, B.S., Bazan, G.C. (2004) Collective optical behaviour of cationic water-soluble dendrimers. *Advanced materials*, 16, **23-24**: 2127-2132

[190] Tomalia, D.A. (2005) Birth of a new macromolecular architecture: dendrimers as quantized building blocks for nanoscale synthetic polymer chemistry. *Progress in Polymer science*, **30**: 294-324

[191] Shi, X., Patri, A.K., Lesniak, W., Islam, M.T., Zhang, C., Baker, J.R., Balogh, L.P. (2005) Analysis of PAMAM-succinamic acid dendrimers by slab-gel electrophoresis and capillary zone electrophoresis, *Electrophoresis*, **26**:2960-2967

[192] Brothers, H.M., Piehler, L.T., Tomalia, D.A. (1998) Slab-gel and CE characterization of PAMAM dendrimers. *Journal of Chromatography A*, **814**: 233-246

[193] Hawker, C.J.; Frechet, J.M.J. (1990) Preparation of polymers with controlled molecular architecture - a new convergent approach to dendritic macromolecules. J*ournal of the American Chemical Society*, **112**: 7638-7647

[194] Zeng, F., Zimmerman, S.C., Kolotuchin, S.V., Reichert, D.E.C., Ma, Y. (2002) Supramolecular polymer chemistry: design, synthesis, characterization, and kinetics, thermodynamics, and fidelity of formation of self-assembled dendrimers. *Tetrahedron*, **58**: 825-843

[195] Maraval, V.; Laurent, R.; Donnadieu, B.; Mauzac, M.; Caminade, A.M.; Majoral, J.P. (2000) Rapid Synthesis of Phosphorus-Containing Dendrimers with Controlled Molecular Architectures: First Example of Surface-Block, Layer-Block, and Segment-Block Dendrimers Issued from the Same Dendron. *Journal of the American Chemical Society*, **122**: 2499-2511.

[196] Padias, A.B.; Hall, H.K.; Tomalia, D.A.; McConnell, J.R. (1987) Starburst polyether dendrimers. *Journal of organic chemistry*, **52**: 5305-5312

[197] Newkome, G.R.; Young, J.K.; Baker, G.R.; Potter, R.L.; Audoly, L.; Copper, D.; Weis, C.G. (1993) Cascade polymers - pH dependence of hydrodynamic radii of acid-terminated dendrimers. *Macromolecules*, **26**: 2394-2396

[198] Prosa, T.J.; Bauer, B.J.; Amis, E.J.; Tomalia, D.A.; Scherrenberg, R. (1997) A SAXS study of the internal structure of dendritic polymer systems. *Journal of Polymer Science Part B*, **35**: 2913-2924.

[199] Prosa, T.J., Bauer, B.J., Amis, E.J. (2001) From Stars to Spheres: A SAXS Analysis of Dilute Dendrimer Solutions. *Macromolecules*, **34**: 4897-4906

[200] Topp, A.; Bauer, B.J.; Tomalia, D.A.; Amis, E.J. (1999) Effect of Solvent Quality on the Molecular Dimensions of PAMAM Dendrimers. *Macromolecules*, **32**: 7232-7237

[201] Li, J., Piehler, L.T., Qin, D., Baker J.R., Tomalia, D.A. (2000) Visualization and characterization of PAMAM dendrimers by atomic force microscopy. *Langmuir*, **16**: 5613-5616

[202] Betley, T.A.; Holl, M.M.B.; Orr, B.G.; Swanson, D.R.; Tomalia, D.A.; Baker, J.R. (2001) Tapping Mode Atomic Force Microscopy Investigation of Poly(amidoamine) Dendrimers: Effects of Substrate and pH on Dendrimer Deformation. *Langmuir*, **17**: 2768-2773

[203] Li, J., Qin, D., Baker, J.R., Tomalia, D.A. (2001) The characterization of high generation poly(amidoamine) G9 dendrimers by atomic force microscopy (AFM). *Macromolecular Symposia*, **167**: 257-269

[204] Betley, T.A.; Hessler, J.A.; Mecke, A.; Holl, M.M.B.; Orr, B.G.; Uppuluri, S.; Tomalia, D.A.; Baker, J.R. (2002) Tapping Mode Atomic Force Microscopy

Investigation of Poly(amidoamine) Core-Shell Tecto(dendrimers) Using Carbon Nanoprobes. *Langmuir*, **18**: 3127-3133

[205] Jackson, C.L., Chanzy, H.D., Booy, F.P., Drake B.J., Tomalia, D.A., Bauer, B.J., Amis, E.J. (1998) Visualization of dendrimer molecules by transmission electron microscopy (TEM): staining methods and cryo-TEM of vitrified solutions. *Macromolecules*, **31**: 6259-6265

[206] Hood, R., Watson, J.T., Jones, A.D. (2006) Resolution and Mass Accuracy of high-mass ions in TOF mass spectrometry: Applications to PAMAM dendrimers. *54th Annual Conference on Mass Spectrometry*

[207] Felder, T., Schalley, C.A., Fakhrnabavi, H., Lukin, O. (2005) A combined ESI- and MALDI-MS(/MS) study of peripherally persulfonated dendrimers false negative results by MALDI-MS and analysis of defects. *Chemistry A European Journal*, **11**: 5625-5636

[208] Baytekin, B., Werner, N., Luppertz, F., Engeser, M., Brüggemann, J., Bitter, S., Henkel, R., Felder, T., Shalley, C.A. (2006) How useful is mass spectrometry for the characterization of dendrimers? "Fake defects" in the ESI and MALDI mass spectra of dendritic compounds. *International Journal of Mass Spectrometry*, **249-250**: 138-148

[209] Subbi, J., Aguraiuja, R., Tanner, R., Allikmaa, V., Lopp, M. (2005) Fragmentation of PAMAM dendrimers in matrix-assisted laser desorption. *European Polymer Journal*, **41**: 2552-2558

[210] Zhou, L., Russell, D.H., Zhao, M., Crooks, R.M. (2001) Characterization of PAMAM dendrimers and their complexes with Cu^{2+} by MALDI mass spectrometry. *Macromolecules*, **34**: 3567-3573

[211] Schwartz, B. L.; Rocwood, A. L.; Smith, R. D.; Tomalia, D. A.; Spindler, R. (1995) Detection of high molecular weight starburst dendrimers by electrospray ionization mass spectrometry. *Rapid Communications in Mass Spectrometry*, **9**: 1552-1555.

[212] Kallos, G. J.; Tomalia, D. A.; Hedstand, D. M.; Lewis, S.; Zhou, J. (1991) Molecular weight determination of a polyamidoamine Starburst polymer by electrospray ionization mass spectrometry. *Rapid Communications in Mass Spectrometry,* **5**: 383-386.

[213] Tolic, K.P., Anderson, G.A, Smith, R.D., Brothers, H.M., Spindler, R., Tomalia, D.A. (1997) ESI-FT-ICR mass spectrometric characterization of high molecular mass Starburst™ dendrimers. *International Journal of Mass Spectrometry and Ion Processes*, **165/166**: 405-417

[214] Frauenrath, H. (2005) Dendronized polymers - building a new bridge from molecules to nanoscopic objects. *Progress in Polymer science*, **30**: 325-384.

[215] Han, M., Chen, P., Yang, X. (2005) Molecular dynamics simulation of PAMAM dendrimer in aqueous solution. *Polymer*, **46**: 3481-3488.

II. Publications

In this chapter four paper proposals are presented.

The first paper is concerned with the analysis of seven high molecular weight proteins with molecular weights higher than 200 kDa using CGE-on-the-chip, planar SDS-PAGE and MALDI-TOF-MS. All proteins were analyzed under non reducing as well as under reducing conditions. The presented work focuses on two main issues. First, a direct comparison of high molecular weight protein sizing with two gel electrophoretical techniques, CGE-on-the-chip and planar SDS-PAGE, was performed. Secondly, the benefits and limitations of MALDI-MS in the high molecular weight range were investigated. Five of seven analyzed proteins were plasma derived. This group of proteins included Fibronectin, Apolipoprotein B-100, α2-Macroglobulin, Fibrinogen and Immunoglobulin M. Moreover, Hemocyanin from Keyhole limpet and Thyroglobulin from bovine thyroid gland were analyzed. In this work it was demonstrated that all three described techniques, CGE-on-the-chip, planar SDS-PAGE and MALDI-TOF-MS, were capable of analyzing high molecular weight protein samples. With the aid of MALDI-TOF-MS the exact molecular weights of all seven high molecular weight proteins were determined which were in good agreement with the values given in literature.

The second paper is concerned with with the analysis of N-linked glycan structures covalently bound to glycoproteins. The primary topic of this article is the analysis of enzymatic de-N-glycosylation of two human serum glycoproteins (Antithrombin III and Coagulation Factor IX) using PNGase F (N-Glycosidase F). To monitor the progress of de-N-glycosylation three different analytical techniques (CGE-on-the-chip, planar SDS-PAGE and MALDI-TOF-MS) were applied. The performance of both applied gel electrophoretical methods provided very similar results and it was possible to distinguish between the various glycoforms. While analysis with MALDI-TOF-MS provided the most accurate molecular weights, molecular weight determination with CGE-on-the-chip was heavily affected by extensive protein glycosylations.

In the third paper the characterization of PAMAM dendrimers from generation two (G2) up to generation ten (G10) using Matrix Assisted Laser Desorption/Ionization Time-Of-Flight Mass Spectrometry (MALDI-TOF-MS) in the linear mode and nano-Electrospray-Gas-phase Electrophoretic Molecular Mobility Analysis (nES-GEMMA) is presented. For the first time

the molecular masses of real large dendrimers G8-G10 were determined by MALDI mass spectrometry and by nES-GEMMA, techniques which are based on different physico-chemical principles. Obtained experimental data allowed the determination of the exact molecular mass, the spherical size and the calculation of the density of all dendrimer generations G2 to G10. Amounts in the picomole range were sufficient for analysis and measurements could be performed within several minutes. The results based on the two new methods for dendrimer research exhibited an excellent correlation and open up new avenues. Furthermore the results were compared with published data using techniques based on different principles.

The topic of the fourth paper is the molecular weight determination of very high molecular weight biomolecules with Matrix Assisted Laser Desorption/Ionization Time-Of-Flight Mass Spectrometry (MALDI-TOF-MS). For this purpose the applied analytes were polyclonal human Immunoglobulin M and a Poly(amindo amine) (PAMAM) dendrimer of generation 10. According to literature both samples have molecular weights of about 1000 kDa. For the first time molecular weight determination of both samples was carried out on a commercial MALDI mass spectrometer. In this work it was demonstrated that molecular weight determination of very high molecular mass analytes with good mass accuracy and sensitivity (despite their structural heterogeneity in terms of polydispersity and glycosylation) is possible on an instrument, containing no special instrumental features as e.g. cryo detectors or unusual high acceleration voltages and which is at the present time available on the market. However, the main limitation for analysis in the very high molecular weight range with MALDI-TOF-MS was the availability of suitable calibration standards.

Journal of Biomolecular Techniques, *in preparation* (2006)

Molecular weight determination of several high molecular weight proteins using CGE-on-the-chip, planar SDS-PAGE and MALDI-TOF-MS

Roland Müller[1], M. Kratzmeier[2], H. Elgass[2], Günter Allmaier[1*]

[1]Institute of Chemical Technologies and Analytics, Vienna University of Technology, A-1060 Vienna, Austria

[2]Agilent Technologies, Waldbronn, Germany

Corresponding author: Günter Allmaier, Institute of Chemical Technologies and Analytics, Vienna University of Technology, Getreidemarkt 9/164, A-1060 Vienna, Austria

Tel: +43 1 58801 15160 Fax: +43 1 58801 15199

E-mail: guenter.allmaier@tuwien.ac.at

Keywords: High molecular weight proteins; CGE-on-the-chip; planar SDS-PAGE; MALDI-TOF-MS; molecular weight determination

Abstract

The molecular weight of seven proteins with molecular weights higher than 200 kDa was determined with CGE-on-the-chip, planar SDS-PAGE and MALDI-TOF-MS. While the analysis of high molecular weight proteins with planar SDS-PAGE was an already well established technique, the feasibility of MALDI-TOF-MS for the exact molecular weight determination of high mass proteins was only partly described in literature so far. CGE-on-the-chip is the newest of all three applied analytical techniques and was so far not tested and evaluated for the analysis of high molecular weight proteins. All proteins were analyzed under non reducing as well as under reducing conditions. The presented work focuses on two main issues concerning high molecular weight proteins. First, a direct comparison of high molecular weight protein sizing with two gel electrophoretical techniques, CGE-on-the-chip and planar SDS-PAGE, was performed. Secondly, the benefits and limitations of MALDI-MS in the high molecular weight range were investigated. Five of seven analyzed proteins were plasma derived. This group of proteins included Fibronectin, Apolipoprotein B-100, α2-Macroglobulin, Fibrinogen and Immunoglobulin M. Moreover, Hemocyanin from Keyhole limpet and Thyroglobulin from bovine thyroid gland were analyzed.

Introduction

Analytical techniques. The most common techniques for the molecular weight determination of proteins are mass spectrometry [1-4], denaturing gel electrophoresis and gel filtration [5-7]. In this paper one mass spectrometric and two gel electrophoretical techniques were applied for the molecular weight determination of seven different high mass proteins. Today, planar SDS-PAGE is the most wide-spread method for separating proteins electrophoretically. The popularity of this technique comes from its simplicity, efficiency, reproducibility and sensitivity. In 1969 the reliability of molecular weight determination of several proteins in the

molecular weight range between 12 and 200 kDa was demonstrated by Weber and Osborn [8]. Consequently, planar SDS-PAGE became a generally accepted technique for determining the molecular weights of proteins. For the analysis of proteins with SDS-PAGE the analytes are denatured with the aid of heat and sodium dodecyl sulphate (SDS), an ionic detergent. In turn SDS/protein complexes are formed which consist of a rather constant weight ratio of 1,4 g SDS to 1 g protein. Due to the high molar ratio of SDS the intrinsic charge of the protein becomes insignificant. Afterwards the SDS/protein complexes are separated electrophoretically with the aid of a sieving polymer called gel matrix. Since the SDS/protein complexes have identical charge densities and conformations, electrophoretic migration through the gel matrix is only based on the size of the SDS/protein complexes. Molecular weight determination in SDS gel electrophoresis is performed by comparing the migration behaviour of individual SDS/protein complexes with the migration behaviour of known standards [9]. In gel electrophoresis the most commonly used way of visualizing proteins is based on staining procedures which are performed after the electrophoretical separation is finished. For the experiments presented in this paper Coomassie Brilliant Blue R-250 (CBB R-250) was used for protein visualization after planar SDS-PAGE. CBB R-250 is a triphenylmethane dye with high extinction coefficients and high protein affinity [10]. CGE-on-the-chip is based on Lab-on-the-chip technology. While no exact scientific for the term Lab-on-a-chip technology can be given, all commercially available Lab-on-the-chip devices are based on microfluidic systems and chips capable of performing multiple functions [11]. Generally, the term microfluidics merely refers to microstructures carrying fluids which are can be applied for the analysis of proteins, DNA, RNA, drugs or entire cells [12-15]. Major benefits of Lab-on-the-chip instruments over conventional analysis systems are a higher degree of automation and lower amounts of sample solution required for analysis. Due to lower analysis times high-throughput analysis is possible. The first commercially available lab-on-the-chip system was introduced in 1999 by Agilent Technologies and was based on

CGE [16]. The corresponding lab-on-the-chip instrument is called 2100 Bioanalyzer and is a CGE Lab-on-a-chip device which integrates and automates sample handling, separation, staining, destaining, detection and data analysis. At the moment the application range extends to the automated analysis of DNA, RNA, cells and protein samples. Generally the separation principle of CGE-on-the-chip is identical to planar SDS-PAGE, but there are many practical differences. For CGE-on-the-chip linear polymers instead of cross-linked polymer networks are used as gel matrix. The instrument contains 16 individual programmable electrodes which are coupled with a high-voltage power supply and are required for sample injection and separation. Analysis of proteins with CGE-on-the-chip is performed with the aid of microfabricated silica chips which consist of a network of connected micro-channels. These chips are made of glass with photolithographically defined wet-etched channels and have dimensions of 17,5 to 17,5 mm. The CGE-on-the-chip device is equipped with 16 individual programmable high-voltage electrodes which are applied for the electrokinetic injection and separation of protein samples. Sample separation occurs in a separation capillary with an effective separation length of 1,25 cm. Detection is based on laser induced fluorescence (LIF) and the instrument is equipped with a 10 mW semiconductor laser which emits laser light with a wavelength of 630 nm. In order to maintain a constant temperature of 30°C during sample injection and separation the instrument is equipped with a thermostat and an air based cooling system. Today, all commercial CGE-on-the-chip protein assays are limited to a sizing range of about 250 kDa. MALDI-TOF-MS is a well established analytical method for the molecular weight determination of biopolymers [17-23]. This mass spectrometric technique is applied for the analysis of proteins, peptides, oligosaccharides, synthetic polymers and nucleic acids. The linear TOF mass analyzer offers a large analyzable molecular weight range, high sensitivity and high mass accuracy, which cannot be obtained with other biochemical or electrophoretical methods. Theoretically TOF mass analyzers offer an unlimited analyzable mass to charge range [24]. However, there are several practical factors which limit the

analyzable mass to charge range. Limiting factors are unwanted fragmentations of analyte ions during the desorption process and during migration through the drift tube as well as practical limitations of the detector itself. Next to the high analyzable molecular weight range other advantages of MALDI-TOF mass spectrometry are high sensitivity and accuracy. The main disadvantages of MALDI-TOF-MS are the rather high instrumentation cost, the lack of quantification capability and difficulties of finding a proper sample preparation technique for a given type of analyte. An advantage of gel electrophoresis over MALDI-TOF-MS is that the first technique allows the simultaneous molecular weight determination of several proteins in a mixture without suppression effects as well as the quantification of proteins.

High molecular weight proteins. In this paper the term high molecular weight (HMW) protein is referred to proteins which have molecular weights higher than 200 kDa. The seven analyzed HMW proteins can be systematically divided into three different types. The first type of protein consists only of one single polypeptide backbone with a molecular weight higher than 200 kDa. Such proteins might form non covalent aggregates but under denaturing conditions only high molecular weight polypeptide backbones are observed. Hence, reducing agents have no significant influence on this type of protein. Apolipoprotein B-100 and Hemocyanin are examples for this type of HMW protein. The second type comprises HMW proteins which consist of polypeptide chains with molecular weights higher than 200 kDa which are linked together through disulfide bridges. Unlike the first type described above these HMW proteins are significantly affected by reducing agents. Examples for this type of HMW protein are Fibronectin and Thyroglobulin. The third type of HMW proteins consists of proteins build up of polypeptide chains smaller than 200 kDa which are linked together through disulfide bridges. Fibrinogen, Immunoglobulin M and α2-Macroglobulin are examples for this type of HMW proteins. Generally most high molecular weight proteins are produced in higher organisms, but some exceptions are known. While the majority of

mammalian proteins have molecular weights below 100 kDa the importance of HMW proteins should not be underestimated. Some of the most abundant human blood serum proteins like Fibrinogen, α2-Macroglobulin, Immunoglobulin M and Apolipoprotein B-100 belong to the class of HMW proteins [25]. α2-Macroglobulin (α2M) is a major serum protein which belongs to the class of protease inhibitors and is capable of irreversible inhibiting all four classes of proteases by a unique trapping mechanism which forms a molecular trap around proteases. The protein has a peptide stretch, called bait region, which contains specific cleavage sites for different proteases. A maximum of two proteases can be bound per α2-Macroglobulin tetramer and generally two subunits are cleaved per protease molecule bound [26]. When a protease cleaves the peptide stretch a conformational change is induced and in turn the protease is trapped by α2-Macroglobulin. Covalent binding of the protease to α2-Macroglobulin is not required for irreversible inhibition. Nevertheless in addition to non covalent trapping most of the bound protease is covalently bound to α2-Macroglobulin via amide bonds formed between lysyl amino groups and internal cysteine-glutamate thioesters [27]. α2-Macroglobulin is a homotetramer and consists of two pairs of disulfide-linked polypeptide chains. While two subunits are linked covalently through two disulfide bridges, the resulting dimer forms non covalent homotetrameric protein complexes with other dimers. In literature α2-Macroglobulin is described to resemble a hollow cylinder which is comprised of two identical functional halves with three C_2 axes of symmetry and no mirror planes [28]. Known PTMs of tetrameric α2M are several inter- and intra-chain disulfide bridges and 32 N-linked sugar residues. According to literature intact, tetrameric α2-Macroglobulin has a molecular weight of 725 kDa [29-30]. Fibrinogen (FG), also called coagulation factor I, is a plasma glycoprotein essential for blood clotting and produced by hepatic parentchymal cells. Mean serum concentrations of human fibrinogen are about 3 mg/mL. The conversion of soluble fibrinogen monomers into insoluble fibrin monomers which is followed by polymerization and aggregation of fibrin monomers is the terminal step of the blood clotting

cascade. Thrombin triggers the conversion of fibrinogen to fibrin by cleaving fibrinopeptides A and B from the N-termini of α- and β- chains and thus exposing the polymerization sites responsible for clot formation. The resulting fibrin monomers form soft clots which are then converted into hard clots by factor XIIIa which catalyzes the covalent cross-linking of glutamate and lysine amino acid residues between gamma chains and between alpha chains of different monomers. Fibrinogen is found at elevated levels after surgical trauma and pregnancy and is decreased in cases of liver cirrhosis and serum hepatitis. Further fibrinogen acts as a cofactor in platelet aggregation. Fibrinogen is a 340 kDa glycoprotein composed of two pairs of three separate polypeptide chains [31]. The three types of subunits are called α-, β- and γ-chains. While the α-chain has no sugar residues, the β-chain has one N-linked and the γ-chain two N-linked glycan residues. In the literature a molecular weight of 66,2 kDa is stated for the α-chain, while for the β- and γ- chain molecular weights of 54,2 and 48,4 kDa are given [32]. About one-third of all α-chains are phosphorylated. While the β-chain has one N-linked glycan the γ-chain has two N-linked glycan residues. The total reported carbohydrate content of fibrinogen is only about 3% [33]. Next to multiple intra-chain disulfide bridges the individual fibrinogen subunits are linked together by several inter-chain disulfide bridges. By electron microscopy FG appears as a trinodular structure in which the central nodule contains the amino termini of all six chains [34]. Immunoglobulin M (IgM) is an antibody and an important product of the immune system because it plays a critical role in the early protection against bacterial infections. It is the predominant antibody class made against certain antigens such as microbial polysaccharides. With typical concentrations of about 1,5 mg/mL IgM is one of the most abundant proteins found in human blood serum. Normally IgM is found as a pentameric molecule composed of five Y-shaped subunits and one joining J-chain. The five subunits are covalently linked through disulfide bridges and thus form one single molecule under non reducing conditions. The reported average molecular weight of intact IgM under non reducing conditions is between 900 and 1000 kDa [35-36].

Each Y-shaped subunit consists of two heavy and two light chains. Light chain molecules have molecular weights of about 25 kDa and are not glycosylated, while heavy chain molecules have molecular weights of about 75 kDa and are glycosylated. The J-chain has a molecular weight of about 15 kDa and contains one N-linked glycan residue [37]. Thyroglobulin (Thyro) is an iodine-containing protein stored in thyroid gland. When the thyroid is stimulated by thyroid stimulating hormone (TSH) thyroglobulin is coverted into circulating thyroxines. The protein is produced in the thyroid gland and is a precursor of the iodinated thyroid hormones thyroxine (T4) and triiodothyronine (T3). Due to its large size and absence from plasma under normal conditions thyroglobulin is very immunogenic and hence often used as carrier protein for the production of antibodies. Thyroglobulin is an extensively post-translational modified homodimeric protein which consists of two polypeptide subunits. Known post-translational modifications (PTMs) are 14 N-linked glycan residues, three thyroxine residues and one triiodothyronine per subunit. The presence of inter-chain or intra-chain disulfide bridges is not exactly described in literature. According to literature intact, dimeric Thyroglobulin has a molecular weight of 660 kDa [38-39]. The protein is known to be an excellent source of N-linked glycan residues of various structures [40]. The carbohydrate content of thyroglobulin comprises about 10% of the total molecular weight [41]. Despite the presence of two intact polypeptide chains in each thyroglobulin dimer smaller protein fragments ranging down to 20 kDa were observed in SDS-PAGE under reducing conditions and reported in literature [42-43]. Keyhole limpet Hemocyanin (HC) is found in the hemolymph of the mollusc Megathura crenulata and belongs to a large family of giant extracellular respiratory proteins responsible for the oxygen-transport in blood. Hemocyanins are found in many mollusc and athropod species. Each oxygen binding site of a HC subunit contains two copper ions, resulting in the characteristic blue color of the oxygenated molecule. Due to its high molecular weight hemocyanin is widely used as hepten carrier and immune stimulant. HC consists of two structurally and physiologically distinct isoforms (KLH1 and

KLH2) each being based on a subunit consisting of one single polypeptide chain with a molecular weight of approximately 400 kDa [44]. Every KLH subunit comprises 8 different globular functional units of about 50 kDa. At the level of the quaternary structure KLH1 occurs as a cylindrical didecamer, whereas KLH2 exists as a mixture of didecamers and tubular multidecamers with molecular weights of roughly 8 MDa for each didecamer. Such didecamer have diameters of about 35 nm [45]. Both KLH forms have different glycosylation patterns. KLH 1 has a total carbohydrate content of 3,0%, while KLH 2 has a carbohydrate content of 3,4% [46]. Apolipoprotein B-100 (Apo B-100) is the dominant protein constituent of low density lipoproteins (LDL) and is also found in very low density lipoproteins (VLDL). It is a ligand for the LDL receptor and acts as a cofactor in enzymatic reactions and as a recognition signal for the cellular binding and internalization of LDL particles. Furthermore Apo B-100 is necessary for the assembly of VLDL particles. Human Apolipoprotein B-100 is produced in the liver and has a mean serum concentration of about 1 mg/mL. It was also demonstrated that Apolipoprotein B-100 can bind to artery wall proteoglycans and thus appears to be a crucial initiating event in atherogenesis [47]. Apolipoprotein B-100 consists of one single polypeptide backbone which is modified with 19 N-linked glycan residues, one S-palmitoyl cysteine and 8 intra-chain disulfide bridges. Palmitoylation is required for the proper assembly of the hydrophobic core of the lipoprotein particle. The Apo B-100 molecule is modelled as a belt which surrounds the low density lipoprotein (LDL) particle [48]. According to literature Apolipoprotein B-100 has a molecular weight of about 550 kDa [49]. One of the analytical problems in characterizing Apo B-100 is that in the free form the protein is insoluble in aqueous solutions and tends to form aggregates. Fibronectin (FN) is found either as soluble plasma protein or as fibrils in the extracellular matrix. FN mostly forms heterodimers or multimers of alternatively spliced variants which are connected by two disulfide bridges near the carboxyl ends of the polypeptide backbones. To a lesser extend homodimers are observed as well. Plasma FN has a dimeric form, whereas cellular FN is

found as dimer or cross-linked multimer. Plasma FN is secreted by hepatocytes, whereas cellular FN is produced by fibroblasts, epithelial cells or other cell types. Fibronectin has the ability to bind to collagenous and glycosaminoglycan constituents of the connective tissue, to actin, DNA, heparin, fibrinogen and some other plasma proteins as well as to various cell surfaces. Moreover, fibronectins have a variety of different functions like cell adhesion, wound healing, cell motility and maintenance of cell shape. Known PTMs of Fibronectin are seven N-linked and two O-linked glycan residues and one phosphoserine. The carbohydrate content is only about 5% of the total molecular weight of the protein. Next to two inter-chain disulfide bridges which connect the individual subunits, each Fibronectin subunit has almost 30 intra-chain disulfide bridges. A molecular weight of about 220 kDa for each polypeptide chain is reported in literature [50].

Material and Methods

Chemicals and Materials. Water, methanol, acetic acid, formic acid and acetonitrile (ACN) were purchased from Merck. Trifluoroacetic acid was purchased from Riedel-de-Haen. Sinapic acid (SA), 2,4,6-trihydroxyacetophenon monohydrate (THAP), Coomassie Brilliant Blue R-250 and dithiotreitol (DTT) was provided from Fluka. Lithium dodecylsulfate (LDS) was applied from Sigma-Aldrich. All described chemicals from Merck, Riedel-de-Haen, Fluka and Sigma-Aldrich were of analytical grade. Analysis with planar gel electrophoresis was carried out with pre-cast 3-8% Tris-Acetate gels (1,0mm x 10 wells), NuPAGE LDS Sample Buffer (4x) and NOVEX Tris-Acetate SDS Running Buffer (20x) from Invitrogen. Planar SDS-PAGE was calibrated using the HiMark Unstained High Molecular Weight Protein Standard (Invitrogen). For MALDI-TOF-MS calibration the Invitromass High Molecular Weight Mass Calibrant Kit (Invitrogen) was applied. Sample purification for the analysis with MALDI-TOF-MS was performed using ZipTip pipette tips from Millipore which contained C4 and HPL column residues. Gel matrix, sample buffer, protein dye

concentrate, P200 plus ladder, spin filters and protein chips applied for analysis with CGE-on-the-chip were provided in the Protein P200 plus Kit (Agilent Technologies). Bovine thyroid gland Thyroglobulin (Thyro), human polyclonal Immunoglobulin M (IgM), Keyhole limpet Hemocyanin (HC), human plasma Fibrinogen (FG), bovine plasma Fibronectin (FN), human plasma Apolipoprotein B-100 (Apo) and human plasma α2-Macroglobulin were purchased from Calbiochem.

MALDI-TOF mass spectrometry

Instrumentation. The MALDI-TOF-MS experiments were carried out on an Axima TOF^2 instrument from Shimadzu Biotech Kratos Analytical. The device is a high resolution, floorstanding instrument equipped with a pulsed nitrogen laser (wavelength: 337 nm, pulse width: 4 ns), an integrated 1 GHz transient recorder, a curved field reflector, a differential pumped collision gas cell and a flight tube with a flight path length of 1,2 meters. The instrument was operated in the positive ion linear mode applying an accerlerating voltage of 20 kV without delayed extraction. All mass spectra were acquired by averaging 50 to 200 unselected and consecutive laser shots on the same preparation by rastering. In order to obtain statistical reliable results all samples were measured at least ten times and the arithmetic mean values of the determined molecular weights were calculated. Data evaluation was performed using the Shimadzu Biotech Launchpad v.2.4.1. All mass spectra were smoothed using the company-supplied Savitzky-Golay algorithm [CHL-63]. The applied peak detection method was Threshold-Centroid at 50% height of the peak maximum.

Sample preparation and analysis. Prior to analysis with MALDI-TOF-MS matrix solutions were prepared freshly. Sinapic acid and THAP was dissolved in 1/1 (v/v) 0,1% TFA/ACN to give final MALDI matrix concentrations of 6 mg/mL in the case of SA or 10 mg/mL in the case of THAP. The resulting MALDI matrix solutions were vortexed thoroughly for several

seconds. For all high molecular weight proteins except of α2-Macroglobulin THAP was used as MALDI matrix. In the case of α2-Macroglobulin SA was used as MALDI matrix. Three different types of sample preparation techniques were applied for the analysis of high molecular weight proteins with MALDI-TOF-MS. The volume mixture technique was the most simple of all three sample preparation techniques and was used for the analysis of Fibrinogen, Thyroglobulin and α2-Macroglobulin under non reducing conditions. In the case of the volume mixture technique 2 uL sample solution containing between 0,25 and 1 mg/mL protein sample were mixed with 4 uL matrix solution. The second sample preparation technique was applied in order to remove salts from protein solutions. This sample preparation technique was used for the analysis of Hemocyanin and Immunoglobulin M under non reducing conditions. For this method ZipTips pipette tips with reversed-phase C4 resins were applied. 1 uL 1% TFA was added to 10 uL sample solution containing a protein concentration of 1 ug/uL and the mixture was vortexed thoroughly and spinned down afterwards. First a ZipTip C4 pipette tip was put on a 20 uL Gilson pipette which was set to 10 uL. Wetting solution (50%(v/v) acetonitrile, 0,05% TFA) and washing solution (0,1% TFA) were prepared freshly. The ZipTip C4 pipette tip was conditioned by aspirating and dispensing the wetting solution three times. The dispensed solutions were discarded. Then the pipette tip was washed by aspirating and dispensing the washing solution three times. During the binding step the sample solution was aspirated and dispensed at least three times and protein was bound to the reversed-phase column. Before the proteins were eluted the column was washed by aspirating and dispensing the washing solution two times. In the final step the purified proteins were eluted with about 2 to 4 uL MALDI matrix solution. For the analysis of all high molecular weight proteins under reducing conditions sample purification with ZipTip pipette tips containing hydrophilic HPL resins were applied. In order to reduce the proteins' disulfide bridges 10 uL sample solution containing about 10 ug protein were mixed with 0,5 uL 10% LDS and 1 uL 1M DTT in a 0,5 mL Eppendorf tube. The resulting mixture was

vortexed thoroughly, spinned down and incubated in a microwave (12 minutes, 170W). For removing the detergents from the protein sample a ZipTip HPL pipette tip was put on a 20 uL Gilson pipette which was set to 10 uL and solutions A (90%(v/v) acetonitrile, 0,1%(v/v) formic acid) and solution B (50%(v/v) acetonitrile, 0,1%(v/v) formic acid) were prepared freshly. First 10 uL solution A were mixed with the sample solution. For conditioning the ZipTip HPL pipette tip solution B is aspirated and dispensed to waste once. In the next step the pipette tip is equilibrated by aspirating and dispensing solution A three times. The dispensed solutions were pipetted to the waste. Then the protein sample was bound to the chromatographic media by aspirating and dispensing the sample solution seven times. For washing the column and removing detergent molecules solution A was aspirated and dispensed to waste ten times. Finally the purified protein sample was eluted with about 2 to 4 uL MALDI matrix solution. Regardless of the applied type of sample preparation technique 0,5 uL aliquots of the resulting matrix/sample mixtures were deposited on several different spots on a stainless steel microtiterformat MALDI target and dried under a gentle stream of air forming crystalline layers. Molecular weight calibration was performed externally by using the Invitromass High Molecular Weight Mass Calibrant, which contained various recombinant standard proteins with given molecular weights in the mass range from 30 kDa to 160 kDa. The calibration kit was applied according to the manufacturer's instructions, but in contrast to the mentioned instruction manual the two MALDI matrix solutions described earlier above were applied for sample preparation.

Planar SDS-PAGE

Instrumentation. Planar gel electrophoresis was carried out in an EI9001–X Cell II Mini Cell gel chamber from Novex. Prior to the electrophoretical separation 800 mL freshly diluted Tris-Acetate SDS Running Buffer was filled into the gel chamber. The applied electrophoresis power supply PowerEase 500 was provided by Amersham Pharmacia Biotech. After

visualisation the gels were scanned with an Image Scanner from Amersham Pharmacia Biotech. Integration and evaluation of the detected sample spots was performed manually using the Image Master LabScan v.3.01b and ImageQuant TL 1D v.2005 software (Amersham).

Sample preparation and analysis. For analysis of the protein samples under non reducing conditions 6 µL sample solution with a protein content between 0,25 and 1 mg/mL, 3 uL NuPAGE LDS Sample Buffer (4x) and 3 uL water were mixed in a 0,5 mL Eppendorf tube, vortexed for several seconds and spinned down. Analysis under reducing conditions was performed by adding 3 uL 0,1M DTT instead of 3 uL water to the sample solution. Heat denaturation was performed using an Eppendorf Thermoblock (1 minute, 99°C). After heat denaturation the solutions were spinned down again and cooled down to room temperature. Then 10 uL of the resulting sample mixture was applied directly onto the slab gel. For the molecular weight determination with planar SDS-PAGE the HiMark Unstained High Molecular Weight Protein Standard was applied. The HiMark Protein ladder contained of nine standard proteins in the molecular weight range of 40 to 500 kDa. Preparation of the ladder solution was performed by mixing 6 uL HiMark Protein standard solution with 3 uL NuPAGE LDS Sample Buffer (4x) and 3 uL water in a 0,5 mL Eppendorf tube. The mixture was vortexed for several seconds, spinned down and then applied directly onto the slab gel without heat denaturation. For the electrophoretical separation a constant voltage of 150 V was applied. Electrophoresis was stopped when the blue marker front reached the bottom of the slab gels. The typical duration of an electrophoretical separation was about 70 minutes. After the separation was finished the gels were placed in a Fixing solution (45%(v/v) methanol, 5%(v/v) acetic acid) for 30 minutes and incubated under slight agitation. Protein visualisation was performed by replacing the Fixing solution with Coomassie staining solution (0,1%(w/v) Coomassie Brilliant Blue R-250, 45%(v/v) methanol, 9%(v/v) acetic acid). The incubation

time in the Coomassie staining solution was 45 minutes. Finally the staining solution was removed and the gels were placed in a Destaining solution (45%(v/v) methanol, 9%(v/v) acetic acid) for at least 90 minutes. The Destaining solution was changed several times and it was destained until the deep blue gel background was completely removed.

CGE-on-the-chip

Instrumentation. CGE-on-the-chip experiments were carried out using the 2100 Bioanalyzer and the Protein P200 plus assay (Agilent Technologies). The instrument was operated and the obtained results were integrated and evaluated with the aid of the 2100 Expert software v.B.02.02.SI238. In order to adopt the Protein P200 plus assay to the analysis of high molecular weight proteins slight modifications were necessary and some software settings were customized.

Sample preparation and analysis. Prior to analysis gel-dye-mix, destaining solution and denaturing solution were prepared. For the preparation of the gel-dye-mix 650 uL gel matrix were mixed with 25 uL protein dye concentrate, vortexed thoroughly for several seconds and spinned down. Then the gel-dye-mix was pipetted into a spin filter. The destaining solution was prepared by pipetting 650 uL gel matrix solution directly into a spin filter. Both spin filters were centrifuged at 2500g for 15 minutes and the resulting filtrates were pipetted into two Eppendorf tubes. Depending on whether CGE-on-the-chip analysis was performed under reducing or non reducing conditions 200 uL sample buffer were mixed either with 7 uL 1M DTT or 7 uL water. Afterwards the resulting denaturing solutions were vortexed for several seconds. For analysis with CGE-on-the-chip and the Protein P200 plus assay 4 uL sample solution with a protein content between 0,25 and 1 mg/mL were mixed with 2 uL destaining solution in a 0,5 mL Eppendorf tube, vortexed thoroughly and spinned down. For the external protein sizing calibration up to a molecular weight of 210 kDa the Protein P200 plus ladder

was applied. Moreover, the denaturing solution contained two reference proteins called lower and upper marker which act as internal references for molecular weight determination and quantitation. Without adding denaturing solution 6 uL ladder solution were pipetted into a 0,5 mL Eppendorf tube. Heat denaturation of the ladder and sample solutions was performed using an Eppendorf Thermoblock (4 minutes, 95°C). After heat denaturation the protein solutions were spinned down again and cooled down to room temperature. Finally 84 uL water were added to all sample solutions and the ladder solution in order to give a final volume of 90 uL. At this point of the workflow 12 uL gel-dye-mix were filled in the marked well at the right top of a protein chip. The chip was placed into the chip priming station and gel-dye-mix was filled into the micro-channel network by air pressure. Then the remaining gel-dye-mix was removed from the well. Afterwards 12 µL gel-dye-mix and 12 µL destaining solution were filled in the designated wells marked with G and DS. In the final working step 6 uL sample solution and 6 uL ladder solution were pipetted into the wells marked with the numbers 1-10 and with the ladder symbol. After placing the ready chip into the CGE-on-the-chip instrument analysis was started by the Expert software. While peak analysis and integration was not limited by a certain molecular weight, molecular weight determination was only possible up to 210 kDa due to the lack of a proper protein sizing calibration in the high molecular weight range. Consequently, migration times and not molecular weights were given for the characterization of analyte peaks in the molecular weight range above 210 kDa. For this purpose the peaks of the lower and upper marker were used as references with constant migration times of 18 sec (lower marker) and 40 sec (upper marker).

Results and Discussion

α2-Macroglobulin. Analysis of α2M with CGE-on-the-chip under non reducing conditions showed only one significant analyte peak (dimeric α2M) at a migration time of 45,9 sec (Fig. 1 a). Moreover, one analyte peak with very low intensity was found at migration time of about

57,5 sec which could probably be correlated with two covalently linked α2M dimers. Due to its biological function native α2M is known to be capable of forming covalent bonds between various amino acid residues. Under reducing conditions α2M dimers split into monomers, so the most intensive analyte peak was detected at a migration time of 39,1 sec. Because this analyte peak was located between the lower and upper marker and was hence within the CGE-on-the-chip calibration range the molecular weight of the α2M monomer could be determined. Based on CGE-on-the-chip the molecular weight of the monomeric α2M was 199 kDa. Next to the α2M monomer peak also several α2M degradation products in the molecular weight range between 14 kDa and 210 kDa were found under reducing conditions which were not detected under non reducing conditions. With planar SDS-PAGE only one single analyte band was observed under non reducing (α2M dimer) and reducing conditions (α2M monomer) (Fig. 1 b). For the α2M dimer a molecular weight of 361 kDa and for the α2M monomer a molecular weight of 176 kDa was determined. Unlike in the case of CGE-on-the-chip no significant bands of sample degradation products were found under reducing conditions. Analysis of α2M with MALDI-TOF-MS under non reducing conditions showed the singly, doubly and triply charged molecular ion peaks of the α2M dimer (Fig. 1 c). For molecular weight determination the triply charged molecular ion peak was applied and provided a molecular weight of 351,1 kDa for the α2M dimer. Under reducing conditions the singly, doubly and triply charged molecular ion peaks of the α2M monomer were detected with MALDI-TOF-MS (Fig. 1 d). Next to the three molecular ion peaks described above also the singly charged α2M dimer molecular ion peak, the doubly charged α2M trimer molecular ion peak and the triply charged α2M dimer molecular ion peak was observed. It was most likely that the observed α2M multimer peaks were non covalent aggregates formed during the desorption and ionization process. Based on the doubly charged monomeric α2M molecular ion peak a molecular weight of 174,3 kDa was determined for the α2M monomer. The molecular weights determined for α2M with planar SDS-PAGE was only 1-3% lower than the

molecular weight given in literature. According to literature tetrameric α2M has a molecular weight of 725 kDa (Table 1). The results obtained with MALDI-TOF-MS were 4% below the molecular weights stated in literature. With CGE-on-the-chip the determined molecular weight of the α2M monomer was 10% higher than the molecular weight given in literature. However, it was not surprising that the molecular weight determined for α2M with CGE-on-the-chip was higher than the results obtained with other analytical techniques because heavily glycosylated proteins were known to provide measured higher molecular weights with CGE-on-the-chip than non glycosylated proteins.

Fibrinogen. Using CGE-on-the-chip the analyte peaks of two different FG isoforms were observed under non reducing conditions (Fig. 2 a). The smaller isoform (isoform 1) had a migration time of 44,1 sec while the larger isoform (isoform 2) had a migration time of 45,7 sec. Under reducing conditions the α-chain, β-chain and γ-chain was detected. For the α-chain a molecular weight of 79 kDa (27,0 sec) was measured, while for the β-chain a molecular weight of 65 kDa (28,0 sec) and for the γ-chain a molecular weight of 57 kDa (29,1 sec) was obtained with CGE-on-the-chip. With planar SDS-PAGE sample bands of the two FG isoforms were observed under non reducing conditions (Fig. 2 b). For FG isoform 1 a molecular weight of 312 kDa and for FG isoform 2 a molecular weight of 375 kDa was determined. Under reducing conditions the three different subunits were detected. The measured molecular weight of the FG α-chain was 61 kDa. For the β-chain a molecular weight of 50 kDa and for the γ-chain a molecular weight of 46 kDa was measured. With both gel electrophoretical techniques the bands/peaks of the two FG isoforms observed under non reducing conditions were well resolved. Analysis of intact FG with MALDI-TOF-MS under non reducing conditions showed the singly, doubly, triply and four times charged molecular ion peaks of both FG isoforms (Fig. 2 c). Based on the triply charged molecular ion peaks a molecular weight of 305,8 kDa was determined for FG isoform 1 and a molecular weight of

337,6 kDa for FG isoform 2. Like in the case of gel electrophoresis the peaks of the two FG isoforms were well resolved and had similar signal intensities. Under reducing conditions the singly and doubly charged molecular ion peaks of the α-, β- and γ-chains were observed with MALDI-TOF-MS (Fig. 2 d). Interestingly, the analyte peaks of the non modified α-chain were significantly smaller and had a poorer signal to noise ratio compared with the peaks of the glycosylated β- and γ-chain. Based on the singly and doubly charged molecular ion peaks a molecular weight of 65,8 kDa was determined for the α-chain, a molecular weight of 54,0 kDa for the β-chain and a molecular weight of 48,2 kDa for the γ-chain. Hence, all molecular weights determined with MALDI-TOF-MS for the FG subunits were in excellent agreement with the molecular weights given in literature (Fig. 2). Based on the molecular weights determined for the FG subunits intact FG has a calculated molecular weight of 336 kDa. For intact FG a molecular weight of 340 kDa was reported in literature. The molecular weight obtained for intact FG with MALDI-TOF-MS was 1% (isoform 2) and 10% (isoform 1) respectively below the molecular weight given in literature for intact FG. While the molecular weights obtained with planar SDS-PAGE for the FG subunits were 4% to 8% below the data published in literature, all molecular weights obtained with CGE-on-the-chip were 20% higher than the molecular weights stated in literature.

Immunoglobulin M. Under non reducing conditions one single analyte peak with a migration time of 59,6 sec was observed for IgM with CGE-on-the-chip (Fig. 3 a). Under reducing conditions IgM light and heavy chains were detected. For the light chain a molecular weight of 26 kDa was obtained, while for the heavy chain a molecular weight of 111 kDa was determined. Comparable results were obtained with planar SDS-PAGE (Fig. 3 b). For intact IgM without the presence of a reducing agent only one diffuse band close to the gel pocket was found. Under reducing conditions a molecular weight of 25 kDa was determined for the light chain and a molecular weight of 76 kDa for the heavy chain. Because no separation was

possible below a molecular weight of 40 kDa a 10% Bis-Tris gel instead of a 3-8% Tris-Acetate gel for the molecular weight determination of the IgM light chain. Analysis of IgM under non reducing conditions using MALDI-TOF-MS showed analyte peaks of several different charge states of the intact IgM molecule. In the MALDI mass spectra of intact IgM the three times up nine times charged molecular ion peaks of IgM were detected (Fig. 3 c). Based on the seven, eight and nine times charged molecular ion peaks an average molecular weight of 1026,4 kDa was obtained for intact IgM. Under reducing conditions the IgM light chain, heavy chain and a non covalent aggregate of one light and one heavy chain was observed with MALDI-TOF-MS (Fig. 3 d). In all three cases the corresponding singly and doubly charged molecular ions were found. Based on the singly charged molecular ion peaks a molecular weight of 23,3 kDa was obtained for the IgM light chain and a molecular weight of 70,6 kDa for the IgM heavy chain. The molecular weight obtained for intact IgM with MALDI-TOF-MS was in good agreement with the molecular weight stated in literature (Table 3). Concerning the molecular weight determination of the light and heavy chain the measured molecular weights were 6 to 7% below the molecular weights given in literature. The molecular weights obtained for the IgM light chain and heavy chain using planar SDS-PAGE were in very good agreement with the data published in literature. Also the molecular weight obtained with CGE-on-the-chip for the light chain was in very good agreement with literature, whereas the molecular weight measured for the heavy chain was significantly higher (+48%) than the molecular weight given in literature. Like in the case of α2M this significant difference between the results obtained for the IgM heavy chain with planar SDS-PAGE and CGE-on-the-chip can be explained by the fact that the IgM heavy chain was heavily glycosylated. As already mentioned earlier heavily glycosylated proteins have slower migration times and hence higher measured molecular weights in CGE-on-the-chip compared with ordinary non glycosylated proteins.

Thyroglobulin. With CGE-on-the-chip under non reducing conditions monomeric and dimeric Thyro was found (Fig. 4 a). The Thyro dimer peak had a migration time of 56,4 sec, while the Thyro monomer peak had a migration time of 44,4 sec. Under reducing conditions only monomeric Thyro and several degradation products were detected. The measured migration time of the Thyro monomer was slightly lower under reducing conditions than under non reducing conditions. Analysis with planar SDS-PAGE showed protein bands of monomeric and dimer Thyro under non reducing conditions (Fig. 4 b). While the Thyro dimer band was found at a molecular weight higher than 500 kDa and was hence out of the calibration range, a molecular weight of 250 kDa was determined for the Thyro monomer. Furthermore, two more protein bands with molecular weights higher than 500 kDa were observed under non reducing conditions. Like in the case of CGE-on-the-chip only monomeric Thyro was observed in planar SDS-PAGE under reducing conditions. Again, the measured molecular weight was slightly lower under reducing than under non reducing conditions. Based on the results obtained with both gel electrophoretic techniques it was proven that Thyro dimers consist partly of monomers covalently linked through disulfide bridges and partly of non covalently assembled monomers. As already described in the literature Thyro showed several Thyro degradation products with both electrophoretical techniques under reducing conditions. With MALDI-TOF-MS usable results were obtained only under reducing conditions. The MALDI mass spectra of Thyro showed the singly, doubly, triply, four times and five times charged molecular ion peaks of the Thyro monomer (Fig. 4 c). Next to the Thyro monomer analyte peaks other less intensive sample peaks were detected which probably stemmed from impurities also observed with gel electrophoresis. For molecular weight determination of the Thyro monomer based on the triply charged molecular ion peak a molecular weight of 331,6 kDa was obtained. Hence, the determined molecular weight was in excellent agreement with the molecular weight given in literature. According to literature a molecular weight of 660 kDa was expected for dimeric Thyro (Table 4).

Interestingly, the molecular weight determined for the Thyro monomer with planar SDS-PAGE was significantly below (-24%) the molecular weight stated in literature.

Hemocyanin. In the case of Hemocyanin only one single analyte peak/band was observed with both gel electrophoretical methods under reducing and non reducing conditions (Fig. 5 a-b). No degradation products or protein impurities were detected. Analysis with planar SDS-PAGE provided a molecular weight of 360 kDa (reducing and non reducing conditions). With CGE-on-the-chip a migration time of 49,3 sec was observed under reducing and non reducing conditions. The molecular weight determined for Hemocyanin with SDS-PAGE was 10% below the molecular weight given in literature (Table 5). The obtained MALDI mass spectra of Hemocyanin under non reducing conditions showed five analyte peaks (Fig. 5 c). These analyte peaks represented several different charge states of the Hemocyanin molecular ion. While the double charged molecular ion peak was the most intensive analyte peak, all molecular ion peaks with one to five charges were detected. For molecular weight determination only the three times and four times charge molecular ion peaks were applied because the five times charged analyte peak had only a poor signal to noise ratio. The molecular weight of Hemocyanin determined with MALDI-TOF-MS (404,6 kDa) was only 1% higher than the molecular weight given in literature (Tab. 1; 400 kDa). With none of the three applied analytical techniques it was possible to differentiate between the KLH1 and KLH2 isoform.

Apolipoprotein B-100. With CGE-on-the-chip one single sample peak at a migration time of 53,4 sec was observed for Apolipoprotein B-100 under reducing and non reducing conditions (Fig. 6 a). Similar results were observed with planar SDS-PAGE (Fig. 6 b). In this case only one single protein band which had an identical Rf value like the 500 kDa band of the HiMark ladder was found under reducing and non reducing conditions. Some Apo B-100 degradation

products with molecular weights between 200 kDa and 500 kDa were detected with both electrophoretical techniques as well. In the MALDI mass spectra of Apo B-100 under reducing conditions the two, three, four and five times charged molecular ion peaks of Apo B-100 were observed (Fig. 6 c). Since Apo B-100 is a very large and hydrophobic protein a very poor desorption and ionization behaviour was expected. Consequently, all analyte peaks had a comparably poor signal to noise ratio. Based on the four times charged molecular ion peak a molecular weight of 542,9 kDa was determined with MALDI-TOF-MS for Apo B-100 (Table 6). Hence, the determined molecular weight was only 1% below the molecular weight given in literature (550 kDa).

Fibronectin. Under reducing conditions two distinct types of FN subunits were observed with CGE-on-the-chip and planar SDS-PAGE (Fig. 7 a-b). With both electrophoretical techniques the two sample bands/peaks were only poorly resolved. In the case of planar SDS-PAGE a molecular weight of 229 kDa was determined for the smaller FN subunit (FN isoform 1) and a molecular weight of 243 kDa for the larger FN subunit (FN isoform 2). With CGE-on-the-chip migration times of 44,0 sec (isoform 1) and 44,8 sec (isoform 2) were measured. According to the results obtained with both gel electrophoretical techniques the concentration of both FN subunits was roughly similar. Under non reducing conditions only one single sample peak at a migration time of 57,7 sec was detected with CGE-on-the-chip. Planar SDS-PAGE showed two distinct sample bands at molecular weights higher than 500 kDa under non reducing conditions. Moreover, diffuse protein bands close to the gel pocket indicated that some amounts of FN were not separated electrophoretically. Analysis of FN under non reducing conditions using MALDI-TOF-MS showed no usable analyte peaks. On the other hand under reducing conditions the singly, doubly and triply charged molecular ion peaks of both FN subunits were observed (Fig. 7 c). The doubly charged molecular ion peaks had the highest intensity of all analyte peaks. In the case of the singly and doubly charged molecular

ion peaks the two types of subunits were only poorly resolved. FN subunit 1 showed slightly more intensive analyte peaks than FN subunit 2. Next to the FN analyte peaks some non specific peaks were found in the MALDI mass spectra of FN which most likely stemmed from sample impurities also observed with planar SDS-PAGE. For molecular weight determination the doubly and triply charged molecular ion peaks were applied. The determined molecular weights were 249,4 kDa for FN subunit 1 and 263,1 kDa for FN subunit 2 (Table 7). According to literature both FN subunits are reported to have a molecular weight of about 220 kDa so the molecular weights determined with MALDI-TOF-MS was 13-20% higher than the molecular weights given in literature. However, it should be noted that no mass spectrometric data were available for the intact FN subunits so the data given in literature should be regarded conditionally. Comparing the results obtained for both FN subunits with planar SDS-PAGE the molecular weights determined with MALDI-TOF-MS were about 8% higher.

Conclusions

In this work it was demonstrated that all three described techniques, CGE-on-the-chip, planar SDS-PAGE and MALDI-TOF-MS, were capable of analyzing high molecular weight protein samples. It was further shown that the results obtained with CGE-on-the-chip were in very good agreement with the protein band patterns observed with old-fashioned planar SDS-PAGE. In the case of very high molecular weight proteins like IgM CGE-on-the-chip results were superior to the results observed with planar SDS-PAGE. The practical benefits of CGE-on-the-chip over planar SDS-PAGE were faster analysis times, a higher degree of automation and larger accessible sizing range. Until now no commercial planar SDS-PAGE system is capable of separating proteins according to their molecular weight in the molecular weight range from 14 to 1000 kDa. At the moment the main drawback of CGE-on-the-chip was the lack of a suitable sizing calibration in the molecular weight range above 210 kDa. Analysis

with MALDI-TOF-MS using a commercial standard instrument provided exact molecular weights for all high molecular weight proteins. With the aid of a suitable MALDI matrix and sample preparation technique the desorption and ionization of all seven high molecular weight proteins was possible and in all cases the determined molecular weights were in good or excellent agreement with the values given in literature. Exact molecular weight determination with MALDI-TOF-MS was feasible because some multiple charged molecular ion peaks of high molecular weight analytes were detected at mass to charge ratios below 160.000 and hence were within the calibration range. Consequently the usefulness of MALDI-TOF-MS for the exact molecular weight determination of high molecular weight proteins was demonstrated.

Legends to tables

Table 1. Summary of the molecular weights determined for α2-Macroglobulin (o.c. – out of calibration range)

Table 2. Summary of the molecular weights determined for Fibrinogen (o.c. – out of calibration range)

Table 3. Summary of the molecular weights determined for Immunoglobulin M (o.c. – out of calibration range; the value marked with an asterisk was not determined with 3-8% Tris-Acetate gels but 10% Bis-Tris gels from Invitrogen)

Table 4. Summary of the molecular weights determined for Thyroglobulin (o.c. – out of calibration range; n.a. – not available)

Table 5. Summary of the molecular weights determined for Hemocyanin

Table 6. Summary of the molecular weights determined for Apolipoprotein B-100

Table 7. Summary of the molecular weights determined for Fibronectin (n.a. – not available)

Legends to figures

Figure 1. (a) CGE-on-the-chip electropherograms of α2-Macroglobulin (red line: non reducing conditions, blue line: reducing conditions); (b) Planar SDS-PAGE gel of α2-Macroglobulin (left lane: non reducing conditions, middle lane: marker, right lane: reducing conditions); (c) Positive ion MALDI mass spectra of α2-Macroglobulin (non reducing conditions); (d) Positive ion MALDI mass spectra of α2-Macroglobulin (reducing conditions)

Figure 2. (a) CGE-on-the-chip electropherograms of Fibrinogen (red line: non reducing conditions, blue line: reducing conditions); (b) Planar SDS-PAGE gel of Fibrinogen (left lane: non reducing conditions, middle lane: marker, right lane: reducing conditions); (c) Positive ion MALDI mass spectra of Fibrinogen (non reducing conditions); (d) Positive ion MALDI mass spectra of Fibrinogen (reducing conditions)

Figure 3. (a) CGE-on-the-chip electropherograms of Immunoglobulin M (red line: non reducing conditions, blue line: reducing conditions); (b) Planar SDS-PAGE gel of Immunoglobulin M (left lane: non reducing conditions, middle lane: marker, right lane: reducing conditions); (c) Positive ion MALDI mass spectra of Immunoglobulin M (non reducing conditions); (d) Positive ion MALDI mass spectra of Immunoglobulin M (reducing conditions)

Figure 4. (a) CGE-on-the-chip electropherograms of Thyroglobulin (red line: non reducing conditions, blue line: reducing conditions); (b) Planar SDS-PAGE gel of Thyroglobulin (left lane: non reducing conditions, middle lane: marker, right lane: reducing conditions); (c) Positive ion MALDI mass spectra of Thyroglobulin (non reducing conditions)

Figure 5. (a) CGE-on-the-chip electropherograms of Hemocyanin (red line: non reducing conditions, blue line: reducing conditions); (b) Planar SDS-PAGE gel of Hemocyanin (left lane: non reducing conditions, middle lane: marker, right lane: reducing conditions); (c) Positive ion MALDI mass spectra of Hemocyanin (non reducing conditions)

Figure 6. (a) CGE-on-the-chip electropherograms of Apolipoprotein B-100 (red line: non reducing conditions, blue line: reducing conditions); (b) Planar SDS-PAGE gel of Apolipoprotein B-100 (left lane: non reducing conditions, middle lane: marker, right lane: reducing conditions); (c) Positive ion MALDI mass spectra of Apolipoprotein B-100 (reducing conditions)

Figure 7. (a) CGE-on-the-chip electropherograms of Fibronectin (red line: non reducing conditions, blue line: reducing conditions); (b) Planar SDS-PAGE gel of Fibronectin (left lane: non reducing conditions, middle lane: marker, right lane: reducing conditions); (c) Positive ion MALDI mass spectra of Fibronectin (reducing conditions)

References and Notes

[1] Belgacem O, Buchacher A, Pock K, et al. Molecular weight determination of plasma-derived glycoproteins by ultraviolet MALDI-TOF-MS with internal calibration. *J Mass Spectrom* 2002; 37:1118-1130

[2] Luque-Garcia JL, Zhou G, Sun T, Neubert TA. Use of nitrocellulose membranes for protein characterization by MALDI-MS. *Anal Chem* 2006;78:5102-5108

[3] Liu Z, Schey KL. Optimization of a MALDI TOF-TOF mass spectrometer for intact protein analysis. *J Am Soc Mass Spectrom* 2005;16:482-490

[4] Kleinova M, Belgacem O, Pock K, Rizzi A, Buchacher A, Allmaier G. Characterization of cysteinylation of pharmaceutical-grade human serum albumin by ESI-MS and low-energy collision-induced dissociation tandem mass spectrometry. *Rapid Commun Mass Spectrom* 2005;19:2965-2973

[5] Whitaker JR. Determination of molecular weights of proteins by gel filtration on sephadex. *Anal Chem* 1981;35:1950-1953

[6] Andrews P. Estimation of molecular weights of proteins by gel filtration. *Nature* 1962;196:36-39

[7] Steere RL, Ackers GK. Restricted-diffusion chromatography through calibrated columns of granulated agar gel: a simple method for particle size determination. *Nature* 1962;196:475-476

[8] Weber K, Osborn M. The Reliability of molecular weight determinations by SDS-PAGE. *J Biol Chem* 1969;244:4406-4412

[9] Shapiro AL, Vinuela E, Maizel JV. Molecular weight estimation of polypeptide chains by electrophoresis in SDS polyacrylamide gels. *Biochem Biophys Res Commun* 1967;28:815-820

[10] Fazekas de St. Groth S, Webster R, Datyner A. Two new staining procedures for quantitative estimation of proteins on electrophoresis strips. *Biochim Biophys Acta* 1963;71:377-391

[11] Felton M. Lab on a Chip: Poised on the brink. *Anal Chem* 2003;75:505A-508A

[12] Mueller O, Hahnenberger K, Dittmann M, et al. A microfluidic system for high-speed reproducible DNA sizing and quantitation. *Electrophoresis* 2000;**21**:128-134

[13] Ogura M, Agata Y, Watanabe K, et al. RNA chip: quality assessment of RNA by microchannel linear gel electrophoresis in injection-molded plastic chips. *Clin Chem* 1998;44:2249-2255

[14] Woolley A, Mathies R. Ultra-High-Speed DNA Sequencing Using Capillary Electrophoresis Chips. *Anal Chem* 1995;67:3676-3680

[15] Woolley AT, Mathies RA. Ultra-high speed DNA fragment separations using microfabricated capillary assay electrophoresis chips. *P Natl Acad Sci USA* 1994;91,11348-11352

[16] Hawtin P, Hardern I, Wittig R, et al. Utility of lab-on-a-chip technology for high-throughput nucleic acid and protein analysis. *Elelectrophoresis* 2005;26:3674-3681

[17] Perera IK, Kantartzoglou S, Dyer PE. Some characteristics of matrix-assisted UV laser desorption/ionization mass spectrometry analysis of large proteins. *Int J Mass Spectrom* 1996;156:151-172

[18] Hillenkamp F, Karas M, Beavis RC, Chait BT. MALDI mass spectrometry of biopolymers. *Anal Chem* 1991;63:1193-1203

[19] Gross J, Strupat K. MALDI mass spectrometry applied to biological macromolcules. *TrAC-Trends Anal Chem* 1998;17:470-484

[20] Beavis RC, Chait BT. High-accuracy molecular mass determination of proteins using MALDI mass spectrometry. *Anal Chem* 1990;62:1836-1840

[21] Belgacem O, Buchacher A, Pock K, et al. Molecular mass determination of plasma-derived glycoproteins by ultraviolet matrix-assisted laser desorption/ionization time-of-flight mass spectrometry with internal calibration. *J Mass Spectrom* 2002;37:1118-1130

[22] Peacock PM, McEwen CN. Mass Spectrometry of synthetic polymers. *Anal Chem* 2004;76:3417-3428

[23] Nielen MWF. MALDI-TOF mass spectrometry of synthetic polymers. *Mass Spectrom Rev* 1999;18:309-344

[24] Mamyrin BA. Time-of-flight mass spectrometry (concepts, achievements and prospects). *Int J Mass Spectrom* 2001;206:251-266

[25] Anderson NL, Anderson NG. The human plasma proteome. *Mol Cell Proteomics* 2002;1:845-867

[26] Chen BJ, Wang D, Yuan AI, Feinman RD. Structure of α2-macroglobulin-protease complexes. Methylamine competition shows that proteases bridge two disulfide-bonded half-molecules. *Biochemistry* 1992;31:8960-8966

[27] Gettins P, Cunningham LW. Identification of ^{1}H resonances from the bait region of human α2-macroglobulin and effects of proteases and methylamine. *Biochemistry* 1986;25:5011-5017

[28] Feldman SR, Gonias SL, Pizzo SV. Model of α2-macroglobulin structure and function. *P Natl Acad Sci USA* 1985;82:5700-5704

[29] Roche PA, Salvesen GS, Pizzo SV. Symmetry of the inhibitory unit of human α2-Macroglobulin. *Biochemistry* 1988;27:7876-7881

[30] Dangott LJ, Puett D, Cunningham LW. Conformational changes induced in human α2-macroglobulin by protease and nucleophilic modification. *Biochemistry* 1983;22:3647-3653

[31] Peng H, Sahni A, Fay P, et al. Identification of a binding site on human FGF-2 for fibrinogen. *Blood* 2004;103:2114-2120

[32] Vecchione G, Casetta B, Santacroce R, Margaglione M. A comprehensive on-line digestion-liquid chromatography/mass spectrometry/collision-induced-dissociation MS approach for the characterization of human Fibrinogen. *Rapid Commun Mass Spectrom* 2001;15:20011383-1390

[33] Townsend RR, Hilliker E, Li YT, Laine RA, Bell WR, Lee YC. Carbohydrate structure of human fibrinogen. *J Biol Chem* 1982;257:9704-9710

[34] Cote HCF, Pratt KP, Davie EW, Chung DW. The polymerization pocket "a" within the carboxyl-terminal region of the gamma chain of human fibrinogen is adjacent to but independent from the calcium binding site. *J Biol Chem* 1997;272:23792-23798

[35] Yilmaz H, Tantas A, Ilgaz A, Morgan KL. Isolation and preparation of monoclonal antibody to ovine immunoglobulin M. *Turk J Vet Anim Sci* 1999;23:135-140

[36] Plaut AG, Tomasi TB. Immunoglobulin M: Pentameric Fc_{μ} fragments released by trypsin at higher temperatures. *P Natl Acad Sci USA* 1970;65:318-322

[37] Symersky J, Novak J, McPherson DT, DeLucas L, Mestecky J. Expression of the recombinant human immunoglobulin J chain in *E. Coli*. *Mol Immunol* 2000;37:133-140

[38] Vassart G, Verstreken L, Dinsart C. Molecular weight determination of thyroglobulin 33 S messenger RNA as determined by polyacrylamide gel electrophoresis in the presence of formamide. *FEBS J* 1977;79:15-18

[39] Edelhoch H. The properties of Thyroglobulin – the effects of alkali. *J Biol Chem* 1960;235:1326-1334

[40] Spiro MJ. Presence of glucuronic acid-containing carbohydrate unit in human thyroglobulin. *J Biol Chem* 1977;252:5424-5430

[41] Alvino CG, Tassi V, Paterson BM, DiLauro R. In vitro synthesis of 300000 M_r rat thyroglobulin subunit. *FEBS J* 1982;137:307-313

[42] Chernoff SB, Rawitch AB. Thyroglobulin structure-function. Isolation and characterization of a thyroxine-containing polypeptide from bovine thyroglobulin. *J Biol Chem* 1981;256:9425-9430

[43] Spiro MJ. Subunit heterogeneity of thyroglobulin. *J Biol Chem* 1973;248:4446-4460

[44] Kurokawa T, Wuhrer M, Lochnit G, Geyer H, Markl J, Geyer R. Hemocyanin from the keyhole limpet *Megathura crenulata* carries a novel type of N-glycans with Gal(b1-6)Man-motifs. *Eur J Biochem* 2002;269:5459-5473

[45] Markl J, Lieb B, Gebauer W, Altenhein B, Meissner U, Harris JR. Marine tumor vaccine carriers: structure of the molluscan hemocyanins KLH and HtH. *J Cancer Res Clin* 2001;127:R3-R9

[46] Idakieva K, Stoeva S, Voelter W, Gielens C. Glycosylations of *Rapana thomasiana* hemocyanin. Comparison with other prosobranch (gastropod) hemocyanins. *Comp Biochem Phys B* 2004;138B:221-228

[47] Karlsson H, Leanderson P, Tagesson C, Lindahl M. Lipoproteomics I: Mapping of proteins in low-density lipoprotein using two-dimensional gel electrophoresis and mass spectrometry. *Proteomics* 2005;5:551-565

[48] Vrablik M, Ceska R, Horinek A. Major Apolipoprotein B-100 mutations in lipoprotein metabolism and atherosclerosis. *Physiol Res* 2001;50: 337-343

[49] Chulkova TM, Tertov VV. Degradation of human apolipoprotein B-100 by apolipoprotein(a*). FEBS J* 1993;336:327-329

[50] Ingham KC, Brew SA, Broekelmann TJ, McDonald JA. Thermal stability of human plasma fibronectin and its constituent domains. *J Biol Chem* 1984;259:11901-11907

	CGE-on-the-chip [sec]	CGE-on-the-chip [kDa]	SDS-PAGE [kDa]	MALDI-MS [kDa]	literature [kDa]
α2M dimer	45,9	o.c.	361	351,1 kDa	363 kDa
α2M monomer	39,1	199	176	174,3 kDa	181 kDa

Table 1

	CGE-on-the-chip [sec]	CGE-on-the-chip [kDa]	SDS-PAGE [kDa]	MALDI-MS [kDa]	literature [kDa]
FG isoform 1	44,1	o.c.	312	305,8 kDa	~340 kDa
FG isoform 2	45,7	o.c.	375	337,6 kDa	~340 kDa
FG α-chain	27,0	79	61	65,8 kDa	66 kDa
FG β-chain	28,0	65	50	54,0 kDa	54 kDa
FG γ-chain	29,1	57	46	48,2 kDa	48 kDa

Table 2

	CGE-on-the-chip [sec]	CGE-on-the-chip [kDa]	SDS-PAGE [kDa]	MALDI-MS [kDa]	literature [kDa]
IgM intact	59,6	o.c.	o.c.	1026,4 kDa	~1000 kDa
IgM light chain	22,8	26	25*	23,3 kDa	~25 kDa
IgM heavy chain	31,7	111	76	70,6 kDa	~75 kDa

Table 3

	CGE-on-the-chip [sec]	SDS-PAGE [kDa]	MALDI-MS [kDa]	literature [kDa]
Thyro dimer	56,4	o.c.	n.a.	660 kDa
Thyro monomer	44,4	250	331,6 kDa	330 kDa

Table 4

	CGE-on-the-chip [sec]	SDS-PAGE [kDa]	MALDI-MS [kDa]	literature [kDa]
HC	49,3	360	404,6 kDa	~400 kDa

Table 5

	CGE-on-the-chip [sec]	SDS-PAGE [kDa]	MALDI-MS [kDa]	literature [kDa]
Apo	53,4	500	542,9 kDa	550 kDa

Table 6

	CGE-on-the-chip [sec]	SDS-PAGE [kDa]	MALDI-MS [kDa]	literature [kDa]
FN intact	57,7	n.a.	n.a.	n.a.
FN isoform 1	44,0	229	249,4 kDa	~220 kDa
FN isoform 2	44,8	243	263,1 kDa	~220 kDa

Table 7

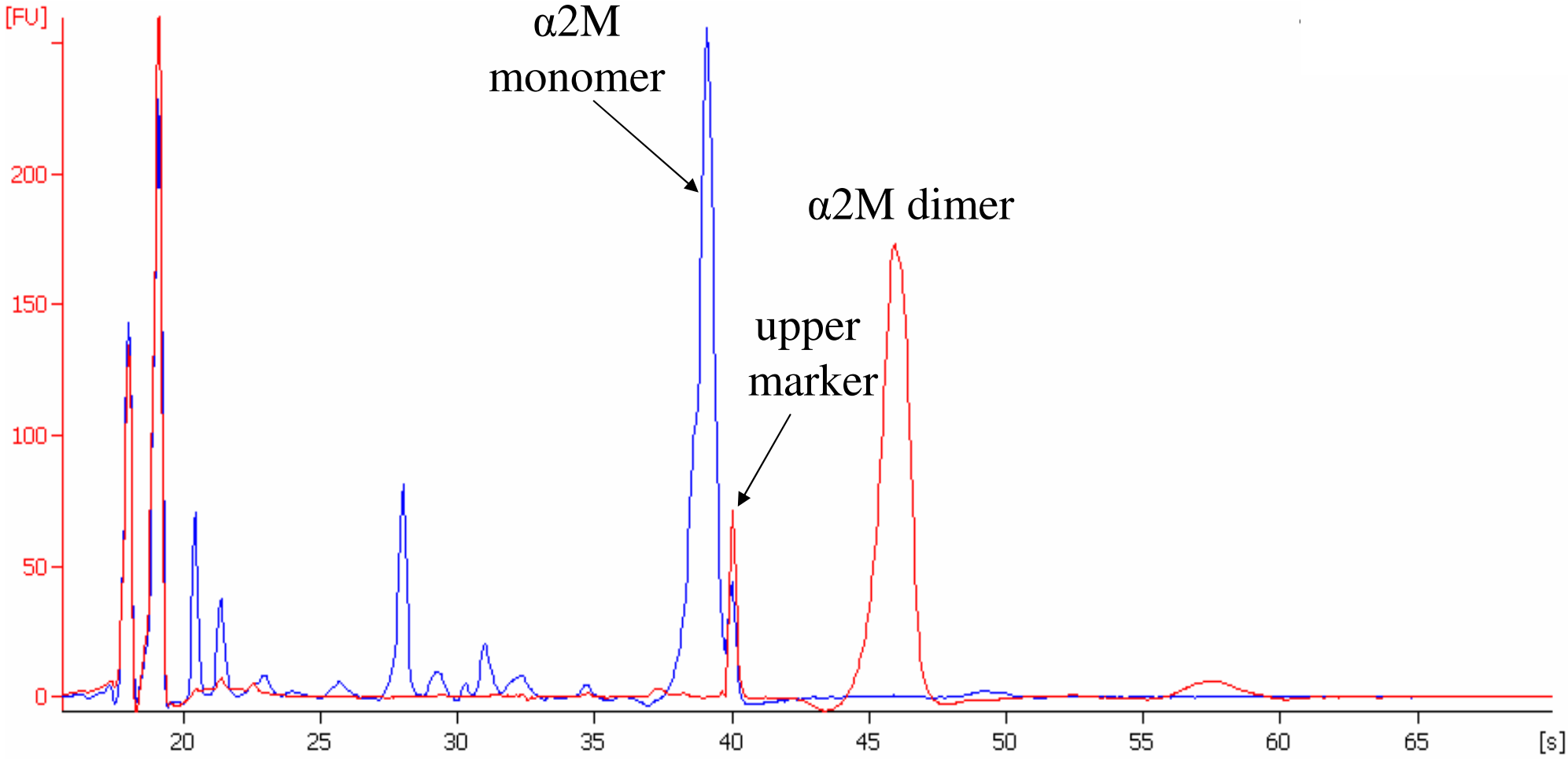
[FU]
200
150
100
50
0
20
25
30
35
40
45
50
55
60
65
[s]
α2M
monomer
α2M dimer
upper
marker

Figure 1a

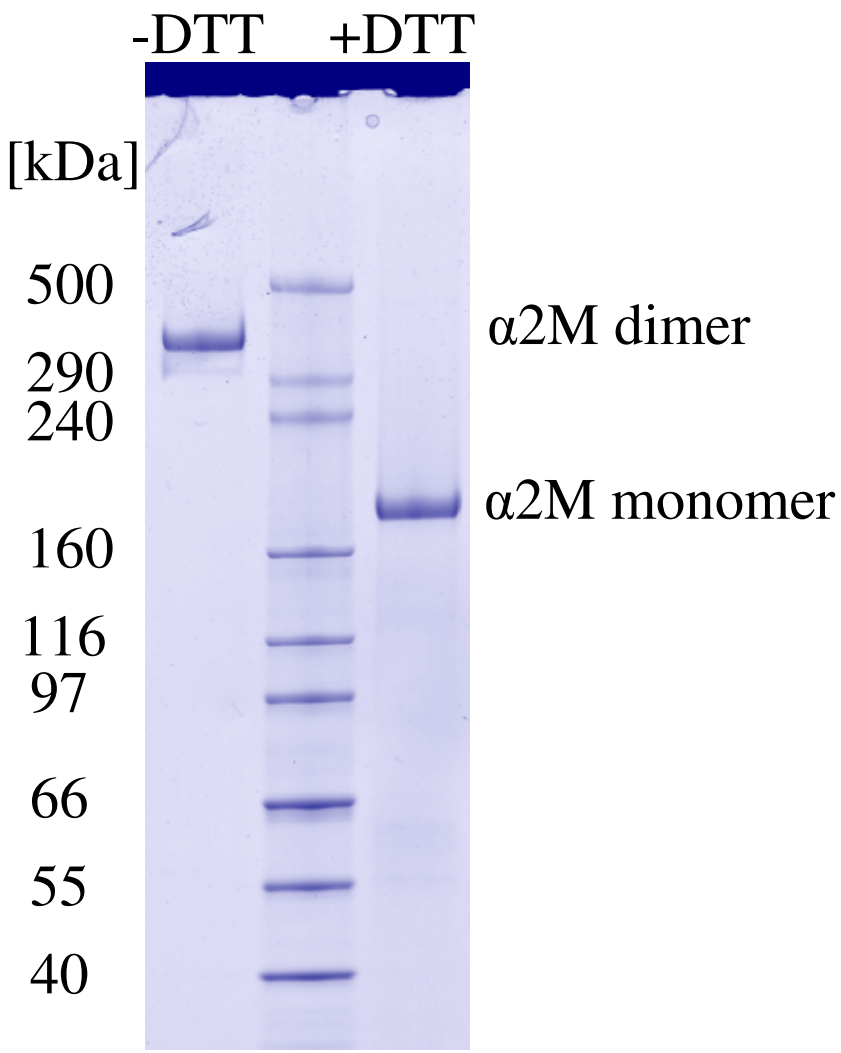
-DTT
+DTT
[kDa]
500
290
240
160
116
97
66
55
40
α2M dimer
α2M monomer

Figure 1b

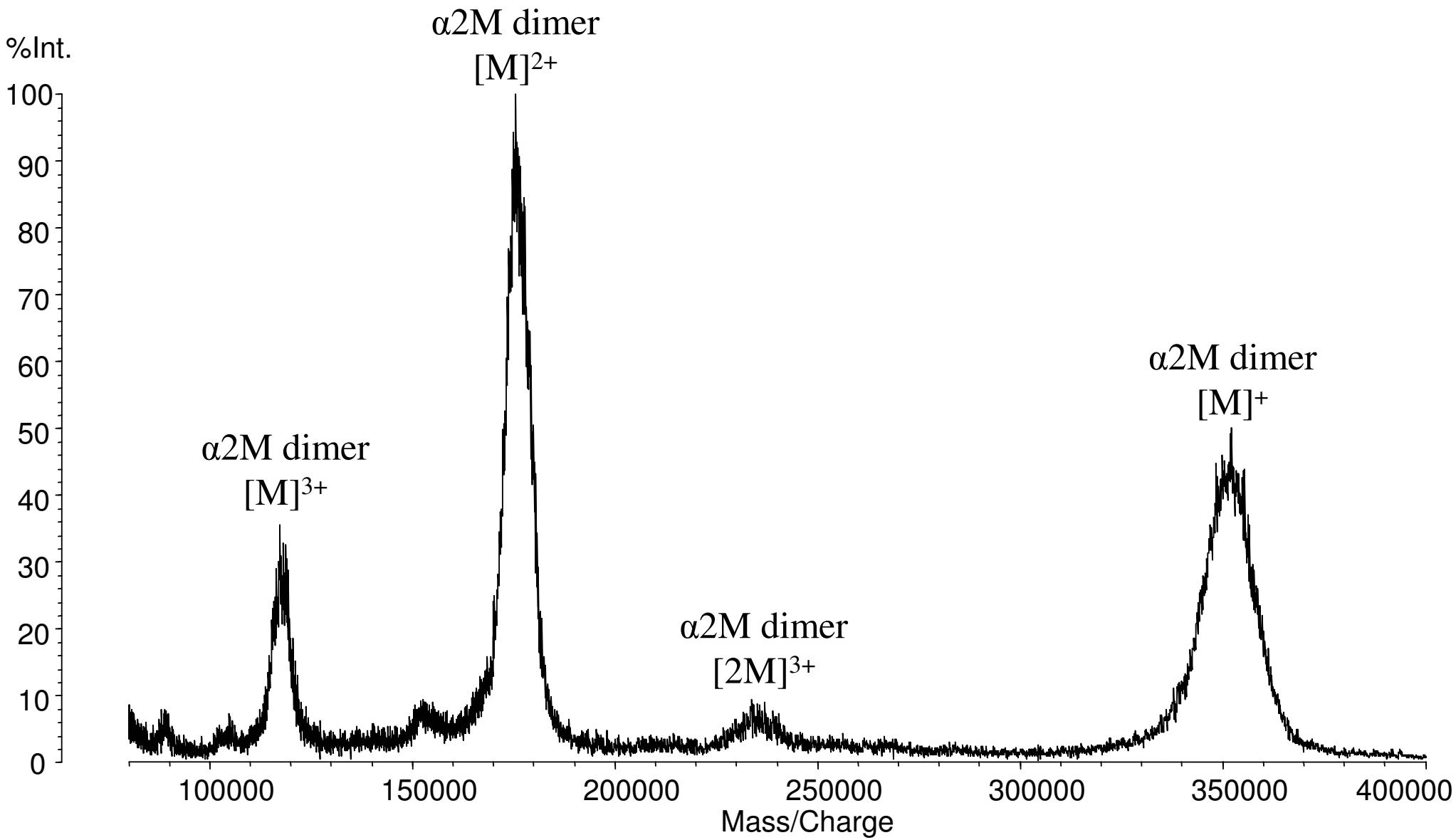
α2M dimer
[M]2+
%Int.
100
90
80
70
60
50
40
30
20
10
0
α2M dimer
[M]3+
α2M dimer
[2M]3+
α2M dimer
[M]+
100000
150000
200000
250000
300000
350000
400000
Mass/Charge

Figure 1c

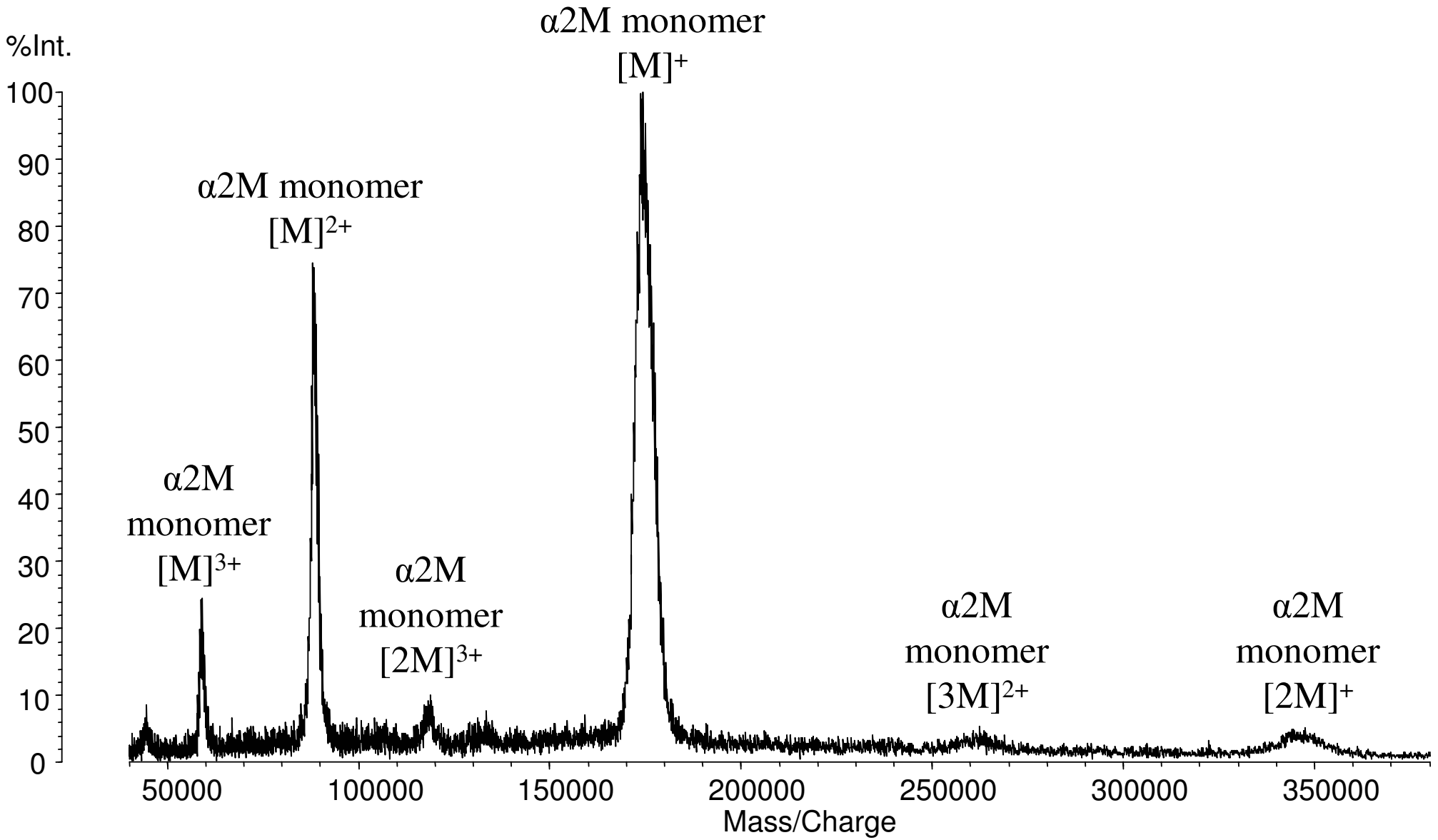
%Int.
100
90
80
70
60
50
40
30
20
10
0
α2M monomer
[M]+
α2M monomer
[M]2+
α2M
monomer
[M]3+
α2M
monomer
[2M]3+
α2M
monomer
[3M]2+
α2M
monomer
[2M]+
50000
100000
150000
200000
250000
300000
350000
Mass/Charge

Figure 1d

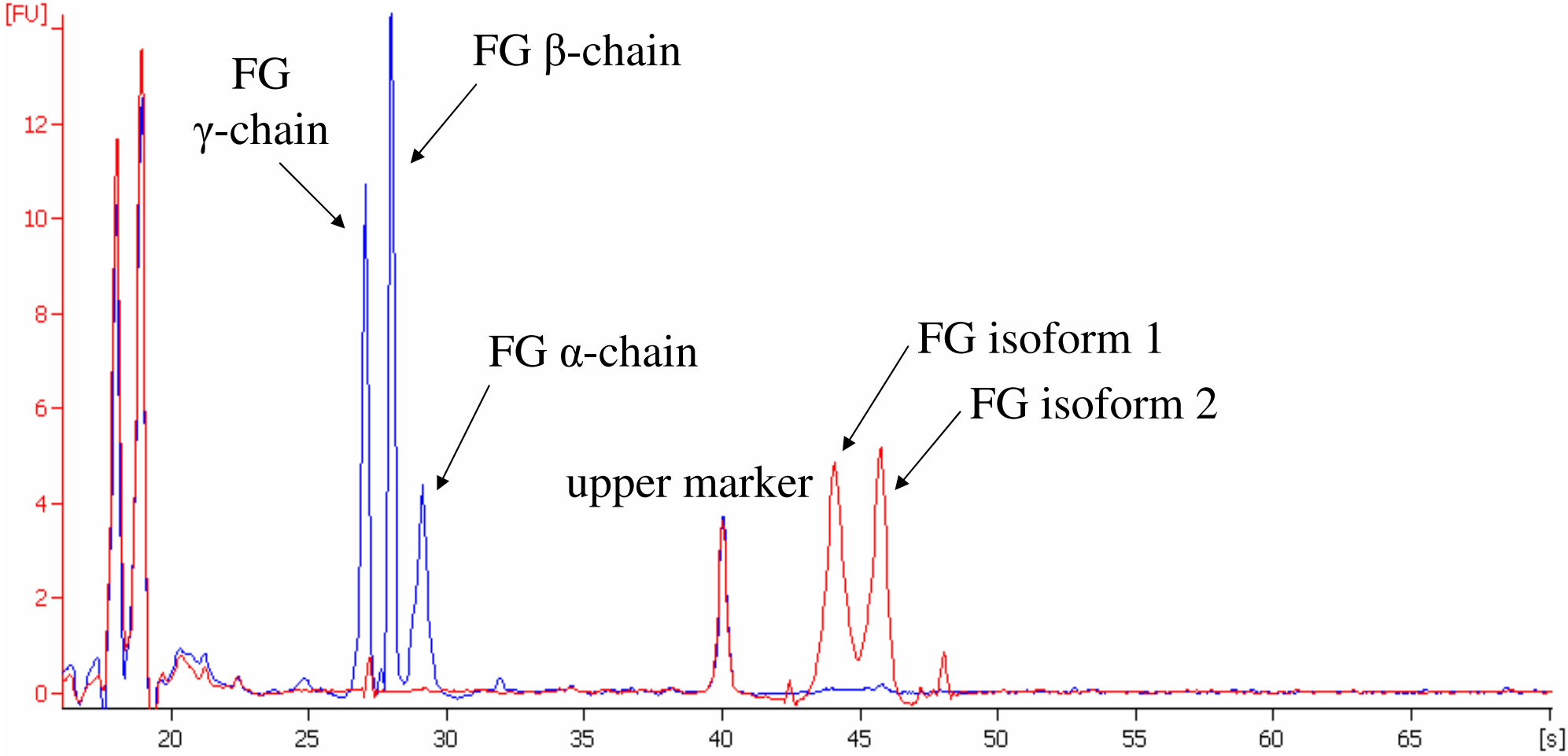
[FU]
12
10
8
6
4
2
0
20
25
30
35
40
45
50
55
60
65
[s]
FG
γ-chain
FG β-chain
FG α-chain
upper marker
FG isoform 1
FG isoform 2

Figure 2a

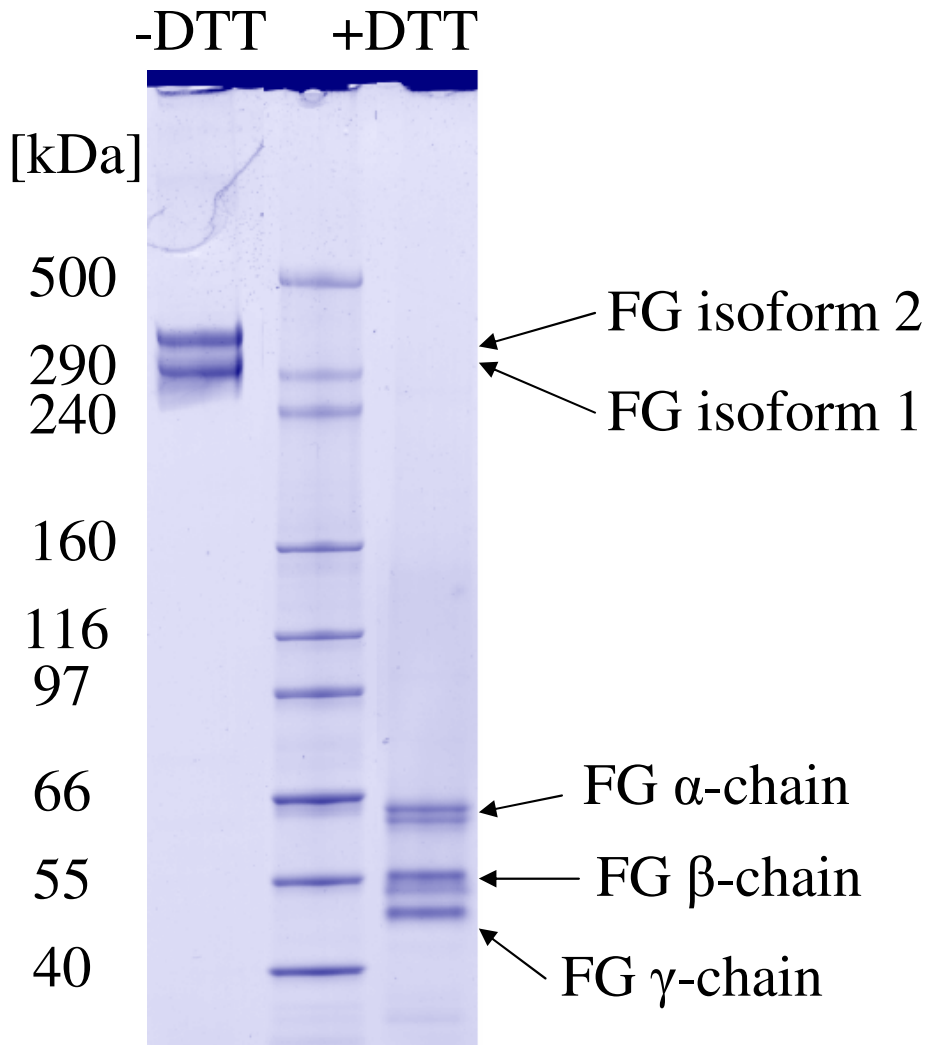
-DTT
+DTT
[kDa]
500
290
240
160
116
97
66
55
40
FG isoform 2
FG isoform 1
FG α-chain
FG β-chain
FG γ-chain

Figure 2b

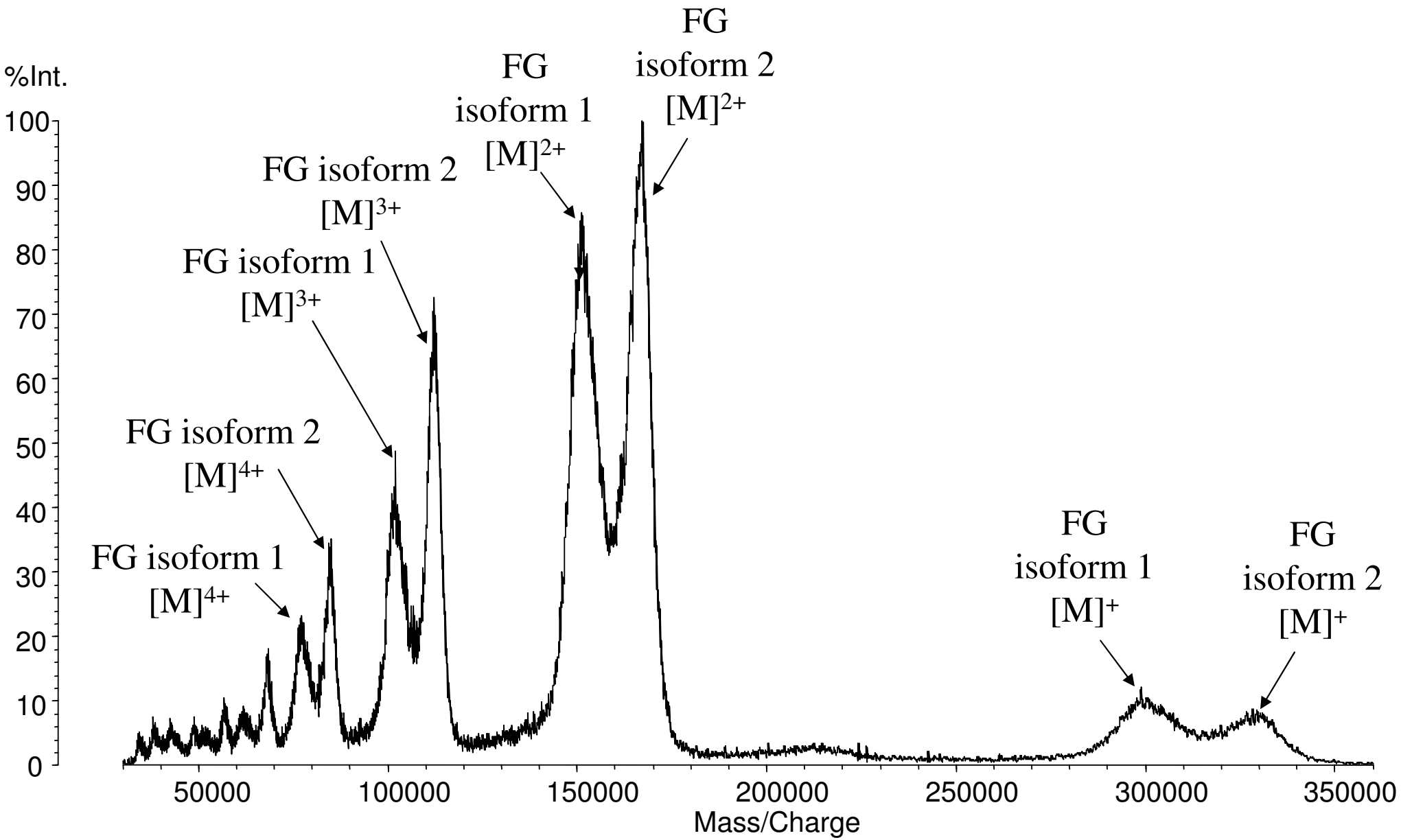
%Int.
100
90
80
70
60
50
40
30
20
10
0
FG isoform 1 [M]4+
FG isoform 2 [M]4+
FG isoform 1 [M]3+
FG isoform 2 [M]3+
FG isoform 1 [M]2+
FG isoform 2 [M]2+
FG isoform 1 [M]+
FG isoform 2 [M]+
50000
100000
150000
200000
250000
300000
350000
Mass/Charge

Figure 2c

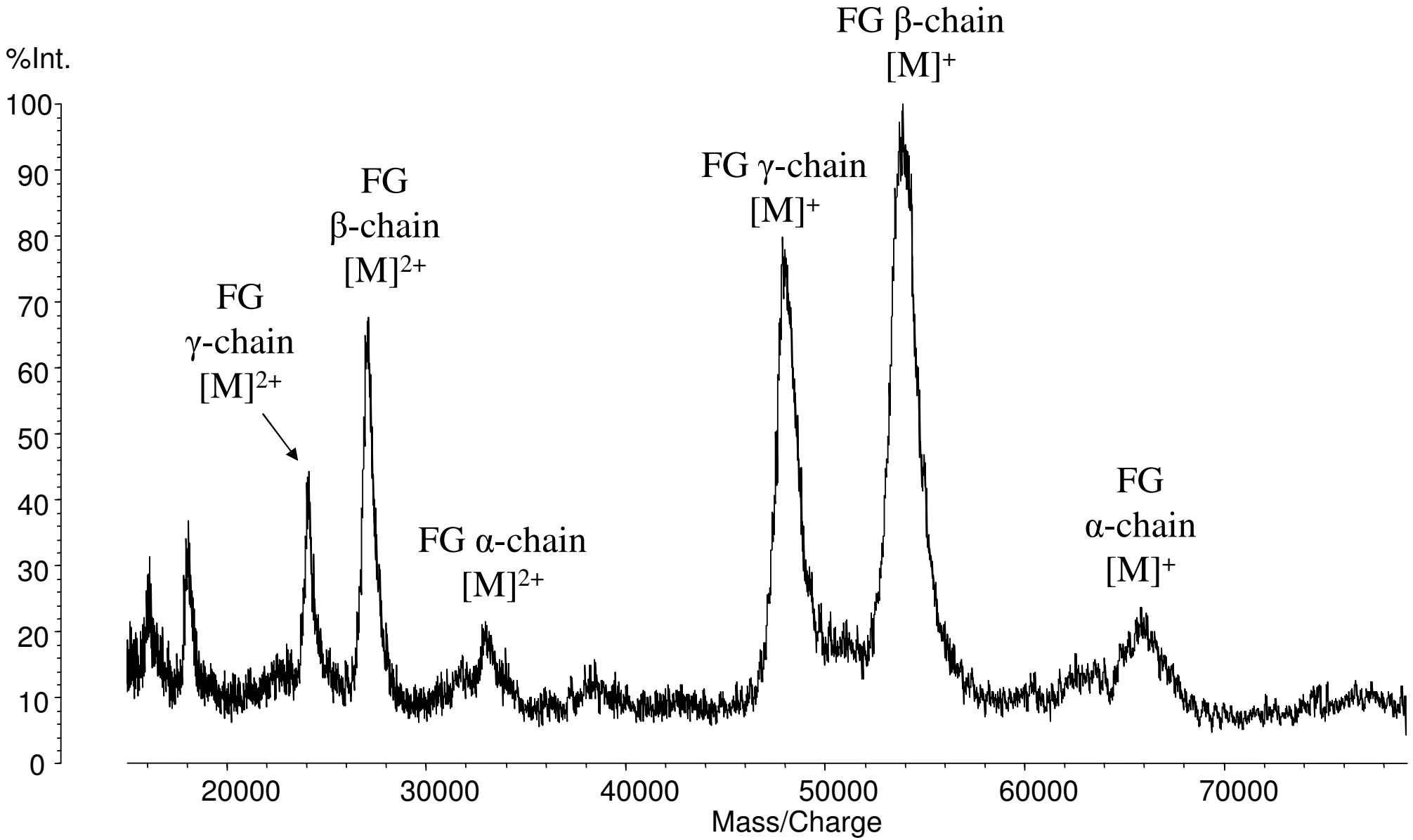
%Int.
100
90
80
70
60
50
40
30
20
10
0
FG γ-chain [M]2+
FG β-chain [M]2+
FG α-chain [M]2+
FG γ-chain [M]+
FG β-chain [M]+
FG α-chain [M]+
20000
30000
40000
50000
60000
70000
Mass/Charge

Figure 2d

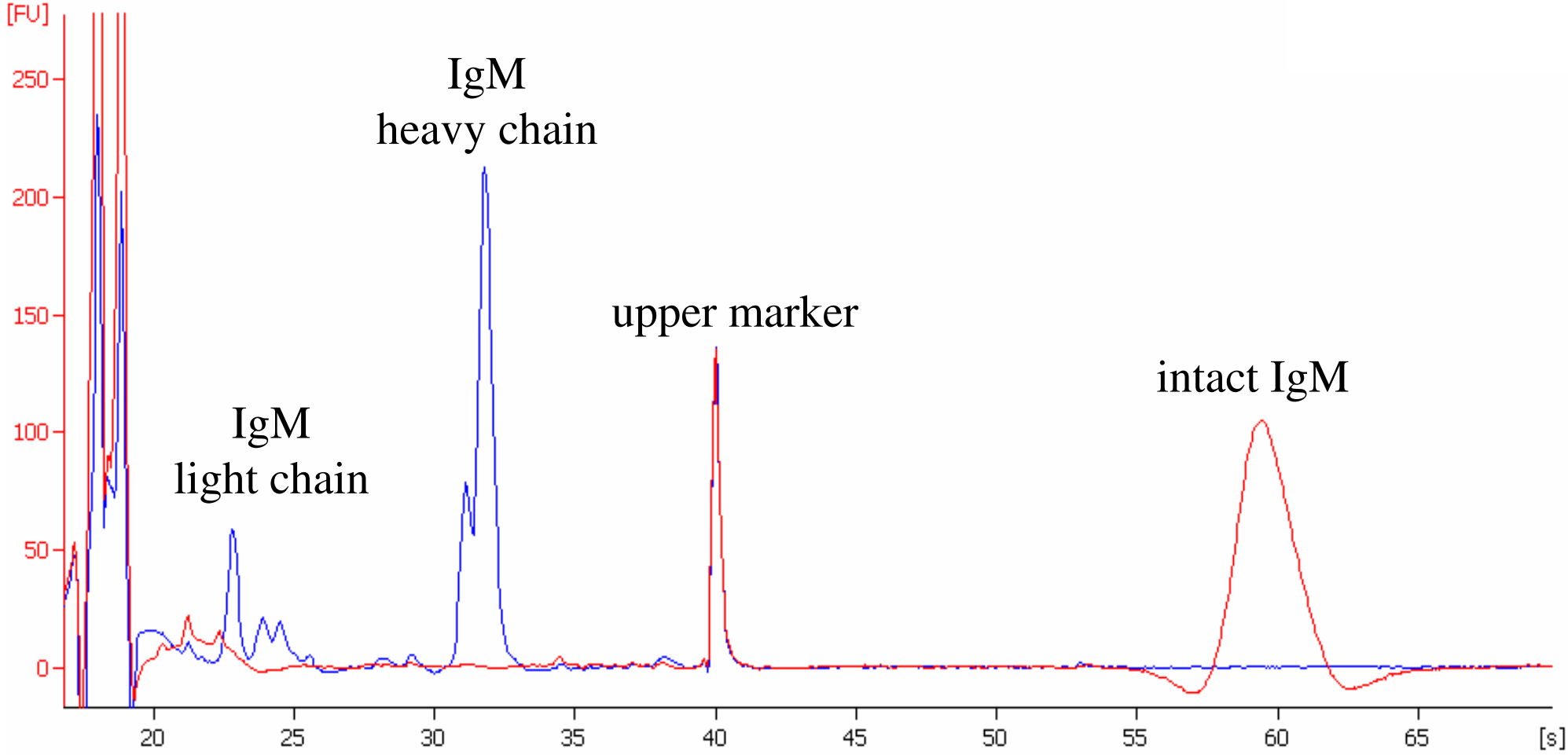
[FU]
250
200
150
100
50
0
IgM
heavy chain
upper marker
intact IgM
IgM
light chain
20
25
30
35
40
45
50
55
60
65
[s]

Figure 3a

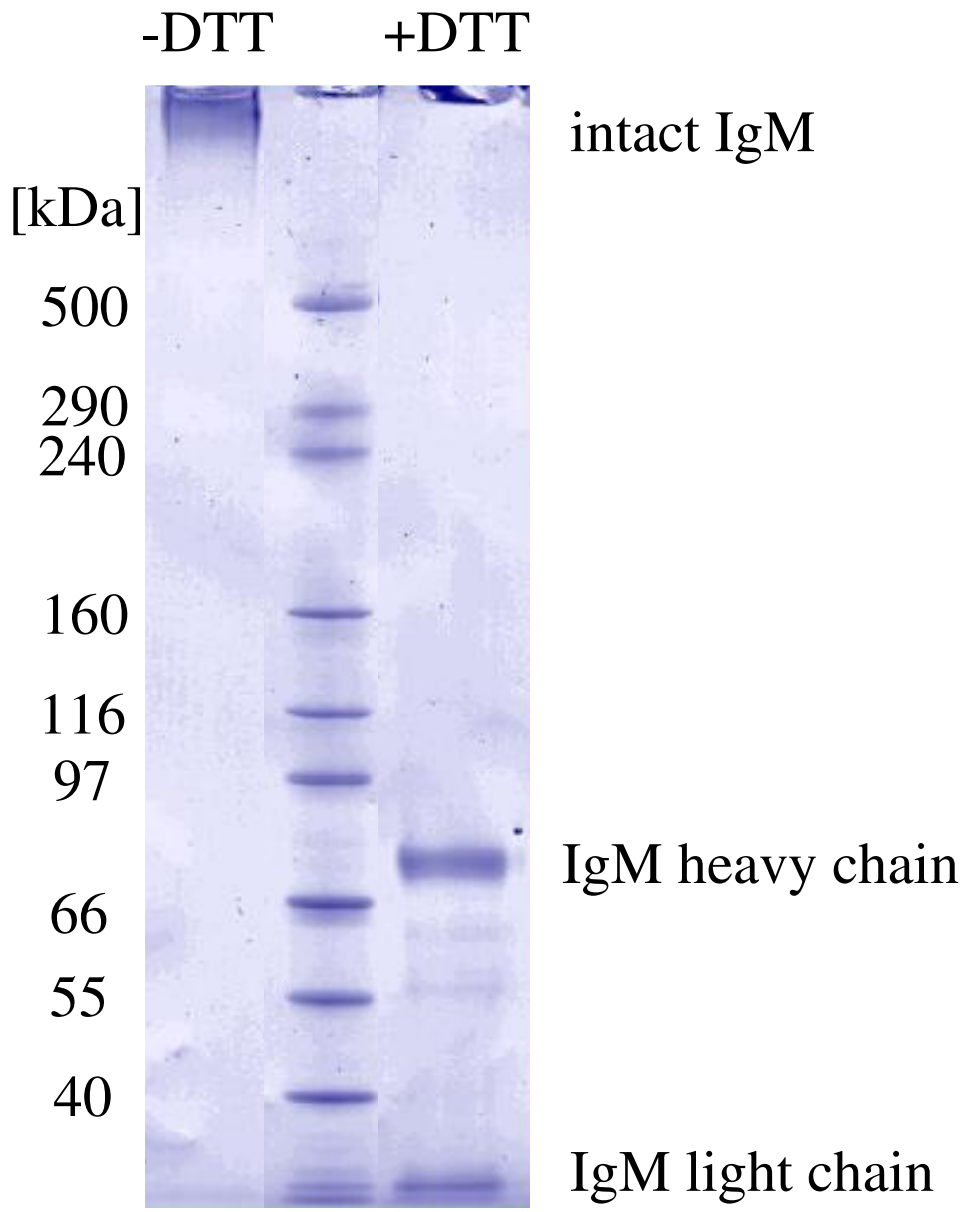
-DTT
+DTT
intact IgM
[kDa]
500
290
240
160
116
97
66
55
40
IgM heavy chain
IgM light chain

Figure 3b

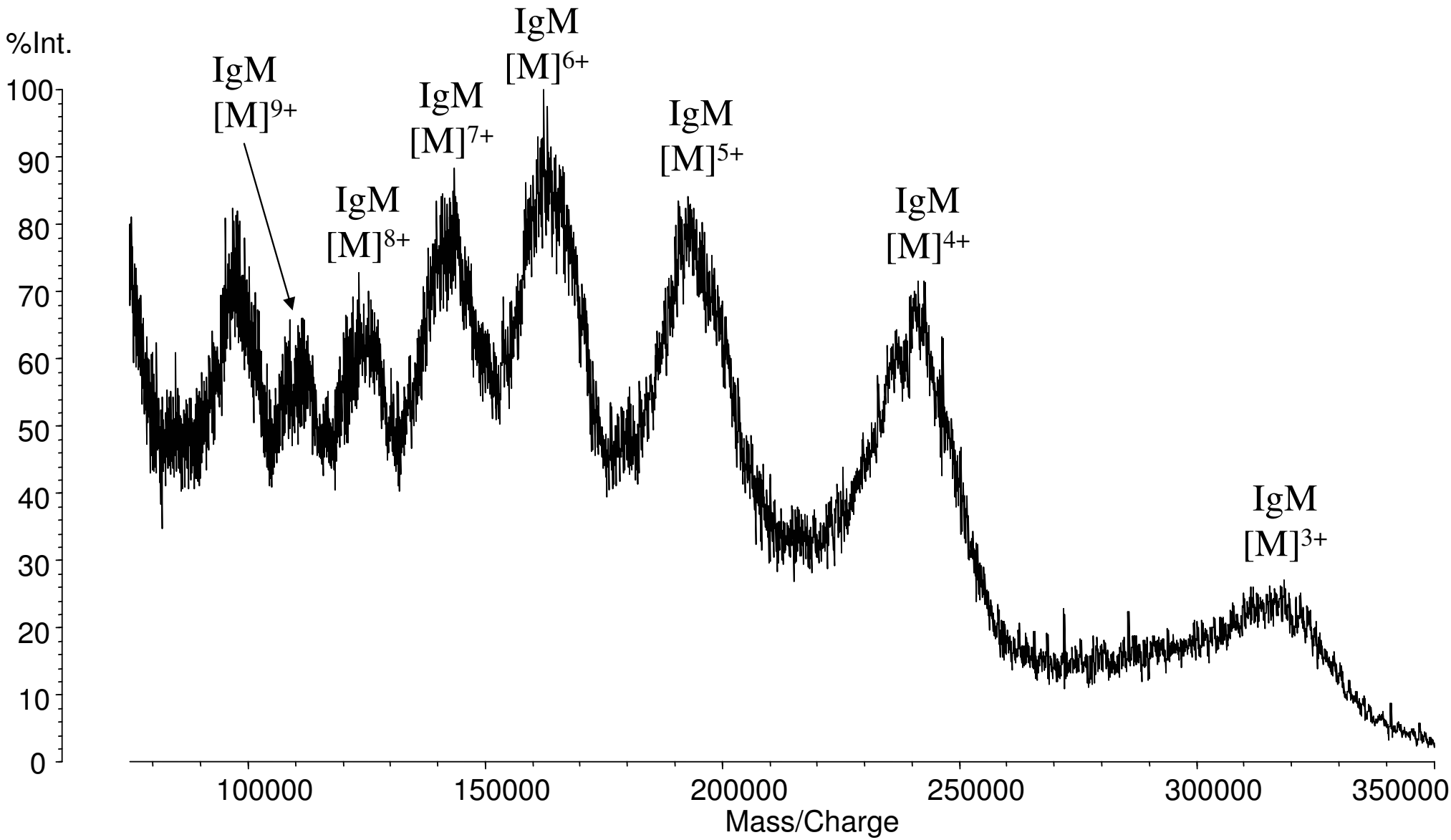
%Int.
100
90
80
70
60
50
40
30
20
10
0
IgM
[M]9+
IgM
[M]8+
IgM
[M]7+
IgM
[M]6+
IgM
[M]5+
IgM
[M]4+
IgM
[M]3+
100000
150000
200000
250000
300000
350000
Mass/Charge

Figure 3c

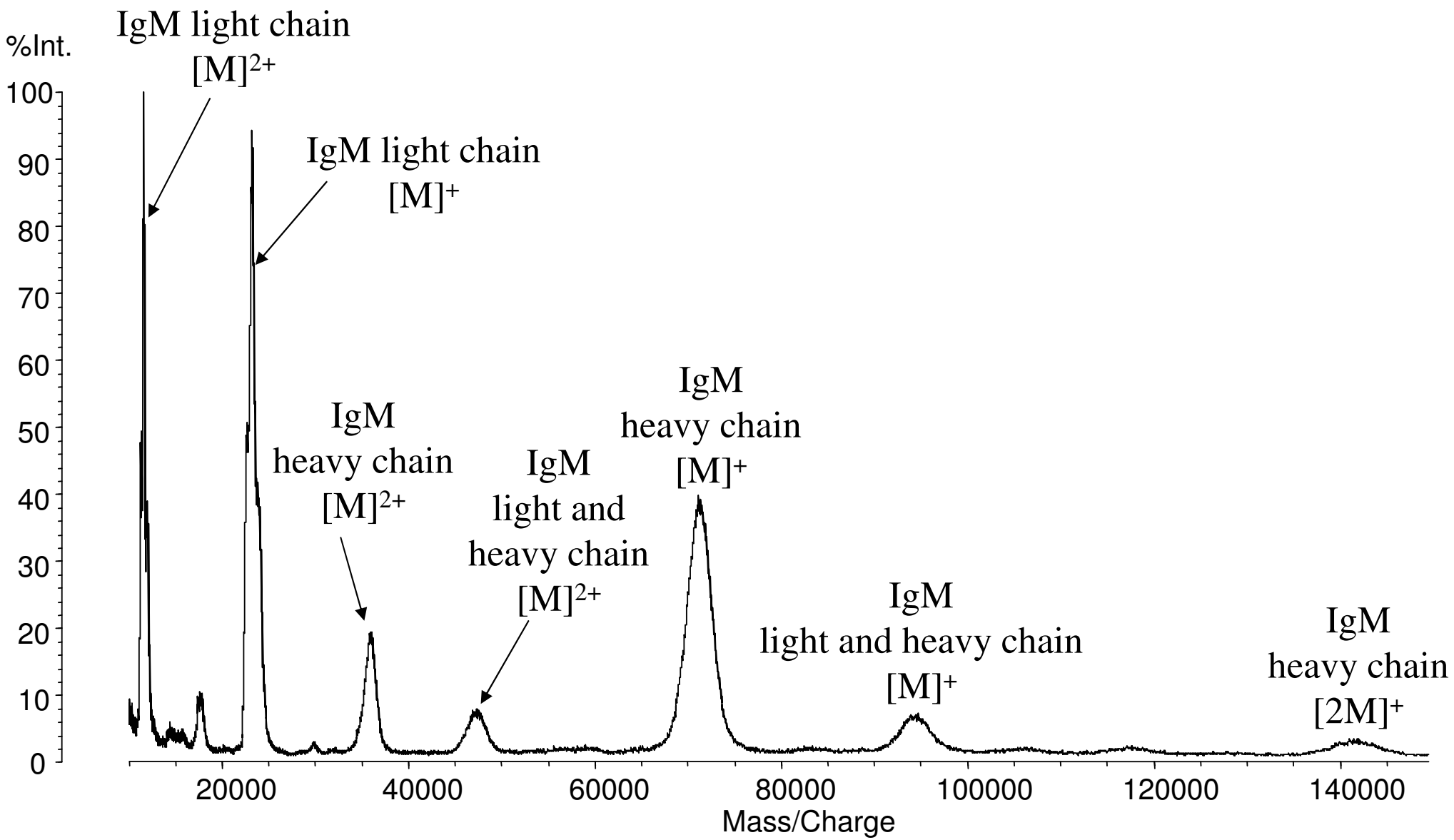
IgM light chain
[M]2+
IgM light chain
[M]+
IgM
heavy chain
[M]2+
IgM
light and
heavy chain
[M]2+
IgM
heavy chain
[M]+
IgM
light and heavy chain
[M]+
IgM
heavy chain
[2M]+
%Int.
100
90
80
70
60
50
40
30
20
10
0
20000
40000
60000
80000
100000
120000
140000
Mass/Charge

Figure 3d

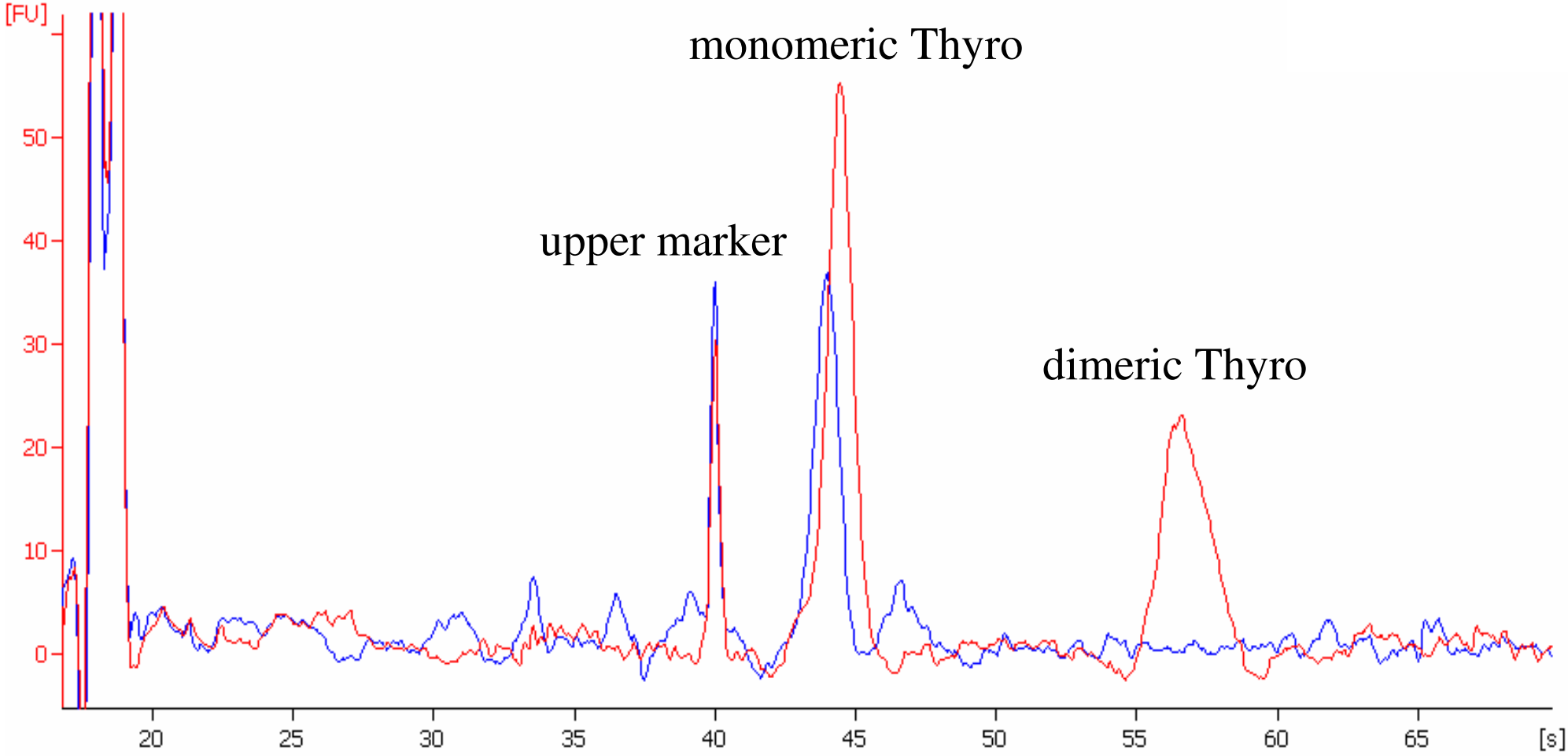
[FU]
50
40
30
20
10
0
monomeric Thyro
upper marker
dimeric Thyro
20
25
30
35
40
45
50
55
60
65
[s]

Figure 4a

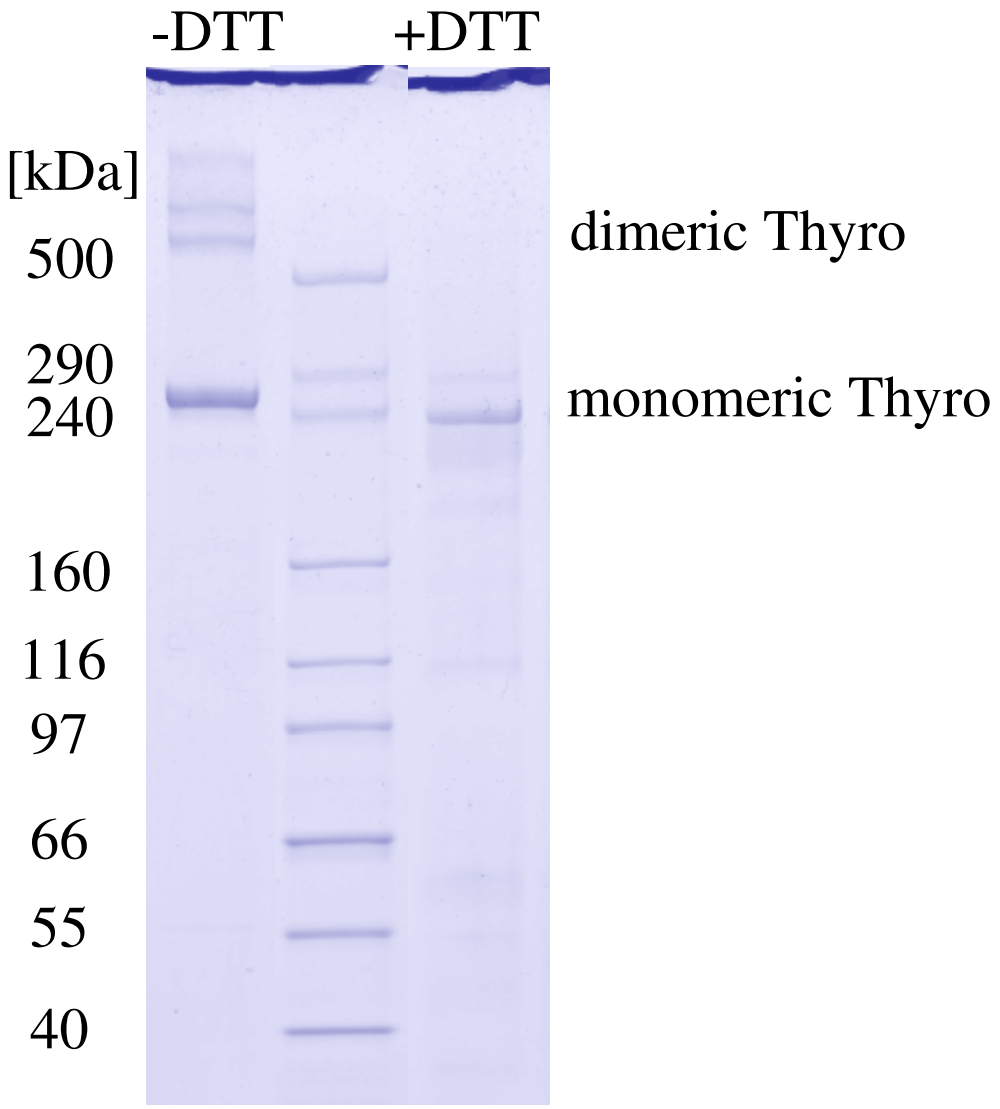
-DTT
+DTT
[kDa]
500
290
240
160
116
97
66
55
40
dimeric Thyro
monomeric Thyro

Figure 4b

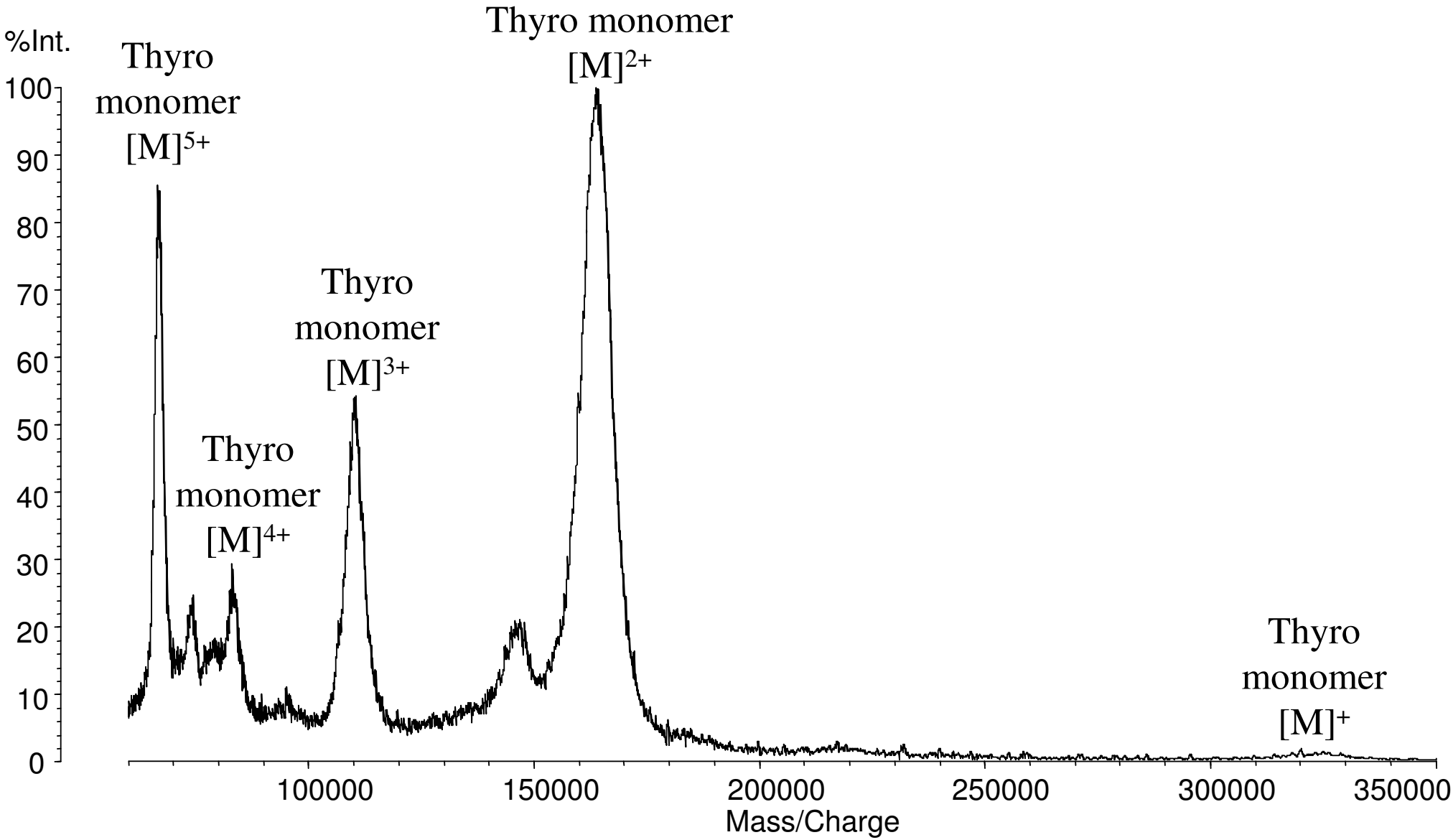
%Int.
100
90
80
70
60
50
40
30
20
10
0
Thyro monomer [M]5+
Thyro monomer [M]4+
Thyro monomer [M]3+
Thyro monomer [M]2+
Thyro monomer [M]+
100000
150000
200000
250000
300000
350000
Mass/Charge

Figure 4c

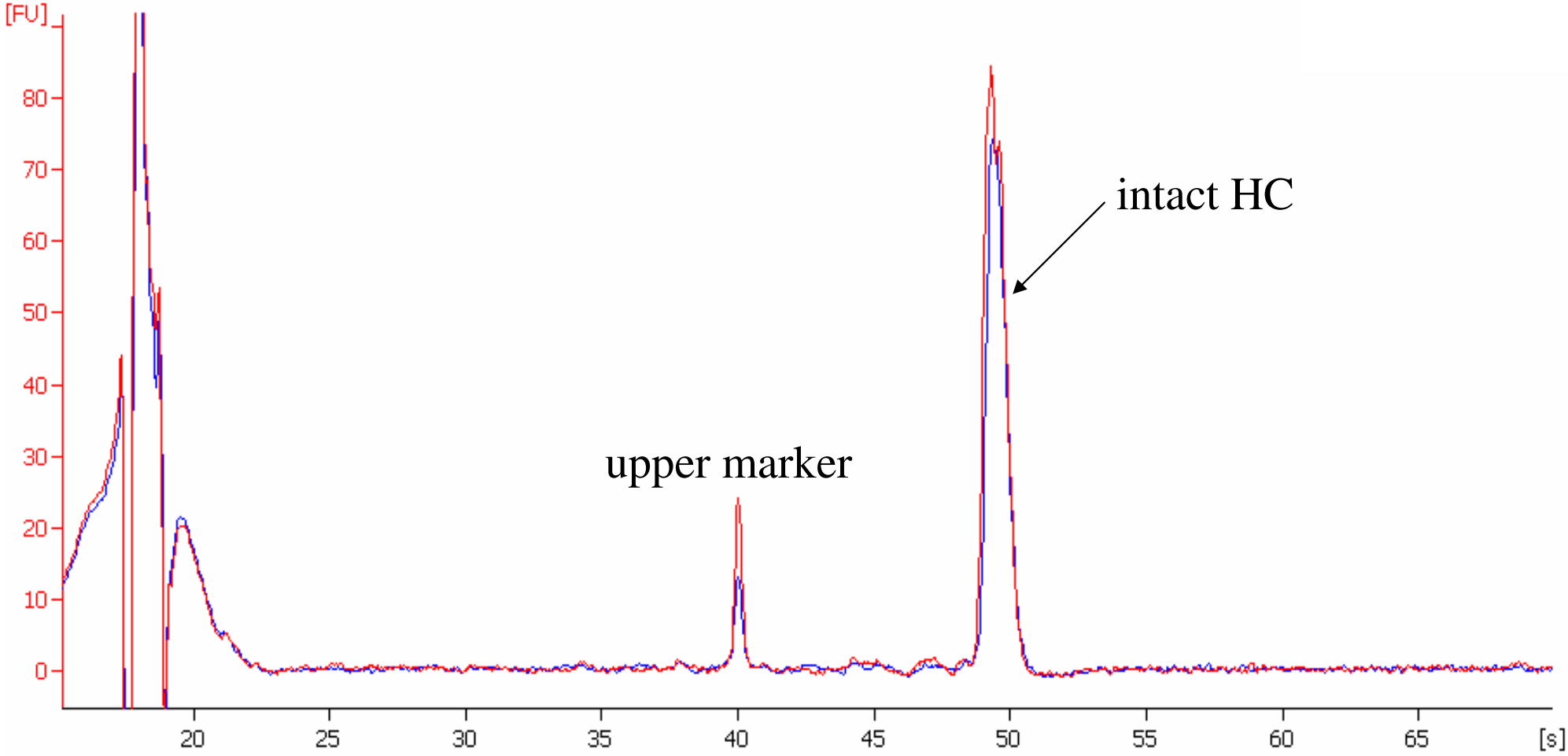
[FU]
80
70
60
50
40
30
20
10
0
20
25
30
35
40
45
50
55
60
65
[s]
intact HC
upper marker

Figure 5a

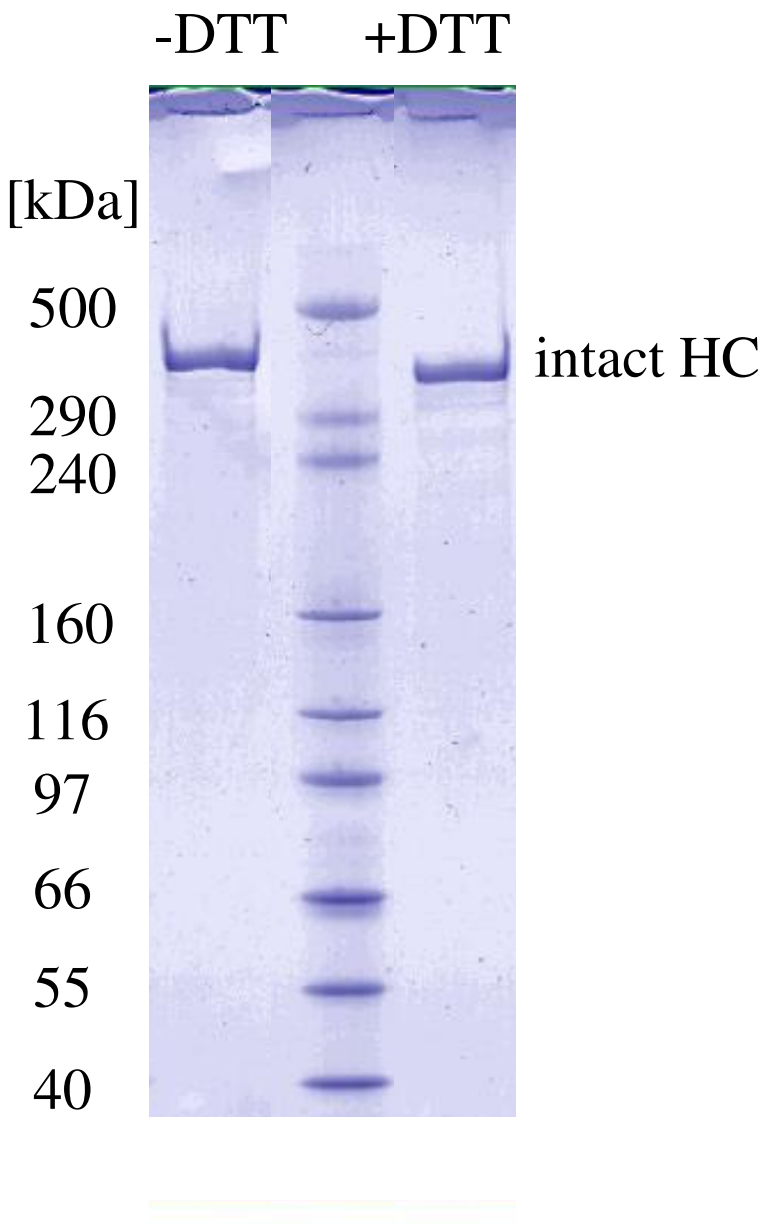

Figure 5b

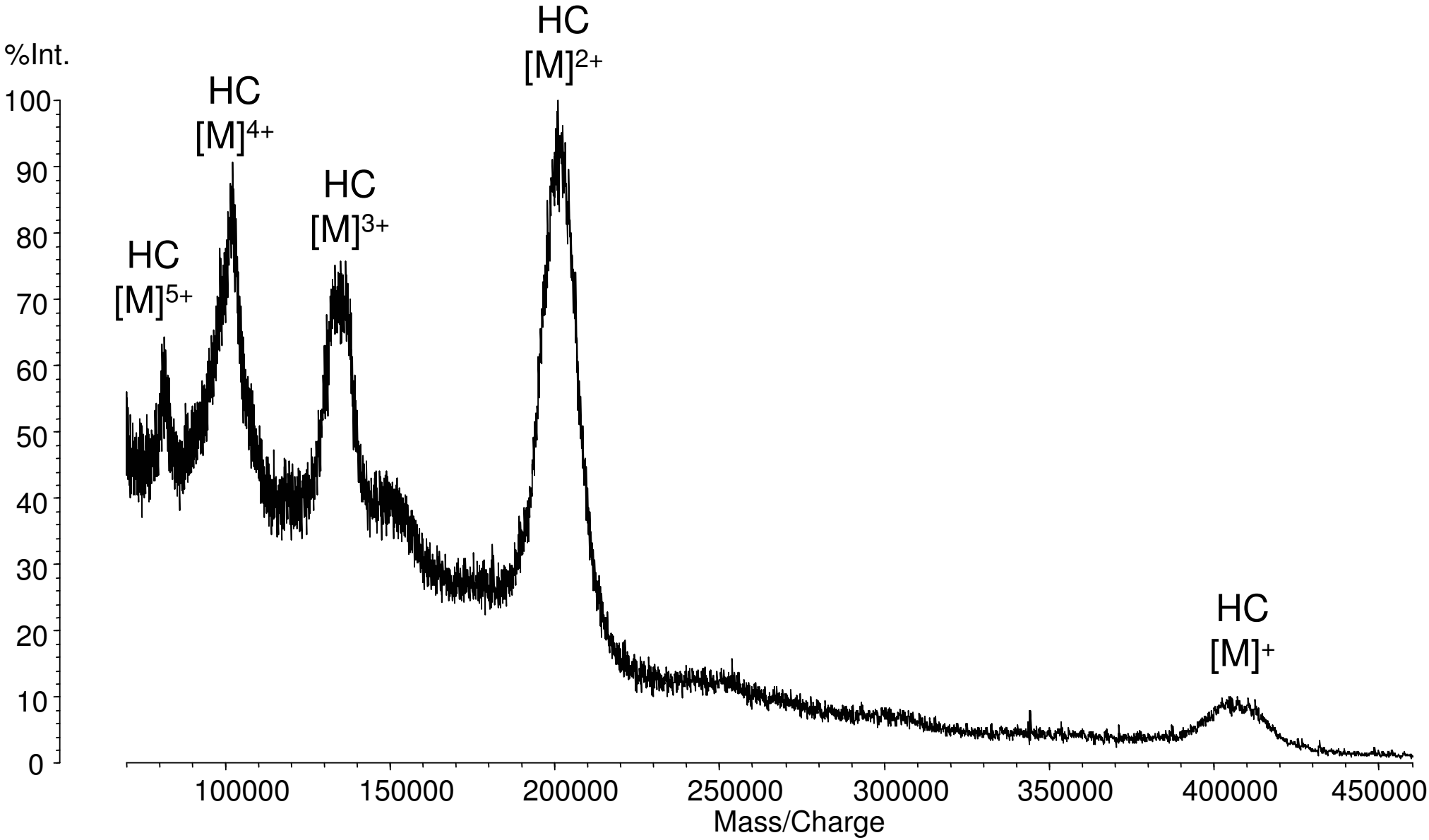
%Int.
100
90
80
70
60
50
40
30
20
10
0
HC
[M]5+
HC
[M]4+
HC
[M]3+
HC
[M]2+
HC
[M]+
100000
150000
200000
250000
300000
350000
400000
450000
Mass/Charge

Figure 5c

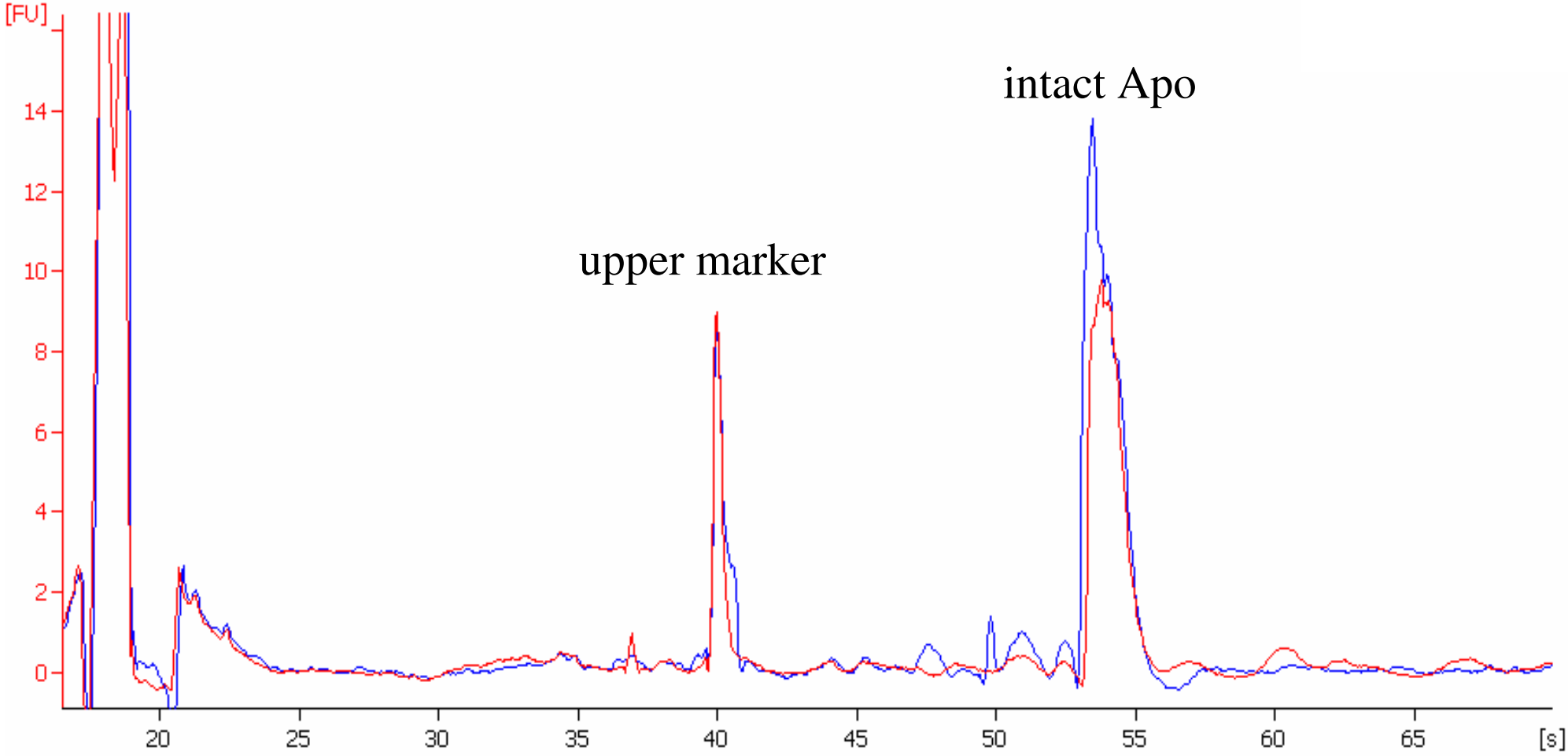
[FU]
14
12
10
8
6
4
2
0
20
25
30
35
40
45
50
55
60
65
[s]
upper marker
intact Apo

Figure 6a

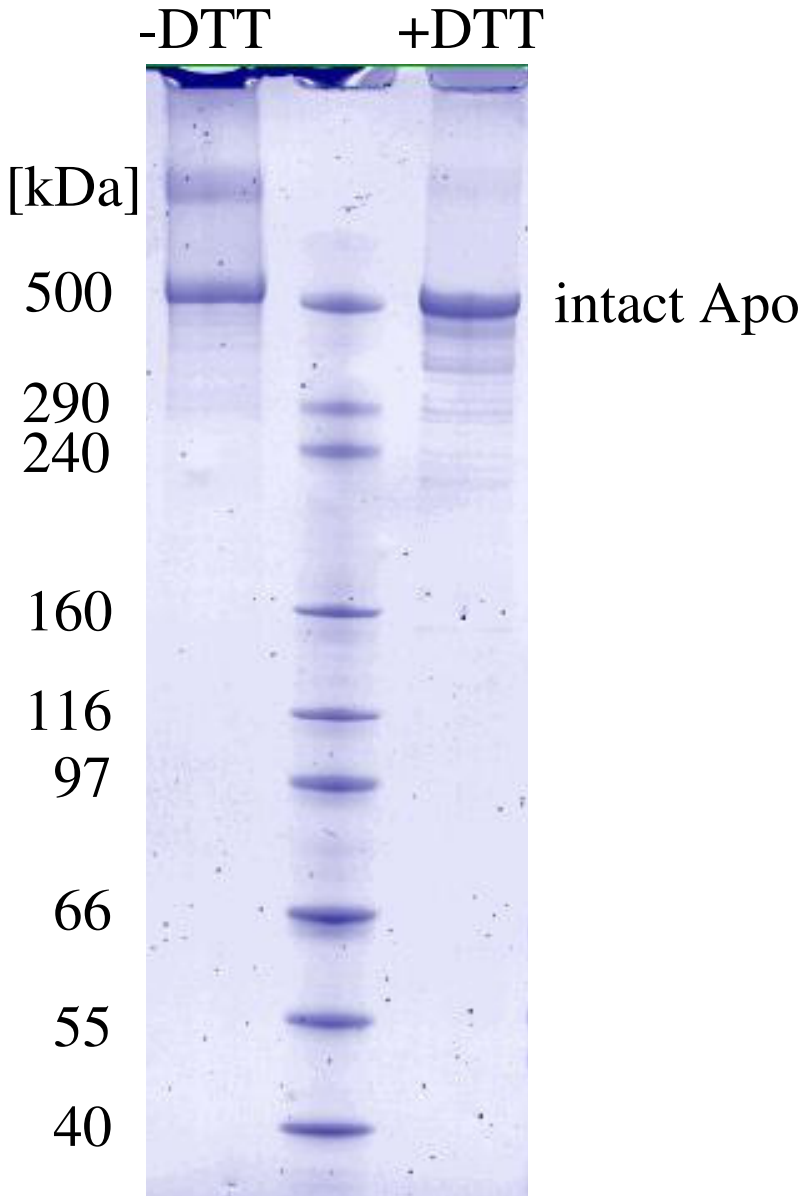

Figure 6b

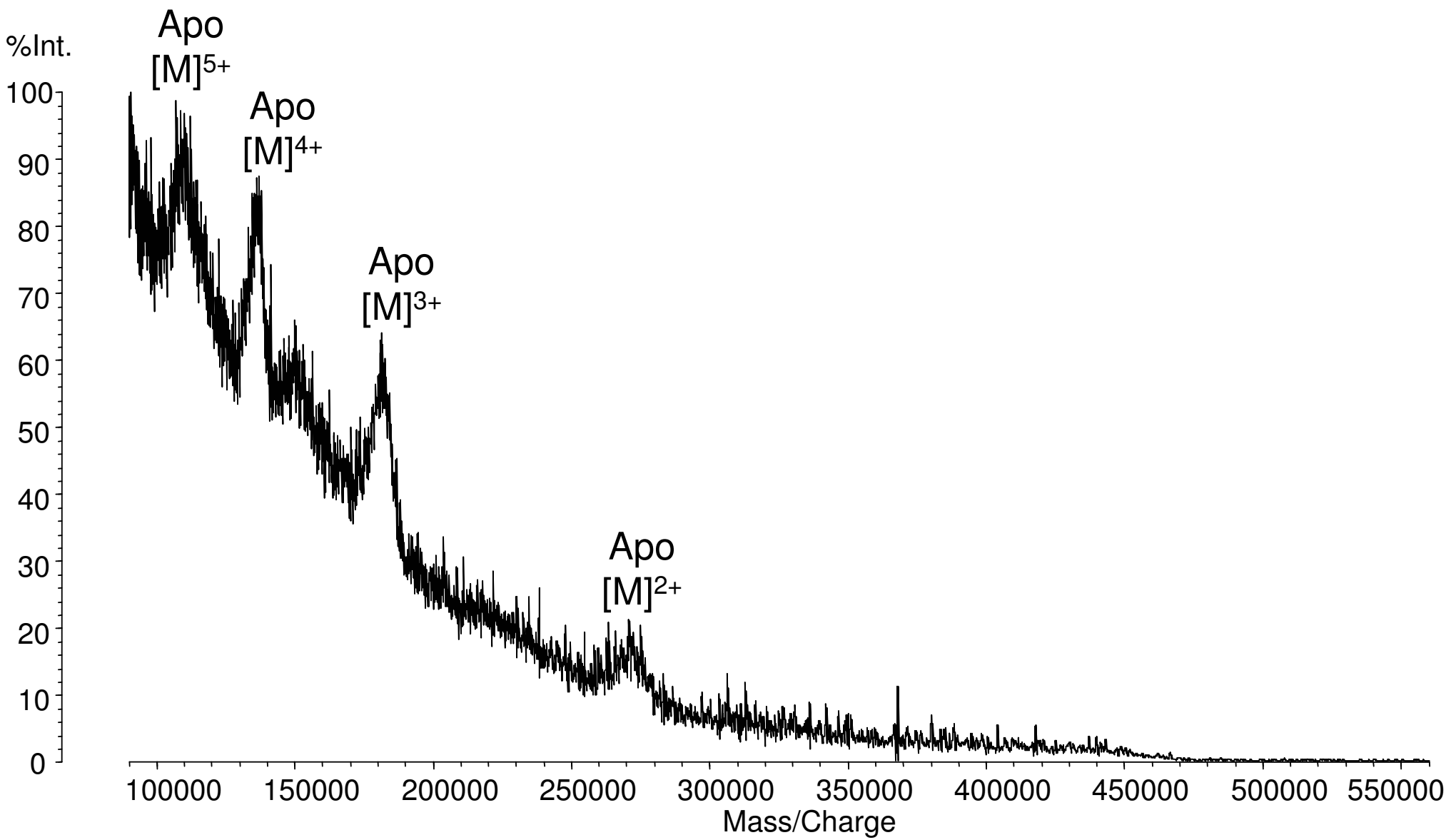
%Int.
100
90
80
70
60
50
40
30
20
10
0
Apo
[M]5+
Apo
[M]4+
Apo
[M]3+
Apo
[M]2+
100000
150000
200000
250000
300000
350000
400000
450000
500000
550000
Mass/Charge

Figure 6c

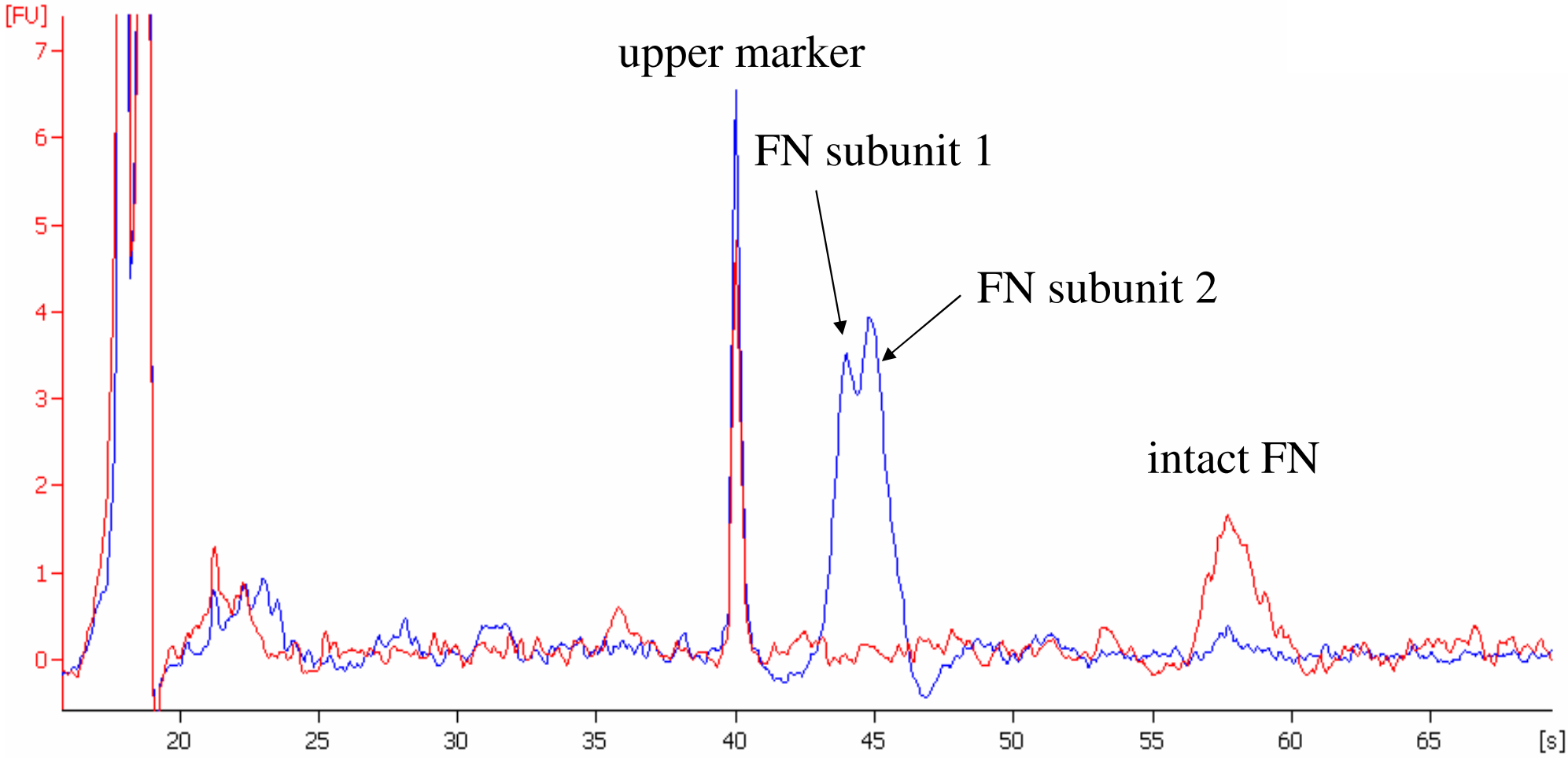
[FU]
7
6
5
4
3
2
1
0
upper marker
FN subunit 1
FN subunit 2
intact FN
20
25
30
35
40
45
50
55
60
65
[s]

Figure 7a

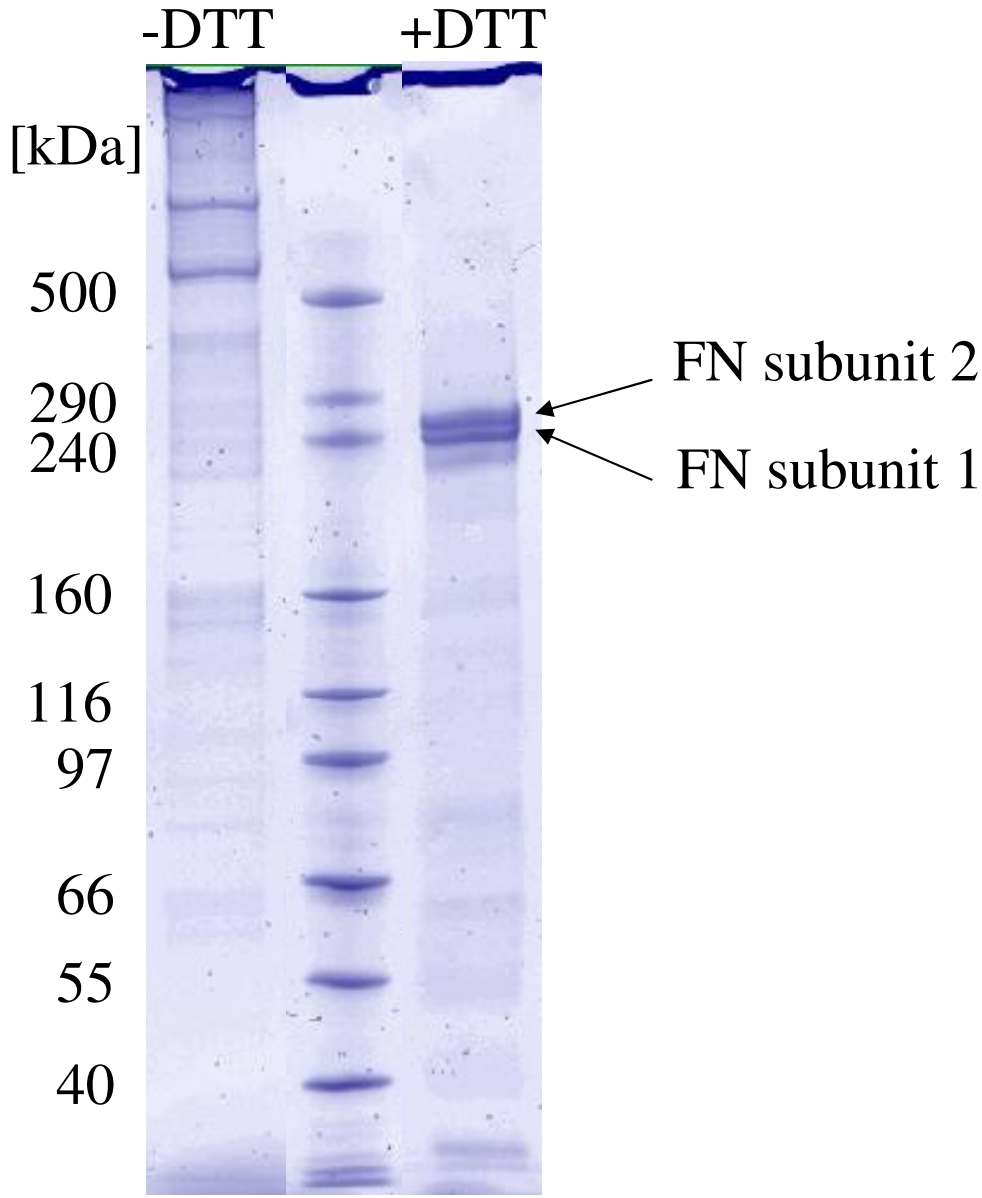
-DTT
+DTT
[kDa]
500
290
240
160
116
97
66
55
40
FN subunit 2
FN subunit 1

Figure 7b

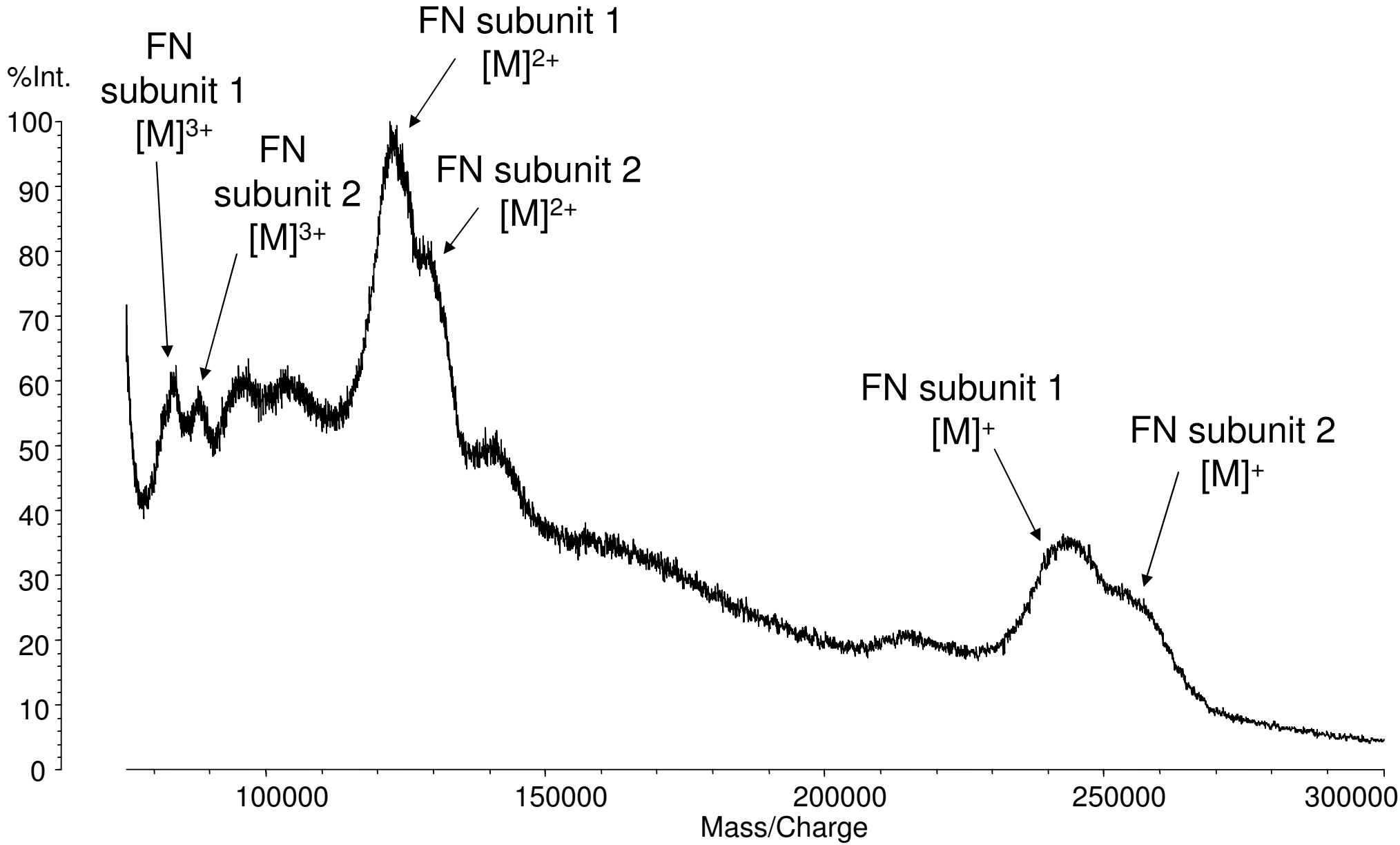
FN subunit 1 [M]3+
FN subunit 2 [M]3+
FN subunit 1 [M]2+
FN subunit 2 [M]2+
FN subunit 1 [M]+
FN subunit 2 [M]+
%Int.
100
90
80
70
60
50
40
30
20
10
0
100000
150000
200000
250000
300000
Mass/Charge

Figure 7c

Analytical Biochemistry, *in preparation* (2006)

Comparison of planar SDS-PAGE, CGE-on-the-chip and MALDI-TOF mass spectrometry for the analysis of the enzymatic de-N-glycosylation of Antithrombin III and Coagulation Factor IX with PNGase F

Roland Müller and Günter Allmaier*

Institute of Chemical Technologies and Analytics, Vienna University of Technology, A-1060 Vienna, Austria

Corresponding author: Günter Allmaier, Institute of Chemical Technologies and Analytics, Vienna University of Technology, Getreidemarkt 9/164, A-1060 Vienna, Austria Tel: +43 1 58801 15160 Fax: +43 1 58801 15199 E-mail: guenter.allmaier@tuwien.ac.at

Keywords: Antithrombin III; Coagulation Factor IX; CGE-on-the-chip; MALDI-TOF mass spectrometry; enzymatic de-N-glycosylation; PNGase F

Abstract

The primary topic of this article is the comparison of three different analytical techniques applied for the molecular weight determination of intact as well as partly and complete de-N-glycosylated human serum glycoproteins (Antithrombin III and Coagulation Factor IX). N-glycans were removed from the protein backbone using PNGase F. N-Glycosidase F, which is also called PNGase F, is an enzyme from the family of the Glycopeptidases, which cleaves all types of Asparagine attached N-glycans of glycoproteins, provided that the oligosaccharide has at least the length of a chitobiose core unit. Two of the applied techniques were based on gel electrophoresis while the third was based on the principle of mass spectrometry. Planar gel electrophoresis and matrix-assisted-laser-desorption-ionization time-of-flight mass spectrometry (MALDI-TOF-MS) are well-established techniques for protein analysis. While gel electrophoresis is used primary for molecular weight (MW) and concentration determination, mass spectrometry provides MW data of biopolymers with extremely high accuracy. Further a novel miniaturised capillary gel electrophoresis on-the-chip (CGE-on-the-chip) instrument, called 2100 “Lab on a Chip” Bioanalyzer, from Agilent Technologies, was applied for analysis.

Introduction

Protein analysis with SDS polyacrylamide gel electrophoresis (SDS-PAGE) based on slab gels has a 45-years old history and countless papers have already described this technique in great detail [1-3]. During sample preparation 1,4 g SDS attach to 1 g protein and cover the charge of the native protein. Normally reducing agents like Dithiothreitol (DTT) or β-Mercaptoethanol (BME) are added during sample preparation as well in order to reduce and thus cleave the disulphide bridges commonly found in proteins. After sample preparation all proteins should be converted into protein/SDS micelles with a roughly ellipsoid shape. Negatively charged SDS molecules on the surface of the micelles prevent protein aggregation and force all micelles to move into one direction during electrophoresis. With the aid of a cross-linked polymeric gel matrix like polyacrylamide, which acts as a molecular sieve, these protein/SDS micelles are separated only according to their molecular weight. Because it is actually separated due to the denatured protein's shape, steric effects like huge glycan structures attached to a protein are known to affect the MW measured with gel electrophoresis. Molecular weight determination with gel electrophoresis is simplified due to the linear correlation of the relative migration distance and the logarithmic molecular weight of protein/SDS micelles. This linear correlation is only observed within a limited molecular weight range and depends above all upon the applied gel type. Following the electrophoretic separation proteins are mostly visualized using Coomassie Brilliant Blue or silver staining [4,5]. Today, the most limiting step in slab gel electrophoresis is the protein detection and visualisation process.

In the year 1988 MALDI-MS was invented by Hillenkamp, Karas and Tanaka and became a breakthrough in protein analysis [6,7]. In 2002 Tanaka was awarded with the

Nobel Prize for his work focused on MALDI-MS. Different types of sample preparations exist, but for protein analysis the dried droplet technique is the most commonly applied method. Proteins are mixed with a matrix, like 2,4,6-Trihydroxyacetophenone (THAP) or Sinapic acid (SA), which absorbs UV light. After the co-crystallisation of matrix and analytes, the matrix molecules are exited with a UV laser and in turn gaseous analyte ions are produced [8,9]. In a final step the analyte ions, which have been successfully desorbed and ionised, are accelerated and afterwards separated by a time-of-flight (TOF) mass analyser according to their mass to charge ratio [10]. Molecular weight (MW) determination with TOF mass analysers is possible, because the square of the flight time of an accelerated analyte ion correlates with its mass-to-charge ratio. An advantage of TOF mass analysers over gel electrophoresis is the fact that the observed MWs are independent of the analyte's shape, because the entire analysis is performed under high vacuum conditions (10^{-6} to 10^{-7} Torr).

Lab-on-a-chip technology is the latest of all three described methods. The term "lab-on-a-chip" (LOC) technology is somewhat irritating, because today not one of the available chips on the market is an entire laboratory on a chip. There is no exact scientific definition what makes up a "lab on a chip" device. The only properties such devices have in common are the use of a chip and microfluidics, which merely indicates microstructures carrying fluids, in order to perform multiple functions on the chip [11]. Further LOC systems are much less labour-intensive than slab-gel electrophoresis and require smaller sample amounts. Protein sizing on a microchip based on the principle of capillary gel electrophoresis (CGE) was first introduced in the year 2000 [12]. The first commercially available instrument based on lab-on-a-chip technology and CGE was the

Agilent 2100 Bioanalyzer, which was developed by Agilent Technologies in collaboration with Caliper Technologies Corporation [13-18]. Basically the principle of this miniaturized CGE device is similar to classical SDS-PAGE, except that analysis is performed in fine capillaries instead of a slab gel. Another significant difference between planar gel electrophoresis and CGE-on-the-chip is that in the first technique the actual separation parameter is the migration distance, while in CGE-on-the-chip the parameter of interest is the migration time. For all performed experiments the Protein 200 Plus assay was applied, which uses a gel matrix based on polymer networks of linear polyacrylamide chains, which are hold together only through physical interactions. This is in contrast to SDS-PAGE with slab gels, where cross-linked slab gels are applied. Separation in a cross-linked gel depends on the pore sizes within the gel, while a linear polymer gel has dynamic pores with variable size, which makes linear polymers much more flexible than their cross-linked counterparts [19]. The Protein 200 Plus assay is capable of analysing the MW and concentration of proteins from 14 to 200 kDa in size [20,21]. Another important parameter is temperature, because its change results in a change of viscosity and thus injection volumes are affected [22]. Therefore the temperature within the Bioanalyzer is kept constant at 30°C with the aid of a thermostat and air-cooling. Sample preparation is similar to planar SDS-PAGE, but in the case of the 2100 Bioanalyzer a single prepared sample can be analysed several times. Sample wells on the chip are linked to a separation capillary through micro channels. Sample injection into the micro channels is performed electrokinetically. Separation is performed in a 1,7 cm separation capillary in the middle of the protein chip. The detection principle is based on laser-induced fluorescence with an excitation wavelength of 630 nm and an emission

wavelength of 680 nm. The gel matrix within the capillaries contains a blue fluorescence dye, which binds to protein/SDS micelles. Shortly before these micelles reach the detector, the gel matrix containing fluorescence dye is diluted with gel matrix without fluorescence dye. Without this dilution step the background signals would be very intensive and thus drastically reduce the limit of detection.

Human Antithrombin III (Expasy accession number: P01008) is a glycoprotein consisting of a 432 amino acids backbone. Depending on the number of attached N-linked sugar residues it is distinguished between α-form (4 glycan residues) and β-form (3 glycan residues). According to published MALDI-TOF-MS data the α-form has a MW of 57,26 kDa, while the β-form has a MW of 55,04 kDa [23]. Next to 3 or 4 N-glycosylations the only other known posttranslational modifications of Antithrombin III are three disulfide bridges. The β-form of Antithrombin III (AT III) makes up less than 8% of all AT III present in human plasma, while the α-form with 4 sugar residues is the most abundant form in blood plasma. Human coagulation Factor IX (Expasy accession number: P00740) is a heavily posttranslational modified single-chain glycoprotein with 415 amino acids. Intact human plasma derived Coagulation Factor IX (pdFIX) is reported to have a MW of 53,75 kDa, while complete de-N-glycosylated FIX has a reported MW of 47,68 kDa [23]. The known posttranslational modifications of FIX are 7 disulphide bridges, 2 N- linked and 6 O-linked glycans, two phosphorylations, one sulfation, one hydroxylation and up to 12 gamma-carboxyglutamic acids. The protein is obtained out of human blood, or produced as a recombinant protein. A recombinant form of FIX (rFIX) is produced from

a Chinese hamster ovary cell line that was engineered for high-level protein processing and expression [24].

Material and Methods

Materials. Antithrombin III and Factor IX, both human plasma-derived, were provided by Octapharma (Vienna, Austria). Recombinant Factor IX (Bene FIX®) was provided by Baxter. For the de-N-glycosylation N-Glycosidase F (PNGase F), recombinant from Roche was used. Protein samples were desalted using Microspin G-25 columns from Amersham Biosciences or C-18 ZipTips from Millipore. The applied slab gels were 4-20% Tris-Glycine gels, 1.0 mm x 10 wells, from Invitrogen. Tris Glycine SDS running buffer (10x), Tris Glycine SDS sample buffer (2x), Mark 12 Unstained Standard Marker and NuPAGE sample reducing agent (10x) were provided by Invitrogen as well. For CGE-on-the-chip experiments Protein Dye Concentrate, Protein 200 Plus gel matrix, Protein 200 Plus Ladder and Protein 200 Plus Sample Buffer from Agilent were applied. All MALDI-TOF-MS standard proteins used for calibration were provided by Sigma. Sinapic acid (p.a., >99%) and 2,4,6-Trihydroxyacetophenone monohydrate (p.a., >99,5%) were from Fluka. Unless noted otherwise water p.a. from Merck was applied.

Instrumentation. The applied slab gel electrophoresis gel chamber was of the type EI9001–X Cell II Mini Cell (Novex), the power supply of the type EPS 300 was provided by Amersham Pharmacia Biotech. On-Chip-CE experiments were carried out with an Agilent 2100 Bioanalyzer (Waldbronn, Germany) and the according Protein 200+ Assay. Data evaluation was performed using the Agilent 2100 Expert Software. All MALDI-

TOF-MS experiments were carried out with a high resolution, floorstanding instrument (AXIMA CFR, Shimadzu Biotech Kratos Analytical, Manchester, UK) equipped with a pulsed nitrogen laser (λ = 337 nm, 4 ns pulse width) in linear, positive ion mode and an accelerating voltage of 20 kV. Mass spectra were acquired by averaging 10 to 1000 unselected and consecutive laser shots. For each sample at least three identically prepared sample spots were analysed. All mass spectra gathered were smoothed using the company-supplied Savitzky-Golay algorithm (width: 150 channels).

Microscale reduction and alkylation of Antithrombin III. An aqueous solution containing 240 µg AT III were lyophilised, redissolved in 200 µL Reduction and Denaturation Buffer (6 M Guadinium HCl; 0,5 M Tris, pH 8,0; 2 mM EDTA) and incubated for 1 hour at 37°C. Afterwards the sample was heat denatured with a Thermoblock at 96°C for 4 minutes. After cooling down to room temperature (RT), 20 µL 100 mM DTT (2 µmol) solution were added to the solution, followed by incubation for 2 hours at 37°C. Finally 10 µL 0,5 M Iodoacetamide (5 µmol) were pipetted to the solution. Alkylation was performed at RT in the dark for 1 hour. From the obtained alkylated protein solution 150 µL were desalted using Microspin G-25 columns.

Enzymatic de-N-glycosylation with PNGase F. 100 Units of PNGase F were dissolved in 1000 µL of water to gain an enzyme solution with an activity of 0,1 units/µL. For a complete de-N-glycosylation 10 µL protein solution containing 5 to 10 µg glycoproteins and 1 µL freshly prepared PNGase F solution were mixed and incubated at 37°C for 18 hours. In the case of AT III the alkylated protein was applied for digestion with

PNGase F. For the kinetic analysis of the PNGase F digest of alkylated AT III 30 µL protein solution and 7 µL freshly prepared PNGase F solution (0,1 units/µL) were mixed. 4 µL aliquots were taken after 1 minute, 30 minutes, 1 hour, 2 hours, 3,5 hours and 5 hours and stored at –80°C. In the case of the kinetic analysis of rFIX the same procedure was applied, except only half of the amounts were used and aliquots were taken after 1 minute, 15 minutes, 30 minutes, 1 hour, 2 hours and 3 hours. For subsequent MALDI-TOF-MS analysis the samples were desalted using C-18 ZipTips. In the final step samples were eluted with 5 µL matrix solution (THAP in the case of FIX and SA for AT III). For the analysis with CGE and SDS-PAGE no desalting step was required.

Planar SDS-PAGE. Analysis was performed under reducing conditions. For the sample preparation a mixture containing 4,8 µL sample solution, 6 µL SDS sample buffer (2x) and 1,2 µL NuPAGE Reducing Agent, which contained DTT, was vortexed for several seconds, spinned down and heat denatured using either a Thermoblock (2 minutes at 85°C). Then the solution was cooled down to RT and spinned down again. For the molecular weight calibration Mark 12 Unstained Standard from Invitrogen was applied, which was diluted 1 to 1 with water. Before 10 µL of the prepared solutions were carefully loaded into each gel pocket, the Running Chambers was filled with 800 mL freshly diluted SDS Running Buffer (1x). The voltage was set to 125 V constant, the running time was 120 minutes. For visualization the gels were silver stained. The gels were scanned using an Image Scanner from Amersham Pharmacia Biotech and the Master LabScan v.3.01b Software. For the data evaluation the Image Master TotalLab v.2.01 was applied.

CGE-on-the-chip. Gel Dye Mix (GDM), Destaining solution (DS) and a Denaturing solution containing BME were prepared according to the Agilent Protein 200+ manual before analysis. For preparing the protein samples 4 uL sample solution and 2 µL of the denaturing solution were mixed in a 0,5 mL Eppendorf tube, vortexed for 10 seconds and spinned down for 15 seconds. Afterwards the sample was heat denatured at 96°C for 4 minutes and cooled to RT subsequently before adding 84 µL water. The tube was vortexed for 10 seconds. For the preparation of the P200+ Ladder 6 uL ladder solution were applied and no water was added, otherwise the same procedure as stated above was applied. To avoid air bubbles in the sample wells during the loading of the chip the sample wells were filled using the reverse pipetting technique. Further it was important that the pipette was held vertically and that the solution was put in the middle of the well, otherwise a poorer performance might occur due to the formation of tiny air bubbles. First 12 µL GDM were filled in the well marked with "G" at the right top of the Chip. With the aid of the Chip Priming Station the GDM was pressed into the fine capillaries of the chip by air pressure for 1 minute. Then the matrix solution was removed from the well and the chip system was checked for bubbles. Bubbles in the capillaries can be detected as bright spots. Afterwards 12 µL GDM were filled in all wells labeled with G and 12 µL DS in the well marked with DS. Finally 6 µL of the sample solutions and 6 µL of the ladder solution, prepared immediately before loading the chip, were applied into the wells labeled with the numbers 1 to 10 and with the ladder symbol respectively. After filling all wells, the chip was placed into the CGE-on-the-chip device and the run was

started through the user software. At the end of analysis the electrodes were washed using an electrode cleaner chip filled with 350 mL water.

MALDI-TOF-MS. Sample preparation was exclusively performed on customary stainless steel MALDI target plates using the dried-droplet technique. First the matrix (SA or THAP) was dissolved in 0,1% TFA/ACN (1/1, v/v) to give a final matrix concentration of 6 mg/mL. The resulting matrix solution was vortexed for 10 seconds, spinned down and finally sonicated for 3 minutes to completely dissolve the matrix. AT III and FIX samples were desalted using C-18 ZipTips before they were deposited on the MALDI target. Wetting, washing and loading steps were performed according to the ZipTip user guide from Millipore, but in the final desalting step 5 µL matrix solution were aspirated once and dispensed into a new tube. Then a 0,5 µL aliquot of this solution was deposited on the target and dried at RT in a gentle stream of air. When the spot had dried, very small crystals were visible and another 0,5 µL aliquot was applied on the same spot, which was then dried again with a gentle stream of air. For the molecular mass assignments of proteins external calibration with 3 standard proteins was applied. These standard proteins were horse skeleton muscle Myoglobin, bakers yeast Enolase and bovine serum albumin. A separate external calibration was performed for each applied matrix. 9 µL matrix solution and 1,5 µL of the following three solutions were mixed together: Bovine serum albumin 1000 ng/µL; Enolase 250 ng/µL, Myoglobin 20 ng/µL. A 0,5 µL aliquot of the protein-matrix-mixture was spotted onto the MALDI target and dried under a gentle stream of air. This step was repeated once. The following average MWs were assumed: BSA 66399 Da, Enolase 46671 Da, Myoglobin 16952 Da.

Results and Discussion

Analysis of Antithrombin III using planar SDS-PAGE. It was impossible to differentiate intact Antithrombin III (AT III) from carbamylated Antithrombin III (AT III alk.) with 4-20% Tris Glycine gels (Fig. 1). A theoretical mass increase of 348 Da was expected after carbamylation. The measured MW was 60,9 kDa for intact AT III and 59,9 kDa for AT III alk., so an actual mass decrease of 1,0 kDa was observed. After 1 minute PNGase F digestion a broader AT III alk. band was observed. This peak broadening was caused by partial digestion of the sample and insufficient resolution in the molecular weight range of interest. After 2 hours five bands were observed, which represented all five possible isoforms, each with a different number of N-glycans. Resolution was poor, but all bands were clearly visible. Digestion was stopped after 2 hours, because further experiments showed, that longer digestion times had no effect on the achieved results. The following molecular weights were observed: AT III alk with 4 sugar residues - 61,3 kDa, with 3 sugar residues - 59,1 kDa, with 2 sugar residues - 57,0 kDa, with 1 sugar residue - 54,5 kDa, without sugar residues - 51,9 kDa. Therefore the MW difference between the bands were 2,2 kDa; 2,1 kDa; 2,5 kDa and 2,6 kDa. The difference between complete and non glycosylated AT III was 9,4 kDa.

Analysis of Coagulation Factor IX using planar SDS-PAGE. After 2 hours digestion time the N-glycans of rFIX were completely removed and only a single band with a MW of 57,6 kDa was visible (Fig 1). In the contrary to AT III, where carbamylation was absolutely necessary for the de-N-glycosylation, PNGase F worked very well with intact

rFIX. For intact rFIX a MW of 67,4 kDa was determined, so a mass decrease of 9,8 kDa was observed after complete PNGase F digestion. After 1 minute of PNGase F digestion, mono-de-N- and complete-de-N-glycosylated rFIX was already visible. The following molecular weights were determined for partial digestion: rFIX with 2 N-glycan residues: 67,1 kDa, rFIX with 1 N-glycan residue: 59,7 kDa, rFIX without N-glycan residues: 55,1 kDa. The observed MW difference was 7,4 kDa between intact rFIX and mono-de-N-glycosylated rFIX and 4,6 kDa between mono-de-N-glycosylated and complete de-N-glycosylated rFIX. Therefore the MW difference between fully glycosylated and complete de-N-glycosylated rFIX was 12,0 kDa. One reason that one time a mass shift of 9,8 and the other time a mass shift of 12,0 kDa between intact and complete de-N-glycosylated rFIX was observed, can be explained through the fact, that in the first case the intensity of both analyte peaks were similar, while in the second case the two bands of partly digested rFIX were much less intensive than the band of intact rFIX.

Analysis of Antithrombin III using CGE-on-the-chip. It was possible to differentiate between α and β form of AT III with CGE-on-the-chip (Fig. 2). For the α form of AT III a MW of 76 kDa was determined, while the β form showed a MW of 67 kDa. Peak areas of both AT III peaks correlated with the typical abundance ratio of α and β form in human plasma. The big difference between the MW stated by the literature, 57,3 kDa, [23] and the obtained MW of α-AT III with CGE was irritating. An explanation for this phenomenon was, that large sugar residues, like 2 kDa glycan residues in the case of AT III, interrupted the stick-like form of denatured proteins and made proteins bulkier [25]. These bulkier proteins travel slower during the gel electrophoresis than proteins

without extensive sugar residues. On the other hand SDS cannot attach to glycan structures, so comparable less SDS was loaded onto glycoproteins. AT III also showed broader peaks compared with other, non-glycosylated proteins due to microheterogenities. For alkylated AT III a MW of 79 kDa was observed, so a mass increase of 3 kDa was determined after alkylation. After 1 minute digestion time with PNGase F, mono- and di-de-N-glycosylated isoforms of AT III alk. were already visible and could be distinguished. After incubating reduced and alkylated AT III with PNGase F for 30 minutes, only a small amount starting material was visible anymore, while after 18 hours no starting material was visible at all (Fig. 3). Peaks 2, 3 and 4 indicate partly de-N-glycosylated alkylated AT III and while these peaks clearly became weaker after 18 hours digestion time, they were still visible afterwards (Table 1). Peak 5 is the complete de-N-glycosylated isoform of alkylated AT III, which was the most intensive peak after a several hours of PNGase digest. The area of peak 6 was correlated with peak 5 and was probably a degradation product of complete de-N-glycosylated AT III. The average MW was 78,8 kDa for peak 1, 68,2 kDa for peak 2, 59,1 kDa for peak 3, 49,6 kDa for peak 4, 46,0 kDa for peak 5 and 42,1 kDa for peak 6. Hence, the MW difference was 10,4 kDa between peak 1 and 2, 8,8 kDa between peak 2 and 3, 9,5 kDa between peak 3 and 4 and 3,6 kDa between peak 4 and 5. The mass difference between peak 4 and 6 was 7,5 kDa. After 2 hours digestion time CGE results were similar to those achieved with SDS-PAGE. During the de-N-glycosylation peak 5 and 6 steadily became larger, while peaks 2 to 4 reached a maximum after some time and afterwards a decrease in the protein amount occurred. This concentration maximum was reached after 1 minute (peak 2), 30 minutes (peak 3) or 1 hour (peak 4). A general problem should also be considered when working

with de-N-glycosylated proteins. Glycosylations are not only required for biological activity, but also to improve the solubility of proteins. It was noticed that, according to the obtained CGE results, the total protein amount in solution was decreased by 20% after 5 hours digestion, which might be due to adsorption and/or sedimentation.

Analysis of Coagulation Factor IX using CGE-on-the-chip. CGE-on-the-chip experiments provided a MW of 90 kDa for pdFIX and 95 kDa for rFIX (Fig. 4). Compared with other analysed proteins the analyte peaks of the FIX samples were very broad due to the numerous post-translational modifications of the protein. It was further noticed, that the analyte peak shape of rFIX was very asymmetric. Concerning the poor mass accuracy the same applies as stated for AT III. Like AT III, both FIX samples have ~2 kDa sugar residues, which interfered with the protein's migration behaviour. Because FIX is more heavily post-translational modified than AT III, the mass accuracy obtained for FIX was even poorer than for AT III. The determined MW of rFIX was about 9 kDa higher than the MW of pdFIX. De-N-glycosylation of rFIX occurred very fast. After only 1 minute digestion time the largest peak was already the complete de-N-glycosylated isoform. Another phenomenon was observed after the PNGase F digest: the more of the original N-glycan structure was removed, the smaller the peak width became. After 3 hours digestion time there was only a very small mono-N-glycosylated peak visible, which area was about 30 times smaller than the peak area of complete de-N-glycosylated rFIX. Thus the digest was almost complete, but even after 18 hours incubation with PNGase F it was not possible to completely digest the small mono-N-glycosylated peak (Fig. 5). On the other hand even after 30 minutes digestion time with PNGase F, no intact

rFIX was observed anymore. These observations were true for both, rFIX and pdFIX (Fig. 6). The average MWs for pdFIX were 90,0 kDa (2 N-glycans), 78,8 kDa (1 N-glycan) and 64,5 kDa (without N-glycans), so the calculated MW difference between intact and mono de-N-glycosylated pdFIX was 11,2 kDa. Between mono-de-N-glycosylated pdFIX and complete de-N-glycosylated pdFIX a MW of 14,3 kDa was observed, so the total MW difference between complete N-glycosylated and complete de-N-glycosylated pdFIX was 25,5 kDa (table 2). In the case of rFIX an average MW of 94,8 kDa was determined for the intact protein, 84,9 kDa for mono-glycosylated rFIX and 63,5 kDa for complete de-N-glycosylated rFIX. The difference between intact and mono-glycosylated rFIX was 15,9 and 16,4 kDa between mono-glycosylated and complete de-N-glycosylated rFIX, hence the total difference between intact and complete de-N-glycosylated rFIX was 32,3 kDa (table 3). This mass shift was higher than in the case of pdFIX. After complete de-N-glycosylation both FIX samples showed very similar MWs, which lead to the assumption that the recombinant protein had different N-glycosylations compared to plasma derived FIX, but a similar protein backbone. When comparing the speed of de-N-glycosylation with the de-N-glycosylation of AT III, both FIX samples were degraded much faster than alkylated AT III.

Analysis of Antithrombin III using MALDI-TOF-MS. The obtained average MW of intact AT III with 4 glycan residues was 57,16 kDa. After carbymylation an average MW of 57,69 kDa was measured, so a mass increase of 0,53 kDa was observed. A theoretical mass increase of 0,35 kDa was expected, so the mass shift was higher than expected. After PNGase F digestion of AT III alk. the average MW obtained with MALDI-TOF-

MS decreased from 57,69 kDa to 49,47 kDa, which was a shift of 8,22 kDa (Fig. 7). The average MW difference of the isoforms was 2,05 kDa. The MW of AT alk. determined with SDS-PAGE (60 kDa) was closer to the MALDI-TOF-MS result (49,5 kDa) than the MW determined with on-chip-CE (79 kDa). The MW obtained with CGE-on-the-chip for complete de-N-glycosylated AT III alk. (46 kDa), however, was very close to the MW determined with MALDI-TOF-MS (47,7 kDa). The MW of complete de-N-glycosylated AT III alk. determined with planar SDS-PAGE (59 kDa) was higher than the results obtained with the other methods (Table 4). Further MALDI-TOF-MS and CGE-on-the-chip results demonstrated that glycosylations generally caused peak broadening due to heterogenities. Hence, the more of the original N-glycan structure was removed, the slighter the peaks became.

Analysis of Coagulation Factor IX using MALDI-TOF-MS. Sinapinic acid (SA) and several other matrices were tested as MALDI matrices for the desorption and ionisation of FIX, but suitable results were only obtained with THAP. For intact rFIX an average MW of 54,70 kDa and for intact pdFIX an average MW of 55,31 kDa was measured (Fig. 8). Hence a significant mass difference of about 0,61 kDa between both FIX samples was observed. rFIX seemed to be of higher purity and more concentrated, so better signals were obtained with rFIX compared with pdFIX. According to literature the MW of FIX was 53,75 kDa, so the determined MW of rFIX was 1,8% higher [50]. The MWs of both, intact and PNGase F digested FIX samples were measured and the MW difference between the intact and de-N-digested protein was calculated. Therefore, the observed mass shifts should not be over-interpreted, since two large molecular weights

were subtracted from each other. When comparing the data of pdFIX obtained with MALDI-TOF-MS, a mass decrease of 6,66 kDa was observed (intact pdFIX: 55,31 kDa, PNGase F digested pdFIX: 48,65 kDa) after complete de-N-glycosylation. In the case of rFIX a mass decrease of 6,98 kDa was observed (intact rFIX: 54,70 kDa; PNGase F digested rFIX: 47,72 kDa). It was likely, that the glycan residues of rFIX were larger than those of pdFIX. This conclusion was also affirmed by CGE-on-the-chip results. Furthermore, complete de-N-glycosylated pdFIX and de-N-glycosylated rFIX seemed to be different, since complete de-N-glycosylated rFIX was 0,94 kDa smaller than complete de-N-glycosylated pdFIX, probably due to other differences between the post-translational modifications of both FIX samples. When comparing the results achieved with MALDI-TOF-MS with the gel electrophoretical methods, the data obtained with slab gel electrophoresis were more accurate than the data observed with CGE-on-the-chip (Table 5).

Conclusions

De-N-glycosylation with PNGase F generally worked with both proteins of interest, but the kinetic of the enzymatic digestion was heavily affected by the nature of the glycoprotein. For FIX an almost quantitative digestion was observed after a rather short time, while in the case of reduced and alkylated AT III a significant amount of only partly digested protein was detected even after more than 18 hours incubation time with PNGase F. All three presented methods were suitable for monitoring the de-N-glycosylation progress. Concerning the performance of the applied methods planar SDS-PAGE with slab gels and on-chip-CE provided very similar results, which was not

surprisingly because both techniques are basically based on gel electrophoresis. On the other hand suppression effects occurred with MALDI-TOF-MS, so analysis of protein mixtures or proteins with different glycosylation states showed different results compared with gel electrophoretical results. CGE-on-the-chip was by far the fastest of all applied methods, while analysis with MALDI-TOF-MS was most labour intensive. Nevertheless the MWs determined with MALDI-TOF-MS were most accurate, while analysis of glycoproteins with SDS gel electrophoresis generally provided too high molecular weights due to attached glycan structures. Especially sizing with CGE-on-the-chip was heavily affected by glycans, which was a benefit for this work.

Acknowledgements. We want to tank F. Weigang (Agilent Technologies, Vienna), M. Kuschel and A. Zenker (Agilent Technologies, Waldbronn, Germany) for providing us with the Agilent 2100 Bioanalyzer. Further we thank K. Pock and A. Buchacher (Octapharma, Vienna) for plasma derived antithrombin III and coagulation factor IX samples.

Legends to tables

Table 1. Results of the PNGase F digestion of alkylated AT III measured with CGE-on-the-chip

Table 2. Results of the PNGase F digestion of rFIX measured with CGE-on-the-chip

Table 3. Results of the PNGase F digestion of pdFIX, measured with CGE-on-the-chip

Table 4. Summary of the results achieved for AT III with all three methods

Table 5. Summary of the results achieved for FIX with all three methods

Legends to figures

Figure 1. Planar SDS-PAGE (4-20% Tris-Glycine gel) of PNGase F digested AT III alk. and rFIX, silver stained; lane 1: AT III (500 ng); lane 2: AT III alk. (500 ng); lane 3: AT III alk. after 1 minutes; PNGase F digest; lane 4: AT III alk. after 2 hours PNGase F digest; lane 5: rFIX intact (3 ug); lane 6: rFIX after 1 minutes PNGase F digest; lane 7: rFIX after 2 hours PNGase digest

Figure 2. CGE-on-the-chip electropherogram of intact AT III

Figure 3. CGE-on-the-chip electropherograms of rather incomplete PNGase F digests of AT III alk.; blue line: after 30 minutes; red line: after 18 hours; peak 1: AT III alk with 4 sugar residues (α form), peak 2: AT III alk with 3 sugar residues (β form), peak 3: AT III alk with 2 sugar residues, peak 4: AT III alk with 1 sugar residue, peak 5: AT III alk with no sugar residues; peak 6 could not be correlated with a specific form of AT III alk and was probably a degradation product

Figure 4. CGE-on-the-chip electropherograms of pdFIX (red line) and rFIX (blue line)

Figure 5. CGE-on-the-chip electropherograms of PNGase F digests of intact rFIX (blue line), rFIX after 30 minutes of PNGase F digest (turquoise line) and rFIX after 3 hours of PNGase F digest (red line)

Figure 6. CGE-on-the-chip electropherograms of PNGase F digests of intact pdFIX (blue line), pdFIX after 1 min PNGase F digest (turquoise line), pdFIX after 15 min PNGase F digest (black line) and pdFIX after 3 hours of PNGase F digest (red line)

Figure 7. MALDI-TOF mass spectra of PNGase F digests of AT III alk. without PNGase F (red line), AT III alk after 30 minutes PNGase F digest (blue line) and AT III alk after 18 hours PNGase F digest (green line); matrix: SA; peak 1 is the fully N-glycosylated protein, peak 2 shows AT III alk. with 3 sugar residues, peak 3 is the di-N-glycosylated and peak 4 the mono-N-glycosylated protein; peak 5 is the complete de-N-glycosylated protein

Figure 8. MALDI-TOF mass spectra of intact rFIX (green line), intact pdFIX (orange line), complete PNGase F digested rFIX (blue line) and complete de-N-glycosylated pdFIX (red line); matrix: THAP

References

[1] Putnam F (1993) *Perspectives in Biological Medicine* 36:323-337

[2] O'Farrell P (1975) *Journal of Biological Chemistry* 250:4007-4021

[3] Görg A, Postel W, Gunther S (1988) *Electrophoresis* 9:531-546

[4] Fazekas de St. Groth S, Webster R, Datyner A (1963) *Biochimica and Biophysica Acta* 71:377-391

[5] Heukeshoven J, Dernick R (1988) *Electrophoresis* 9:28-32

[6] Karas M, Hillenkamp F (1988) *Anal Chem* 60:2299-2301

[7] Tanaka K., Waki H., Ido Y., Akita S., Yoshida Y., Yohida T. (1988) *Rapid Commun Mass Spectrom* 2:151-153

[8] Karas M, Bachmann D, Bahr U, Hillenkamp F (1987) *Int J Mass Spectrom* 78:53

[9] Karas M (1990) *Phys Bl* 5:149-154

[10] Spengler B, Kaufmann R (1992) *Analusis* 20:91-101

[11] Felton M (2003) *Anal Chem* 75:505-508A

[12] Bousse L (2001) *Anal Chem* 76:1207-1212

[13] Heiger D (2000) High performance capillary electrophoresis - an introduction, Agilent Technologies, Waldbronn

[14] Mueller O, Hahnenberger K, Dittmann M, Yee H, Dubrow R, Nagle R, Ilsley D (2000) *Electrophoresis* 21:128-134

[15] Ogura M, Agata Y, Watanabe K, McCormick R, Hamaguchi Y, Aso Y, Mitsuhashi M (1998) *Clin Chem* 44:2249-225

[16] Woolley A, Mathies R (1995) *Anal Chem* 67:3676-3680

[17] Barthmaier P (2002) Application Note 5988-8322EN, Agilent Technologies

[18] Barthmaier P, Kuschel M, Neumann T, Kratzmaier M (2002), *American Biotechnology Laboratory*, publication number 5988-7907EN, Agilent Technologies

[19] Technical Note 5988-3160EN (2001), Agilent Technologies

[20] Barthmaier P (2001) Application Note 5988-4021EN, Agilent Technologies

[21] Neumann T (2002) Application Note 5988-6576EN, Agilent Technologies

[22] Guttmann A (1996) *TrAC-Trend Anal Chem* 15:194-198

[23] Belgacem O, Buchacher A, Pock K, Josic D, Sutton C, Rizzi A., Allmaier G. (2002) *J Mass Spectrom* 37:1118-1130

[24] Bond M, Jankowski M, Patel H, Karnik S, Strang A, Xu B, Rouse J, Koza S, Letwin B, Steckert J, Amphlett G, Scoble H (1998) *Semin Hematol* 35:11-17

[25] Kelly L, Barthmaier P (2003) Application Note 5989-0332EN, Agilent Technologies

sample name	molecular weight [kDa]						concentration [ng/µL]						
	6	5	4	3	2	1	6	5	4	3	2	1	total
AT III alk, not digested	-	-	-	-	70,1	79,0	-	-	-	-	37,2	403	440
AT III alk, 1 min digest	-	-	-	59,5	67,6	77,4	-	-	-	35	101	99,1	235
AT III alk, 0,5h digest	42,0	46,0	49,6	59,1	67,9	78,5	17,1	20,6	84,5	68,9	9,5	1,9	203
AT III alk, 1h digest	42,1	45,7	49,4	59,0	67,8	78,5	26,7	32,6	88,7	49,5	4,4	1,4	203
AT III alk, 2h digest	42,2	46,2	49,5	58,7	67,5	78,9	37,6	35,2	85,3	49,9	3,9	1,3	213
AT III alk, 3,5h digest	42,1	46,1	49,5	59,1	68,1	79,6	43,9	38,6	82	43,4	2,8	1	212
AT III alk, 5h digest	42,1	45,8	49,9	59,2	68,4	80,0	42,9	34,4	68,5	37,1	2,7	0,7	186

Table 1

sample name	MW [kDa]			concentration [ng/µL]			
	3	2	1	3	2	1	total
pdFIX intact	-	-	90,0	-	-	224,1	224,1
pdFIX PNGase F digest t=1min	64,9	78,3	90,0	11,9	35,9	35,2	83,0
pdFIX PNGase F digest t=15min	65,0	78,8	-	84,9	14,5	-	99,4
pdFIX PNGase F digest t=30min	64,2	79,3	-	90,0	10,9	-	100,9
pdFIX PNGase F digest t=1h	64,0	79,0	-	104,1	9,0	-	113,1
pdFIX PNGase F digest t=2h	64,4	78,4	-	85,6	7,3	-	92,9
pdFIX PNGase F digest t=3h	64,5	78,8	-	92,0	3,7	-	95,7

Table 2

sample name	molecular weight [kDa]			concentration [ng/µL]			
	3	2	1	3	2	1	total
rFIX intact	-	-	94,8	-	-	4340	4340
rFIX PNGase F digest t=15min	63,7	85,0	-	3827	352	-	4179
rFIX PNGase F digest t=30min	63,3	85,0	-	3735	260	-	3995
rFIX PNGase F digest t=60min	63,5	84,6	-	3559	110	-	3669

Table 3

sample	molecular weight [kDa]		
	SDS-PAGE	Lab-on-a-chip	MALDI-MS
AT III, intact, alpha form	60,9	76,0	57,2
AT III, alk., alpha form	61,3	78,8	57,7
AT III, alk., mono-de-N-glycosylated	59,1	68,2	55,5
AT III, alk., di-de-N-glycosylated	57,0	59,1	53,5
AT III, alk., tri-de-N-glycosylated	54,5	49,6	51,5
AT III, alk., complete de-N-glycosylated	51,9	46,0	49,5

Table 4

sample	molecular weight [kDa]		
	SDS-PAGE	Lab-on-a-chip	MALDI-MS
pdFIX, intact	61,1	90,0	55,3
rFIX, intact	67,1	94,8	54,7
rFIX, mono-de-N-glycosylated	59,7	78,8	51,2
rFIX, complete de-N-glycosylated	55,1	64,5	47,7

Table 5

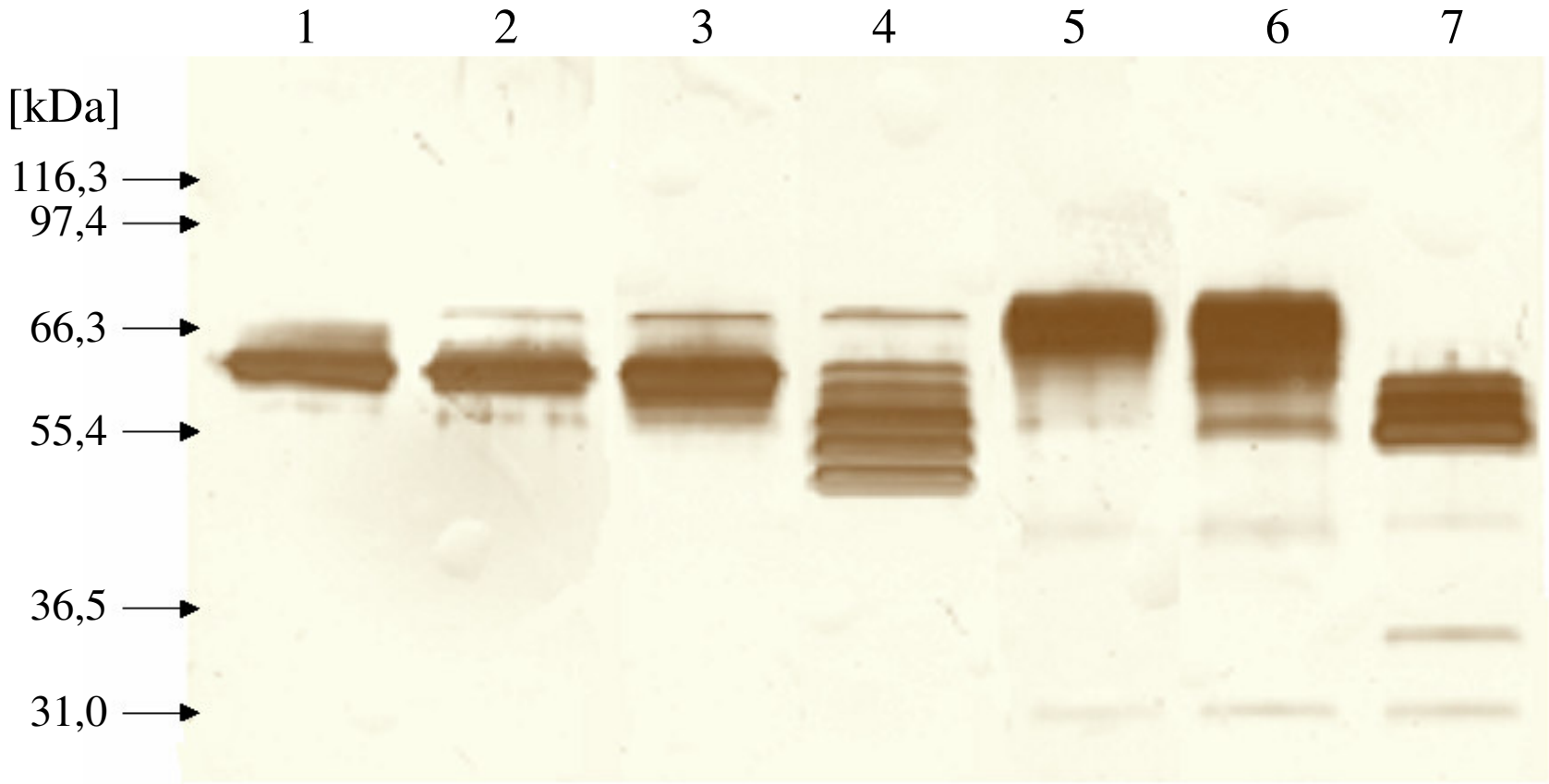

Figure 1

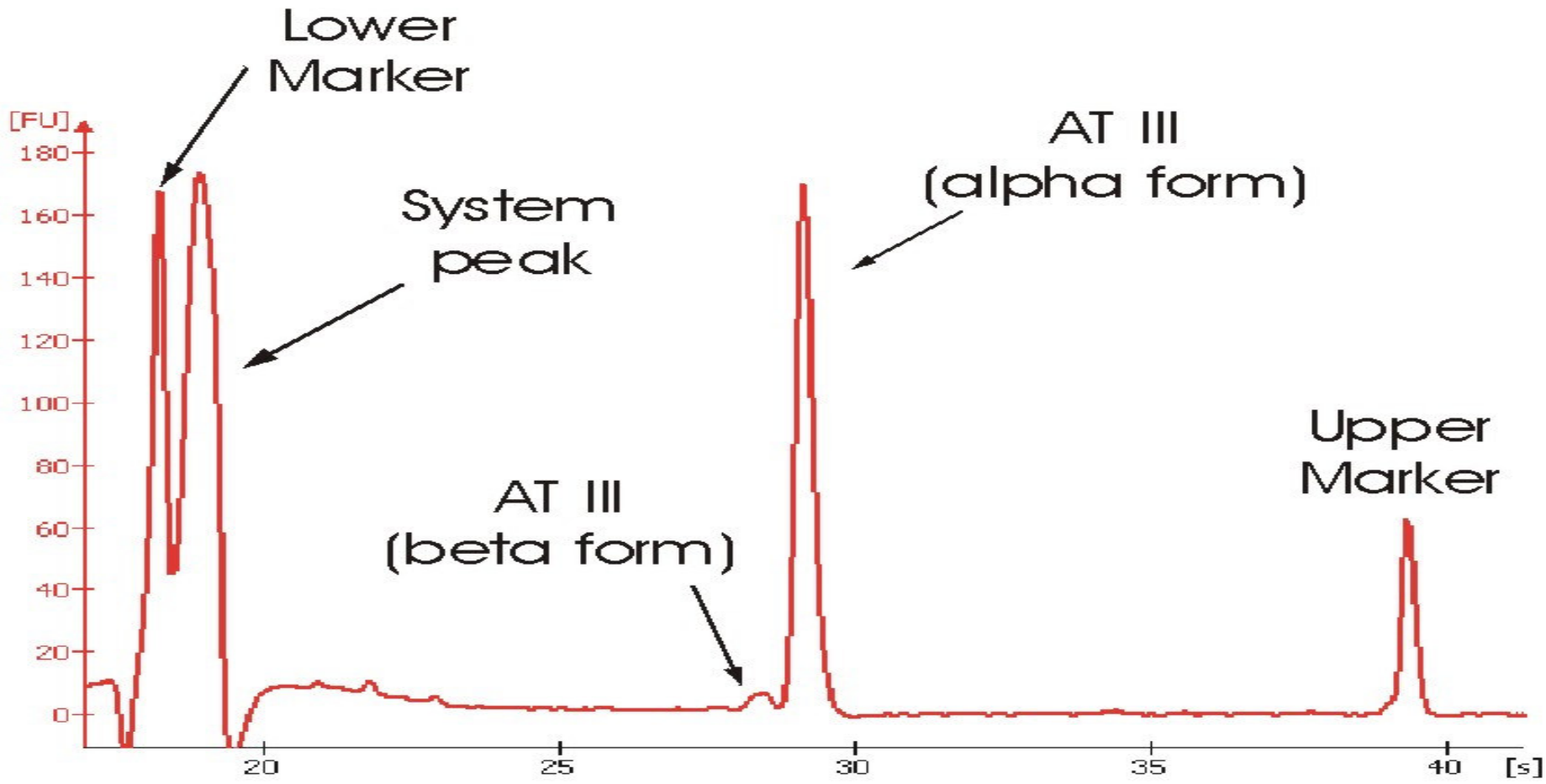
Lower
Marker
System
peak
AT III
(alpha form)
AT III
(beta form)
Upper
Marker
[FU]
180
160
140
120
100
80
60
40
20
0
20
25
30
35
40
[s]

Figure 2

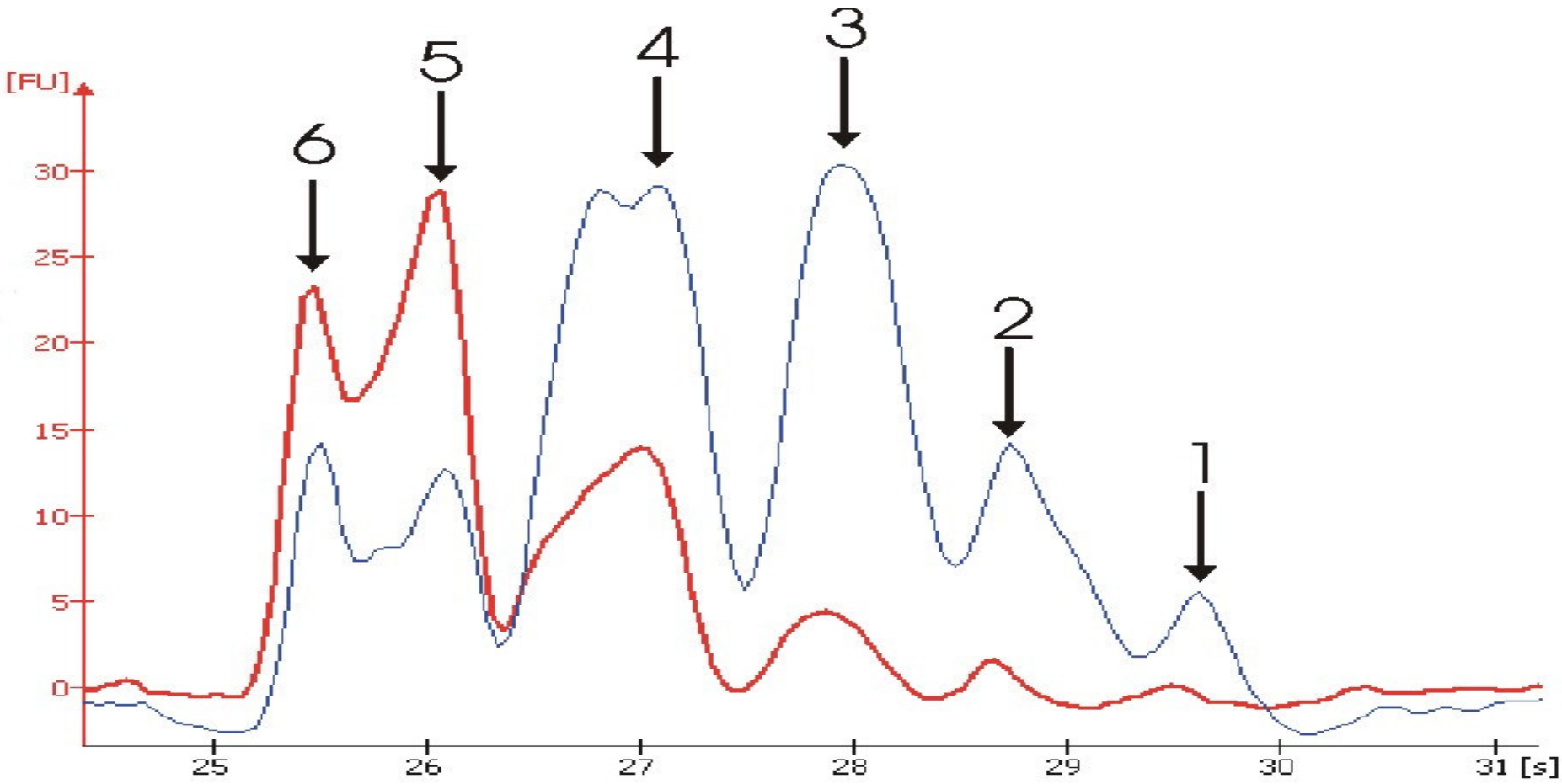

Figure 3

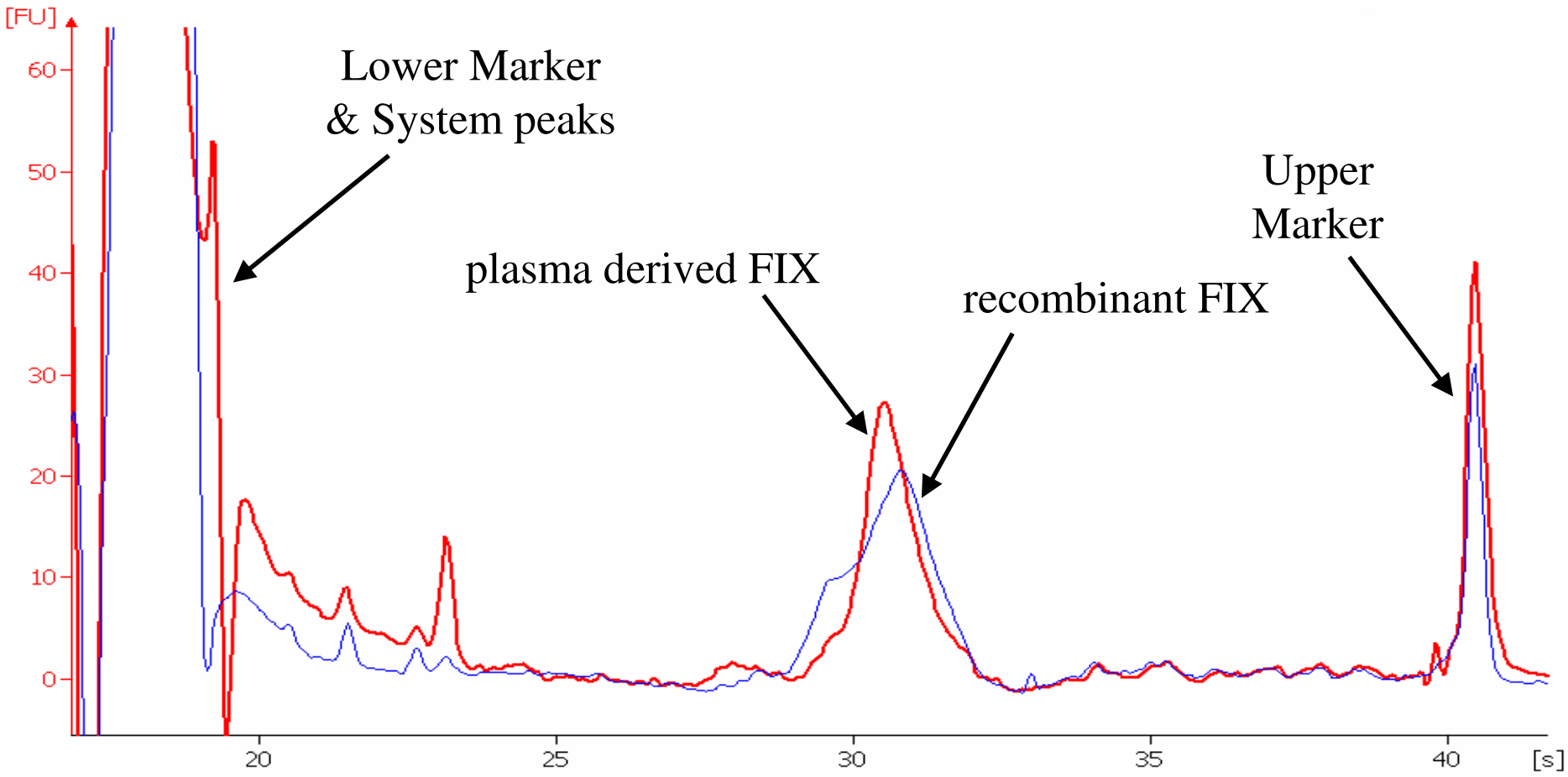
[FU]
60
50
40
30
20
10
0
Lower Marker
& System peaks
plasma derived FIX
recombinant FIX
Upper
Marker
20
25
30
35
40
[s]

Figure 4

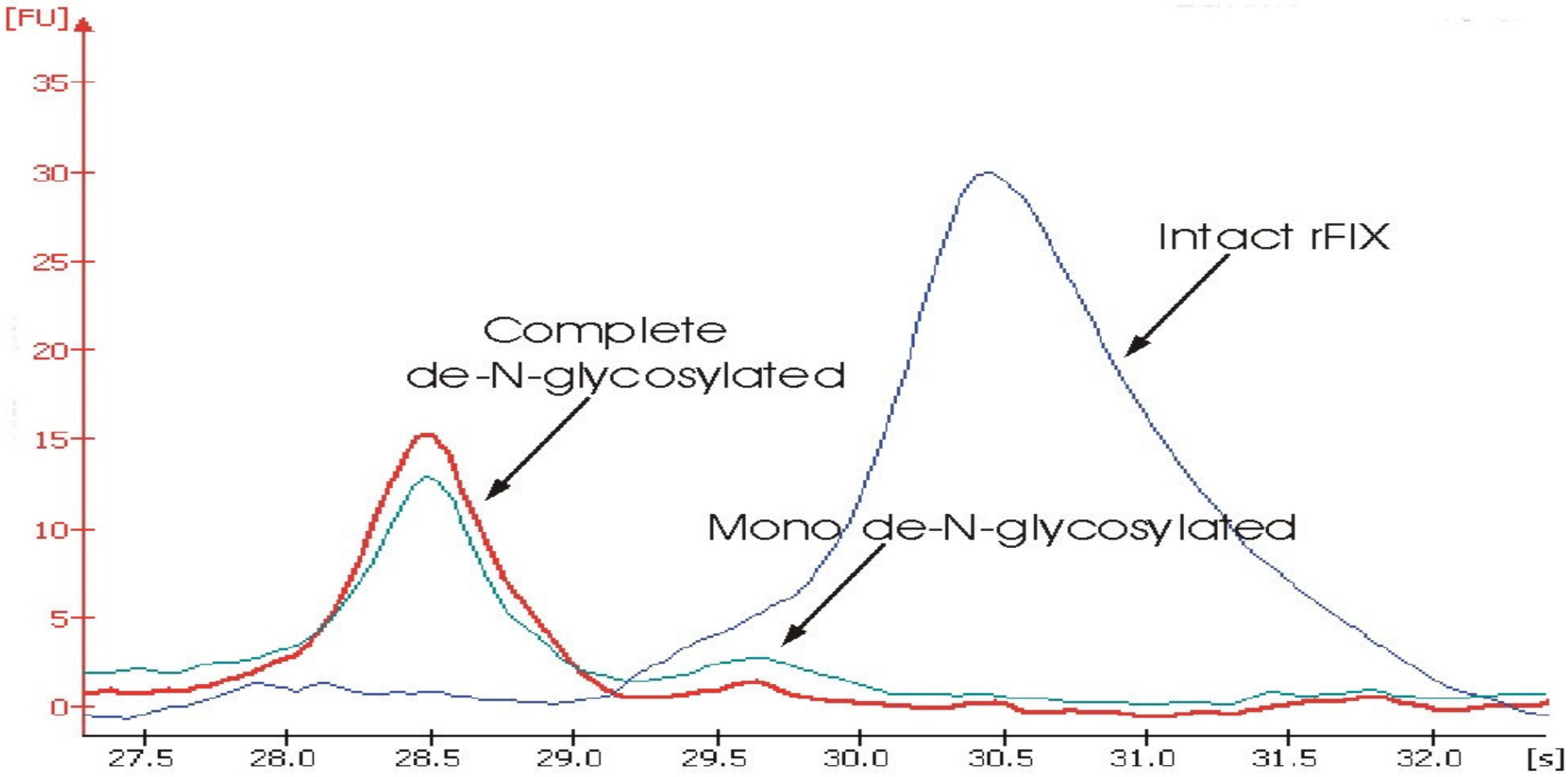
[FU]
35
30
25
20
15
10
5
0
27.5
28.0
28.5
29.0
29.5
30.0
30.5
31.0
31.5
32.0
[s]
Intact rFIX
Complete
de-N-glycosylated
Mono de-N-glycosylated

Figure 5

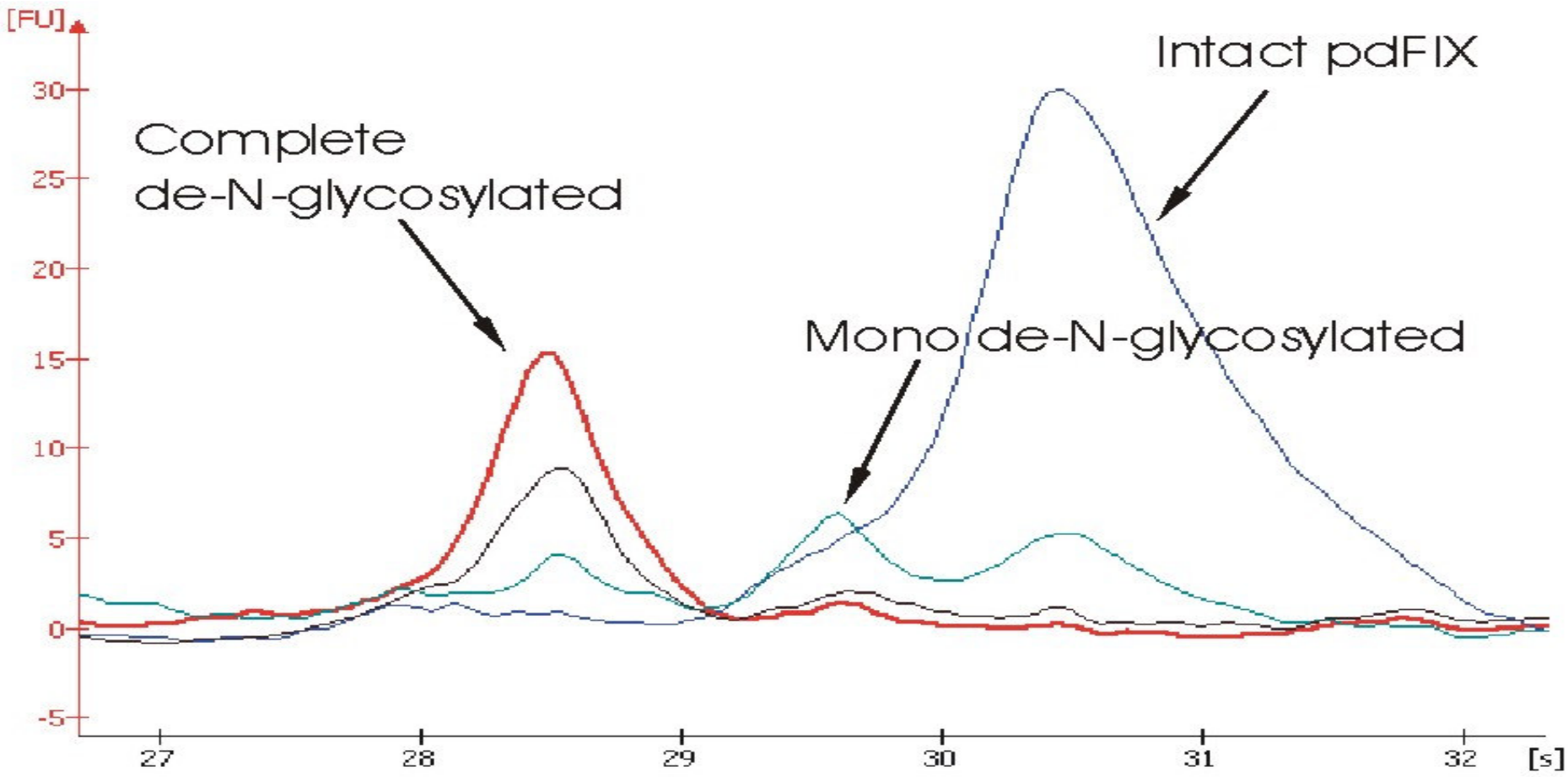
[FU]
30
25
20
15
10
5
0
-5
Complete
de-N-glycosylated
Intact pdFIX
Mono de-N-glycosylated
27
28
29
30
31
32
[s]

Figure 6

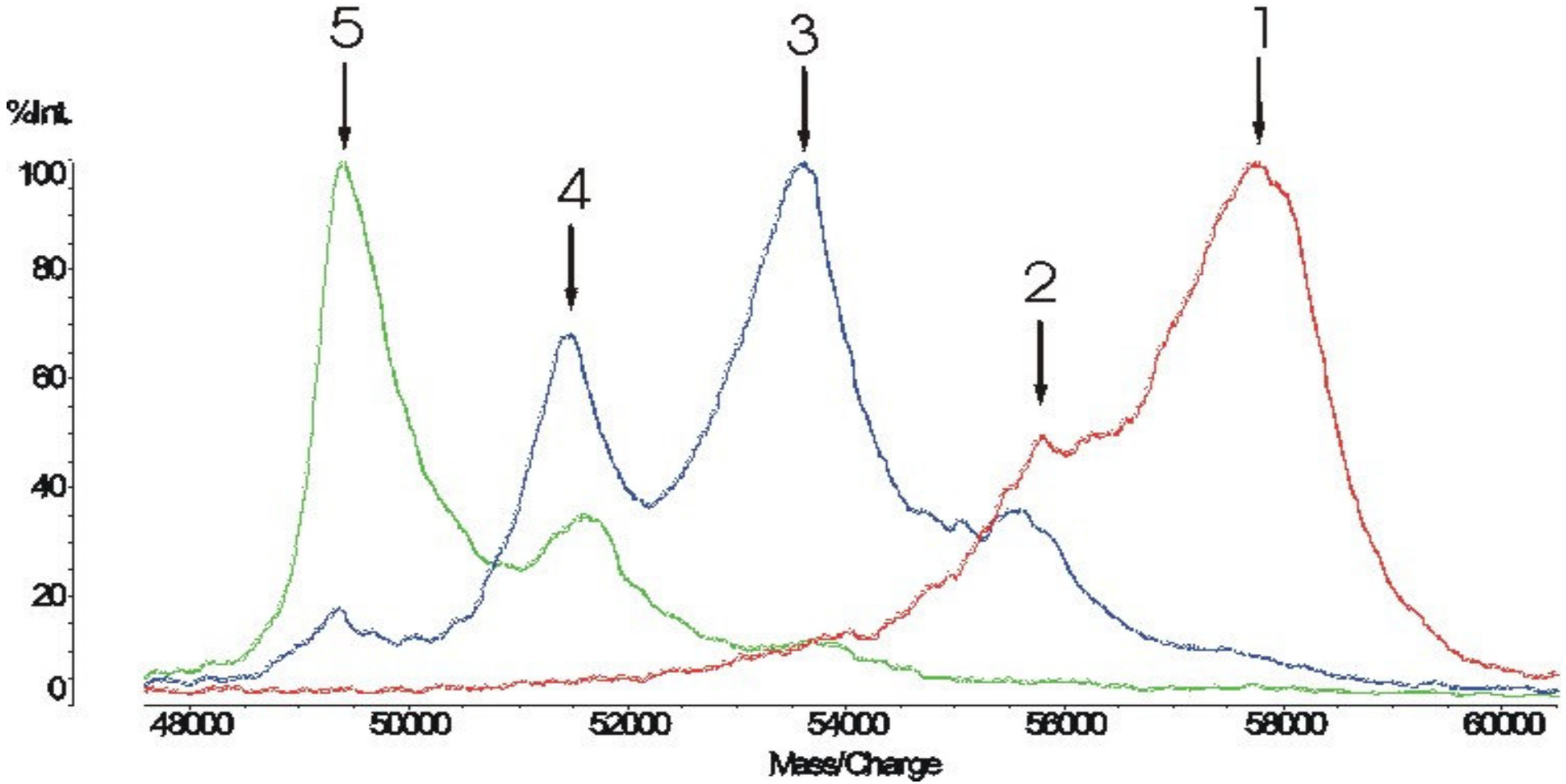
5
3
1
4
2
%Int.
100
80
60
40
20
0
48000
50000
52000
54000
56000
58000
60000
Mass/Charge

Figure 7

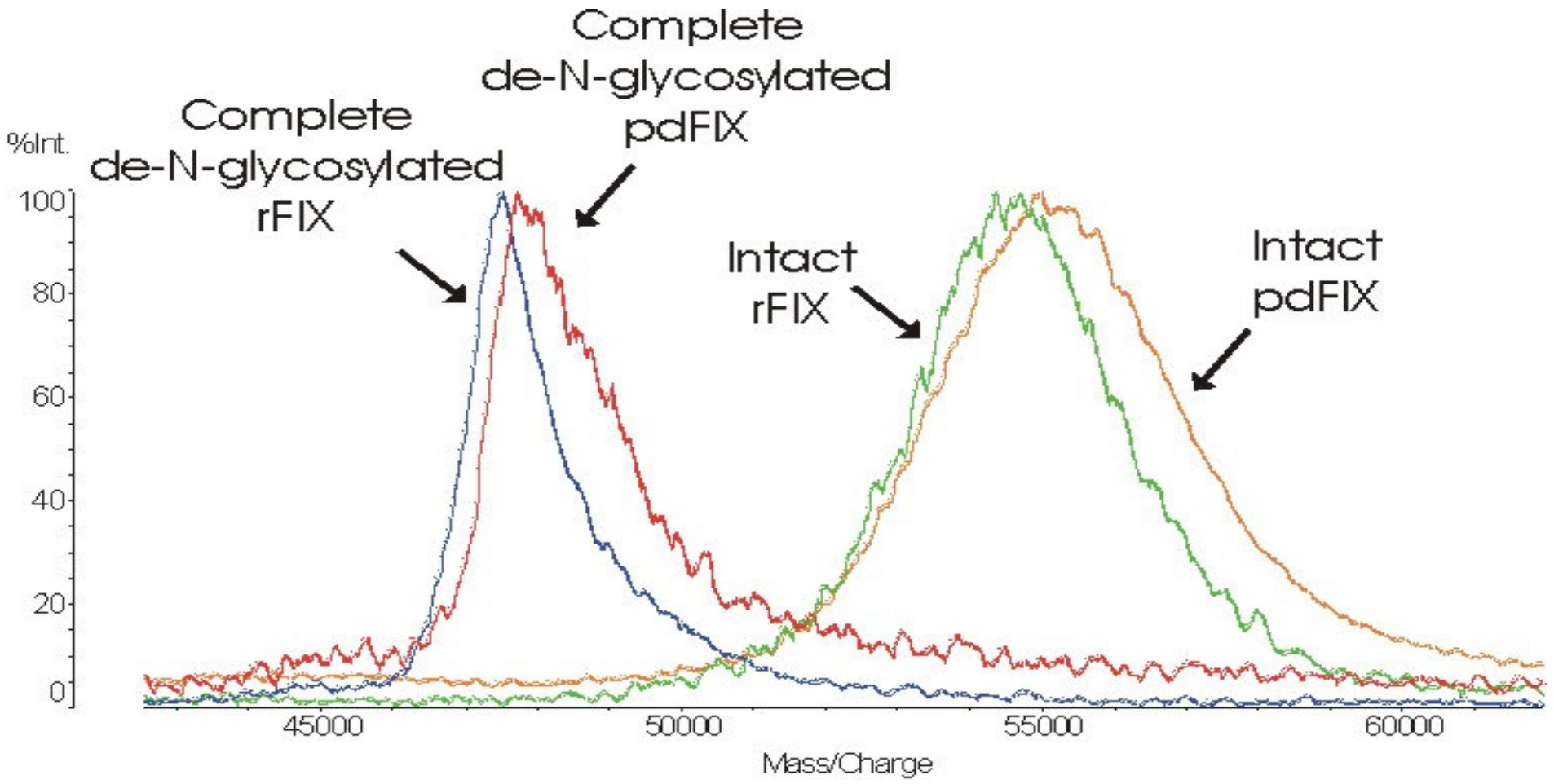
Complete
de-N-glycosylated
pdFIX
Complete
de-N-glycosylated
rFIX
Intact
rFIX
Intact
pdFIX
%Int.
100
80
60
40
20
0
45000
50000
55000
60000
Mass/Charge

Figure 8

Macromolecules, *in preparation* (2006)

Determination of molecular weight, particle size and density of high number generation PAMAM dendrimers using MALDI-TOF-MS and nES-GEMMA

Roland Müller[1+], Christian Laschober[1,2+], Wladyslaw W. Szymanski[2] and Günter Allmaier[1*]

[+]Both have contributed equally to the work.

[1]Institute of Chemical Technologies and Analytics, Vienna University of Technology, A-1060 Vienna, Austria

[2]Institute of Experimental Physics, University of Vienna, A-1090 Vienna, Austria

Corresponding author: Günter Allmaier, Institute of Chemical Technologies and Analytics, Vienna University of Technology, Getreidemarkt 9/164, A-1060 Vienna, Austria

Tel: +43 1 58801 15160 Fax: +43 1 58801 15199

E-mail: guenter.allmaier@tuwien.ac.at

Running title: MALDI-MS and nES-GEMMA of PAMAM dendrimers

ABSTRACT

In this work we present the characterization of PAMAM dendrimers from generation two (G2) up to ten (G10) with a focus on the G5 to G10 with matrix-assisted laser desorption/ionization linear mass spectrometry (MALDI-MS) and nano-electrospray gas-phase electrophoretic mobility molecular analysis (nES-GEMMA). For the first time the molecular masses of high-mass dendrimers G8 to G10 were determined by MALDI-MS and nES-GEMMA, techniques which are based on different physico-chemical principles. Obtained experimental data allowed the determination of the molecular mass (up to 580 kDa with a precision below ±0,9%), of the spherical size (from 3.3 - 14.0 nm with a precision of ±0.2 nm) and the calculation of their densities. Amounts in the nanogramm range were sufficient for analysis could be performed within several minutes. The results based on these methods for high-generation dendrimers exhibited an excellent correlation and were compared with published data using techniques based on different principles.

Introduction

Dendritic (branch like) architecture has been recognized as complete new building scheme for polymers as early as 1926 by Herman Staudinger within his macromolecular hypothesis[1]. This kind of architecture lead to polymeric molecules[2,3], called dendrimers, which faced a rapidly increasing importance in the recent decade[4-8], since they are recognized as a whole new type of well defined functionalised building blocs for a bottom-up synthesis of nanoscale objects with designable properties[9-12]. Unlike other polymers, dendrimers possess a well defined globular size in the low nm range and structure, with a clear distinction between core and surface, which makes them suitable for applications like catalysis and as delivery vehicles[7] for

small drug molecules[13]. Various interesting molecular architectures using dendrimers have already been realised, such as self assembly macromolecule structures between different types of dendrimers[14,15], dendrimers coupled with various polymers in different arrangements[16-19], dendrimers with hydrophobic core and hydrophilic surface, which may be used as artificial liposomes, and dendrimers coupled to peptides, antibodies, DNA and carbohydrates for example. The goal of these architectures is to create a whole set of new macromolecular properties which could not have been realised otherwise.

To be able to create desired dendrimer products and structures, dendrimer properties (e.g. molecular weight, hydrophobic vs. hydrophilic character, number and type of free reaction groups, average diameter and density) have to be sufficiently characterised during macromolecular synthesis steps and before their use in the above mentioned applications. Despite this fact, analysis seems to be a step behind their importance and as was already stated by Caminade et. al.[20]. The main reason for this fact is that dendrimers pose a new challenge to all analytical techniques as they exhibit exponentional growth of surface and mass during their stepwise synthesis (producing the next higher generation) as well as covering a mass range from a few kDa in the case of generation one (G1) to one MDa for generation ten (G10).

A special, very important subclass of the dendrimers, namely poly(amido-)amine (PAMAM) dendrimers, will be the focus of this work. PAMAM dendrimers resemble proteins in their size and particular chemical structure (a huge number of peptide bonds). But while proteins can fold oddly or change their shape, dendrimers are more or less cemented structures with strong and rigid bonds. Due to these attributes they are already used to replace proteins in immunodiagnostics[21,22] and *in vitro* gene expression applications[23], for example. Therefore it is not surprising that PAMAM dendrimers are the first class of dendrimers which have been successfully commercialised[3], which makes their detailed characterisation even more important.

Until now size exclusion chromatography (SEC)[24-28], slab gel electrophoresis (SDS-PAGE)[29], capillary electrophoresis (CE)[29,30], small angle x-ray scattering (SAXS)[31,32], and small angle neutron scattering (SANS)[33,34] atomic force microscopy (AFM)[35-38], transmission electron microscopy (TEM)[39] and mass spectrometry[40,41], have been applied to determine the molecular mass, diameter and shape of PAMAM dendrimers. Other techniques that focus on a chemical characterisation such as the characterisation of surface groups or the abundance of certain structure elements will not be discussed in this work, since the presented experimental data are solely focused on molecular mass, size and density determination. In the following section we give a brief overview of the before mentioned techniques as well as their advantages and disadvantages. A detailed description of other analytical techniques applied to dendrimers can be found in following reviews [20,42-44].

SEC is a widely and routinely used separation technique which allows the separation of analytes according to their size in solution. The main advantages of SEC are easy handling and a high dynamic range concerning molecular weight determination. When this method was applied to determine the molecular mass of dendrimers, a systematic error between expected and with SEC determined molecular mass values was found[24]. This error could be linked to the different shape of the commonly used calibrants, which are linear polystyrol polymers, and the spherically shaped dendrimers. This shape dependency of the molecular weight determination is a general phenomenon of SEC and thus makes this method somehow problematic in the use of molecular weight determination of dendrimers particularly for higher generations.

CE and SDS-PAGE are analytical techniques widely used for the analysis of biopolymers. Both techniques separate analytes according to their electrophoretic migration behaviour, which strongly depends the number of charged surface groups, the pH of the buffer solution and the cross section of the molecule. For molecular weight determination, as it is carried out with proteins, denaturation and the attachment of sodium dodecyl sulphate (SDS) molecules

to the polypeptide backbone is inevitable as it levels the charging differences between different types of proteins and leads to a direct relationship between migration behaviour and molecular weight. Applying these techniques to analyse dendrimers, it is possible to differentiate between different generations of one particular dendrimer species and between dendrimer particles of one generation with different surface modification. Both techniques lack the ability to determine the size or molecular mass of the dendrimers [30]. However, a qualitative analysis of the change of dendrimer populations during synthesis and modification steps has been possible with these methods[20].

SAXS and SANS are both scattering techniques which allow the determination of the radius of gyration of the dendrimer molecules as well as the electron density distribution inside the dendrimer particles in solution. With these techniques it was possible to prove that PAMAM dendrimers change their characteristic shape from star like (varying electron density to radius function) to rigid sphere like (constant electron density along the outer radius of the particle). The advantage of both techniques is that the determined value is an average of a vast amount of scattering events on many dendrimer particles, and that measurements are made with dendrimers in solution. However, both techniques also have their disadvantage, as considerable experimental expense as well as high expertise in interpreting the experimental data is required [31-34].

AFM is a microscopic technique that allows to investigate the shape as well as mechanical properties of single dendrimer particles. The strongest limitation of AFM in the determination of dendrimers is the softness of these organic molecules, which limits the resolution and hampers the analysis of dendrimers smaller than G5 [35-38]. Another observed effect is the deformation and losing of the spherical shape of dendrimers during adsorption on substrate surfaces, which poses problems in the size determination. With scanning the whole dendrimer particle it was possible to circumvent this problem and determine the volume and calculate a spherical–equivalent diameter[35,36,38].

TEM is an additional microscopic method whose resolution depends on the energy of the primary electron beam. For samples which provide enough contrast and regularity even atomic resolution is possible. This method was used to determine the diameter of G5 up to G10 PAMAM dendrimers in vacuum[39]. However, as dendrimers are organic molecules with a weak contrast, a staining step must be carried out before analysis, which may lead to a systematic error in the determined particle dimensions, but as TEM can be carried out at low temperature, the loosing-shape effect as described for AFM can be avoided[39].

Mass spectrometry is an analytical technique preliminary used for the exact molecular weight determination of various high-mass biopolymers. The MALDI-TOF-MS technique was a major break-through for the mass spectrometric analysis of molecules with molecular weights higher than 2 kDa and was first presented in 1988 by Hillenkamp, Karas and Tanaka [45,46]. Whereas today most MALDI-MS experiments are performed with proteins, carbohydrates and oligonucleotides [47], the analysis of dendrimers with this technique is also already described in literature up to G4 [40,41,47-50]. Observed imperfections and deviations from the calculated molecular weights of the dendrimer samples were attributed to chemical defects. Additionally fragmentation of dendrimers was observed for dendrimers absorbing at a similar wavelength of the applied laser wavelength used for desorption/ionization [48,49]. Like in the case of proteins or DNA fragments post-source decay (PSD) fragmentation of PAMAM dendrimers of small size (up to G4) was also observed with MALDI-TOF-MS [50]. Beside MALDI-MS, electrospray ionization (ESI)-MS is another mass spectrometric technique for the exact molecular weight determination already applied to dendrimers [51,52]. Advantages of MALDI-TOF-MS (in the linear mode) are its high molecular weight range, sensitivity and mass accuracy [53]. The main disadvantages of this technique are the rather high instrumentation cost and the search for an optimal matrix and a proper sample preparation method for a given analyte. ESI-MS has the advantage of generating highly charged molecular ions which reduces the mass-to-charge ratio and makes molecules with higher mass accessible to mass

analysers other than TOF systems. But for the determination of the actual molecular mass, the exact charge states of the multiply charged ions are required. For this purpose peaks representing adjacent charge states have to be resolved, which is difficult for many high mass molecules[54] and was not possible for e.g. a PAMAM G6 dendrimer (for higher generation dendrimer it is even more difficult) despite combining ESI with a Fourier-transform ion cyclotron analyzer[40].

The nano-ES-GEMMA (electrospray gas phase electrophoretic mobility molecular analyser), which is used in this study, is a relatively new technique that combines the benefits of the low charge levels (one or two charges per molecule) of the MALDI with the process of desorption/ionisation from the bulk solution by the nano-ES process. It uses a differential mobility analyser (DMA) for the separation of the singly charged particle by their electrophoretic mobility diameter (EMD) at atmospheric pressure. Such devices have been in use since a long time in aerosol physics for the analysis of submicrometer to micrometer particle aerosols[55]; their design was recently adapted to extend the measurable size range into the low single digit nanometer region, or in terms of molecular mass, into the low kDa mass range. A condensation particle counter (CPC) is used for the detection of the separated singly charged particles (ions), offering single particle detection allowing high sensitivity (10^3 particles or ions / cm^3). Furthermore a direct relationship between molecular mass and diameter has already been demonstrated for globular proteins[56] and small DNA fragments[57], allowing the use of the nES-GEMMA to determine the molecular mass of high molecular weight proteins and non-covalent protein complexes. Also the size analysis of bacteriphages[58], viruses and virus fragments[59], high mass protein complexes [56,60] and polyethylene-glycol polymer mixtures[61] as well as small (≤ G4) PAMAM dendrimers[62] was demonstrated with this method.

In this work we present now the characterisation (molecular mass, size and average density) of PAMAM dendrimers up to G10 with the two independent techniques MALDI-TOF-MS

and nES-GEMMA as well as the comparison with other techniques as SAXS, SANS, AFM, TEM and data provided by the manufacturer as well as theoretical values based on molecular dynamics calculations[63].

Material and Methods

Chemicals. All amine-terminated PAMAM dendrimers with an ethylenediamine core were obtained as 5-20% solutions in methanol (G2 to 7 from Sigma-Aldrich, G9 and 10 from Dendritech). Ammonium acetate and acetonitrile (ACN) of analytical grade were acquired from Merck. Trifluoroacetic acid (TFA, 99%) was purchased from Riedel-de-Haen and 2,4,6-trihydroxyacetophenon monohydrate (THAP) from Fluka, both analytical grade. Ammonium acetate and TFA solutions were made by means of analytical grade water from Merck. For MALDI-TOF-MS calibration bovine insulin (Sigma-Aldrich) and the Invitromass HMW Calibrant Kit (Invitrogen) were applied.

MALDI-TOF-MS instrument. MALDI mass spectrometry was carried out on an Axima TOF^2 tandem instrument from Shimadzu Biotech Kratos Analytical. The device is a high resolution, floor-standing instrument equipped with a pulsed nitrogen laser (wavelength: 337 nm, pulse width: 4 ns), an integrated 2 GHz transient recorder, a curved field reflector and a differential pumped collision gas cell. The instrument was operated in the positive ion linear (flight path 1,2 m) mode applying an accelerating voltage of 20 kV without delayed extraction.

Calibration for PAMAM dendrimers from G4 to G10 was performed externally by using the Invitromass HMW Calibrant Kit, which contained various recombinant standard proteins with given molecular weights in the mass range from 30 kDa to 160 kDa. The calibration kit was applied according to the manufacturer's instructions, but in contrast to the instruction manual THAP as MALDI matrix solution was applied for external calibration. Calibration for

PAMAM dendrimer G2 was performed externally using the singly and doubly protonated molecule of bovine insulin. All mass spectra were acquired by averaging 50 to 200 unselected and consecutive laser shots on the same preparation by automatic rastering. In order to calculate relative standard deviations (RSDs) for molecular weight determination each PAMAM dendrimer sample was analyzed ten times using different sample spots on the same MALDI target. All mass spectra were smoothed using the company-supplied Savitzky-Golay algorithm [64]. The applied peak (m/z determination) detection method was threshold-centroid at 50% height of the peak maximum.

Sample preparation for MALDI MS analysis. Prior to analysis, THAP was dissolved in 1/1 (v/v) 0,1% TFA/ACN mixture to give a final MALDI matrix concentration of 10 mg/mL. Prior to use the all day freshly prepared matrix solution was vortexed thoroughly. For MALDI-TOF-MS analysis 1 uL PAMAM dendrimer stock solution was vacuum dried at RT in order to remove all solvents. Afterwards, the residue was dissolved completely in a 9/1 (v/v) 0,1% TFA/ACN solvent mixture to give a final PAMAM dendrimer concentration of 10 nmol (assuming an ideal molecular weight)/mL which was equivalent to the following mass concentrations: 0,03 mg/mL (G2), 0,14 mg/mL (G4), 0,29 mg/mL (G5), 0,58 mg/mL (G6), 1,16 mg/mL (G7), 4,67 mg/mL (G9) and 9,34 mg/mL (G10). One part of the resulting PAMAM dendrimer solution was mixed with two parts of THAP matrix solution in an Eppendorf tube. 0,5 uL aliquots of this matrix/sample mixture were deposited on several different spots on a stainless steel microtiter format MALDI target and dried under a gentle stream of air at RT forming smooth crystalline layers.

nES-GEMMA instrument. The GEMMA system consists of a nano-electrospray (nES) unit, a nano-differential mobility analyzer (nDMA) and an ultrafine condensation particle counter (uCPC) as detector (all parts from TSI Inc). The nano-ES generated multiple charged particles are charge reduced in a bipolar air environment produced by α-radiation from a Po-210 radioactive source (NRD). This charge-reduction process results in neutral and only singly

charged molecules/nanoparticles. The operating particle size range of the instrument combination is between 3 nm (limited by the particle detection with the uCPC) and 65 nm (the upper scan limit of the nDMA when using maximum sheath flow for maximum nDMA resolution). The nDMA was operated with negative high voltage polarity on the central electrode, thus separating and detecting the positively charged fraction of the generated molecules/nanoparticles. The detection limit of the complete GEMMA system in terms of particle concentration is 1 singly charged nanoparticle/cm³. However, due to the limited efficiency of charge manipulation process concentration of airborne dendrimer particles of at least 10000 particles (equivalent to approx. 4 pg for G5 molecules)/cm³ are necessary to obtain appropriate particle count statistics across the whole sizing (3 nm to 30 nm)/scanning range within a reasonable time frame (120 s per scan). Ten scans were averaged for each final size spectrum presented in this paper.

Nano electrospray conditions. For all measurements, the settings of the nano-ES source, buffer concentrations, and solution conductivity were identical. Samples in 20 mM ammonium acetate buffer (pH 7.4) were electrosprayed. For this solvent system and spray-chamber design we found that a stable cone-jet mode operation was obtained at 2 kV and 0.3 L/min CO_2 (99.995%, Air Liquide)/1L/min compressed air (99.999% synthetic air, Air Liquide). A pressure of 4 psi was applied onto the sample solution for sample introduction, which resulted in a sample solution flow of 67 nL/min through the fused silica capillary (25 µm inner diameter and 160 µm outer diameter, length 25 cm uncoated; supplied by TSI Inc). The primary generated droplet size, which is determined by the conductivity of the solvent system and the sample flow through the capillary as well as the inner diameter of the capillary was 150 nm, corresponding to a flow of 2×10^{11} droplets/minute or about 1.7×10^{8} droplets/cm³. The electrospray process was operated in the positive ion mode, which means that droplets with a high initial number of positive charges were produced.

Sample preparation for nES-GEMMA analysis. For the nES-GEMMA all above mentioned commercially available PAMAM dendrimer stock solutions were diluted directly with a 20 mM aqueous ammonium acetate buffer (pH 7.4) to a concentration avoiding the formation of PAMAM cluster ions ($[nM]^+$, $n \geq 2$) consisting of 2 and more dendrimer molecules through the ES process. This concentration was 20 µg/mL for G5, G6, G7, G9 and G10 and 2 µg/mL for G2 and G4.

Results and Discussion

Exact molecular weight determination with MALDI mass spectrometry. The MALDI-TOF mass spectra of PAMAM dendrimers G2 to G10 are shown in Fig. 1 a-g. Most mass spectra exhibit mainly singly charged molecular ions and to a lesser degree doubly charged molecular ions (see Fig. 1 a-e). Sometimes the mass spectra show additionally (e.g. in case of G5 and G6, Fig. 1 c and d) singly charged dimeric molecular ions. Beside the singly charged molecular ion peak the doubly charged molecular ion peak was found as well. The mass spectrum of PAMAM dendrimer G9 showed beneath singly and doubly charged molecular ions also an abundant signal at m/z ~94000 (Fig. 1 f).The peak observed at this m/z ratio was not a triply charged molecular ion peak of PAMAM G9 but either a fragment ion of the analyte molecule or with a much higher probability an impurity. Since no comparable molecular ion peaks (or fragment ions) were observed in the mass spectra of PAMAMs with generations lower than 9, it is most likely that this peak derived from an impurity within the original sample. Possible impurities are precursors of earlier synthesis steps, like G7 or G8, which were not completely removed or converted. Given a similar chemical structure of analytes, molecules with lower molecular weight tend to show more intense peaks in MALDI mass spectrometry due to better desorption/ionization yield. Thus, the impurity can actually

be present in the sample solution in a much lower concentration than the PAMAM dendrimer G9. In the case of PAMAM G10 only the doubly and triply charged molecular ions, but no singly charged molecular ion was observable (Fig. 1 g) despite the instrument can handle a m/z range up to 600000. Concerning the full peak widths at half maximum (FWHM) of the singly charged molecular ion analyte peaks it was interesting to notice, that well-defined proteins of similar molecular weight had several times lower FWHMs than dendrimers. The high FWHM values of the PAMAM dendrimer analyte peaks could be explained by incomplete synthesis and non-optimized purification after synthesis. In the case of PAMAM dendrimer G2 to G7 the singly charged molecular ion peaks were used for molecular weight determination (Table 1). Because molecular weight calibration was limited to 160 kDa for PAMAM G9 the doubly charged and for PAMAM G10 the triply charged molecular ion peak was applied for molecular weight determination. Nevertheless the molecular weight of the triply charged molecular ion peak of PAMAM G10 was slightly out of external calibration range, which was limited with m/z 159081. The molecular weights of all PAMAM dendrimer samples determined with MALDI-TOF-MS were below the calculated molecular weight for ideal synthesis (Table 1). This difference between measured and calculated molecular weight increased continuously with increasing generation of the PAMAM dendrimers and was already surprisingly high for lower PAMAM dendrimer generations (G4: minus 6,3%, G5: minus 10,1%). This observation was corroborated by nES-GEMMA data shown and discussed below. Most likely the synthesis of PAMAM dendrimers was not complete and as a consequence the difference between the calculated and actual molecular weight increased with every synthesis step. It has to be stated in this context that the MALDI mass spectrometric derived molecular weight in the linear mode is independent of 3-dimensional structure of the dendrimer molecule and that under our MALDI conditions no considerable metastable decay was observed[49,50]. The obtained precision of molecular weight determination with MALDI-TOF-MS in the linear mode across all analytes was ± 0,4%.

Size determination with nES-GEMMA. Fig. 2 shows the GEMMA size spectra of PAMAM dendrimers G4, G6, G9 (Fig. 2a) and G2, G5, G7, G10 (Fig. 2b). The typical amount of particles being characterised within one spectrum is between 10^4-10^7, thus characterising bulk and not single particle properties as it is done in TEM, AFM, SAXS and SANS. As can be seen, the $[M]^+$ peak maximum increases steadily with the number of the generation. For G7, G9 and G10 cluster dimers ($[2M]^+$ ion) could be observed (Fig. 2). Furthermore, in the GEMMA spectrum of PAMAM dendrimer G9 and G10 some impurities (particles of smaller size) could be detected (Fig. 2). As these impurities are also high molecular weight components, which is also confirmed by MALDI-MS, it can be assumed that they are either incomplete products of the G9 and G10 dendrimer synthesis, or dendrimers of smaller generation which were not successfully removed after the synthesis. As can be seen in Table 2, the diameters determined by nES-GEMMA measurements agree well with values derived from AFM measurements of different origin [35,36,38] , the average particle diameter found for dendrimer particles in vitrified solutions by TEM[39], and the diameter of gyration found in SAXS[31,32] and SANS[33,34] studies with an average difference of about 10% concerning one dendrimer generation. This difference in size between the different studies are well within there described standard deviations resulting from the experimental method uncertainties and the polydispersity of the dendrimers themselves. The only exception are the two SAXS studies, whose results for generations smaller than 7 agree with TEM, AFM and GEMMA measurements, but which found significantly smaller diameters than the other methods for PAMAM dendrimers G7 and higher. This phenomenon is discussed in literature[31,32] and can be attributed to higher order scattering events inside the particle, which distort the scatter angle and results subsequently in an underestimation of the particle diameter.

Molecular weight and density determination based on nES-GEMMA.

As mentioned before, the nES-GEMMA data can not only be used for the determination of the average particle diameter, but also, with appropriate calibration, for the determination of

the molecular weight. For this reason, the GEMMA system was calibrated with common globular proteins, which are all of spherical shape according to Bacher et al.[56]. Another approach to estimate the molecular mass of a dendrimer particle is the calculation of the average particle volume and the calculation of its mass with an assumed density. As was found by molecular dynamics calculations of dendrimers [63] a density of about 50 atoms/nm³, or, when multiplied with the average atom mass of the PAMAM dendrimers, 0.52 kg/L can be assumed for the bulk volume of the dendrimer particle. Both approaches were used for the calculation and determination of the molecular mass from GEMMA derived particle diameters (Tab. 3).

As can be seen in Table 3, both approaches clearly overestimate the molecular mass of the PAMAM dendrimer G2 particle. This result can be explained by the fact that such small dendrimers cannot be viewed as rigid spheres, but more as star-like branched molecules (disk-like), with a significant distance between its branches, thus neither possessing spherical shape, which is known to bias the determined electrophoretic mobility diameter, nor the assumed bulk density. For higher generation PAMAM dendrimers, where spherical shape, rigidity and bulk properties of the dendrimer particle can be assumed, both approaches do not over- but underestimate the molecular weight of the dendrimers by ~18% but agree very well with each other.

The reason for this difference can either be rooted in the determined particle diameter, or in the explicitly (derived from molecular dynamics) or implicitly (as in case of the protein calibration curve) set particle density. As particle diameters between different analytical methods showed good agreement (as discussed in the paragraph before), particle densities were calculated from molecular dynamics[63] , from the manufacturer[65] and from MALDI mass spectrometric and nES-GEMMA data (Fig 3).

As can be seen in Figure 3 the by means of nES-GEMMA determined average protein density (~0,54 kg/L) is nearly identical to the average dendrimer density found in molecular dynamics

calculations, thus explaining the good agreement between the molecular mass derived from protein calibrations and calculated from the determined particle volume and the theoretical density. The series representing the density values derived from MALDI-TOF-MS and nES-GEMMA data shows an increase of the particle density from 0.31 (G2) to 0.65 (G5). PAMAM generations above G5 show constant density, thus confirming the change from star-like branching to rigid spheres with bulk properties as was found by SAXS[31,32], SANS[33,34] and AFM[35,36,38] studies.

However, the density difference between proteins and with molecular dynamics calculated values for dendrimers[63] to experimental data leads directly to the observed differences between the molecular masses derived from MALDI-MS and the protein calibration and via density calculated values from the nES-GEMMA experiments. One reason for this difference to theory might be that the dendrimer particles are not surrounded by solvent environment as in the molecular dynamics simulation. This amplifies intramolecular forces and might lead to a more dense packing inside the particle and a higher average bulk density. Proteins, as used in the calibration, are not branch like, but linear in their primary structure, which also might lead to differences in particle density, even when the elemental distribution is roughly the same.

The theory of ideal dendrimer growth behaviour postulates a nearly constant growth of the diameter of dendrimers, especially for generations above 4, where globular particle shape can be assumed, but an exponentional molecular mass growth (values derived from manufacturer[61]). This leads to a steady increase of the postulated dendrimer density (dashed line in Fig. 3) with every generation above 4; for smaller generations a slight decrease of density is postulated, since there the star like branching leads to an increase of the distance between the different branches (dashed line with triangles in Fig. 3). Theory and determined densities agree very well until G7. However, the density of G9 and G10 PAMAM dendrimers is significantly below theoretical values according to our MALDI-MS and nESI-GEMMA

data. The reason for this difference from our experimental values and values calculated for ideal dendrimer structures is probably a congestion-induced *De Gennes dense packing*[9,66,67] , as was postulated for high generation dendrimers in literature, which leads to incomplete saturation of free branching spots during the synthesis of the next generation.

Conclusions

In this work we have shown, that molecular mass determination of PAMAM dendrimers up to G10 was generally possible with MALDI-TOF-MS analysis. The observed average precision was ±0.4%. An increasing difference between the theoretical molecular masses for ideal dendrimer growth/synthesis and molecular masses determined with MALDI-TOF-MS with increasing number of generation was found. Analysis with MALDI-TOF-MS provided molecular weights up to 40% below the calculated theoretical molecular weight. nESI-GEMMA analysis of the electrophoretic mobility diameter of dendrimer particles of all generations was possible with a precision of ±0.2 nm. All diameter values were in excellent agreement with values found by various other analytical techniques such as SAXS, SANS, TEM and AFM. The polydispersity of the molecular mass and the distribution of diameters of the analysed dendrimer generations were found to be significantly higher than for proteins in the same molecular mass and size range. It was attempted to calculate the molecular mass of PAMAM dendrimers via their particle diameter with different approaches, but all resulted in a significant discrepancy to the MALDI-MS data. The calculated density of the dendrimer particles based on the MALDI-MS and nES-GEMMA data showed a significant difference to protein densities (0.54 kg/L), densities calculated from molecular dynamic results (0.52 kg/L) as well as to densities derived from dendrimer growth theory (up to 1.2 kg/L). Our results indicate that PAMAM dendrimer particles of G4 or higher possess a constant average density of 0.65 kg/L, which is determined by tight packing of the branches inside the particle.

Acknowledgements. This research was partially supported by the Austrian Science Foundation grants P15008 (to G.A.) and P16185 (to W.W. S.).

Legends to tables

Table 1. Summary of the average molecular weights determined with MALDI-TOF mass spectrometry and the calculated molecular weights of various generations of PAMAM dendrimers. The differences (given in percents) shown in the right column refer to the measured molecular weights compared with the calculated molecular weights in case of ideal structure/synthesis. (Unless noted otherwise, the given molecular weights are based on the singly charged molecular ion peak)

[+] Molecular weight determination based on the doubly charged molecular ion peak

[++] Molecular weight determination based on the triply charged molecular ion peak

Table 2. Average particle diameter ontained in this work with nES-GEMMA and in literature. SAXS, SANS, TEM and AFM. AFM diameters were calculated from determined particle volumes, assuming sphere like shape. n.d., not determined; -, not available.

[a] According to manufacturer medium diameter determined with dilution viscosimetry, SAXS, and SANS.

Table 3. Molecular mass determination based on MALDI-TOF-MS and nES-GEMMA and molecular dynamics[63]

[a] External Protein calibration

[b] Calibration function molecular mass(Da) = $131.77 \times x^{3.106}$; R^2=0.9943 derived from measurements of well-defined proteins as standards.

[c] Assuming a particle density of 0.52 kg/L which was obtained by molecular dynamics calculations [63].

Legends to figures

Figure 1. Positive ion MALDI mass spectra in the linear mode of PAMAM dendrimers of generation (a) G2, (b) G4, (c) G5, (d) G6, (e) G7, (f) G9 and (g) G10.

Figure 2. nES-GEMMA spectra of PAMAM dendrimers (a) G4, G6 and G9 as well as (b) G2, G5, G7 and G10.

Figure 3. Plot of theoretical and experimental PAMAM dendrimer particle densities vs particle diameter.

References and Notes

(1) Staudinger, H. *From organic chemistry to macromolecules*; Wiley-Interscience: New York, NY, USA, 1970.
(2) Frechet, J. M. J.; Tomalia, D. A. *Dendrimers and other dendritic polymers*; Wiley: Chichester, UK, 2001.
(3) Tomalia, D. A.; Baker, H.; Dewald, J. R.; Hall, M. J.; Kallos, G.; Matrin, S. *Polym. J. (Tokyo)* **1985**, *17*, 117-132.
(4) Tomalia, D. A.; Hedstrand, D. M.; Ferrito, M. S. *Macromolecules* **1991**, *24*, 1435-1438.
(5) Tomalia, D. A. *Macromol. Symp.* **1996**, *101*, 243-255.
(6) Naj, A. K. *Wall Street Journal* **1996**, *B1*.
(7) Hecht, S.; Frechet, J. M. J. *Angew. Chem. Int. Edit.* **2001**, *40*, 74-91.
(8) Gauthier, M.; Moller, M. *Macromolecules* **1991**, *24*, 4548.
(9) Tomalia, D. A.; Naylor, A. M.; W.A. Goddard, I. *Angew. Chem. Int. Edit.* **1990**, *29*, 138-175.
(10) Frechet, J. M. J.; Hawker, C. J.; Gitsov, I.; Leon, J. W. *JMS Pure Appl. Chem.* **1999**, *A33*, 1399.
(11) Voit, B. I. *Acta Polym* **1995**, *46*, 87-99.
(12) Fischer, M.; Vögtle, F. *Angew. Chem. Int. Edit.* **1999**, *38*, 884-905.
(13) Boas, U.; Heegaard, P. M. H. *Chem. Soc. Rev.* **2004**, *33*, 43-63.

(14) Tomalia, D. A.; Uppuluri, S.; Swanson, D. R.; Li, J. *Pure Appl. Chem.* **2000**, *72*, 2343-2358.
(15) Tomalia, D. A.; Swanson, D. R. In *Dendrimers and other dendritic polymers*; Frechet, J. M. J.; Tomalia, D. A., Eds.; Wiley: Chichester, UK, 2001; pp 617-629.
(16) van Heerbeek, R.; Kamer, P. C. J.; van Leeuwin, P. W. N. M.; Reek, J. N. H. *Chem. Rev.* **2002**, *102*, 3717-3756.
(17) Hedrick, J. L.; Magbitang, T.; Conner, E. F.; Glauser, T.; Volksen, W.; Hawker, C. J.; Lee, V. Y.; Miller, R. D. *Chem. Eur. J.* **2002**, *8*, 3308-3319.
(18) Jenkins, A. D.; Kratochvil, P.; Stepto, R. F. T.; Sutter, U. W. *Pure Appl. Chem.* **1996**, *68*, 2287-2311.
(19) Schlüter, A. D. *Top. Curr. Chem.* **1998**, *197*, 165-191.
(20) Caminade, A.-M.; Laurent, R.; Majoral, J.-P. *Adv. Drug Deliver. Rev.* **2005**, *57*, 2130-2146.
(21) Singh, P.; Moll, F. I.; Lin, S. H.; Ferzli, C. *Clin. Chem.* **1996**, *42*, 1567-1569.
(22) Singh, P. In *Dendrimers and other dendritic polymers*; Tomalia, D. A.; Frechet, J. M. J., Eds.; Wiley: Chichester, UK, 2001; pp 463-484.
(23) Bieniarz, C. In *Enceclopedia of pharmaceutical chemistry*; Marcel Dekker: New York, NY, USA, 1998; pp 55-89.
(24) Hawker, C. J.; Frechet, J. M. J. *J. Am. Chem. Soc* **1990**, *112*, 7638-7647.
(25) Zeng, F.; Zimmerman, S. C.; Kolotuchin, S. V.; Reichert, D. E. C.; Ma, Y. *Tetrahedron* **2002**, *58*, 825-843.
(26) Maraval, V.; Laurent, R.; Donnadieu, B.; Mauzac, M.; Caminade, A.-M.; Majoral, J.-P. *J. Am. Chem. Soc* **2000**, *122*, 2499-2511.
(27) Padias, A. B.; Hall, H. K.; Tomalia, D. A.; McConnell, J. R. *J. Org. Chem.* **1987**, *52*, 5305-5312.
(28) Newkome, G. R.; Young, J. K.; Baker, G. R.; Potter, R. L.; Audoly, L.; Copper, D.; Weis, C. G. *Macromolecules* **1993**, *26*, 2394-2396.
(29) Shi, X.; Patri, A. K.; Lesniak, W.; Islam, M. T.; Zhang, C.; Jr., J. R. B.; Balogh, L. P. *Electrophroesis* **2005**, *26*, 2960-2967.
(30) Brothers, H. M.; Phieler, L. T.; Tomalia, D. A. *J. Chromatogr. A* **1998**, *814*, 233-246.
(31) Prosa, T. J.; Bauer, B. J.; Amis, E. J.; Tomalia, D. A.; Scherrenberg, R. *J. Polym. Sci.* **1997**, *35*, 2913-2924.
(32) Prosa, T. J.; Bauer, B. J.; Amis, E. J. *Macromolecules* **2001**, *34*, 4897-4906.
(33) Amis, E. J.; Topp, A.; Bauer, B. J. In *29th ACS Central Regional Meeting*: Midland, MI, 1997.
(34) Topp, A.; Bauer, B. J.; Tomalia, D. A.; Amis, E. J. *Macromolecules* **1999**, *32*, 7323-7237.
(35) Li, J.; Piehler, L. T.; Qin, D.; Jr., J. R. B.; Tomalia, D. A.; Meier, D. J. *Langmuir* **2000**, *16*, 5613-5616.
(36) Betley, T. A.; Holl, M. M. B.; Orr, B. G.; Swanson, D. R.; Tomalia, D. A.; jr., J. R. B. *Langmuir* **2001**, *17*, 2768-2773.
(37) Li, J.; Qin, D.; jr., J. R. B.; Tomalia, D. A. *Macromol. Symp.* **2001**, *166*, 257-269.
(38) Betley, T. A.; Hessler, J. A.; Mecke, A.; Holl, M. M. B.; Orr, B. G.; Uppuluri, S.; Tomalia, D. A.; jr., J. R. B. *Langmuir* **2002**, *18*, 3127-3133.
(39) Jackson, C. L.; Chanzy, H. D.; Booy, F. P.; Drake, B. J.; Tomalia, D. A.; Bauer, B. J.; Amis, E. J. *Macromolecules* **1998**, *91*, 6259-6265.
(40) Tolic, L. P.; Anderson, G. A.; Smith, R. D.; II, H. M. B.; Spindler, R.; Tomalia, D. A. *Int. J. Mass Spectrom. Ion Proc.* **1997**, *165*, 405-418.
(41) Zhou, L.; Russel, D. H.; Zhao, M.; Crooks, R. M. *Macromolecules* **2001**, *34*, 3567-3573.
(42) Esfand, R.; Tomalia, D. A. *Drug Discov. Today* **2001**, *6*, 427-436.

(43) Frauenrath, H. *Prog. Polym. Sci.* **2005**, *30*, 325-384.
(44) Tomalia, D. A. *Prog. Polym. Sci.* **2005**, *30*, 294-324.
(45) Karas, M.; Hillenkamp, F. *Anal. Chem.* **1988**, *60*, 2299-2301.
(46) Tanaka, K.; Waki, H.; Ido, Y.; Akita, S.; Yoshida, Y.; Yohida, T. *Rapid Commun. Mass Sp.* **1988**, *2*, 151-153.
(47) Hood, R.; Watson, J. T.; A.D.Jones. In *54th Annual conference in Mass Spectrometry, ASMS, May 29th - June 1st*: Seattle, WA, 2006.
(48) Felder, T.; Schalley, C. A.; Fakhrnabavi, H.; Lukin, O. *Chem-Eur. J.* **2005**, *11*, 5625-5636.
(49) Baytekin, B.; Werner, N.; Luppertz, F.; Engeser, M.; Brüggemann, J.; Bitter, S.; Henkel, R.; Felder, T.; Shalley, C. A. *Int J. Mass Spectrom.* **2006**, *249-250*, 138-148.
(50) Subbi, J.; Aguraiuja, R.; Tanner, R.; Allikmaa, V.; Lopp, M. *Eur. Polym. J.* **2005**, *41*, 2552-2558.
(51) Schwartz, B. L.; Rocwood, A. L.; Smith, R. D.; Tomalia, D. A.; Spindler, R. *Rapid Commun. Mass Sp.* **1995**, *9*, 1552-1555.
(52) Kallos, G. J.; Tomalia, D. A.; Hedstand, D. M.; Lewis, S.; Zhou, J. *Rapid Commun. Mass Sp.* **1991**, *5*, 383-386.
(53) Covey, T. R.; Huang, E. C.; Henion, J. D. *Anal. Chem.* **1991**, *63*, 1193-1200.
(54) Tito, M. A.; Tars, K.; Valengard, K.; Hajdu, J.; Robinson, C. V. *J. Am. Chem. Soc.* **2000**, *122*, 3550-3551.
(55) Liu, B. Y. H.; Pui, D. Y. H. *J. Colloid Interface Sci.* **1974**, *74*, 155-171.
(56) Bacher, G.; Szymanski, W. W.; Kaufman, S. L.; Zöllner, P.; Blaas, D.; Allmaier, G. *J. Mass Spectrom.* **2001**, *36*, 1038-1052.
(57) Mouradian, S.; J.W., S.; F.D., D.; Zarrin, F.; S.L., K.; Smith, L. M. *Anal. Chem.* **1997**, *69*, 919-925.
(58) Wick, C. H.; McCubbin, P. E. *Toxicol. Meth.* **1999**, *9*, 245-252.
(59) Hogan, C. J.; Kettleson, E. M.; Ramaswami, B.; Chen, D.-R.; Biswas, P. *Anal. Chem.* **2006**, *28*, 844-852.
(60) Loo, J. A.; Berhane, B.; Kaddis, C. S.; Wooding, K. M.; Xie, Y.; Kaufman, S. L.; Chernushevich, I. V. *J. Am. Soc. Mass Spectrom.* **2005**, *16*, 998-1008.
(61) In *http://www.tsi.com/documents/CHEMC-006-Water-solublePEGPolymer.pdf*; TSI Inc.: Minneapolis, MN.
(62) In *http://www.tsi.com/appnotes/images/gemma-starburst.gif*; TSI Inc.: Minneapolis, MI.
(63) Han, M.; Chen, P.; Yang, X. *Polymer* **2005**, *46*, 3481-3488.
(64) Savitzky, A.; Golay, M. J. E. *Anal. Chem.* **1964**, *36*, 1627-1639.
(65) In *http://www.dendritech.com/pamam.html*; Dendritech Inc.: Midland, MI.
(66) Tomalia, D. A.; Mardel, K.; Henderon, S. A.; Holan, G.; Esfand, R. In *Handbook of nanoscience, engeneering and technology*; W.A. Goddard, I., Ed.; CRC Press: Boca Raton, FL, USA, 2003; pp 1-34.
(67) Tomalia, D. A.; Frechet, J. M. J. In *Dendrimers and other dendritic polymers*; Tomalia, D. A.; Frechet, J. M. J., Eds.; Wiley: Chichester, UK, 2001; pp 3-44.
(68) In http://www.dendritech.com/pamam.html , Dendritech Inc., Midland, MI, USA

PAMAM Generation	Theoretical number of NH_2 groups [67]	Theoretical MW [kDa] [67]	MALDI-TOF-MS derived MW [kDa]	RSD [%]	MW difference [%]
2	16	3,256	3,233	0,0	-0,6
4	64	14,21	13,32	0,2	-6,3
5	128	28,82	25,92	0,4	-10,1
6	256	58,05	50,16	0,3	-13,6
7	512	116,49	90,97	0,9	-21,9
9	2048	467,14	$323,30^{+}$	1,2	-30,8
10	4096	934,69	$\sim 580^{++}$	1,4	-37,9

Table 1

	GEMMA	AFM[35]	AFM[36]	AFM[38]	TEM[39]	SAXS[31]	SAXS[32]	SANS[33]	SANS[34]	SEC [68]
	Average particle diameter (nm)									
G2	3,3	-	-	-	-	-	-	-	-	2,9
G3	n.d.	-	-	-	-	3,2	2,9	3,3	-	3,6
G4	4,3	-	-	-	-	3,4	3,6	3,9	-	4,5
G5	5,1	4,5	-	4,9	4,3	4,8	4,4	4,9	4,4	5,4
G6	6,4	5,6	5,9	5,9	6,9	5,3	5,7	6,1	-	6,7
G7	7,6	7,2	7,1	7,1	8,0	6,4	6,5	7,2	-	8,1
G8	n.d.	9,2	9,0	8,9	10,2	8,1	7,8	-	8,4	9,7
G9	11,2	12,5	10,5	10,5	12,4	9,8	9,2	-	-	11,4
G10	14,0	15,6	-	-	14,7	11,5	10,8	-	-	13,5

Table 2

PAMAM generation	MALDI MS [a]	nESI-GEMMA [b]	Molecular dynamics [c]
	Molecular Mass (kDa)		
G2	3,24	5,17	5,68
G4	13,32	12,3	13,1
G5	25,92	20,5	21,5
G6	50,16	41,6	42,6
G7	90,97	71,0	71,4
G9	323,3	239	231
G10	580	482	454

Table 3

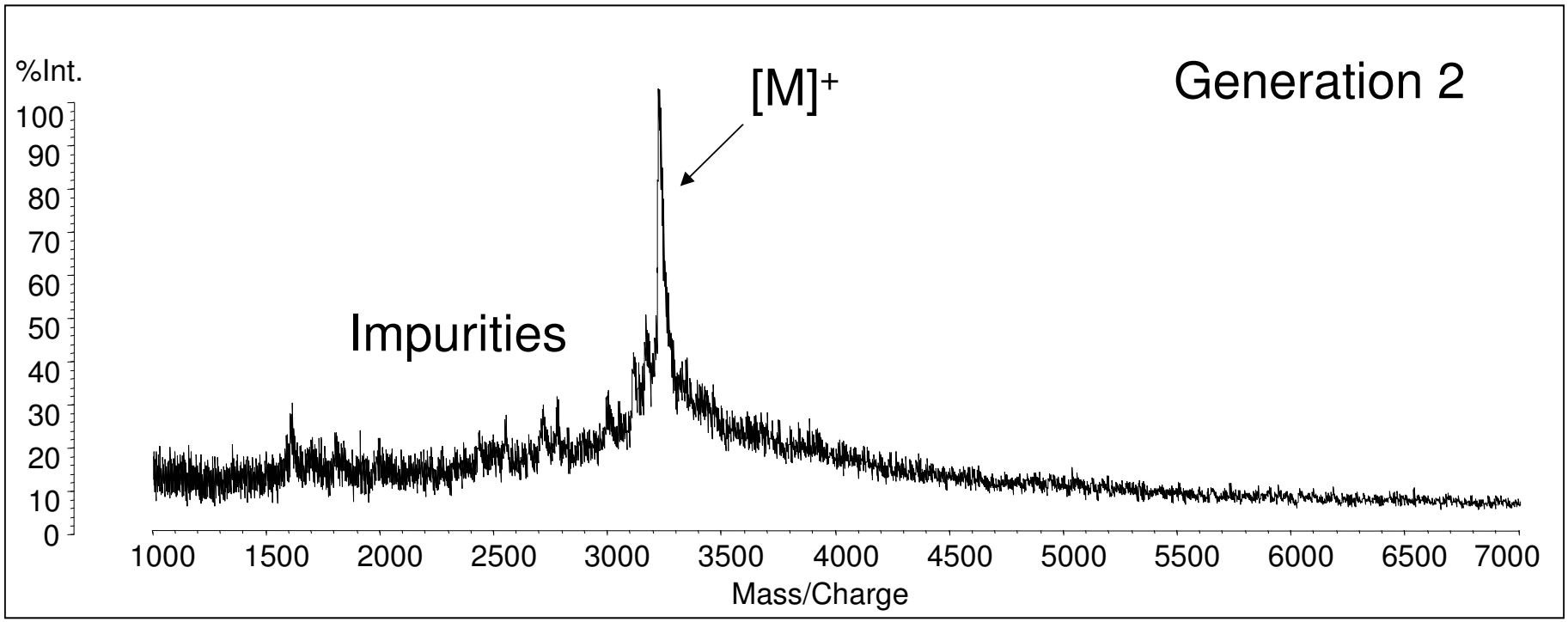
%Int.
100
90
80
70
60
50
40
30
20
10
0
[M]+
Generation 2
Impurities
1000
1500
2000
2500
3000
3500
4000
4500
5000
5500
6000
6500
7000
Mass/Charge

Figure 1a

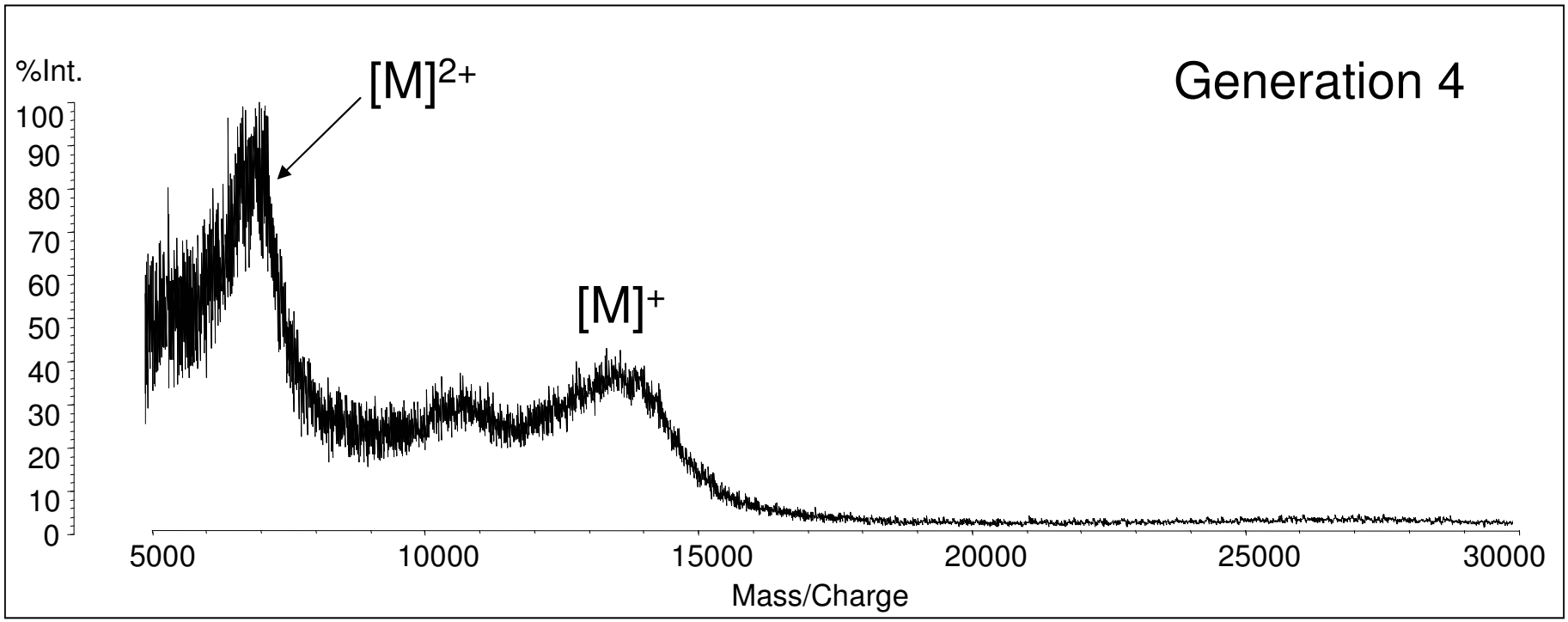
%Int.
100
90
80
70
60
50
40
30
20
10
0
[M]2+
[M]+
Generation 4
5000
10000
15000
20000
25000
30000
Mass/Charge

Figure 1b

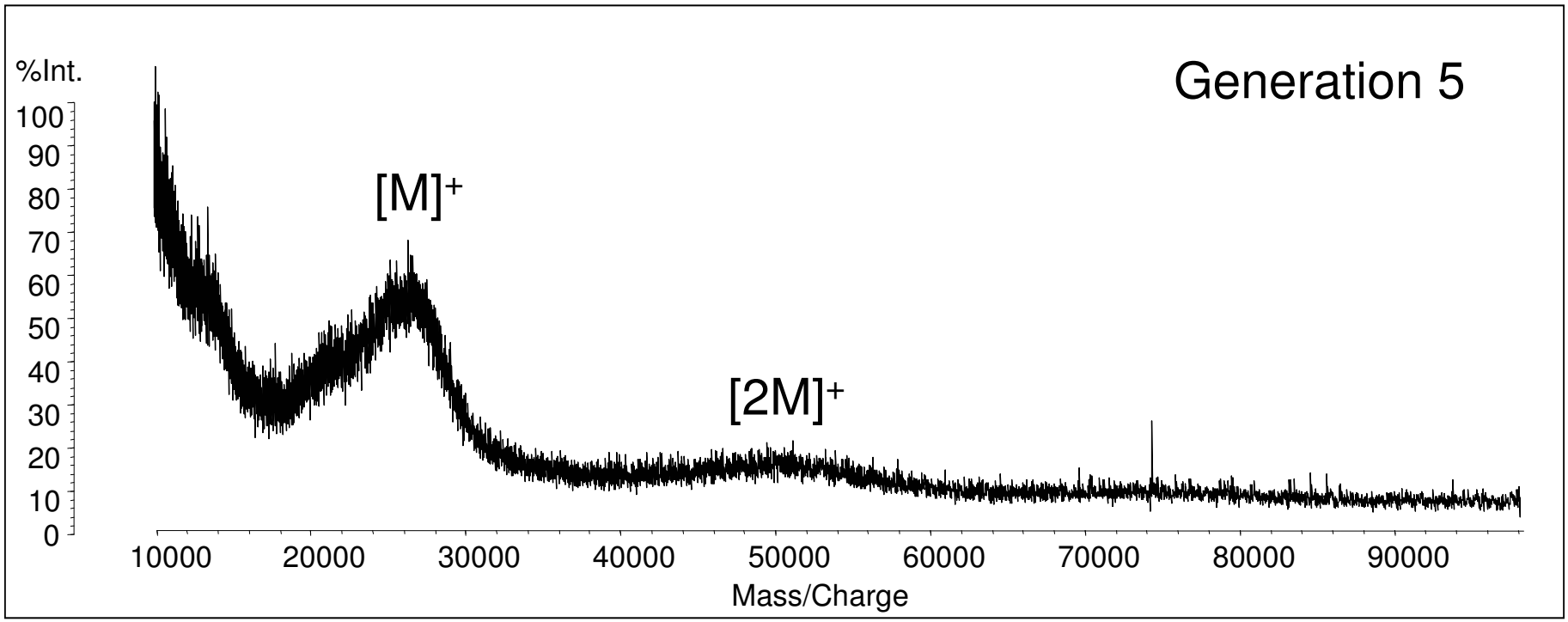
%Int.
100
90
80
70
60
50
40
30
20
10
0
Generation 5
[M]+
[2M]+
10000
20000
30000
40000
50000
60000
70000
80000
90000
Mass/Charge

Figure 1c

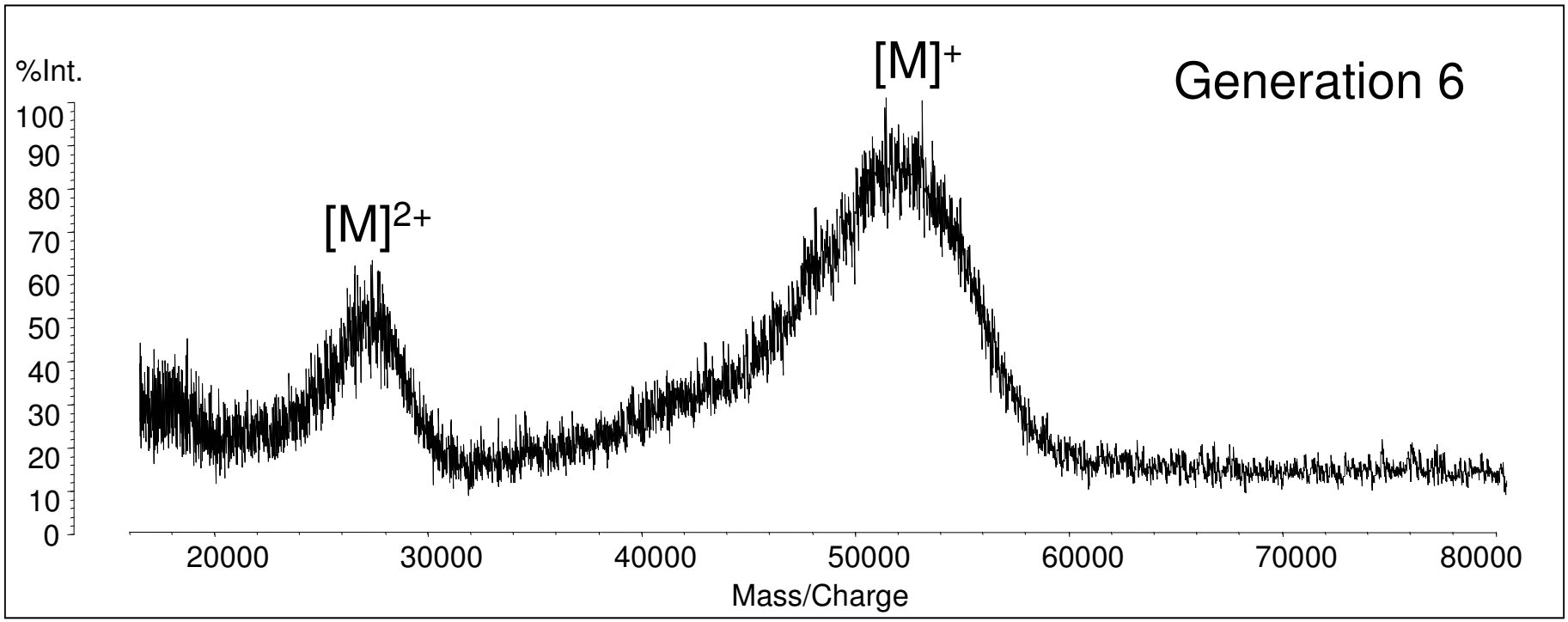
%Int.
100
90
80
70
60
50
40
30
20
10
0
[M]2+
[M]+
Generation 6
20000
30000
40000
50000
60000
70000
80000
Mass/Charge

Figure 1d

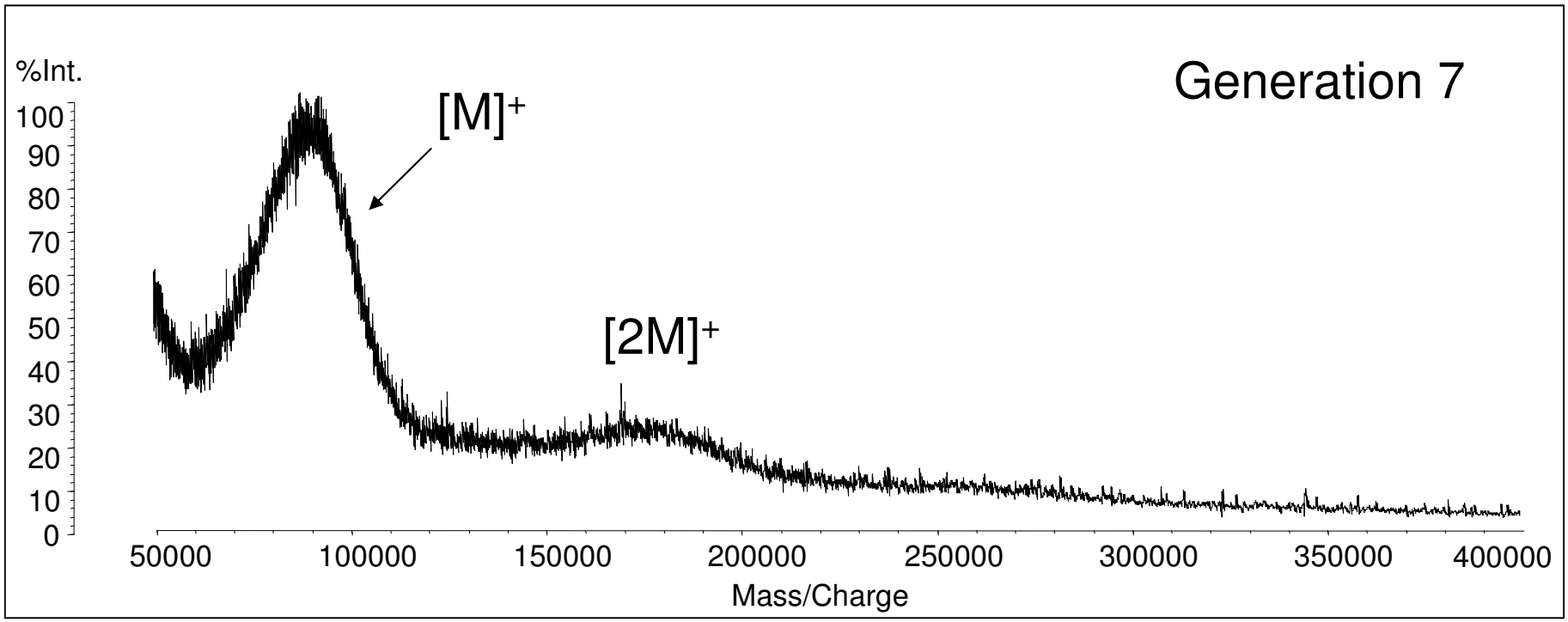
%Int.
100
90
80
70
60
50
40
30
20
10
0
[M]+
[2M]+
Generation 7
50000
100000
150000
200000
250000
300000
350000
400000
Mass/Charge

Figure 1e

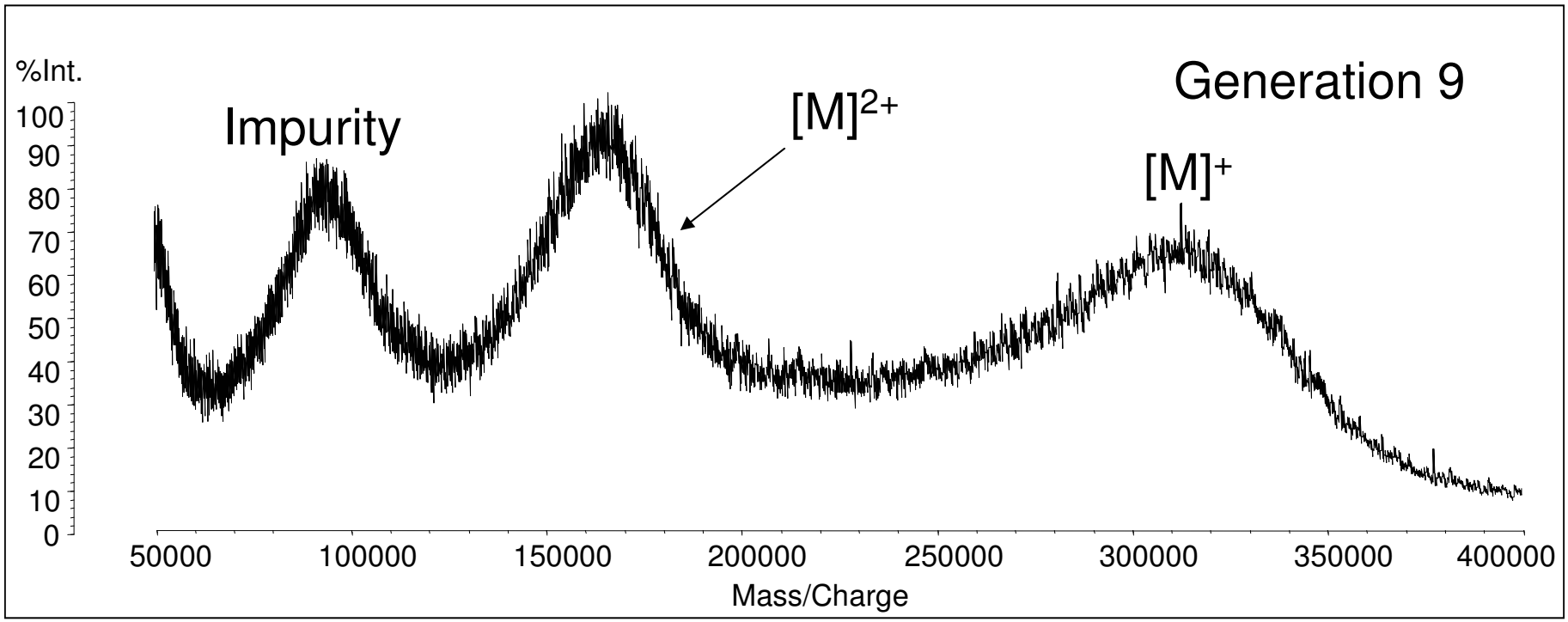
%Int.
100
90
80
70
60
50
40
30
20
10
0
Impurity
[M]2+
Generation 9
[M]+
50000
100000
150000
200000
250000
300000
350000
400000
Mass/Charge

Figure 1f

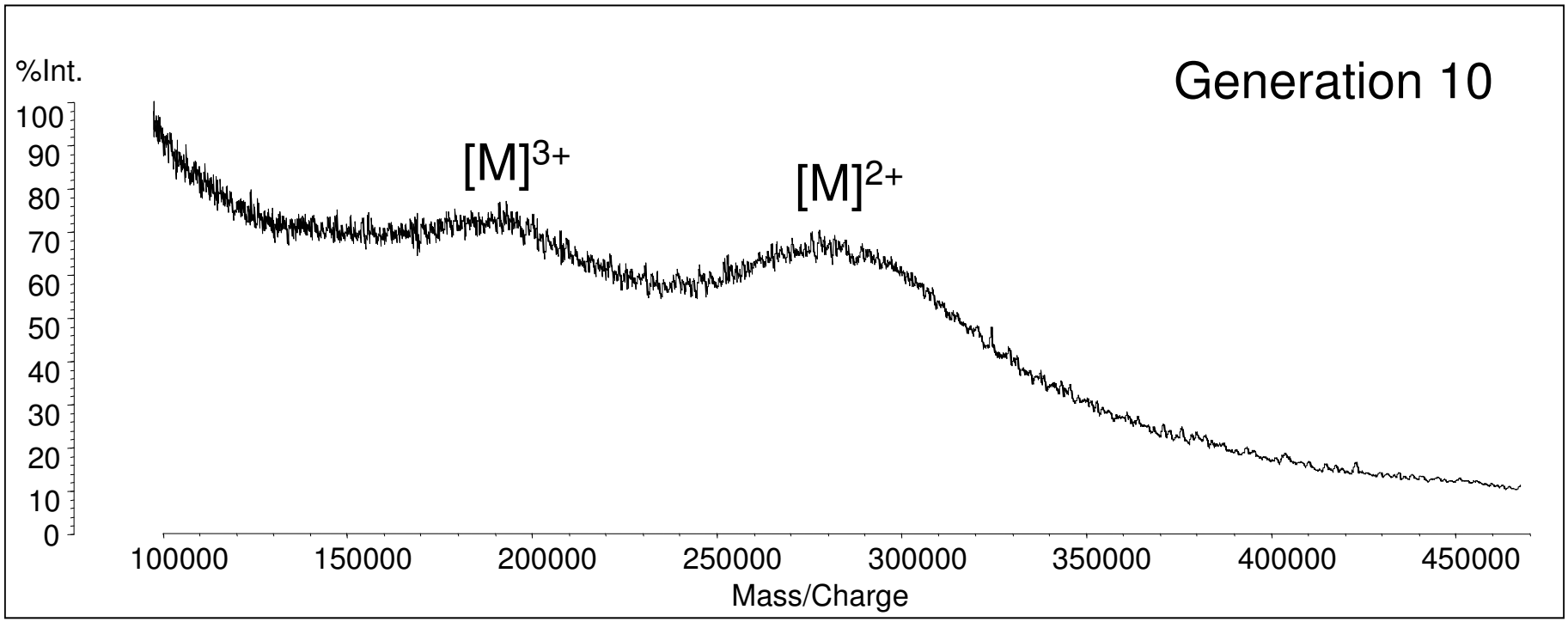
%Int.
Generation 10
100
90
80
70
60
50
40
30
20
10
0
[M]3+
[M]2+
100000
150000
200000
250000
300000
350000
400000
450000
Mass/Charge

Figure 1g

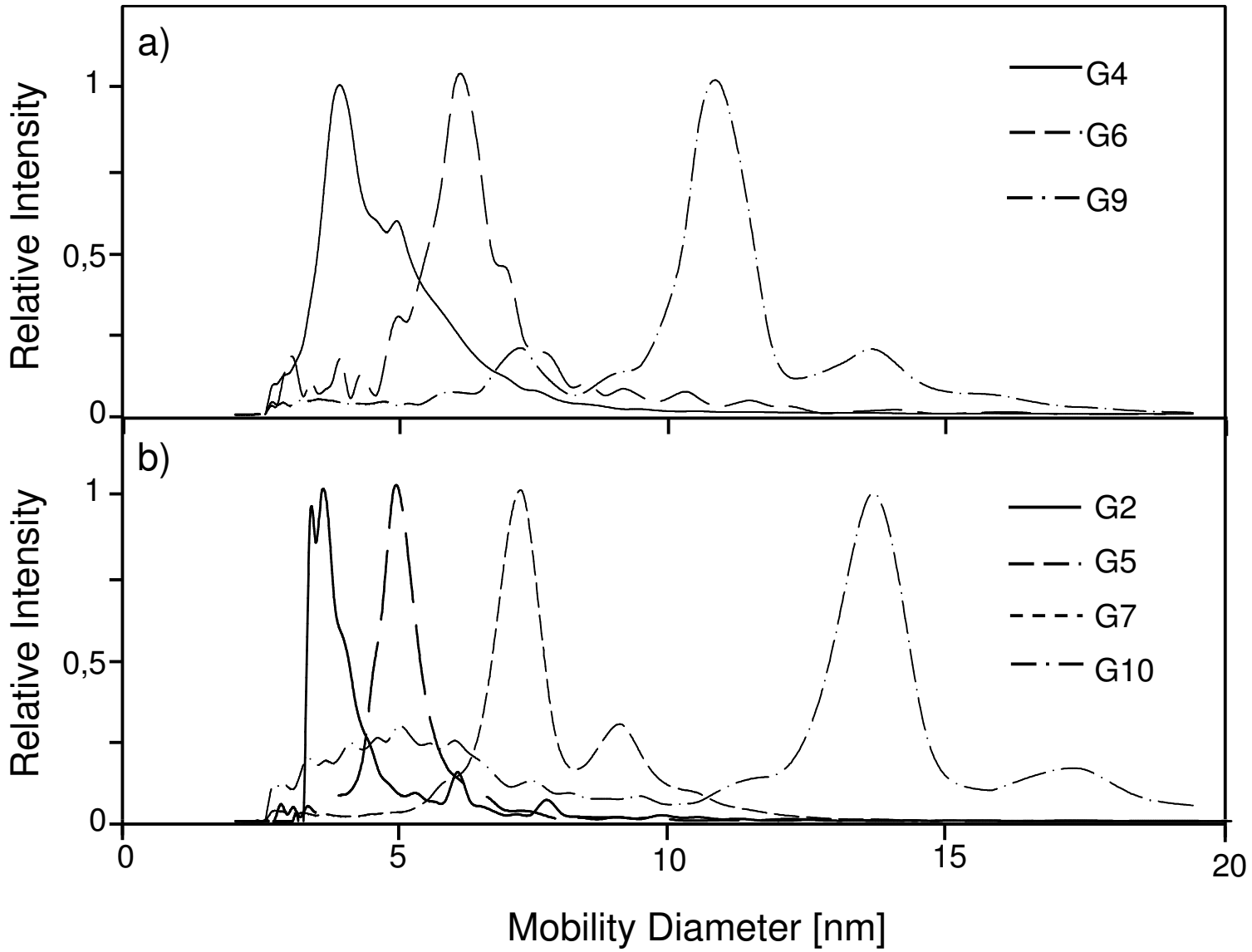
a)
b)
Relative Intensity
Relative Intensity
1
0,5
0
1
0,5
0
G4
G6
G9
G2
G5
G7
G10
0
5
10
15
20
Mobility Diameter [nm]

Figure 2

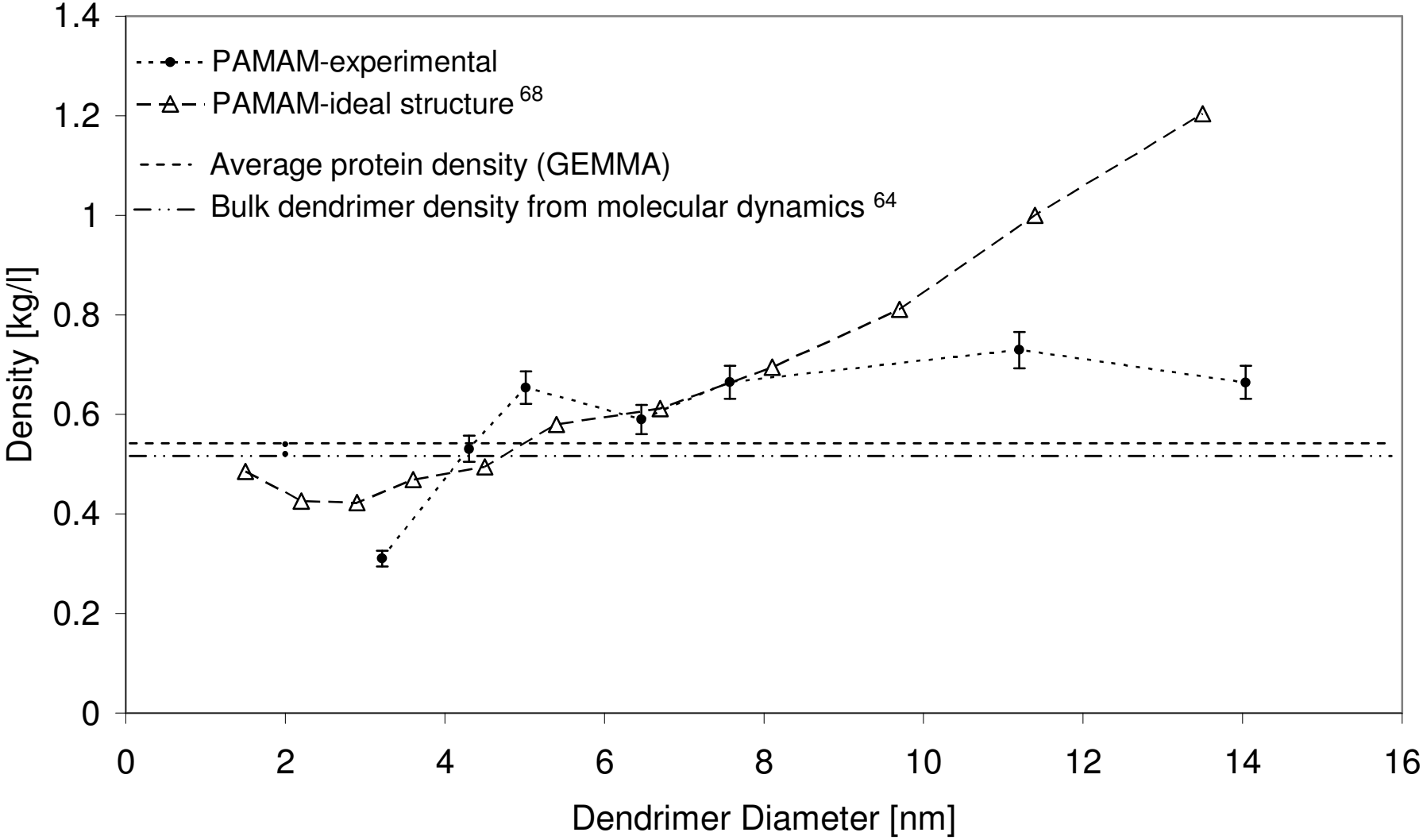
PAMAM-experimental
PAMAM-ideal structure [68]
Average protein density (GEMMA)
Bulk dendrimer density from molecular dynamics [64]
Density [kg/l]
Dendrimer Diameter [nm]
0
0.2
0.4
0.6
0.8
1
1.2
1.4
0
2
4
6
8
10
12
14
16

Figure 3

Rapid Commun. Mass Spectrom., *in press* (2006).

Letter to the Editor

To the Editor-in-Chief

Sir,

Molecular weight determination of ultra-high mass compounds on a standard MALDI TOF mass spectrometer: PAMAM dendrimer generation 10 and immunoglobulin M

Running title: MALDI TOF MS of PAMAM generation 10 dendrimer and Ig M

Key words: MALDI, PAMAM dendrimer, Immunoglobulin M, Molecular weight determination, TOF mass spectrometry, Ultra-high molecular mass

Matrix Assisted Laser Desorption/Ionization Time-Of-Flight Mass Spectrometry (MALDI-TOF-MS) is a well established analytical method particular for the molecular weight determination of high mass biopolymers and to a lesser extent of synthetic polymers [1-5]. The linear TOF mass analyzer combined with vacuum MALDI offers a large molecular weight range, unsurpassed sensitivity and high mass accuracy, which cannot be obtained in this combination by any other methods. Theoretically a TOF analyzer offers an unlimited m/z range [6]. However, there are several practical factors which limit the usable m/z range in MALDI TOF MS. The first limitation is the MALDI process itself. Generally the desorption/ionization of larger monodisperse molecules is more difficult than the desorption/ionization of smaller molecules so resulting in a situation that higher laser powers must be applied often. This in turn facilitates the metastable decay of high molecular weight analytes [7]. The second limitation is the detection itself [8-9] which is related to the detector principles commonly applied (secondary electron multiplier or multichannel plate). A further problem of MALDI-TOF-MS is the difficulties of finding a proper sample preparation technique for a given type of analyte. Optimization of the sample preparation technique is usually based on the *trial-and-error* principle and is often required in order to get results at all or improve the results obtained with MALDI-MS [10]. Routine analysis of proteins and polymers with molecular weights up to 200 kDa is at moment possible, whereas above this limit molecular weight determination seems to be still a challenge. Now we want to demonstrate the feasibility of the molecular weight determination for two classes of compounds, namely a synthetic polymer nanoparticle and a glycoprotein, beyond 500 kDa on a standard MALDI TOF mass spectrometer.

Dendrimers are synthetic polymers with multiple branched structures and variable surface groups. Since dendrimers are nanoparticles (at least at higher generations) and possess particle sizes as well as structures similar to proteins various interesting biological applications like drug delivery are described in literature [11-12]. While at the moment more than 100

compositionally different dendrimer families have been synthesized and characterized so far [13], poly(amindoamine) (PAMAM) dendrimers were the first complete dendrimer family to be synthesized, characterized and commercialized [14]. Synthesis of PAMAM dendrimers involves an iterative 2-step reaction sequence that produces concentric shells around a central starter molecule [15] Starting with a core molecule like ethylene diamine the first reaction sequence creates a PAMAM dendrimer of generation 0 (G0). Repeating this iterative sequence produces higher generations of PAMAM dendrimers. A PAMAM dendrimer of G10 was selected which has a calculated molecular weight of 934,7 kDa and is covered only with primary amine groups in case of ideal synthesis. Molecular weight determination of PAMAM dendrimers is usually performed using size exclusion chromatography [16-20] or mass spectrometry. For this purpose the most commonly applied mass spectrometric techniques are MALDI-MS [21-23] and ESI-MS [24]. However, until now all MALDI-MS analysis of PAMAM dendrimers which are described in literature only analyse dendrimers up to G4 [25-26]. Further, the analysis of a PAMAM dendrimer G10 was performed using ESI-quadrupole [27] and -FT-ICR-MS [28]. Due to extreme high number of charge states generated in the case of high molecular weight analytes during the ESI process, correct assignment between the individual charge states and the detected analyte peaks was almost impossible in the form of a direct measurement. Hence, the general usefulness of ESI-MS for the analysis of very high molecular weight analytes is limited [29].

Immunoglobulin M (Ig M) is an antibody and an important product of the immune system because it plays a critical role in the early protection against bacterial infections. Normally Ig M is found as a pentameric molecule composed of five Y-shaped subunits and one or sometimes two joining J-chain. All subunits are covalently linked through disulfide bridges and thus forming one single molecule. The reported average molecular weight of intact Ig M under non reducing conditions is between 940 and 1100 kDa depending on the biological source [30-34]. Each Y-shaped subunit consists of two heavy and two light chains. Light

chain molecules have molecular weights of about 25 kDa and are not glycosylated, while heavy chain molecules have molecular weights of about 75 kDa and are heavily glycosylated. The J-chain has a molecular weight of about 15 kDa and contains one N-linked glycan residue [35].

Chemicals and materials. Acetonitrile (ACN) and water were purchased from Merck (Darmstadt, Germany), 2,4,6-trihydroxyacetophenon monohydrate (THAP) from Fluka (Buchs, Switzerland) and trifluoroacetic acid (TFA) from Riedel-de-Haen (Seelze, Germany). All chemicals mentioned above were of analytical grade. The PAMAM dendrimer sample of generation 10 (in case of ideal synthesis 4096 primary amines are located at the surface of the molecule/spherical particle and an ethylene diamine is the core structure, product number 53677-6) was obtained as a 3,24 % (w/v) solution in methanol from Dendritech (Midland, MI, USA). Polyclonal human immunoglobulin M (Ig M, product number 401799) isolated from blood was provided from Calbiochem (San Diego, CA, USA) as a saline solution (200 mM NaCl, 50 mM Tris, pH 8,0, 0,05% sodium azide) with a protein content of 1,09 mg/mL. For MALDI mass spectrometric calibration the Invitromass High Molecular Weight Mass (HMW) Calibrant Kit from Invitrogen (Carlsbad, CA, USA) was applied. ZipTip™ C4 pipette tips for protein purification were obtained from Millipore (Billerica, MA, USA).

Instrumentation. All experiments were carried out on a vacuum MALDI-TOF/RTOF instrument (Axima TOF^2) from Shimadzu Biotech Kratos Analytical (Manchester, UK). The device is a vertical floor standing instrument allowing the operation either in the linear, reflectron or tandem MS mode and is equipped with a pulsed nitrogen laser (wavelength: 337 nm, pulse width: 4 ns), an integrated 2 GHz transient recorder, a differential pumped collision gas cell and a standard discrete-dynode electron multiplier (type ETP ActiveFilm 870, SGE, Sydney, Australia). The instrument was operated in the positive ion linear mode (flight path 1.2 m) applying an accelerating voltage of 20 kV without delayed extraction (the use of delayed extraction resulted in no improvement). All mass spectra were acquired by averaging

50 to 200 unselected and consecutive laser shots on the same preparation by rastering (applied laser power was between 100 and 120 units on a scale between 0 an 180). All data were smoothed using the company-supplied Savitzky-Golay algorithm and the applied peak detection method was threshold-centroid mode at 50% height of the peak maximum. Exact molecular weight determination is based on 15 independent analyses on the same target.

Sample preparation and instrument calibration. Prior to all MS analysis the matrix solution was prepared freshly. THAP was dissolved in 0,1% TFA/ACN 1/1 (v/v) to give a final MALDI matrix concentration of 10 mg/mL. The resulting MALDI matrix solution was vortexed thoroughly for several seconds before use immediate use. Different sample preparation or purification techniques were applied for PAMAM G10 and Ig M.

For the analysis of the polymer PAMAM G10, 1 uL dendrimer stock solution was vacuum dried at RT in order to remove the methanol. Afterwards, the residue was dissolved completely in 0,1% TFA/ACN 9/1 (v/v) to give a final dendrimer concentration of 9,34 mg/mL. The acidification of the sample solution supports the protonation of the amino groups at the dendrimer surface. Then 2 uL of this sample solution were mixed with 4 uL matrix solution in an Eppendorf tube.

Prior the MALDI-MS sample preparation of the glycoprotein Ig M, an extensive ZipTip™ C4 purification/desalting procedure was applied. 1 uL 1% TFA was added to 10 uL original protein solution containing a protein concentration of 1.1 ug/uL and the mixture was vortexed thoroughly and spinned down shortly afterwards. The wetting solution (50% ACN/TFA solution (0,05 % aqueous TFA) (v/v)) and washing solution (0,1% aqueous TFA) for the ZipTip™ purification were prepared freshly. The pipette tip was conditioned by aspirating and dispensing the wetting solution three times and subsequently washed by aspirating and dispensing with the washing solution three times. The binding step was performed by aspirating and dispensing the Ig M solution between three and six times (depending on the tip behaviour) resulting in the binding to the reversed-phase silica/polymer material. Before the

sample was eluted the column was washed by aspirating and dispensing with the washing solution two times. In the final step the purified as well as desalted Ig M was eluted with about 2 to 4 uL MALDI matrix solution into an Eppendorf tube.

Regardless of the type of sample 0,5 uL aliquots of the resulting matrix/protein or matrix/polymer sample mixtures were deposited on different spots on a stainless steel microtiter format MALDI target with a restriction ring with a diameter of 3 mm (product number DE1271TA, Shimadzu Biotech Kratos Analytical) and dried under a gentle stream of air forming crystalline layers.

Molecular weight calibration was performed externally by using the HMW calibrant kit, which contained various recombinant proteins without any posttranslational modifications and no disulfide bridges with given molecular weights in the mass range from 30 kDa to 160 kDa (given by the manufacturer: 29851 Da, 49824 Da, 69204 Da, 89712 Da and 159080 Da). The calibration kit was applied according to the manufacturer's instructions, but in contrast to the mentioned instruction manual the MALDI matrix solution described above was applied for sample preparation. The calibration spots were deposited on the same target as the samples. For the molecular weight calibration the singly and double charged molecular ion peaks of the 160 kDa protein standard were applied.

The MALDI mass spectrometric analysis of PAMAM G10 from 1.56 µg on target gave a relatively clean mass spectrum at a reasonable relative laser power (around 100 in the possible range 0 to 180) and showed a doubly and triply charged molecular ion, but no singly charged ion (Fig. 1 A). THAP was particularly successful, maybe due the non-acid character of this matrix. Other solid (as usually applied for technical polymers) or liquid (e.g.. glycerol/sodiumhexacyanoferrat, a binary liquid matrix) MALDI matrices resulted in no better mass spectra. For the doubly charged molecular ion peak a m/z ratio of 283000 was determined, while the triply charged molecular ion peak was observed at a m/z ratio of 193000. Since the external molecular weight calibration was limited to a m/z ratio of 159081,

both molecular ion peaks were out of the calibration range, but nevertheless that was the only way to calibrate this mass spectrum correctly. Based on the triply charged molecular ion peak of PAMAM dendrimer G10 the molecular weight was determined to be 579 kDa ± 8 kDa. Based on the doubly charged molecular ion peak a molecular weight of 566 kDa ± 8 kDa was obtained. Hence the average molecular weight (based on $[M]^{2+}$ and $[M]^{3+}$) determined for PAMAM dendrimer G10 was 573 kDa which was significantly (-39%) below the molecular weight of 935 kDa calculated for ideal dendrimer synthesis. This value was calculated for an optimal dendrimer synthesis, generating an ideal structure without any chemical defects. This significant deviation from the calculated molecular weight and width of the multiply charged molecular ion peaks can be attributed to chemical defects (which are often observed during the synthesis of higher generations of dendrimers) and was corroborated by another techniques, namely gas phase electrophoretic molecular mass analyses [36] (482 ± 24 kDa, data not shown), which is based on different physical principle. In this context it has to be stated that the molecular weight derived from MALDI mass spectrometry is independent of 3-dimensional structure of the dendrimer molecule which is in contrast to techniques usually used for molecular weight determination of dendrimers [37].

The MALDI mass spectrum of human Ig M, seven multiply charged molecular ion peaks were observed (Fig. 1 B) from 2 pmole material on target (without considering any loss during the handling, purification and desalting steps; the amount has to seen also under viewpoint of the high glycoheterogeneity of Ig M). THAP turned out to be the matrix of choice and delivered the best S/N ratios, the highest number of positive charges as well as best peak shapes compared to sinapinic acid, which was used in an earlier work for Ig M [34]. The analyte peak with the highest m/z value was the triply charged molecular ion peak, while the analyte peak with the lowest observed m/z value related to Ig M was the nine times charged molecular ion peak. Obviously, analyte peaks representing all charge states between 3+ and 9+ were found in the mass spectrum with high abundance, too. Despite the instrument

allowed in principle ion detection up to m/z 600000, no peaks with m/z values above 320000 (triply charged molecular ion peak region) were found in the mass spectrum of Ig M. At the region below the 9+ charged molecular ion peak other peaks were detected, which represent impurities or degradation products (degraded subunits). However, based on the determined molecular weight for intact Ig M these peaks can not be correlated with higher charged molecular ion species of Ig M. Three of the seven observed molecular ion peaks were within the calibration range of the recombinant protein calibrant (159080 Da). These analyte peaks were the 7+, 8+ and 9+ charged molecular ion peaks of Ig M. The 6+ charge molecular ion peak was so close to the calibrant molecular weight that it was included in the analysis. For the 6+ charged molecular ion peak (the base peak) an average m/z value of 170280 was measured, while for the 7+ charged molecular ion peak a m/z value of 147490, for the 8+ peak of 128560 and for the 9+ peak of 113150 was determined. The relative standard deviations of the determined m/z values was between 0,2% and 0,5% (15 subsequent determinations). Based on these four multiply charged molecular ion peaks an average molecular weight of 1025,3 kDa ± 28,2 kDa was determined for intact polyclonal human Ig M, which turned out to be in good agreement with published data [30-34]. When evaluating full peak widths at half maximum (FWHM) of the multiple charged molecular ion peaks of Ig M a resolution (FWHM) of 13.6 ($[M]^{6+}$ base peak) and 14 ($[M]^{3+}$ highest detected ion) was obtained in the linear mode, which is considerable better than published data [32-34]. This resolution was of course not sufficient to differentiate the present numerous glycoisoforms (known from the individual subunits) of Ig M.

In this work it was demonstrated that molecular weight determination of very high molecular mass analytes belonging to the group of synthetic polymers (dendrimers) and of biopolymers (glycoproteins) with good mass accuracy and sensitivity (despite their structural heterogeneity in terms of polydispersity and glycosylation) is possible on an instrument, containing no special instrumental features as e.g. cryo detectors or unusual high acceleration voltages and

which is at the present time available on the market. Molecular weight determination of the intact high molecular weight biomolecules was feasible due to optimized sample purification, the use of well-defined high mass calibrants and the generation of multiple charged molecular ions which exhibited m/z ratios close or within the calibration range. Due to the limited available calibration range (up to m/z 159080) and the lower charged molecular ions the molecular weight determined for PAMAM G10 dendrimer exhibits a higher uncertainty than the molecular weight determination of the even larger Ig M. The mass spectrometric analysis of the PAMAM G10 dendrimer (to our knowledge the largest commercial available) revealed a molecular weight considerable below the calculated molecular weight based on a perfect synthesis. However, this determined low molecular weight can be explained by chemical defects of the PAMAM dendrimer particle, which demonstrates the usefulness of MALDI-TOF-MS analysis in the linear mode during synthesis for higher generation dendrimers.

Acknowledgement

This work was supported in part by a grant from the Austrian Science Foundation (P15008) and Agilent Technologies. Furthermore we thank O. Belgacem and E. Raptakis (Kratos Analytical, Manchester, UK) for their helpful discussions.

Yours sincerely,

Roland Müller and Günter Allmaier*

Institute of Chemical Technologies and Analytics, Vienna University of Technology, Getreidemarkt 9/164, A-1060 Vienna, Austria

Corresponding author: Günter Allmaier, Institute of Chemical Technologies and Analytics, Vienna University of Technology, Getreidemarkt 9/164, A-1060 Vienna, Austria

Tel: +43 1 58801 15160 Fax: +43 1 58801 15199 E-mail: guenter.allmaier@tuwien.ac.at

Figure legend

Figure 1 Positive ion MALDI mass spectrum (linear mode) of the synthetic polymer PAMAM dendrimer generation 10 (A) and of purified human blood-derived immunoglobulin M (B).

References

[1] Karas M, Hillenkamp F. *Anal. Chem.* 1988; **60**: 2299

[2] Tanaka K, Waki H, Ido Y, Akita S, Yoshida Y, Yohida T. *Rapid Commun. Mass Spectrom.* 1988; **2**: 151

[3] Belgacem O, Buchacher A, Pock K, Josic D, Sutton C, Rizzi A, Allmaier G. *J. Mass Spectrom.* 2002; **37**: 1118

[4] Schriemer DC, Li L. *Anal. Chem.* 1996; **68**: 2721

[5] Peacock PM, McEwen CN. *Anal. Chem.* 2004; **76**: 3417

[6] Mamyrin BA. *Int. J. Mass Spectrom.* 2001; **206**: 251

[7] Zenobi R, Knochenmuss R. *Mass Spectrom. Rev.* 1998; **17**: 337

[8] Frank M, Labov SE, Westmacott G, Benner WH. *Mass Spectrom. Rev.* 1999; **18**: 155

[9] Peng W-P, Cai Y, Chang H-C. *Mass Spectrom. Rev.* 2004; **23**: 443.

[10] Dreisewerd K. *Chem. Rev.* 2003; **103**: 395.

[11] Hecht S, Frechet JMJ. *Angew. Chem. Int. Edit.* 2001; **40**: 74

[12] Boas U, Heegaard PMH. *Chem. Soc. Rev.* 2004; **33**: 43

[13] Esfand R, Tomalia DA. *Drug Deliv. Today* 2001; **6**: 427

[14] Tomalia DA, Baker H, Dewald JR, Hall MJ, Kallos G, Matrin S, Roeck J, Ryder J, Smith P. *Polym. J. (Tokyo)* 1985; **17**: 117

[15] Tomalia DA. *Prog. Polym. Sci.* 2005; **30**: 294

[16] Hawker CJ, Frechet JMJ. *J. Am. Chem. Soc.* 1990; **112**: 7638

[17] Zeng F, Zimmerman SC, Kolotuchin SV, Reichert DEC, Ma Y. *Tetrahedron* 2002; **58**: 825

[18] Maraval V, Laurent R, Donnadieu B, Mauzac M, Caminade AM, Majoral JP. *J. Am. Chem. Soc.* 2000; **122**: 2499

[19] Padias AB, Hall HK, Tomalia DA, McConnell JR. *J. Org. Chem.* 1987; **52**: 5305

[20] Newkome GR, Young JK, Baker GR, Potter RL, Audoly L, Copper D, Weis CG. *Macromolecules* 1993; **26**: 2394

[21] Felder T, Schalley CA, Fakhrnabavi H, Lukin O. *Chem.-Eur. J.* 2005; **11**: 5625

[22] Baytekin B, Werner N, Luppertz F, Engeser M, Brüggemann J, Bitter S, Henkel R, Felder T, Shalley CA. *Int. J. Mass Spectrom.* 2006; **249-250**: 138

[23] Subbi J, Aguraiuja R, Tanner R, Allikmaa V, Lopp M. *Eur. Polym. J.* 2005 ; **41**: 2552

[24] Kallos GJ, Tomalia DA, Hedstand DM, Lewis S, Zhou J. *Rapid Commun. Mass Spectrom.* 1991; **5**: 383

[25] Hood JR, Watson JT, Jones AD. *54th Annual Conference of the American Society of Mass Spectrometry,* Seattle, WA, USA (May 28 – June 1, 2006) Poster MP11 230.

[26] Zhou L, Russell DH, Zhao M, Crooks RM. *Macromolecules*, 2001 **34**: 3567

[27] Schwartz BL, Rockwood AL, Smith RD, Tomalia DA, Spindler R. *Rapid Commun. Mass Spectrom.* 1995; **9**: 1552

[28] Tolic KP, Anderson GA, Smith RD, Brothers HM, Spindler R, Tomalia DA. *Int. J. Mass Spectrom.* 1997; **165/166**: 405

[29] Fuerstenau SD, Benner HW. *Rapid Commun. Mass Spectrom.* 1995; **9**: 1528

[30] Yilmaz H, Tantas A, Ilgaz A, Morgan KL. *Turk. J. Vet. Anim. Sci.* 1999; **23**: 135

[31] Plaut AG, Tomasi TB. *Proc. Natl. Acad. Sci. USA* 1970; **65**: 318

[32] Wenzel RJ, Matter U, Schultheis L, Zenobi R. *Anal. Chem.* 2005; **77**: 4329

[33] Nelson RW, Dogruel D, Williams P. *Rapid Commun. Mass Spectrom.* 1995; **9**: 625

[34] Nelson RW, Dogruel D, Williams P, Beavis R. *Rapid Commun. Mass Spectrom.* 1994; **8**: 627

[35] Symersky J, Novak J, McPherson DT, DeLucas L, Mestecky J. *Mol. Immunol.* 2000; **37**: 133

[36] Bacher G, Szymanski WW, Kaufman SL, Zöllner P, Blaas D, Allmaier G. *J. Mass Spectrom.* 2001, **36**: 1038

[37] Caminade AM, Laurent R, Majoral JP. *Adv. Drug Deliver. Rev.* 2005; **57**: 2130

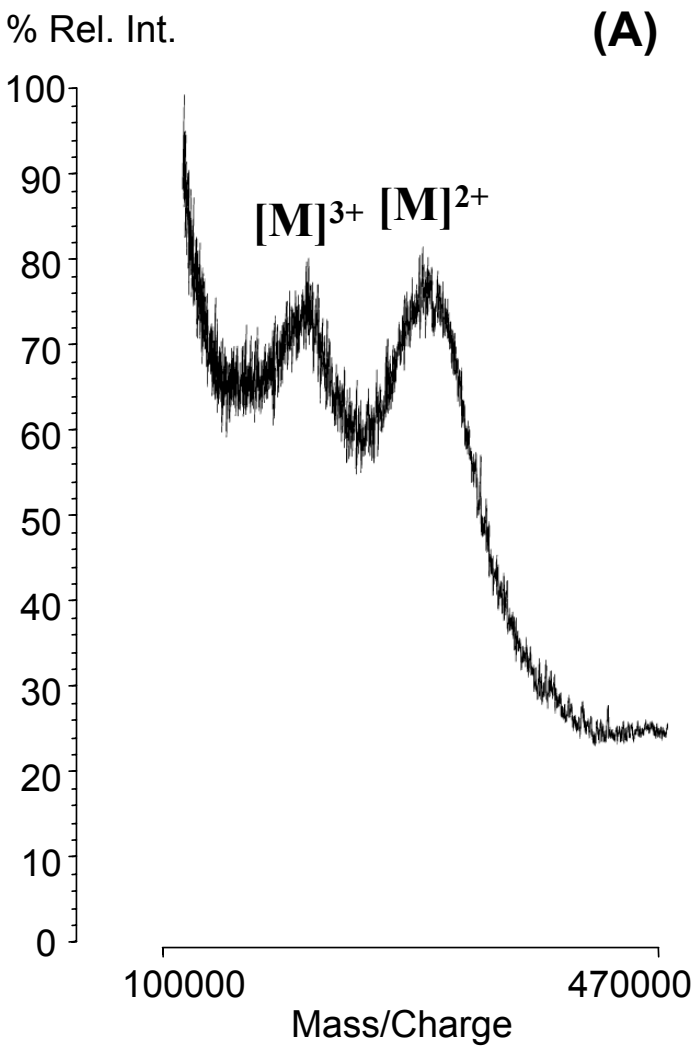

Figure 1 A Positive ion MALDI mass spectrum (linear mode) of the synthetic polymer PAMAM dendrimer G10.

R. Müller and G. Allmaier

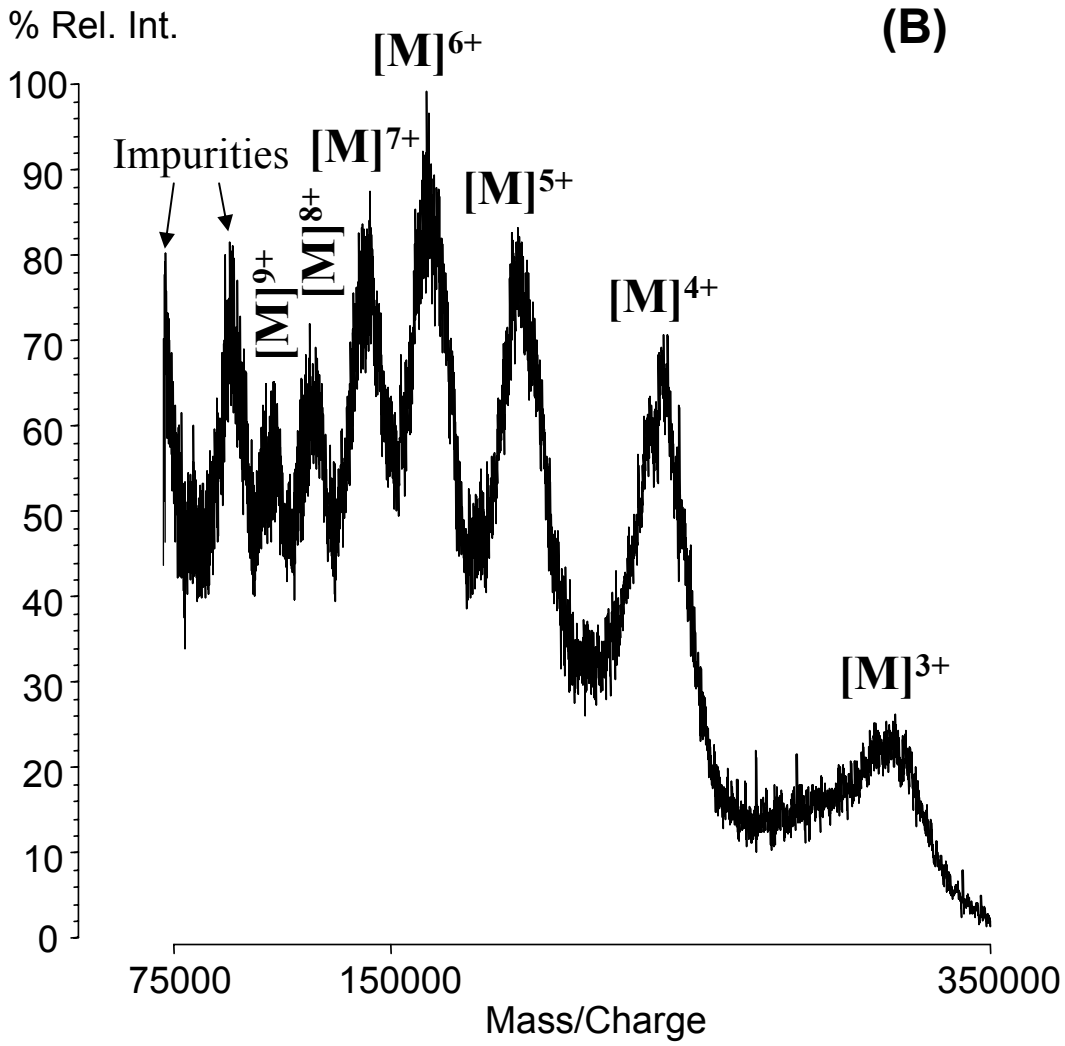

Figure 1 B Positive ion MALDI mass spectrum (linear mode) of purified human blood-derived immunoglobulin M (B).

R. Müller and G. Allmaier

III. Conclusions

It was demonstrated that all three described analytical techniques, CGE-on-the-chip, planar SDS-PAGE and MALDI-TOF-MS, were capable of analyzing high molecular weight protein samples. Further it was shown that the results obtained with CGE-on-the-chip were in very good agreement with the protein bands observed with old-fashioned planar SDS-PAGE. In the case of very high molecular weight proteins like IgM CGE-on-the-chip results were superior to the results observed with planar SDS-PAGE. The practical benefits of CGE-on-the-chip over planar SDS-PAGE were faster analysis times, a higher degree of automation and larger accessible sizing range. Until now no commercial planar SDS-PAGE system is capable of separating proteins according to their molecular weight in the molecular weight range from 14 to 1000 kDa. Analysis with MALDI-TOF-MS using a commercial standard instrument provided exact molecular weights for all analyzed high molecular weight proteins. With the aid of a suitable MALDI matrix and sample preparation technique the desorption and ionization of all seven high molecular weight proteins was possible and in all cases the determined molecular weights were in good or excellent agreement with the values given in literature. Exact molecular weight determination with MALDI-TOF-MS was feasible because of multiple charged molecular ion analyte peaks which were detected at mass to charge ratios below 160000 and hence were within the calibration range. Consequently the usefulness of MALDI-TOF-MS for the exact molecular weight determination of high molecular weight proteins was demonstrated. Moreover, it was shown that molecular mass determination of PAMAM dendrimers up to G10 was generally possible using MALDI-TOF-MS. With an increasing generation number a significant difference between the theoretical molecular masses for ideal dendrimer growth/synthesis and the molecular masses determined with MALDI-TOF-MS was found. The molecular weight differences between theoretical and measured values were lower for smaller dendrimers and steadily increased with the number of generation. Analysis with MALDI-TOF-MS provided molecular weights significantly (up to 40%) below the calculated theoretical molecular weight. The polydispersity of the analysed dendrimer samples was found to be significantly higher than the polydispersity for proteins in the same mass and size range. It was attempted to calculate the mass of the dendrimers via their particle diameter with different approaches, but all resulted in a significant discrepancy to the MALDI-MS data. The calculated density of the dendrimer particles based on the MALDI-MS and nES-GEMMA results showed a significant difference to protein densities (0.54 kg/L), densities calculated from molecular dynamic results (0.52 kg/L) as well as to

densities derived from dendrimer growth theory (up to 1.2 kg/L). The obtained results indicated that PAMAM dendrimer particles of G4 or higher possess a constant density of 0.65 kg/L, which is determined by tight packing of the branches inside the particle. Concerning the molecular weight determination of very high molecular mass analytes belonging to the group of synthetic polymers (dendrimers) and of biopolymers (glycoproteins) with MALDI-TOF-MS good mass accuracy and sensitivity (despite their structural heterogeneity) was possible on an instrument, containing no special instrumental features as e.g. cryo detectors or unusual high acceleration voltages and which is at the present time available on the market. Molecular weight determination of intact high molecular weight biomolecules was feasible due to extensive sample purification, the use of well-defined high mass protein calibrants and the generation of multiple charged molecular ions which exhibited m/z ratios close or within the calibration range. The mass spectrometric analysis of the PAMAM G10 dendrimer, which is the largest commercial available dendrimer, revealed a molecular weight considerable below the calculated molecular weight based on a perfect synthesis. However, this determined low molecular weight can be explained by chemical defects of the PAMAM dendrimer particle, which demonstrates the usefulness of MALDI-TOF-MS analysis in the linear mode during synthesis for higher generation dendrimers.

Lebenslauf

Name: Mag. Roland Müller

Geburtsdatum: 10.02.1979

Geburtsort: Wien

Staatsbürgerschaft: Österreich

Familienstand: Verheiratet

Name der Ehegattin: Sabine Müller (geb. Barna), 07.01.1982, Kleinkindpädagogin

Name der Eltern: Ilse Müller (geb. Kerber), 11.08.1949, Volksschuloberlehrerin
Harald Müller, 5.12.1950, Nachrichtentechniker

Werdegang:

1985 – 1989
Volksschule Dietrichgasse, 1030 Wien

1989 – 1997
Bundesgymnasium Wien 3, Kundmanngasse, 1030 Wien
Abschluß mit ausgezeichnetem Erfolg

1997 – 1999
Chemiestudium an der Uni Wien

1999 – 2000
Zivildienst am Polizeikommissariat Juchgasse, 1030 Wien

2000 – 2004
Fortsetzung des Chemiestudiums an der Uni Wien

Juni 2003 – April 2004
Diplomarbeit bei Prof. G. Allmaier am Institut für Analytische Chemie der Uni Wien mit dem Titel: „MALDI-MS, SDS-PAGE, CE-on-the-chip of glycosylated and non glycosylated proteins“, Abschluß mit ausgezeichnetem Erfolg

Juni 2004 – Oktober 2004
Call Center Tätigkeit bei der Firma Mastermanagement im Call Center der UTA Telekom; Betreuung von Business Kunden

November 2004 – November 2006
Dissertation bei Prof. G. Allmaier am Institut für chemische Technologien und Analytik der TU Wien in Zusammenarbeit mit Agilent Technologies (Waldbronn, Deutschland).
Titel: „CGE-on-the-chip, planar SDS-PAGE and MALDI-TOF-MS investigations of proteins and dendrimers with molecular weights beyond 200 kDa”

Wissenschaftliche Publikationen:

Leščić I., Zehl M., Roland Müller, Vukelić B., Abramić M., Pigac J., Allmaier G., Kojić-Prodić B. Primary structure and disulfide bond linkage of an extracellular lipase from *Streptomyces rimosus* determined by MALDI mass spectrometry. *European Journal of Biochemistry*.

Wissenschaftliche Vorträge:

„Charakterisierung von Proteinen mittels MALDI-TOF-MS, SDS-PAGE und dem Agilent 2100 Bioanalyzer", Agilent Technologies Bioabend (Mai 2004 in Innsbruck, Wien und Graz)

„CGE-on-the-chip, planere SDS-PAGE und MALDI linear TOF Massenspektrometrie: die Analyse von (Glyko-)proteinen im Molekulargewichtsbereich jenseits von 100 kDa?", 23. Agilent Forum Analytik (Februar 2006 in Wien)

„CGE-on-the-chip: Entwicklung und Optimierung eines Assays für hochmolekulare (> 200 kDa) Proteine", 2. ASAC Junganalytikerforum (Juni 2006 in Graz)

Wissenschaftliche Posterpräsentationen:

"CGE-on-chip of proteins beyond molecular weight 250 kDa", 26th International Symposium on the Separation of Proteins, Peptides and Polynucleotides (Oktober 2006 in Innsbruck)

Wissenschaftliche Auslandsaufenthalte:

November und Dezember 2004: Forschungsaufenthalt im Zuge der Dissertation in der Forschungs- und Entwicklungsabteilung von Agilent Technolgies in Waldbronn, Deutschland unter der Betreuung von Martin Kratzmeier und Helmuth Elgass.

Besondere Kenntnisse und sonstiges:

Vertiefendes Wissen in den Bereichen Analytischer Chemie, Organischer Chemie und Biochemie; Englisch perfekt in Wort und Schrift; sehr gute PC Kenntnisse; Führerschein (B)

Mitglied der Gesellschaft Österreichischer Chemiker (GÖCH) und der Österreichischen Gesellschaft für Analytische Chemie (ASAC)